DOE/PC/90362–T1(Vol.2)
(DE95004264)

ENHANCED NO_x REMOVAL IN WET SCRUBBERS USING METAL CHELATES

Final Report

Volume 2 of 2

December 1992

Work Performed Under Contract No. AC22-90PC90362

For
U.S. Department of Energy
Pittsburgh Energy Technology Center
Pittsburgh, Pennsylvania

By
Dravo Lime Company
Pittsburgh, Pennsylvania

DISCLAIMER

DOE/PC/90362--T1(Vol.2)
(DE95004264)
Distribution Category UC-105

ENHANCED NOX REMOVAL

IN WET SCRUBBERS

USING METAL CHELATES

DOE CONTRACT DE-AC22-90PC90362

FINAL REPORT

VOLUME 2 OF 2

PREPARED FOR THE

U.S. DEPARTMENT OF ENERGY

PITTSBURGH ENERGY TECHNOLOGY CENTER

SUBMITTED BY

DRAVO LIME COMPANY

DLC-5237

DECEMBER, 1992

III. DESCRIPTION AND RESULTS OF NOx REMOVAL TESTS

A. PHASE I SUMMARY OF TESTING

This section summarizes the results of testing performed in Phase I of the project, "Enhanced NOx Removal in Wet Scrubbers Using Metal Chelates". Each task's testing will be briefly reviewed with emphasis placed on the purpose of testing, measures of success, results of testing including any unexpected data or problems encountered, and an interpretation of the results of each task's tests. Charts and graphs are included where necessary. An effort was made to generate testing data to support and where necessary, modify the following liquid-film limited, pseudo-first order absorption rate NO removal model:

(Refer to Background Document)

$$\text{NO Removal (NTU)} = \frac{(k_2\,[Fe^{++}]\,D_{NO})^{1/2}}{H/P_T} \quad \frac{a\ Z}{p_M\ v}$$

TESTING PERFORMED:

TASK 3.1.1.1 Start-up of Testing

Purpose of Test: Bring pilot plant to a steady operating condition; add ferrous EDTA to the system to achieve a steady ferrous concentration at a total iron concentration of 35-40 millimolar (mM).

Measures of Success: Determine NOx removal while operating the plant at a steady condition and utilizing the available ferrous EDTA without addition of reducing agents or antioxidants.

Results of Tests: Operating conditions for the task were as follows: 3 ft. absorber tower, single 30% open tray, two spray levels with single Bete MP 1125M nozzles, single quench header with a single Bete TF 40NN nozzle. Steady operating conditions were established and maintained at a flue gas velocity (FGV) of 10 fps and a liquid to gas ratio (L/G) of 50. (L/G expressed as GPM liquid per 1000 acfm gas flow).

Steady-state total iron concentration was 40 mM and the ferrous iron concentration was 1-6 mM. Problems with the inlet NOx analyzer prevented generation of consistent NOx removal data (inlet NOx values below 400 ppm should be discarded), but when both analyzers were functional typical NOx removal appeared to be between 2% and 4% at steady-state conditions. (See Figure 1)

Interpretation: As expected, the iron EDTA solution was not capable of sustaining sufficient ferrous iron concentrations at steady-state conditions to provide much NOx removal. It was decided that in order to achieve desirable ferrous levels, chemical reducing agents/antioxidants would have to be added to the system for the remainder of the project to effect acceptable NOx removals.

TASK 3.1.1.2: Transfer Unit Tests: Subtask 1) Simple Retrofit Tests:

Purpose of Tests: Determine the levels of NOx removal achievable in a simple retrofit mode by the addition of ferrous EDTA and chemical reducing agents/antioxidants to the scrubber liquor of absorbers designed only for SO_2 removal.

Measures of Success: Determine NOx removal at 3 absorber liquid to gas ratios (L/G) and determine the ratios of SO_2 removal in NTU to NOx removal in NTU.

Results of Tests: Operating conditions for this subtask were identical to start-up conditions with the exception of the quench nozzle being switched from the Bete TF 40NN to a Bete TF 56NN to avoid plugging of the smaller nozzle. Sodium dithionite and ascorbic acid were used as the chemical reducing agent/antioxidant mix (250 # sodium dithionite and 55 # ascorbic acid) to maintain ferrous EDTA concentrations. The screw feeder which introduced the chemical mix into the recycle tank for this purpose became inoperable due to faulty electronics requiring batch feeding of the chemical mix once per hour for the majority of the week.

Ferrous levels (10-15mM) and NOx removal (5-12%) were improved by the addition of the sodium dithionite/ascorbic acid mix. (See Figure 2 and Table 1) Continuous addition of the chemical mix with the screw feeder resulted in a higher and more consistent ferrous level and subsequent NOx removal than batch addition of the chemical mix by hand.

Increasing L/G ratio predictably increased SO_2 removal NTU but showed surprisingly little effect on NOx removal NTU. Thus under these scrubber conditions the ratio of SO_2 to NOx removal ratios in NTU increased with increasing L/G. (See Table 1)

Interpretation: As expected from the removal model, NOx removal increased with increasing ferrous concentration and the reducing agent/antioxidant chemical mix was responsible for the increased ferrous concentration, primarily by ferric EDTA reduction to ferrous EDTA. Ferrous iron levels in the system can be controlled by continuous feed of the chemical mix. A higher and more consistent ferrous level is achieved by continuous addition rather than batch addition. The dithionite when batched reacts with and reduces itself resulting in decreased utilization and a "peak and valley" ferric reduction pattern. NOx removal was expected from the theoretical model to increase with increasing L/G. This trend did not develop in the single tray mode and is not reflective of the model per se but of the inability of this absorber configuration to maintain sufficient gas to liquid contact to promote NO absorption into the liquid phase. Gas-liquid contact and mass transfer criteria must be better established before SO_2/NOx removal ratios can be usefully employed under these conditions.

TASK 3.1.1.2: Transfer Unit Tests: Subtask 2) Complex Retrofit/New Plant Tests:

Purpose of Tests: Determine NOx removal achievable in a more complicated retrofit plant mode where additional gas-liquid contact equipment (multiple perforated plate trays) is installed in an absorber design based upon NOx removal requirements rather than SO_2 removal. Determine more fundamental

mass-transfer criteria compared to the first subtask to provide guidance for scale-up to larger absorbers. Determine most suitable tray configuration (number of trays and tray open area) and perform a ferrous oxidation rate study in the complex retrofit mode.

Measures of Success: Determine NOx removal with multiple trays installed. Determine the operational boundaries of the absorber through absorber pressure drop tests with various tray configurations. Determine NOx removal for various ferrous iron concentrations at a satisfactory tray configuration mode (ferrous iron oxidation rate study).

Results of Tests: Initial tests were conducted with 3 and 5 trays of 40% open area to determine the operational boundaries of the absorber. The results of these tests versus tray pressure drop are illustrated in Figure 3. Next, as a result of exceptionally high pressure drop across multiple trays, liquid recycle rates versus single tray pressure drop at various tray open areas were conducted (See Figure 4). Using the criteria of maximum NOx removal and reasonable tray pressure (-10" WC), the most promising configuration found consisted of two trays with 20% open area apiece. The ferrous oxidation rate study was conducted in this configuration with the results shown in Figure 5.

Interpretation: The 3, 4, and 5 tray configurations proved unsatisfactory because pressure drop exceeded the operational boundaries of the absorber (>10" WC). This was due to mechanical limitations of the equipment. The ferrous oxidation test carried out under the most suitable configuration of two 20% open trays revealed the expected direct proportionality of ferrous concentration versus NOx removal. However, a multiple linear regression shows the NOx removal to be proportional to ferrous concentration only to the .13 power rather than to the 0.5 power indicated by the model. It was subsequently discovered that air leakage into the outlet NOx analyzer resulted in a false low outlet NOx reading by dilution with air. This had the effect of elevating the apparent NOx removal. This dilution effect is illustrated by Figure 6 in which the outlet O_2 is on the average a full 2% greater than the inlet O_2 concentration. This had the effect of raising NOx removal by 0.15 to 0.20 NTU's and all NOx removal data up to this point must be corrected for this

factor. In addition to the air leak in the outlet NOx analyzer, a malfunction in the inlet NOx analyzer resulted in a false high reading further skewing the data. Analyzer circuit repairs were made at this point and all NOx removal data from herein is considered reliable.

TASK 3.1.1.3: Effect of Increase in Flue Gas SO_2/NOx Ratio:

Purpose of Test: Start-up and debug new SO_2 injection system. Determine the effect of increased flue gas SO_2 concentration and subsequent increased SO_2/NOx ratio on NOx removal.

Measures of Success: Determine the change in NOx removal with increased SO_2/NOx ratio compared to earlier tests under the same gas-liquid contact conditions. Determine if this increased ratio has the effect of reducing the required amount of chemical reducing agent mix fed to the system to maintain the desired ferrous concentration.

Results of Tests: The new SO_2 injection system performed splendidly with no major operational defects. A slight difficulty was encountered controlling the inlet SO_2 on the automatic mode but control on the manual mode of $\pm$100 ppmv at 2500 ppmv proved easy and reliable. The desired increased SO_2/NOx ratio was thus achieved. No significant change in either NOx removal or chemical additive feed rate was observed under these increased ratio conditions.

Interpretation: NOx removal shows no definite dependance upon SO_2/NOx ratio under these conditions. In addition, the reducing agent/antioxidant chemical mix feed rate appears to be more a function of oxygen concentration than SO_2/NOx ratio.

TASK 3.1.1.4: Simulation of NOx Removal Following Low-NOx Combustion:

Purpose of Test: Determine level of NOx removal with relatively lower inlet flue gas NOx concentration and determine relationship of ferrous concentration versus NOx removal in this mode.

Measures of Success: Determination of NOx removal at lower relative inlet flue gas NOx levels than previously tested. Determination of proportional relationship of ferrous concentration versus NOx removal under varying NOx inlet levels.

Results of Test: During this test period the ratio of SO_2 to NOx fluctuated roughly between 4 and 6 depending on boiler load. Inlet O_2 levels varied between 6% and 11% and inlet NOx levels varied between 400 ppmv and 750 ppmv. Figures 7 and 8 (normalized for ferrous concentration) show quite clearly that NOx removal is independent of inlet O_2 and NOx levels. The regression analysis resulting in the plot of ferrous concentration versus NOx removal shown in Figure 9 reveals NOx removal to be very nearly a function of the square root of the ferrous concentration (.56 power).

Interpretation: This test data is further indication of the applicability of this NOx removal process and model to low as well as high NOx inlet flue gas levels. Figure 8 demonstrates this fact quite clearly. The much better correlation of NOx removal to the square root of the ferrous concentration is a resounding verification of the NOx removal model and much confidence was gained in its application. The more realistic figure of .56 versus the previously generated .13 was the result of the correction of the inlet and outlet NOx analyzer problems discussed in the previous task and careful maintenance and calibration of the analyzers.

TASK 3.1.1.5: Testing of Glyoxal as Reducing Agent/Antioxidant:

Purpose of Test: Determine effectiveness of glyoxal as an alternative reducing/antioxidant agent for ferrous regeneration. Glyoxal is attractive for this purpose because of its relatively lower cost at 100% utilization and the fact that at 100% utilization the final reaction product of the glyoxal redox train is carbon dioxide.

Measures of Success: Determine if glyoxal is an effective chemical reducing agent for the NOx removal process by monitoring the ferrous concentration and NOx removal while controlling glyoxal feed rate.

Results of Test: Glyoxal was initially batch fed into the scrubber recycle tank and later added with a metering pump that fed the additive at a constant rate. A comparison of glyoxal feed rate versus ferrous concentration and NOx removal are shown in Figure 10. For the most part, NOx removal and ferrous concentration showed a close relationship to each other. After a sluggish start, ferrous concentration increased with addition of glyoxal and more or less fluctuated with glyoxal addition rate. The control of ferrous concentration with glyoxal did not seem as precise as it did with the sodium dithionite/ascorbic acid mix.

Interpretation: Glyoxal addition certainly increased the ferrous concentration in the system. However ferrous level control was not as sharp as with the previous chemical mix and a certain "lag time" was evident. More testing is needed with glyoxal before a comparison with the sodium dithionite-based mix can be made. NOx removal is dependent on ferrous concentration in this system and is independent of the reagent used to maintain ferrous levels.

SUMMARY OF PHASE I TESTING:

The previously discussed NOx removal model was generally verified and reinforced by the data generated in this Phase I testing program. A majority of the data was in agreement with the model. Some aspects of the model may need to be modified or expanded as more experimental data becomes available. Better and more consistent quantification of H_t, height of gas-liquid contact zone, and a, interfacial gas-liquid contact area is necessary. Means of increasing these two components of the model need to be investigated and implemented. Glyoxal is an attractive alternative reducing agent and further testing with glyoxal is recommended to better evaluate its effectiveness.

One of the more pleasant surprises encountered in Phase I testing not previously mentioned in this report was the excellent dewatering of the belt filter cake produced during this test phase.

Suppression of ferrous oxidation via chemical antioxidants had the effect of suppressing sulfite oxidation as well. This resulted in a filter cake less hindered by sulfate crystal inclusions. This cake was more ordered in layers than conventional thiosorbic filter cake and dewatered beautifully. Percent solids in the filter cake increased from a baseline of 30%-35% at the outset to 65%-70% for most of the test phase. (See Figure 11). This represents a potentially enormous savings in disposal costs and chemicals associated with scrubber operations in this mode. Savings realized by lower sludge disposal costs and better utilization and reuse of chemicals will help to offset the increased costs associated with NOx removal and make it a more attractive process. Continued improvement in solids dewatering and waste characterization are important areas of future research associated with this NOx removal process.

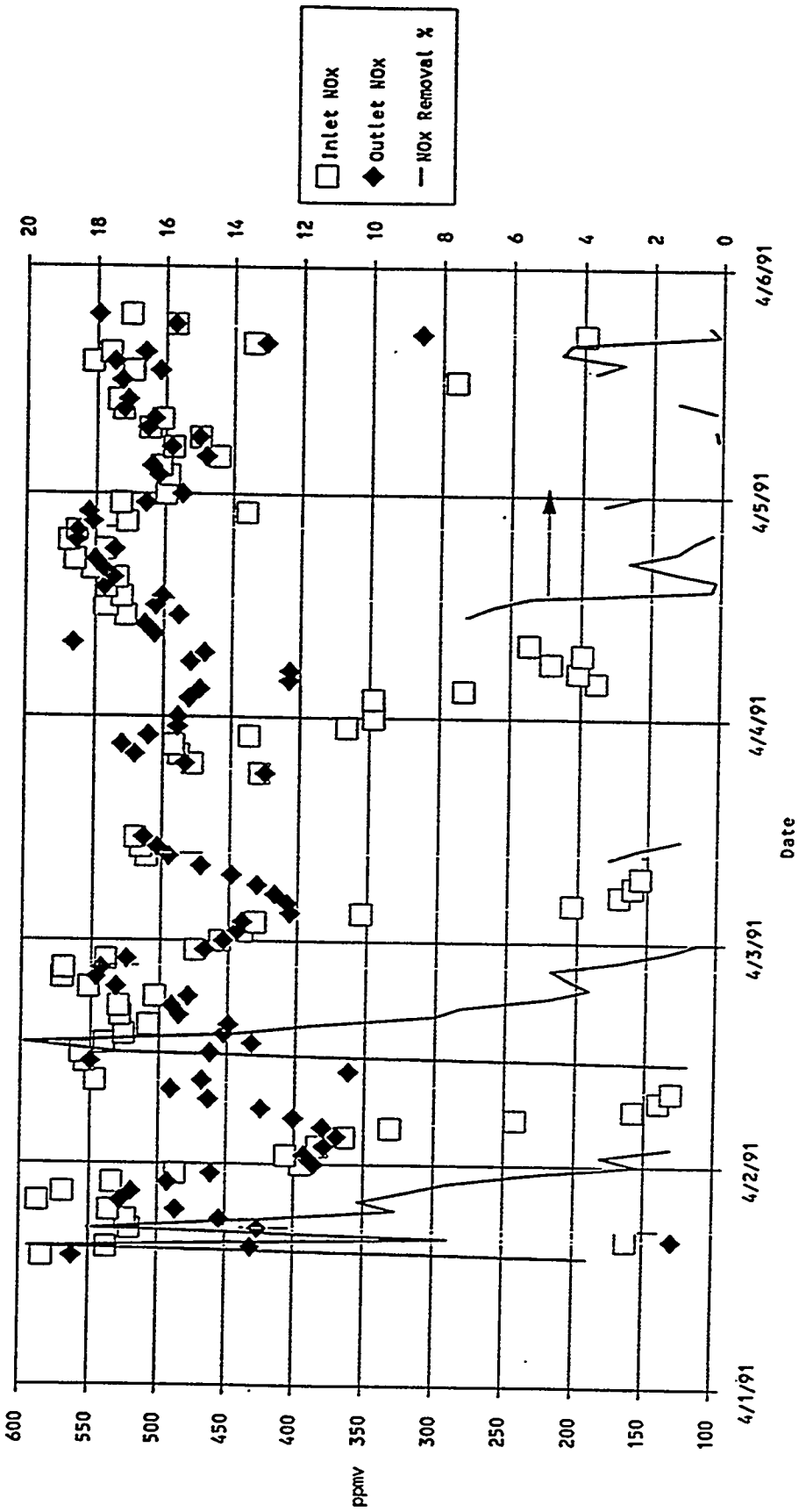

Figure 1

Figure 1

FIGURE 2

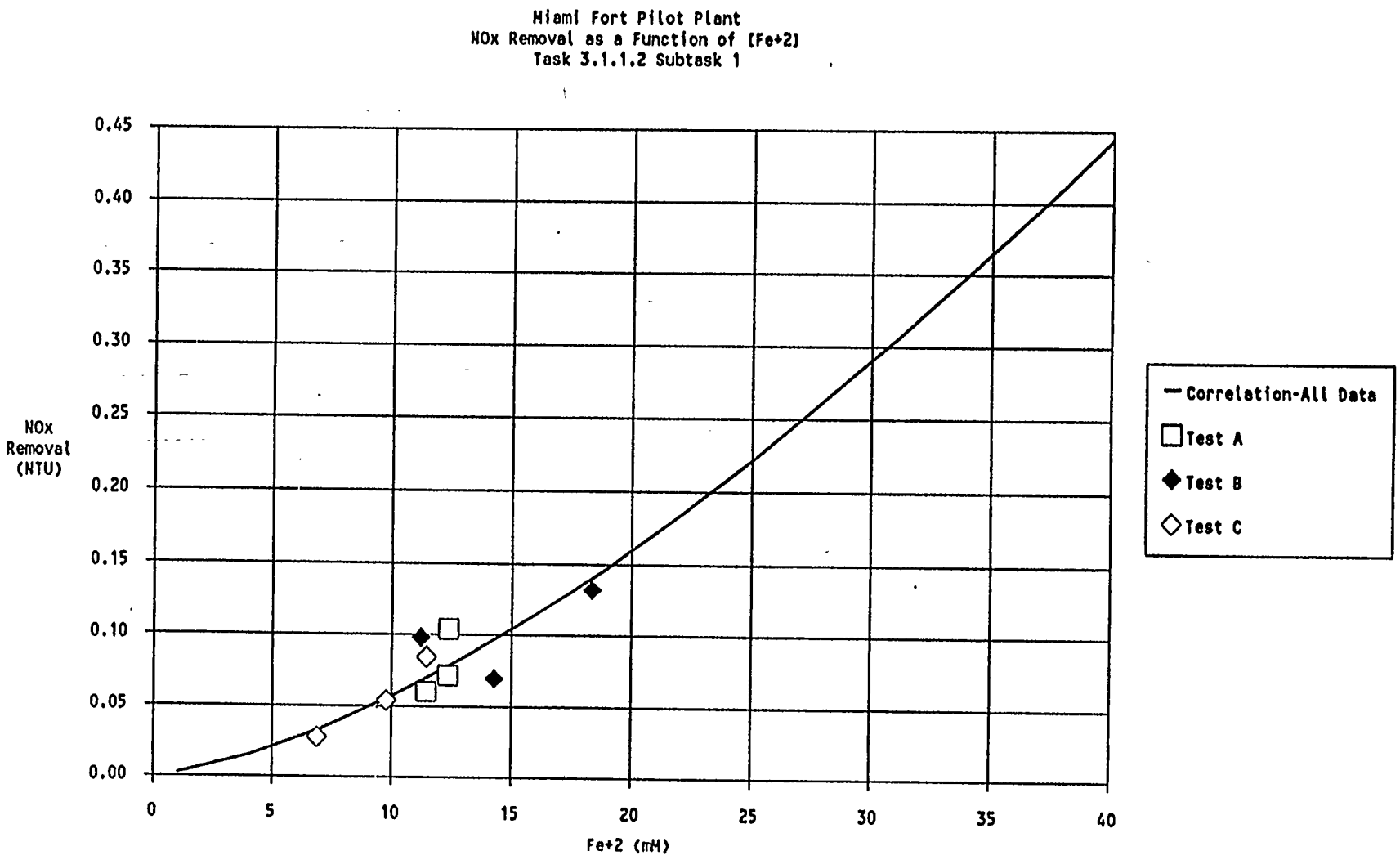

Figure 2

FIGURE 3

Miami Fort Pilot Plant
Complex Retrofit/New Plant NOx Removal Testing
3.1.1.2 Transfer Unit Tests

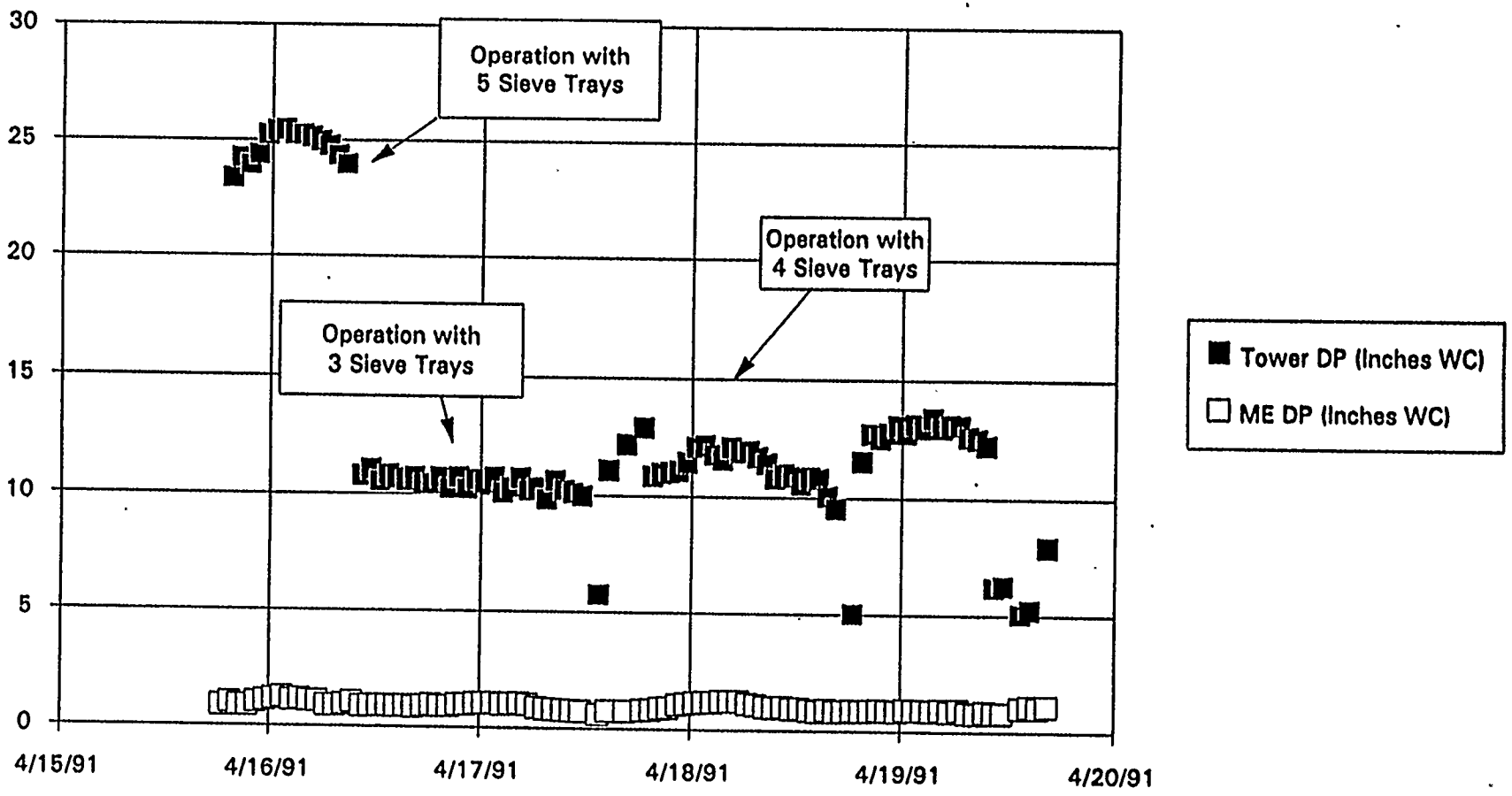

Figure 3

Figure 4

Single Tray Pressure Drop Characterization

Nozzle Configuration:
Quench Nozzle: Bete 1-56FCN
R2&R3 Nozzles: Bete 1-MP1125M
TRAY POSITION #2

Operating Conditions:
10 fps, 6.5 pH
12 - 18 mM Fe+2
M.E. Wash On

Test	R2 GPM	R3 GPM	Total GPM	Tray Open Area Absorber DP (in. WC) 20%	25%	30%	40%
A	0	0	0	2.8	1.8	1.3	1.0
B	50	0	50	6.2	3.2	2.0	1.7
C	100	0	100	14.4	4.1	2.6	2.1
D	100	50	150		12.3	3.6	2.6
E	100	100	200			6.8	3.3
F	125	125	250			8.0	4.0
G	135	128	263			10.9	4.4

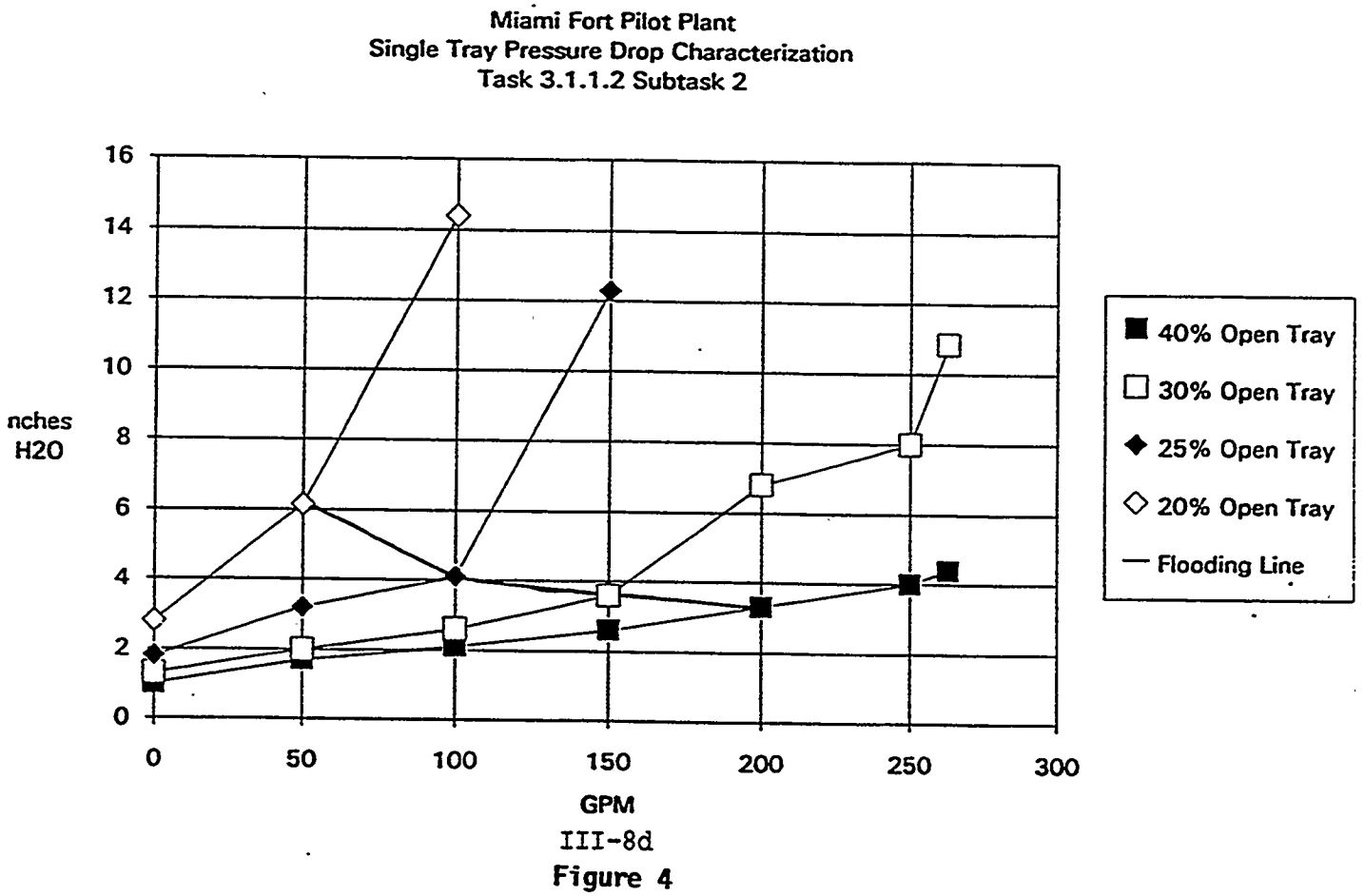

Figure 4

FIGURE 5

Miami Fort Pilot Plant
Task 3.1.1.2 Subtask 2
Ferrous Oxidation Rate Study
4/30/91

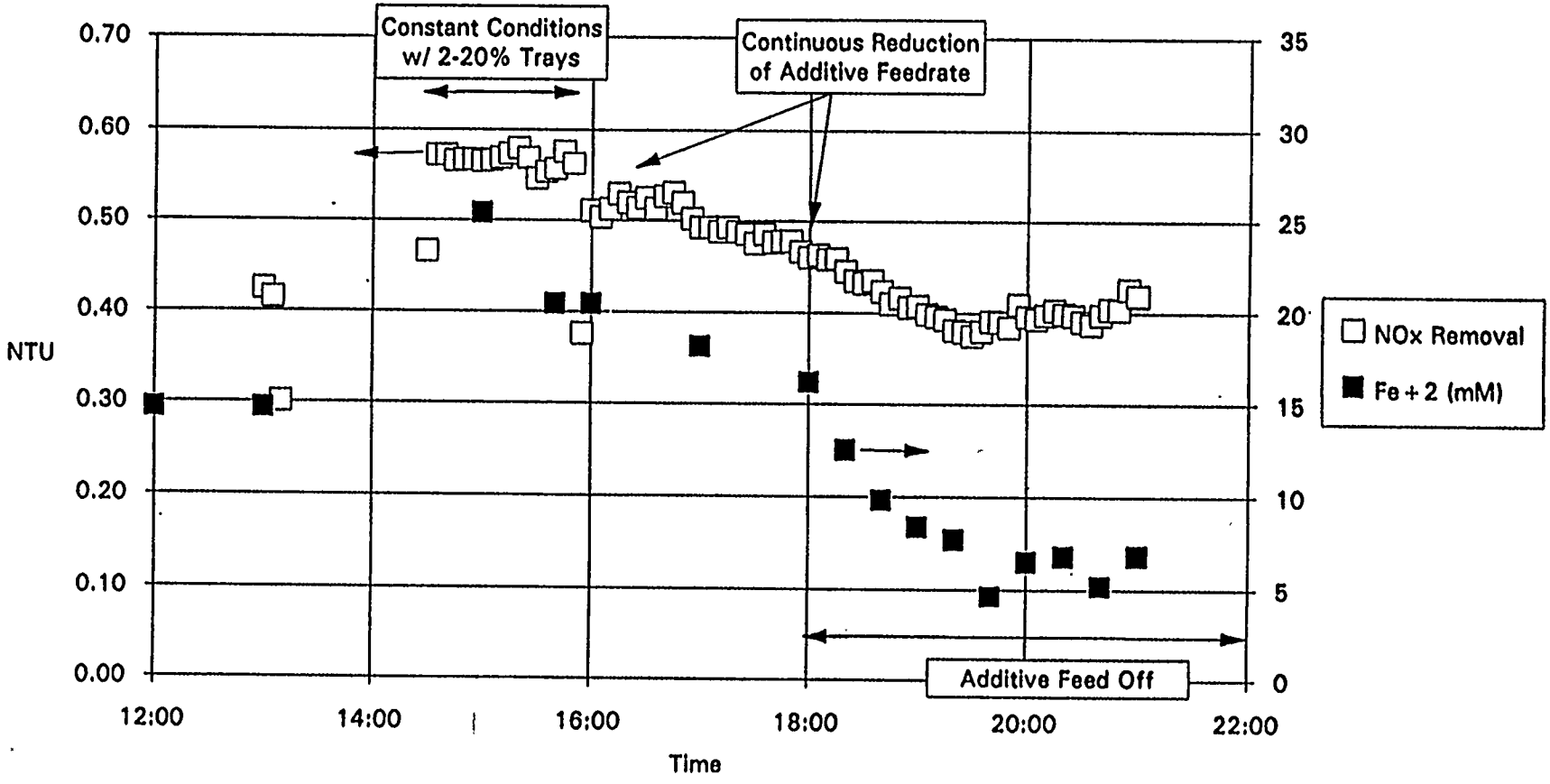

Figure 5

Figure 5

FIGURE 6

Miami Fort Pilot Plant

Complex Retrofit/New Plant NOx Removal Testing; Continued

3.1.1.2 Transfer Unit Tests

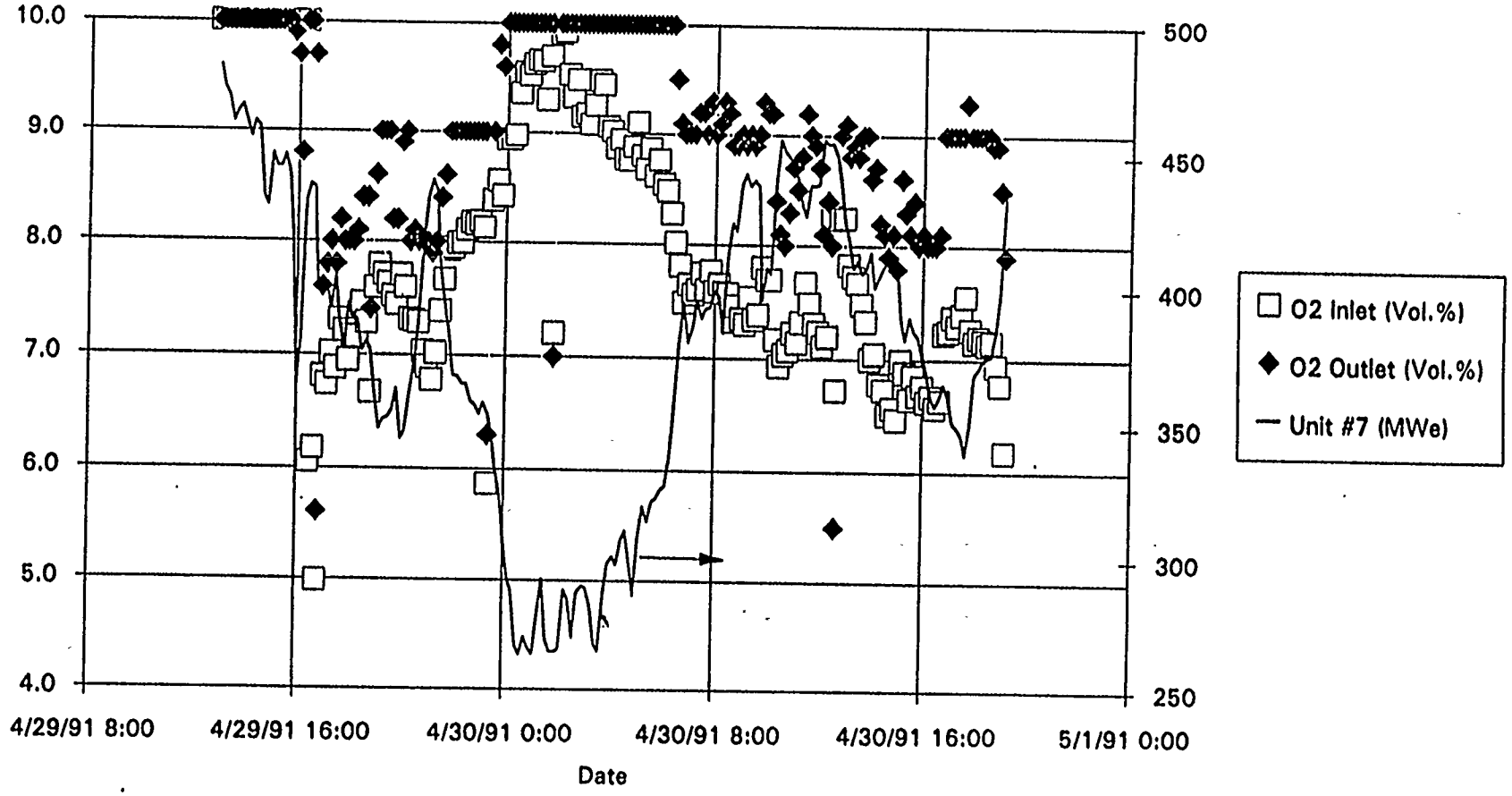

Figure 6

Figure 6

Summary of Regression Analysis of NOx Removal and Inlet O2 and NOx

	NOx NTU =f(O2)		
	m1=02%	b=Const.	
	0.0012	0.1795	
Std. err. Coef.	0.0043	0.0374	Std. err. Coef.
r^2	0.00	0.04	Std. Err. of Y Est.
F	0.08	62	d.f.
SSreg.	0.00	0.12	SSresid.

	NOx NTU =f(NOx In)		
	m1=Inlet NOx	b = Const.	
	-0.0001	0.2329	
Std. err. Coef.	0.0001	0.0399	Std. err. Coef.
r^2	0.02	0.04	Std. Err. of Y Est.
F	1.19	62	d.f.
SSreg.	0.00	0.12	SSresid.

Figure 7

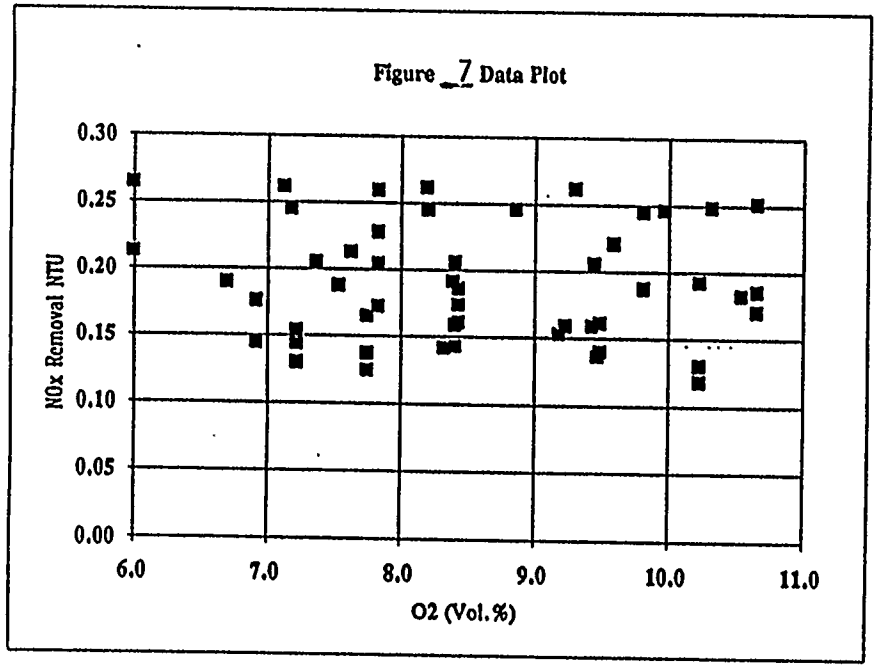

Figure 7

Figure 8

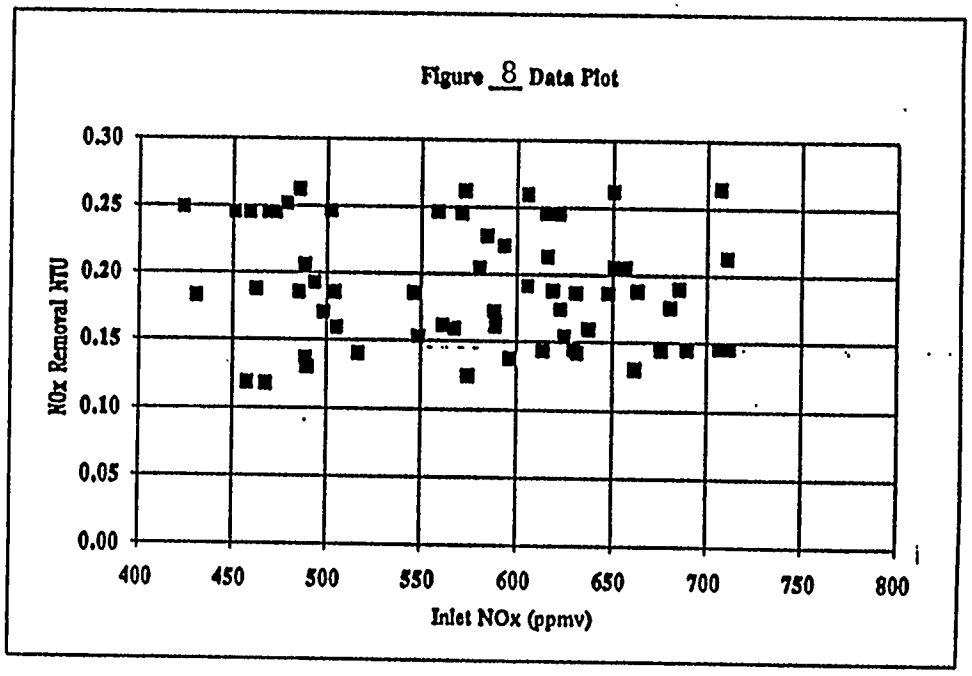

Figure 8

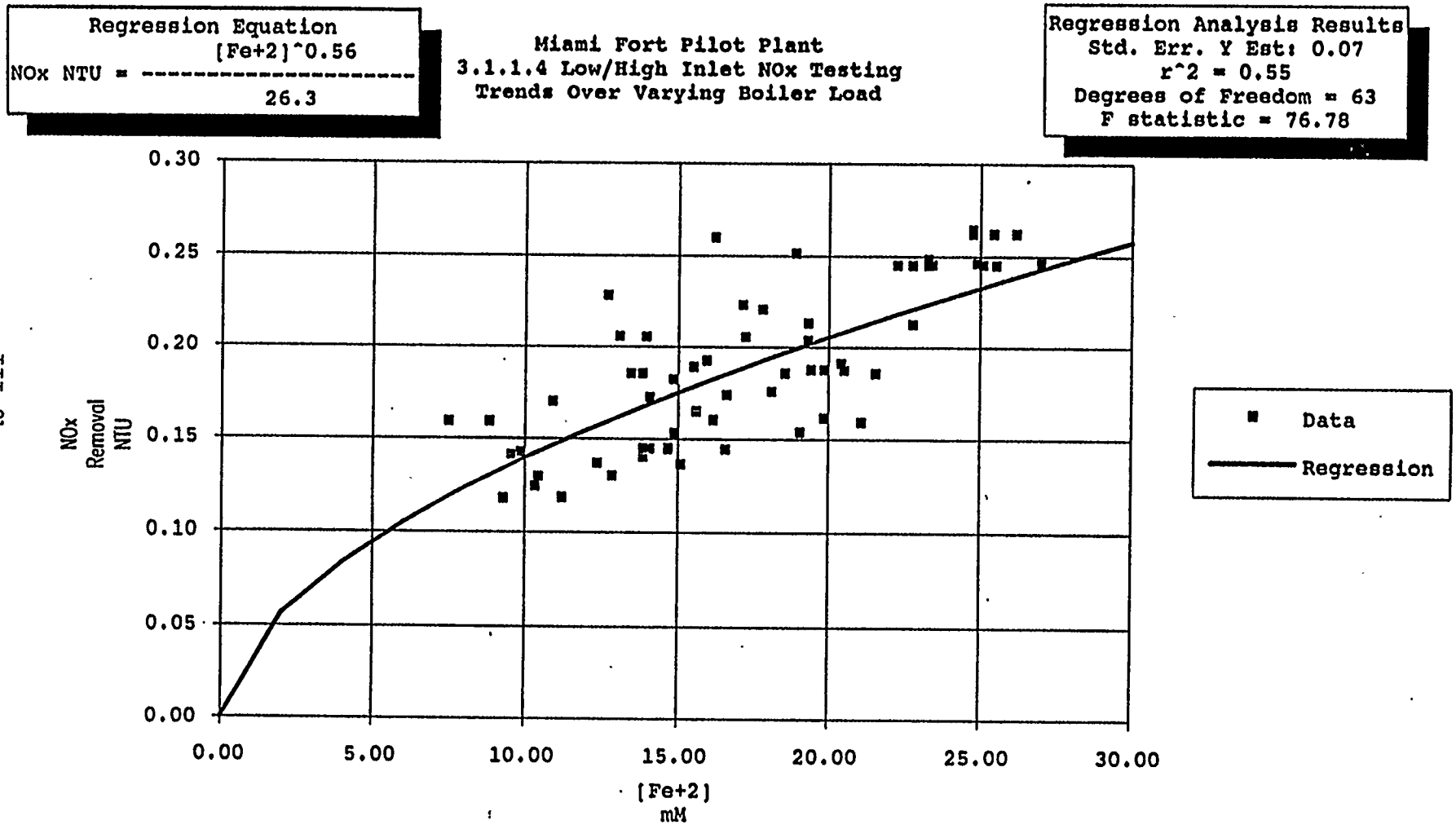
Regression Equation
NOx NTU = [Fe+2]^0.56 / 26.3
Miami Fort Pilot Plant
3.1.1.4 Low/High Inlet NOx Testing
Trends Over Varying Boiler Load
Regression Analysis Results
Std. Err. Y Est: 0.07
r^2 = 0.55
Degrees of Freedom = 63
F statistic = 76.78
NOx Removal NTU
0.30
0.25
0.20
0.15
0.10
0.05
0.00
0.00
5.00
10.00
15.00
20.00
25.00
30.00
[Fe+2] mM
Data
Regression

Figure 9

Miami Fort Pilot Plant

3.1.1.5 Alternative Antioxidant/Reducing Agent Testing

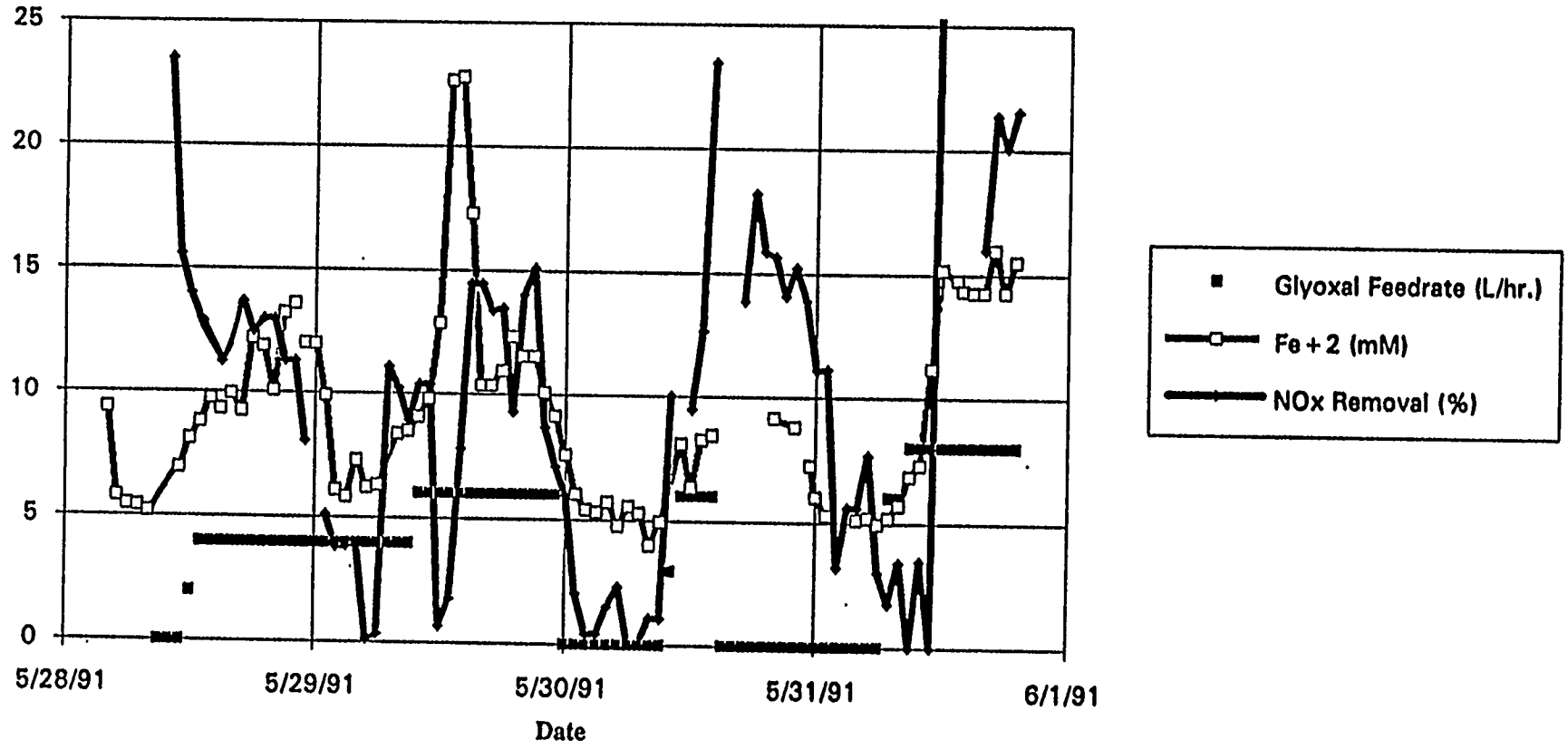

Figure 10

Figure 10

Figure 11

Solids Settling & Filtration Results Summary

Date	Maximum Thickened Solids Conc. (~23 hrs) (wt. %)	Expected TUF Concentration w/unit area of 20 ft2/tpd (wt. %)	Actual Thickener Solids Conc. (wt. %)	Lab Filter Cake Solids (wt. %)	Actual Filter Cake Solids (wt. %)	Comments
4/2/91	33.7	22.6		44.9		1) All actual pilot plant
4/4/91	32.0	19.9	22.8	40.7		data reflect the highest
4/5/91	32.1	23.6	29.3	42.4		values recorded that day.
4/8/91	32.6	17.4	36.4	43.3	45.5	
4/9/91	47.2	38.9	38.8	55.8	45.5	2) Excluded are initial
4/10/91	52.6	46.2	54.8	61.3	52.0	readings of thickener
4/11/91	46.4	37.1	37.9	55.9	54.0	underflow solids after
4/12/91	53.1	50.7	55.6	63.2		restart.
4/15/91					59.5	
4/16/91	55.4	52.0	62.8	65.9	59.3	
4/17/91	57.3	52.0	60.3	65.5		
4/18/91	55.7	52.4	55.7	64.9	67.1	
4/19/91	57.5	56.2	58.7	65.4		
4/22/91					67.5	
4/23/91	58.4	52.5	56.9	66.7		
4/24/91	58.3	52.9	58.3	65.9		
4/25/91	58.4	53.7	61.0	68.7		
4/26/91	69.0	55.4	56.2	65.1	70.5	
4/29/91	57.2	53.6	60.1	64.8		
4/30/91	78.7	73.8	60.9	66.2		
5/1/91					65.6	
5/3/91	63.7	58.2	62.5	68.5		
5/6/91	56.1	51.6	57.3	64.8		
5/7/91	64.3	53.2	58.7	63.1	68.8	
5/8/91	58.1	56.2	60.0	64.1		
5/9/91	60.8	53.2	60.1	64.7		
5/10/91	55.2	52.4	57.6	64.3	70.4	
5/13/91			56.2			
5/14/91	58.0	55.8	61.8	65.5		
5/15/91	58.2	57.2	61.1	66.0	68.9	
5/16/91	56.3	53.5	60.0	66.2		
5/17/91	58.9	55.2	62.0	67.4		
5/20/91	60.9	53.7	64.3	67.8	70.2	
5/21/91	61.4	60.6	64.1	68.7		
5/22/91	63.6	59.5	63.3	67.7		
5/23/91	62.2	57.2	63.4	68.7	72.6	
5/24/91	57.9	57.0	63.2	65.1		
5/28/91	64.1	56.6	62.7	68.5	67.7	
5/29/91	59.3	55.2	62.2	67.0		
5/30/91	61.6	56.9	62.4	67.5		
5/31/91	60.8	55.3	56.0	64.7		

Figure 11
Miami Fort Pilot Plant
Solids Settling & Filtration Data

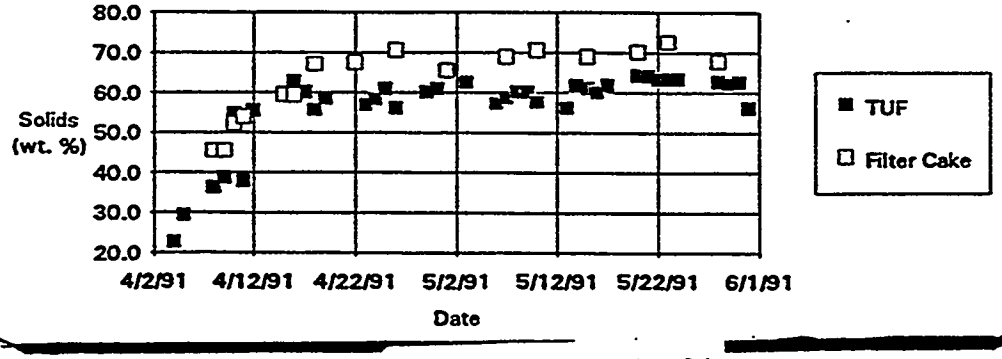

Figure 11

TABLE 1

Summary of NOx Removal Tests Correlations

Date	EDTA	Tot. Fe (mM)	Fe+2 (mM)	SO2 NTU	NOx NTU	Log(NOx Rem.)	Log(Fe+2)	Comments
4/11/91 16:15		32.81	12.38	2.83	0.10	-0.98	1.09	Test A
4/11/91 18:15			12.34	2.62	0.07	-1.14	1.09	L/G=41; SMD=2698 microns
4/11/91 20:15	29.85	32.1	11.45	2.61	0.06	-1.22	1.06	
4/11/91 20:15	29.85	32.1	11.45	4.64	0.08	-1.07	1.06	Test C
4/11/91 22:15			9.77	4.45	0.05	-1.27	0.99	L/G=64; SMD=1717 microns
4/12/91 0:15		32.81	6.88	4.69	0.03	-1.56	0.84	
4/12/91 2:15			11.2	3.39	0.10	-1.01	1.05	Test B
4/12/91 4:15	33.95	31.05	14.27	3.35	0.07	-1.16	1.15	L/G=51; SMD=2041 microns
4/12/91 6:15			18.31	3.20	0.13	-0.88	1.26	

Regression Output:	Test A
Constant	-6.36
Std Err of Y Est	0.11
R Squared	0.59
No. of Observations	3
Degrees of Freedom	1
X Coefficient(s)	4.85
Std Err of Coef.	4.02

Regression Output:	Test C
Constant	-3.36
Std Err of Y Est	0.03
R Squared	0.99
No. of Observations	3
Degrees of Freedom	1
X Coefficient(s)	2.14
Std Err of Coef.	0.21

Regression Output:	Tests A, B, &C
Constant	-2.72
Std Err of Y Est	0.11
R Squared	0.75
No. of Observations	9
Degrees of Freedom	7
X Coefficient(s)	1.47
Std Err of Coef.	0.33

Regression Output:	Test B
Constant	-1.73
Std Err of Y Est	0.17
R Squared	0.23
No. of Observations	3
Degrees of Freedom	1
X Coefficient(s)	0.62
Std Err of Coef.	1.14

Table 1

Table 1

B. PHASE II SUMMARY OF TESTING

This section summarizes the results of testing performed in Phase II of the project, "Enhanced NOx Removal in Wet Scrubbers Using Metal Chelates". Each task's testing will be briefly reviewed with emphasis placed on the purpose of testing, measures of success, results of testing including any unexpected data or problems encountered, and an interpretation of the result of each task's tests. Tables and graphs are included where necessary. An effort was made to generate testing data to support the liquid-film limited, pseudo-first order absorption rate NO removal model previously discussed in the Phase I Summary of Testing and having the following form:

$$\text{NO Removal (NTU)} = \frac{(k_2 \cdot [Fe^{++}]\ D_{NO})^{1/2}}{H/P_T} \quad \frac{a\ Z}{p_M\ v}$$

All testing was performed under test series 3.1.2, "Testing of Ferrous EDTA with Glyoxal Additive and Characterization of Complex Retrofit/New Plant NO Absorber Configurations."

TESTING PERFORMED:

TASK 3.1.2.1: Start-up of Testing:

Purpose of Test: Establish absorber liquid chemistry from service water. Add magnesium hydroxide to establish magnesium enhanced FGD chemistry and ferrous EDTA to establish baseline ferrous iron levels to promote NOx removal.

Measures of Success: Determine baseline NOx removal obtained without addition of reducing agents or antioxidants.

Results of Tests: All liquor remaining from Phase I testing was flushed from the system to eliminate residual sodium and provide a better evaluation of glyoxal. The scrubber configuration consisted of 20% open trays at the T2 and T5 locations and a quench flow of 50 GPM utilizing a Bete TF 56 XPN nozzle. Initial operating conditions were flue gas velocity (FGV) of 8 fps and a liquid recycle rate maintained at 120 GPM through one Bete MP 1125 nozzle at the R3

location to provide a liquid to gas ratio (L/G) of 63. (L/G expressed as GPM liquid per 1000 acfm gas flow.) The SO_2 injection system was used to maintain SO_2 concentration at 2500 ppmv. The chelate additives and magnesium hydroxide were batch fed into the system to bring the chemistry rapidly to the desired levels. Glyoxal was not added during this start-up period.

At the steady operating conditions outlined above and without the addition of reducing agents/antioxidants, ferrous concentration reached equilibrium in the 2 to 3 mM range, resulting in NOx removals of 7% to 9%.

Interpretation: Batch feeding magnesium hydroxide and ferrous chelate to the absorber solution to accelerate building process chemistry was proved. Ferrous iron levels and NOx removal were typical for this regime.

TASK 3.1.2.2: Addition of Glyoxal as Reducing Agent/Antioxidant

Purpose of Test: Determine the efficiency and cost effectiveness of glyoxal as an iron reducing/antioxidant agent. Observe the long term effects of glyoxal addition on absorber operation and scrubber liquor chemistry.

Measures of Success: Successful maintenance of ferrous EDTA concentration in the 10 mM to 20 mM range.

Results of Test: The addition of glyoxal was according to a predetermined schedule based upon boiler load and flue gas oxygen content. Glyoxal additions were typically 8 liters per hour from 0800 hours to 2300 hours and 10 liters per hour from 2300 hours to 0800 hours. Initial indications of lower than anticipated NOx removals and scrubber pressure drop prompted the replacement of the one nozzle configuration with two Bete MP 1125 nozzles at the R3A and R3B positions. This duplicated the configuration found in Phase I (See Figure 1). The use of glyoxal as reducing agent in the above configuration resulted in ferrous iron concentrations for the most part in the 15 mM to 25 mM range and NOx removals in the .04 to .18 NTU range (4% to 18% removal range) with typical NOx removal being 12% (See Figure 2). Two unanticipated effects were noted with glyoxal addition. The first effect was a definite "lag time" between

initial glyoxal addition and the elevation of ferrous iron concentrations (FIC) (See Figure 3) which was previously noted during Phase I testing with glyoxal. The second effect was the sudden and unabated rise in calcium concentrations in the scrubber liquor during the time of glyoxal addition (See Figure 4). These levels, approaching 6000 ppm, were highly unusual for a Thiosorbic FGD process and were cause for alarm because of the scaling potential of such calcium levels. Since magnesium levels were in the normal range of 6000-8000 ppm, it was surmised that the calcium could only be going into solution to balance an excess negative charge. In order to moderate the increase in calcium concentration it was necessary to add magnesium hydroxide to the system to suppress the calcium concentration and balance the excess anionic charge.

Interpretation: Both observed effects, "lag time" in ferrous level increase and the sudden elevation of calcium concentration, can be explained by the formation in the scrubber solution of a bisulfite addition product (BSAP) with glyoxal addition. The chemical literature reveals that bisulfite reacts via a reversible nucleophilic addition to most aldehydes to form negatively charged bisulfite addition products.

It appears that the glyoxal reacts preferentially with bisulfite rather than with ferric EDTA so that until the addition reaction reaches equilibrium not enough glyoxal is available for the reduction of ferric EDTA to ferrous EDTA to proceed in the expected manner. The observed "lag time" is this period leading up to the BSAP reaction equilibrium. Moreover, in order to satisfy this equilibrium requirement, continued addition of glyoxal leads to a constantly increasing anionic BSAP level.

This in turn leads to increasing calcium levels to maintain charge balance in the system. In addition, the binding of the sulfite and glyoxal likely inhibited the sulfite from "cleaving" the NO off the ferrous-EDTA-NO adduct which contributed to lower NOx removals for any particular ferrous concentration than was observed in Phase I. Refer to the attached report on the effects of glyoxal addition for a more detailed explanation of the BSAP hypothesis. The proposed formation of the BSAP seriously compromises the use of glyoxal in this application at this time.

TASK 3.1.2.3: Study of Effect of pH on NOx Removal:

Purpose of Tests: Determine the effect of absorber liquor pH on NOx removal and ferrous iron concentration. Tests to be conducted at pH levels of 5.5, 6.5, and 7.5 to determine if any trend exists.

Measures of Success: Determine the effect of the three pH levels (5.5, 6.5, 7.5) on NOx removal and on ferrous iron concentration.

Results of Tests: Glyoxal continued to be used as the reducing/antioxidant agent. The absorber tower configuration consisted of two 20% trays in the #2 and #5 positions with Bete 1125 M nozzles installed on recycle headers R3A and R3B (See Figure 1). Operating conditions were flue gas velocity of 8 fps and L/G of 65. The inlet SO_2 concentration was maintained at 2500 ppmv with the SO_2 injection system. NOx removal data was not complete during this task due to analyzer problems. Magnesium hydroxide additions to the system were continued in an effort to suppress the elevated calcium levels.

Ferrous iron concentration must be utilized to determine the effects of pH because of the NOx analyzers' failure. The pH testing is nicely summarized in Figure 5. The pH was increased from the usual operation level of 6.5 to 7.5 and then glyoxal feed was initiated. A relatively stable ferrous concentration (10-15 mM) was maintained with constant glyoxal addition at pH = 7.5. The pH was then allowed to drop to the 5.5 level. The ferrous concentration began to drop to the 5 mM level during the latter half of the pH = 5.5 phase. Before returning the pH to the usual operating level of 6.5 pH, glyoxal feed was suspended. In spite of the glyoxal feed termination the ferrous concentration rose dramatically, peaking near 30 mM and remaining over 12 mM for fifteen hours after glyoxal feed had been suspended. Sampling of N_2O was conducted at the pH 5.5 and 7.5 levels and no detectable amounts of N_2O were found at these pH levels just as no significant levels were ever detected at the normal operating pH of 6.5. Lower total iron levels were noted at the pH 7.5 level possibly due to ferric hydroxide precipitation.

Interpretation: No such dramatic trend had been envisioned when these pH tests were planned. Once again the unique reaction of the glyoxal and bisulfite ion dominated the picture. Sulfite ion and bisulfite ion are maintained in equilibrium by the presence of hydrogen ion. Bisulfite dominates at low pH whereas sulfite pre-dominates at higher pH because of the relative scarcity of hydrogen ion. At pH = 5.5, the higher level of bisulfite increased the formation of the BSAP and in effect tied up more glyoxal in the complex leaving it unavailable for ferric EDTA reduction. Conversely, when increasing the pH, the bisulfite concentration decreased and the BSAP equilibrium reaction caused the glyoxal to be "freed" from the complex and thus become available for ferric EDTA reduction. The effective use of glyoxal for ferric-EDTA reduction may thus be limited to relatively high pH conditions where sulfite predominates the sulfite/bisulfite equilibrium.

TASK 3.1.2.4: Fine Spray Tests:

Purpose of Tests: Conduct tests using spiral type nozzles to produce a finer spray thus increasing gas-liquid interfacial area which the NOx removal model suggests should increase NOx removal. Use seven spiral nozzles at two or three spray levels to further increase surface area. Vary flue gas velocity for the tests.

Measures of Success: Increased NOx removal at lower gas velocity and increased NOx removal at higher L/G.

Results of Tests: Glyoxal use as reducing agent was discontinued due to the problems related previously. A mixture of sodium dithionite and ascorbic acid (250#/55#) was utilized for this purpose as was done in Phase I. The absorber tower configuration consisted of a single 40% open tray in the #1 position and seven Bete TF 28 XPN nozzles on recycle headers #2 and #3 (See Figure 6). A test matrix consisting of three flue gas velocities and two liquid recycle rates was conducted and the test results are summarized in Table 1.

Interpretation: Increasing flue gas velocity while maintaining a constant recycle liquid rate decreased NOx removal while decreasing velocity increased NOx removal. With one exception, increasing L/G increased NOx removal. This is consistent with the premise of the model due to increased interfacial surface area and was the expected behavior of the system. The slope of the L/G vs NOx removal line decreases with increasing L/G suggesting that decreasing utilization of additional liquor for NOx removal occurred. It is most likely that this is due to "wall-wetting" effects on the relatively small 3′ diameter pilot plant tower.

TASK 3.1.2.5: Study of Effect of Saddle Packing on NOx Removal:

Purpose of Tests: Investigate the effects of packing in the NOx removal process. Unlike perforated trays, packing has a more clearly defined height of contact zone and the interfacial area, physical area, and mass transfer coefficients are well known and controllable. These factors enable data generated to be easily fitted into the NOx removal model for verification purposes. NOx removal to be determined using 6 feet of 2" plastic Norton Intalox saddles. If absorber gas pressure drop is excessive, 3" plastic Norton Intalox saddles will be used.

Measures of Success: Increased NOx removal compared to tray configurations, especially at lower gas velocities.

Results of Tests: Both the 2" and 3" packing were tested. The absorber tower configuration consisted of 6 feet of packing with seven Bete TF 28 XPN nozzles installed on recycle header #3 and on recycle header #4 there were seven Bete TF 40 XPN nozzles (See Figure 7). A test matrix, consisting of various flue gas velocities and total liquid recycle rates was conducted. Table 2 summarizes the results of the 3" packing tests and Table 3 summarizes the results of the 2" packing tests.

The data from the 3" saddle tests shows that increasing flue gas velocity while maintaining total recycle liquid rate increases NOx removal, which is the opposite of what was expected. The data from the 2" saddle tests shows that

decreasing flue gas velocity while maintaining total recycle liquid rate increases NOx removal as expected. Both data sets reveal that increasing L/G at constant velocity increases NOx removal which can be expected from the model.

Interpretation: Testing was intended to primarily focus on the 2" saddles with the 3" saddles to be used on a contingency basis if tower pressure drop (delta P) proved excessive with the 2" saddles. The delta P experienced with the 2" saddles proved to be 3-4 times higher than that assigned to it by the manufacturer and so the 3" saddles were installed.

When delta P also was much too high with the 3" saddles, concern was raised over the reliability of both the delta P and flue gas velocity (FGV) measurements. The tower differential pressure (DP) transmitter checked out fine. The DP transmitter on the inlet gas venturi responsible for FGV measurements had originally been spanned for 15 fps in the 4' tower. The low flue gas velocities utilized for NOx testing coupled with use of the 3' tower rendered the FGV measurements incorrect by a considerable factor. This was due to the fact that the DP transmitter readings were now on the very low end of the calibration curve (0"-2") where accuracy was poor. This caused the actual FGV readings to be higher than that recorded which in turn caused the pressure drop readings to be much higher than expected for the velocities measured. The inlet gas venturi DP transmitter was checked. Adjustments made included adjusting the zero reading which was off slightly, respanning the calibration curve to 0"-5", and making subsequent adjustments to the data acquisition system. The 2" saddles were reinserted into the scrubber. The pressure drops measured after these corrections for the 2" saddles were then in general agreement with the manufacturer's figures. The data generated for the 2" saddles is thus considered more reliable than that for the 3" saddles, although the trends seen for the 3" saddles are still considered valid.

Examination of the results of regression analyses performed for the packing tests reveals why a small upward drift in flue gas velocity measurement results in such an increase in tower pressure drop. Whereas pressure drop is usually proportional to air flow squared, the results summarized in Figure 8 reveal an even higher exponential factor associated with FGV when packing is installed in

the scrubber tower. Even with the DP transmitter adjustments described above, the results of pitot tube traverse measurements reveal that the actual flue gas velocity measurements are still higher than those recorded. This difference is again more pronounced at lower FGVs (less than 8 fps) where DP's are low (0"-1.5"). Velocity data were subsequently adjusted for this disparity to insure more reliable NOx removal correlations.

In order to explain the dissimilarity in trends for NOx removal for the two types of saddles it is necessary to once again examine the NOx removal model.

$$\text{NO Removal (NTU)} = \frac{(k_2\ [Fe^{++}]\ D_{NO})^{1/2}}{H/P_T} \quad \frac{a\ Z}{p_M\ v}$$

The parameters of interest here are a, the interfacial surface area, and v, the flue gas velocity. One reason for using packing in this project is that the surface area of a packing is considered to be independent of velocity. With this parameter held constant for any packing it is expected that at a constant ferrous iron concentration NOx removal should increase with a decrease in flue gas velocity. This was true for all packing tested except the 3" saddles. The only explanation feasible from the model is that for the 3" saddles the interfacial surface area increased with increasing velocity and thus NOx removal did likewise. Visual inspection of the packing through the tower window port supports this rationale. Inspection of the packing with 3" saddles installed revealed a liquid "rivulet" pattern flowing down through the packing in a relatively mild "non-turbulent" regime. Inspection of all other packing tested revealed a much more turbulent environment characterized by a "droplet" pattern. This suggests that sufficient wetting of the packing surface area occurred for the 2" saddles and the other packing to the extent that the interfacial surface area was independent of velocity. There was not, however, sufficient wetting of the smaller surface area of the 3" saddles for this to be the case. Consequently, increased velocity served to increase liquid holdup on the 3" saddles effectively increasing this packing's interfacial surface area. An increase in SO_2 removal with increasing velocity using the 3" saddles also supports the view that the surface area increased. Otherwise for a constant interfacial surface area SO_2 removal would be expected to decrease with increasing flue gas velocity since it is a gas film controlled process.

TASK 3.1.2.6: Study of Effect of Snowflake Packing on NOx Removal:

Purpose of Tests: Determine the effect on NOx removal of using Norton snowflake random packing. This is a new packing resembling a three dimensional snowflake that has a lower pressure drop and a greater mass transfer capacity than the two inch saddle packing, and has the potential to produce the highest NOx removals.

Measures of Success: Determine NOx removal with the snowflake packing and compare it with the removal obtained with 2" saddles.

Results of Tests: A test matrix consisting of various flue gas velocities and total liquid recycle rates was conducted using the snowflake packing. The results of these tests is summarized in Table 4.

As with the #2 saddles, NOx removal increased with decreasing flue gas velocity at a constant total recycle liquid rate. In like manner, increased L/G at a constant velocity increased NOx removal. The pressure drop across the snowflake packing was only about half that for the 2" saddles over all conditions. It did not appear that the snowflake packing greatly outperformed the #2 saddle packing as the NOx removal rates for the two packing were comparable.

Interpretation: Comparable NOx removal rates between the snowflake packing and the #2 saddles might be expected based upon their relatively similar dry surface areas (33 ft^2/ft^3 for the #2 saddles and 28 ft^2/ft^3 for the snowflake packing). It does appear that the #2 saddles slightly outperform the snowflake packing under similar L/G conditions. However the much lower pressure drop associated with snowflake packing translates into potentially higher L/G ratios and NOx removals with its use.

TASK 3.1.2.7: Study of Effect of PN Fill Packing on NOx Removal:

Purpose of Tests: Determine the effect on NOx removal using Munter's PN Fill packing. This structured packing is designed for installation in commercial FGD scrubbers, has a very open structure to avoid solids plugging, and exhibits a low pressure drop. Once again a packing bed depth of 6 feet was utilized.

Measures of Success: Determine NOx removal with the PN Fill packing and compare it to the results obtained with the other packing.

Results of Tests: A test matrix consisting of various flue gas velocities and total liquid recycle rates was conducted using the PN Fill packing. The results of these tests are summarized in Tables 5 & 6. These tests reveal a trend similar to the other packing tested of increasing NOx removal with decreasing flue gas velocity at a constant total recycle liquid rate. The trend of increased L/G resulting in increased NOx removal at constant flue gas velocity was also observed. The pressure drop across the bed of PN Fill was the lowest of all packing tested to date. For the most part NOx removals were comparable to the #2 saddles and the snowflake packing under similar conditions.

Interpretation: As with the preference for snowflake packing over #2 saddles because of a lower pressure drop at comparable NOx removal rates, so too PN Fill must be considered the most attractive packing choice because of its lowest pressure drop at similar NOx removal.

Task 3.1.2.3: Study of Effect of pH on NOx Removal:Revisited:

Purpose of Tests: To determine the effect of pH on NOx removal using sodium dithionite/ascorbic acid as reducing agent/anti-oxidant. The effect of pH on ferrous iron concentration and NOx removal was skewed by the use of glyoxal as detailed previously. Subsequently the pH tests were repeated at "standard" reducing conditions.

Measures of Success: Determine what effect change in pH has on NOx removal using sodium dithionite as reducing agent.

Results of Tests: Phase I configuration of single Bete MP 1125 nozzles at recycle headers R3A and R3B with two 20% open trays at the T2 and T5 levels was utilized for the pH testing. The results of this second set of pH testing are shown in Figures 9 and 10. No really significant difference was discernible in NOx removal at pH levels of 5.5, 6.5, and 7.5, nor was antioxidant feed rate moderated by higher pH.

Interpretation: The reaction of sulfite with the ferrous EDTA nitrosyl adduct, resulting in lower chemical reducing agent consumption, is believed to be more significant at higher pH. However, under the time constraints and conditions of these tests no such trend was seen.

However one interesting pattern did emerge. The sodium dithionite/ascorbic acid reducing agent/antioxidant mixture usage leveled out at a higher level of consumption at pH 7.5, even though the pH 5.5 test was carried out under higher oxygen conditions. This may be because ferric hydroxide formation at higher pH levels, decreases the total iron content available for reduction. This in turn requires higher reducing agent consumption to maintain desired ferrous iron levels. The effect of ferric hydroxide precipitation may well have overshadowed the sulfite-adduct reaction expected to decrease reducing agent consumption at higher pH.

TASK 3.1.2.4: Fine Spray Tests: Revisited:

Purpose of Tests: To determine what effect different spray nozzles have on NOx removal using sodium dithionite/ascorbic acid as reducing agent/antioxidant.

Measures of Success: Determine if a difference in NOx removal results occurs using different spray nozzles at similar operating conditions using sodium dithionite as reducing agent.

Results of Tests: The first series of fine spray tests used 7 Bete TF 28 XPN nozzles installed on recycle headers R3A and R3B. The second series used 5 Bete TF 40 XPN nozzles on headers R3A and R3B with the nozzles canted inward to minimize "wall-wetting". The results of this series of fine spray tests are summarized in Tables 7 & 8. The TF 28 XPN nozzles generally outperform the TF 40 XPN nozzles even at lower flow rates.

Interpretation: Finer spray nozzles appear to promote higher NOx removal. This is consistent with the model prediction of increased gas-liquid interfacial area being conducive to higher levels of NOx removal.

SUMMARY OF PHASE II TESTING:

Much progress was made toward verification of the NOx removal model during this phase of testing. Despite the setbacks encountered using glyoxal as reducing agent, NOx removal was shown to be roughly half-order with respect to ferrous iron concentration for any given set of scrubber conditions. The model predicts this should be the case regardless of the reducing agent employed. An exception would be in a case such as glyoxal wherein complexing of chemical species inhibits the normal reaction pathways. The data derived from testing fine sprays and various packings made possible the calculation of effective gas-liquid interfacial areas which were very close to the published data for the packing. As predicted, NOx removal was observed to be a function of flue gas velocity to the minus one power and was far less a function of liquid rate in comparison to flue gas velocity. Much greater confidence in the predictive capabilities of the model was gained. Instead of using NOx removal data empirically, the model can now be utilized for design purposes and emphasis will be placed in Phase III of the program on model confirmation and new plant design.

The dramatic improvement in belt filter cake solids dewatering during the NOx removal process continued in Phase II. Regardless of which reducing agent/antioxidant was used, solids content of the belt filter cake was consistently in the 65% to 70% range (See Figure 11). Normal thiosorbic filter cake solids typically average in the 35% to 45% range. This excellent dewaterability of the filter cake is one of the more pleasant and potentially significant outcomes of the project.

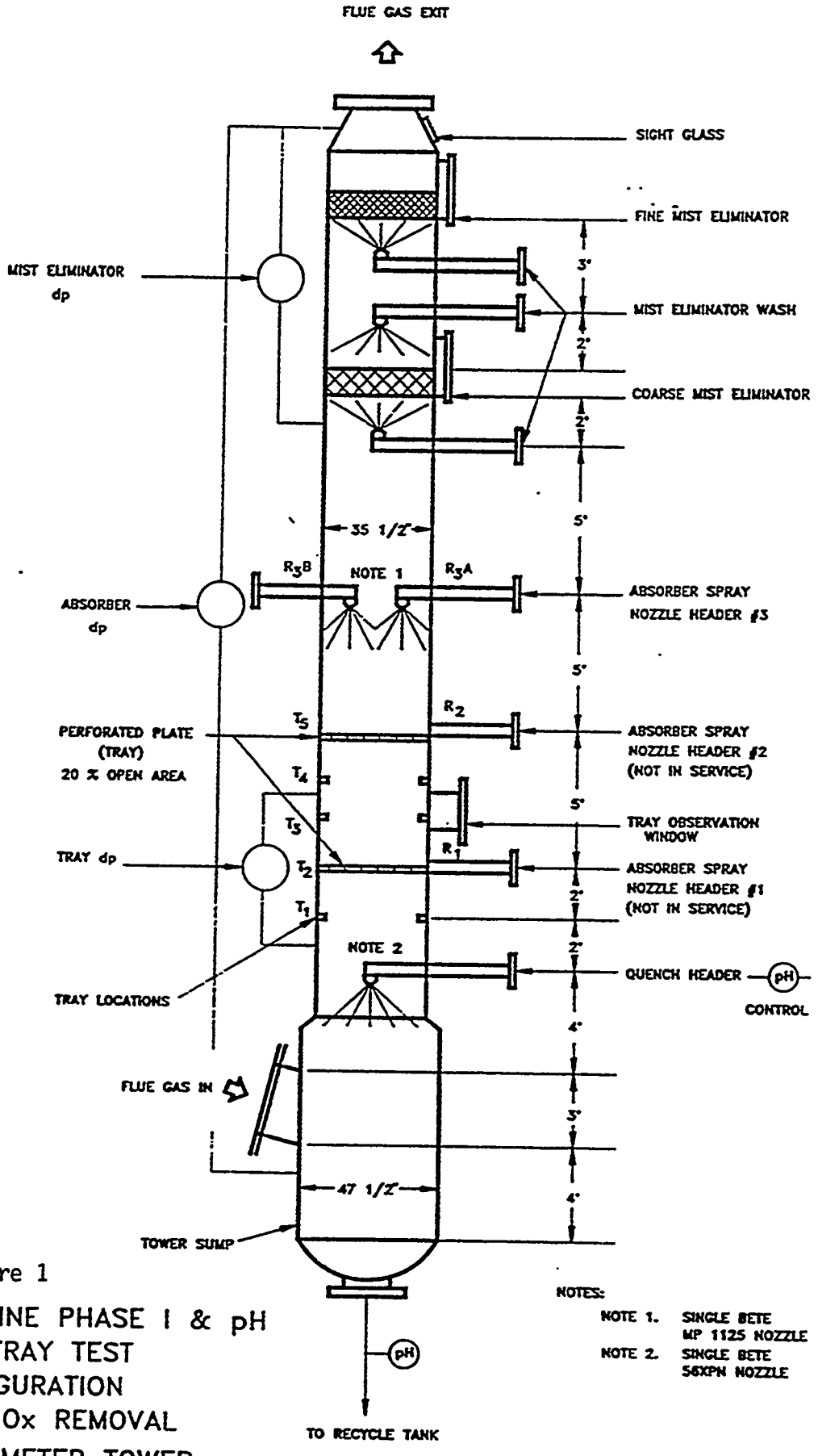

Figure 1

BASELINE PHASE I & pH
TWO TRAY TEST
CONFIGURATION
FOR NOx REMOVAL
3' DIAMETER TOWER

Figure 1

Figure 2

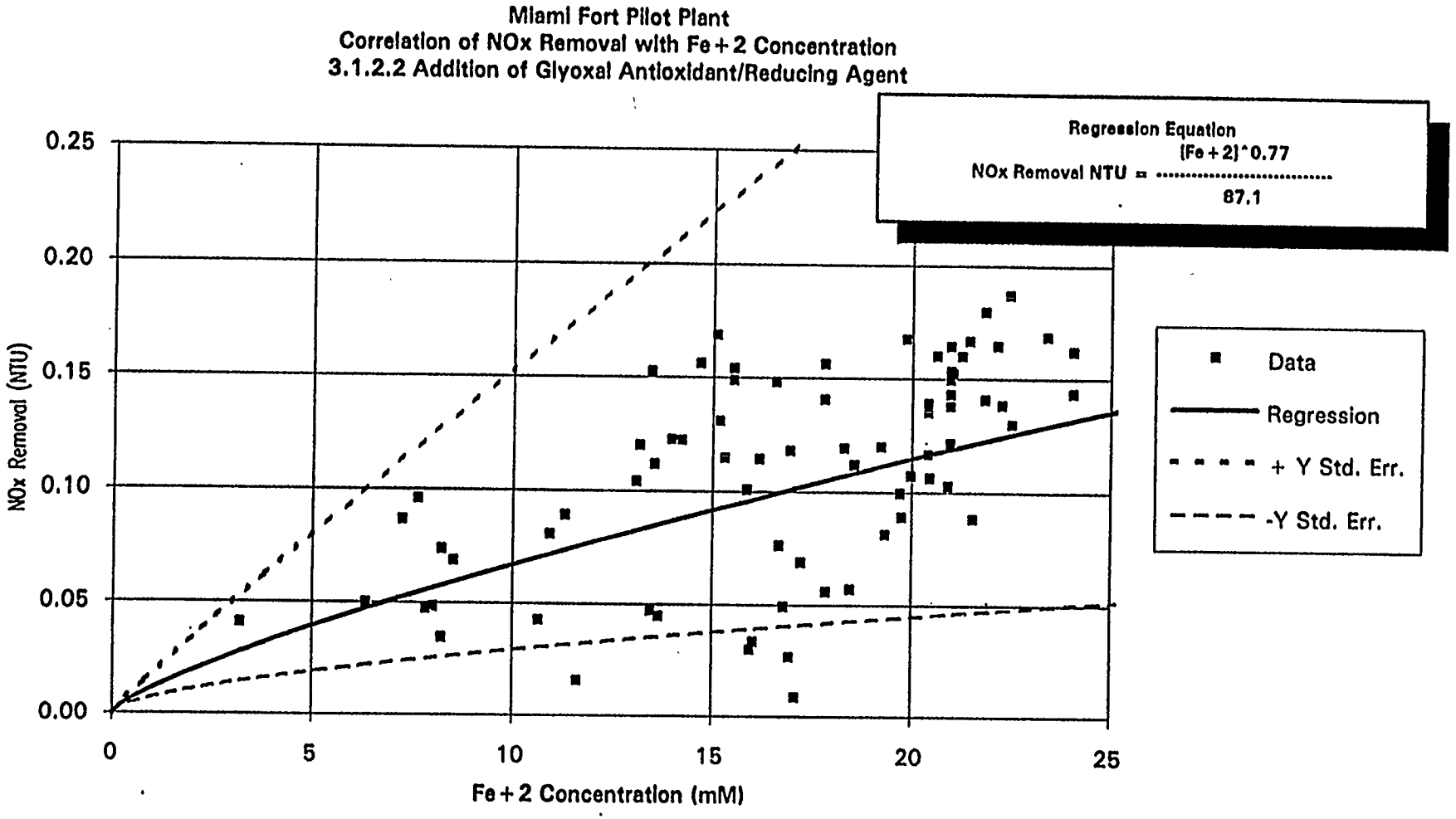

Figure 2

Figure 2

Figure 3

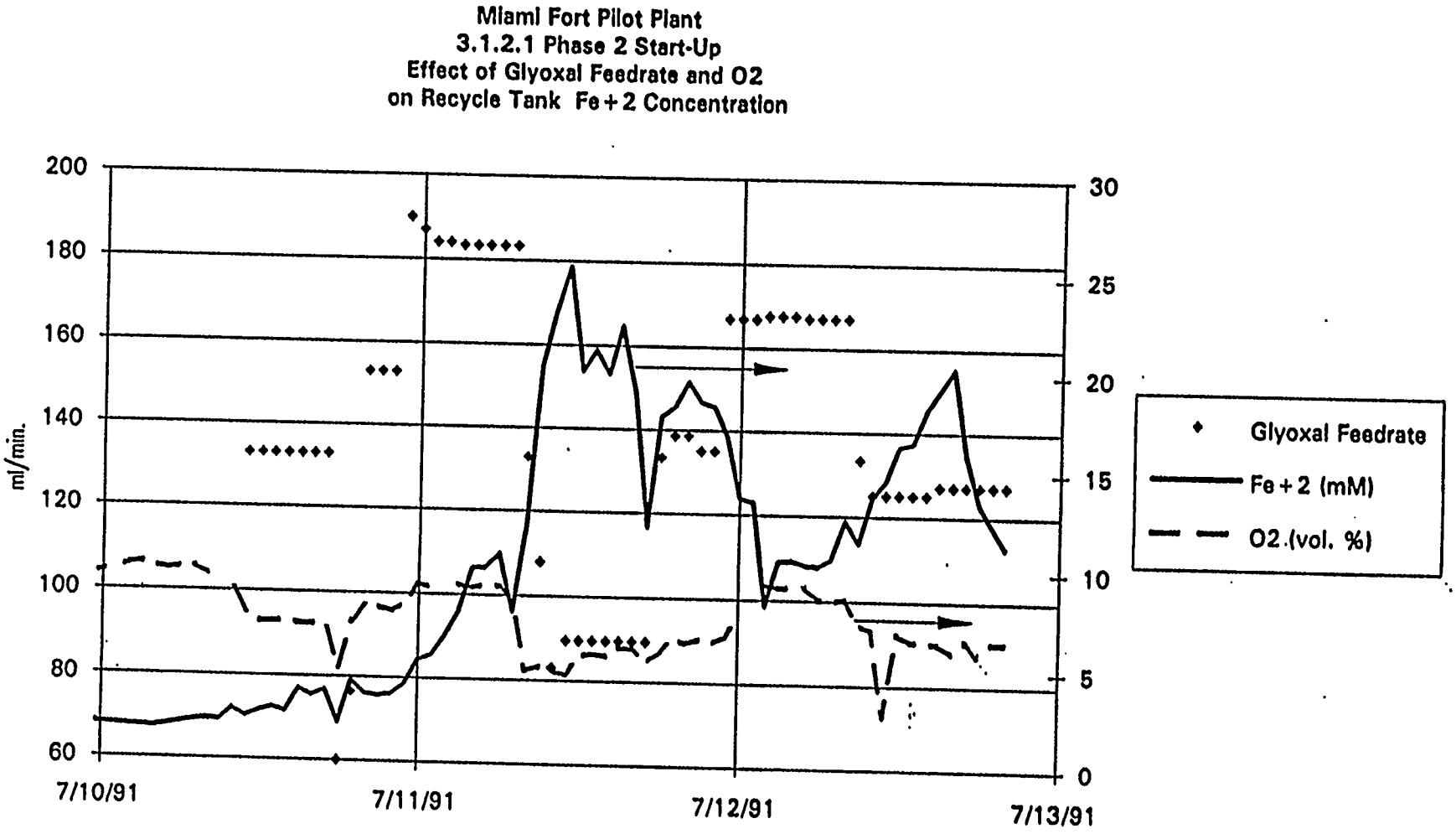

Figure 3

Figure 3

Figure 4

Miami Fort Pilot Plant
Task 3.1.2.2 Glyoxal Testing
Trend of S-N Compounds and Ca + 2

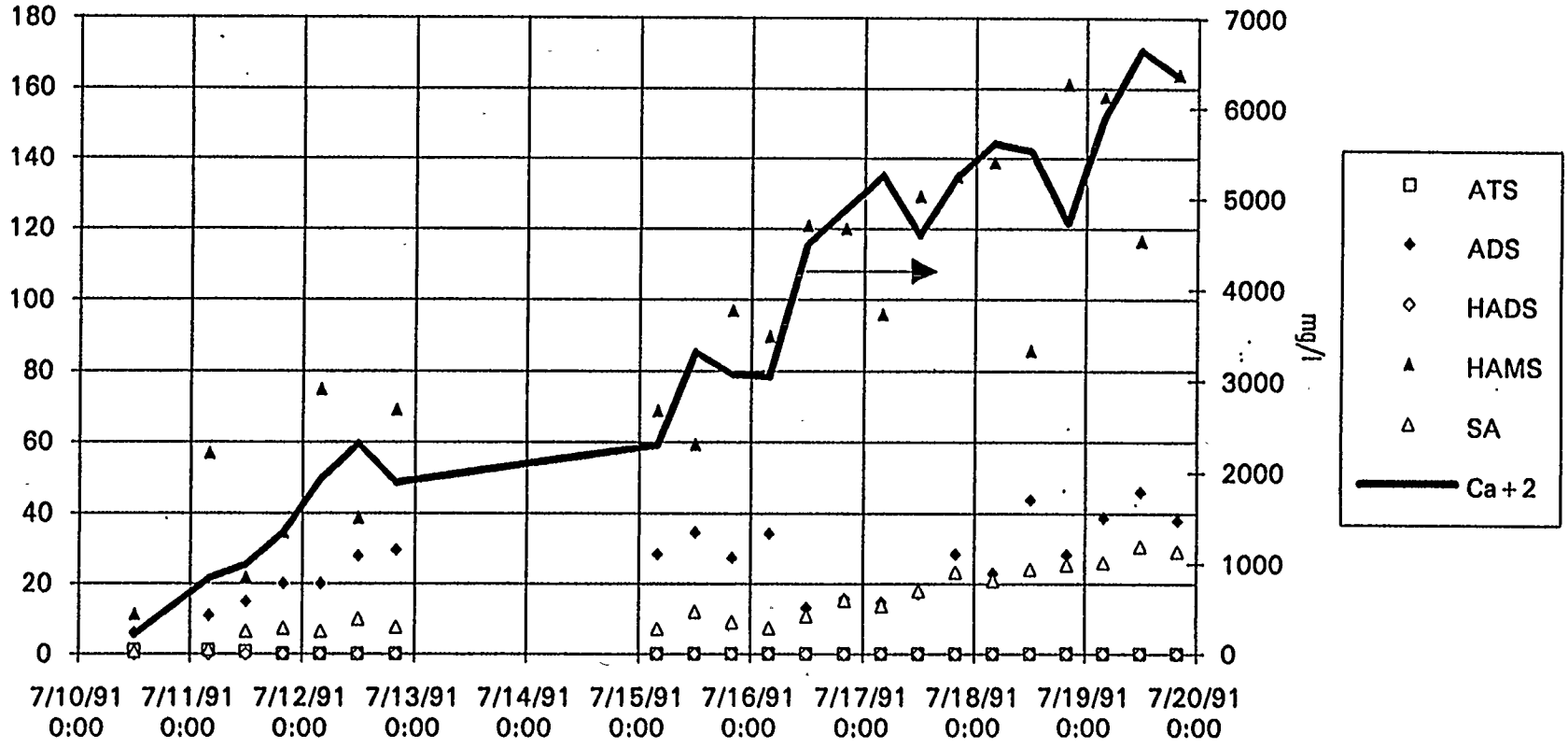

Figure 4

Figure 4

Figure 5

Miami Fort Pilot Plant
Task 3.1.2.3
Effect of pH on NOx Removal

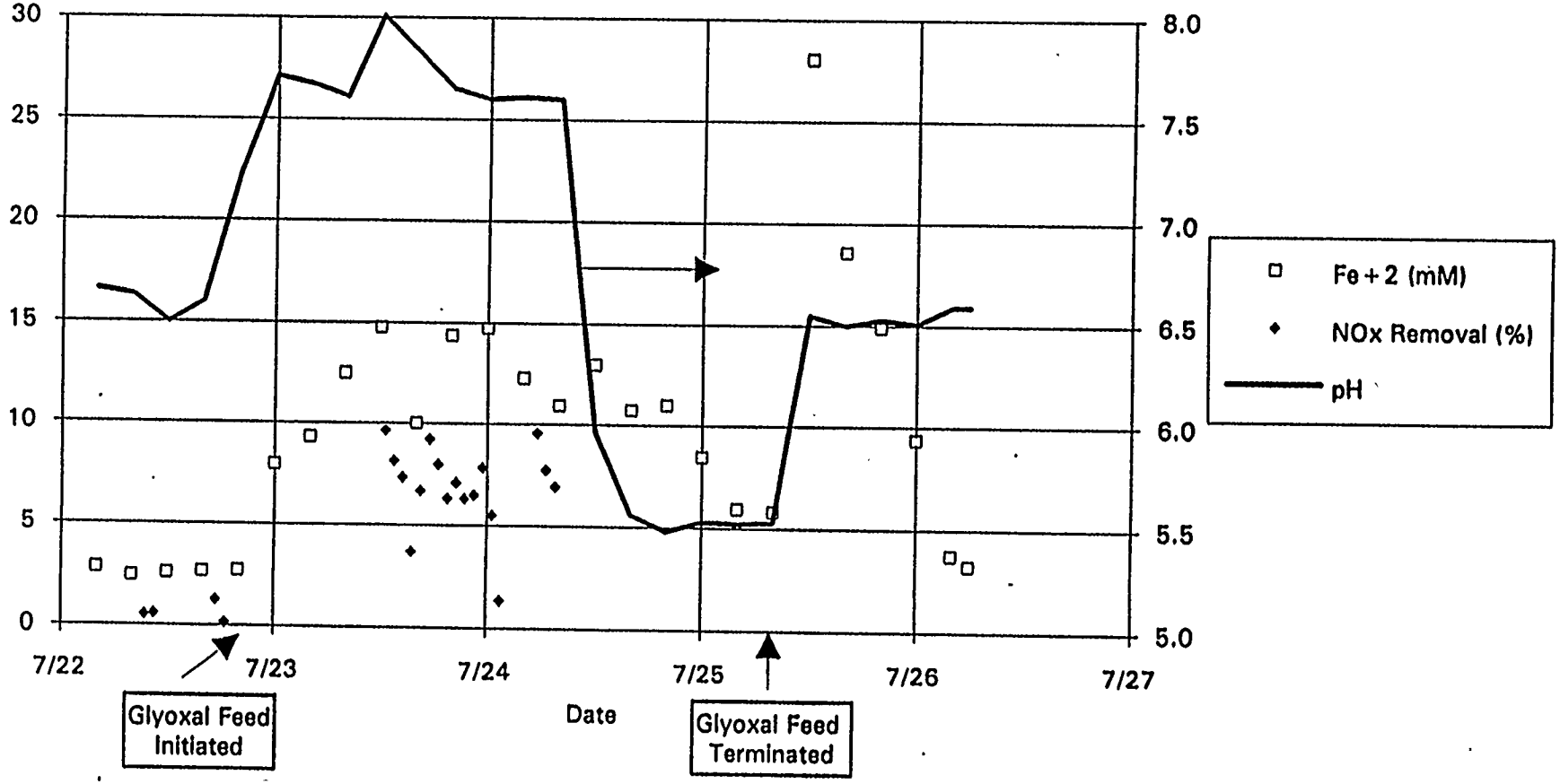

Figure 5

Figure 5

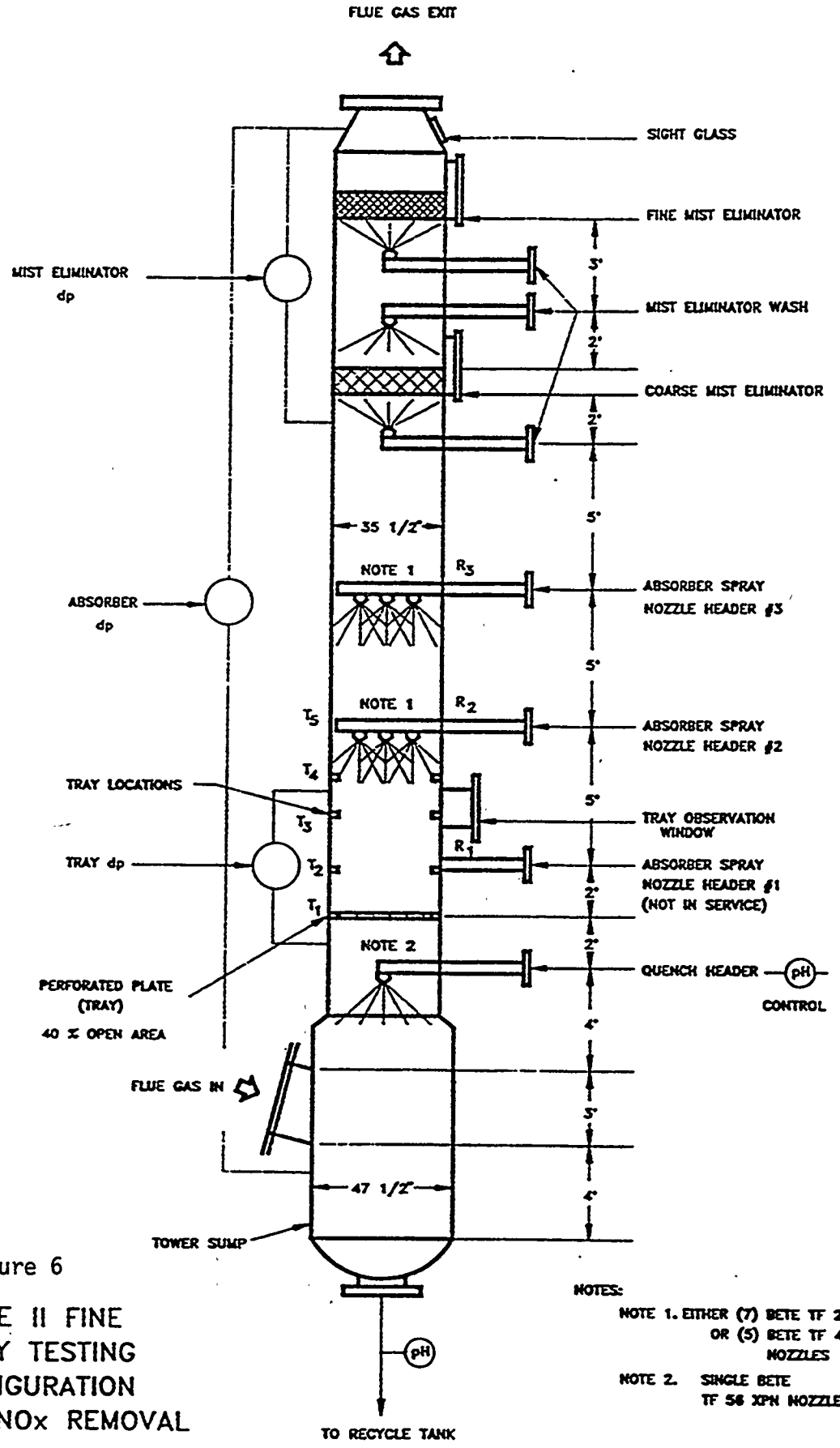

Figure 6

PHASE II FINE SPRAY TESTING CONFIGURATION FOR NOx REMOVAL 3' DIAMETER TOWER

Figure 6

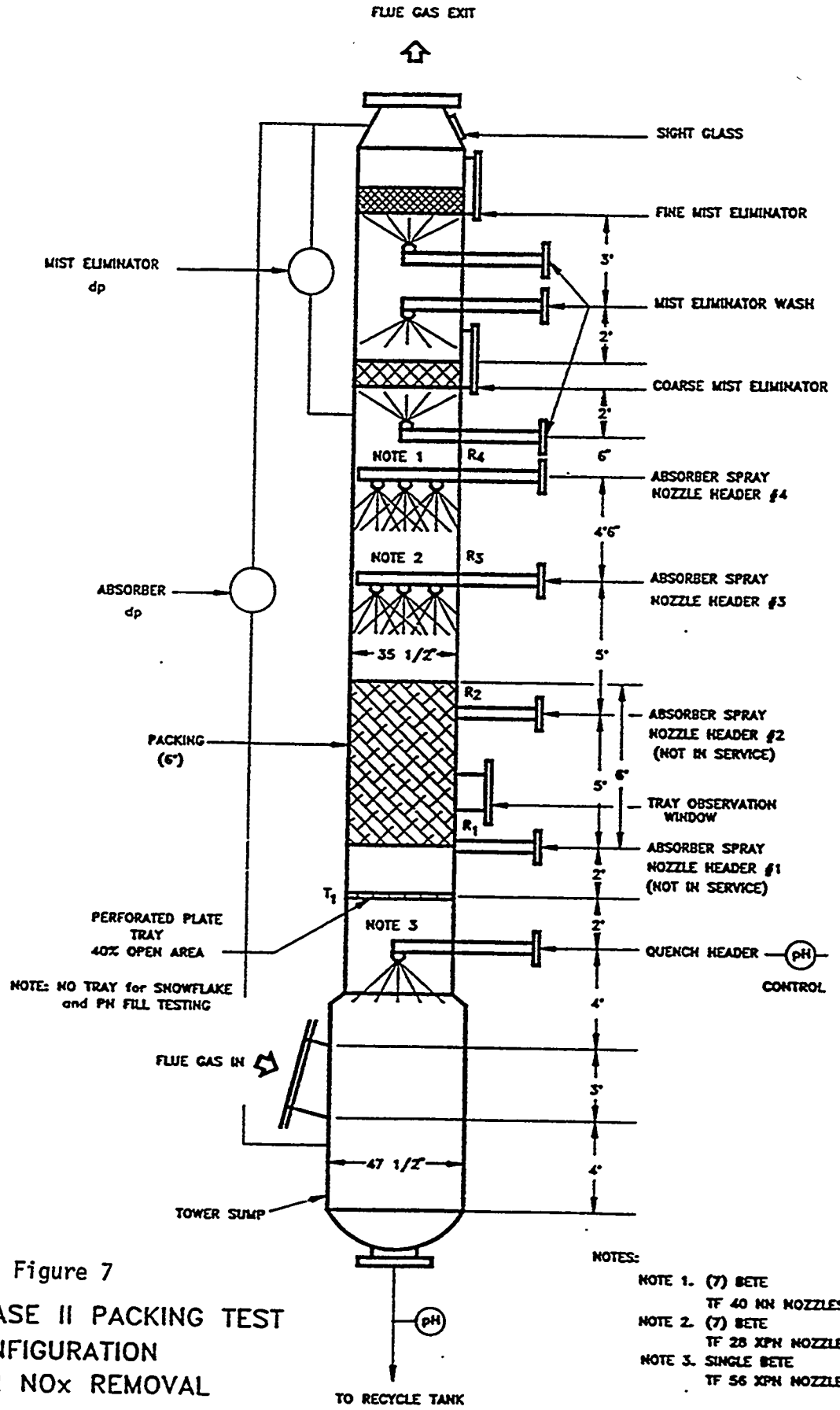

Figure 7

PHASE II PACKING TEST
CONFIGURATION
FOR NOx REMOVAL
3' DIAMETER TOWER

Figure 7

Figure 8

Comparison of Regression Constants								
	NOx Removal Correlations				Pressure Drop Correlations			
Packing	a	b	c	R2	A	B	C	R2
#2 Saddle	-1.13	0.49	-0.61	0.99	4.25	1.04	-4.84	0.93
#3 Saddle	0.09	0.9	-2.59	0.88	2.15	0.44	-1.91	0.92
Snowflake	-0.74	0.62	-1.3	0.99	2.67	0.83	-3.74	0.87
PN Fill	-1.06	0.35	-0.39	0.72	3.64	1.26	-5.54	0.96
Single 40% Tray								
w/TF28XPN	-0.72	1.51	-3.52	0.65	0.99	2.72	-6.47	0.98
w/TF40XPN	-0.9	n/a	-0.09	0.79	0.95	n/a	-0.56	0.97
Double Trays								

Equation (1) NOx Removal (NTU) = (FPS)^a*(GPM)^b*10^c

Equation (2) Packed Bed Pressure Drop ("WC) = (FPS)^A*(GPM)^B*10^C

Notes

1) #3 Saddle and TF40XPN test series limited in scope.
2) PN Fill correlation coefficients derived from dry additive feed test points only.

Figure 8

Figure 9

Miami Fort Pilot Plant
Task 3.1.2.3 Revisited
Effect of Recycle Tank pH on NOx Removal

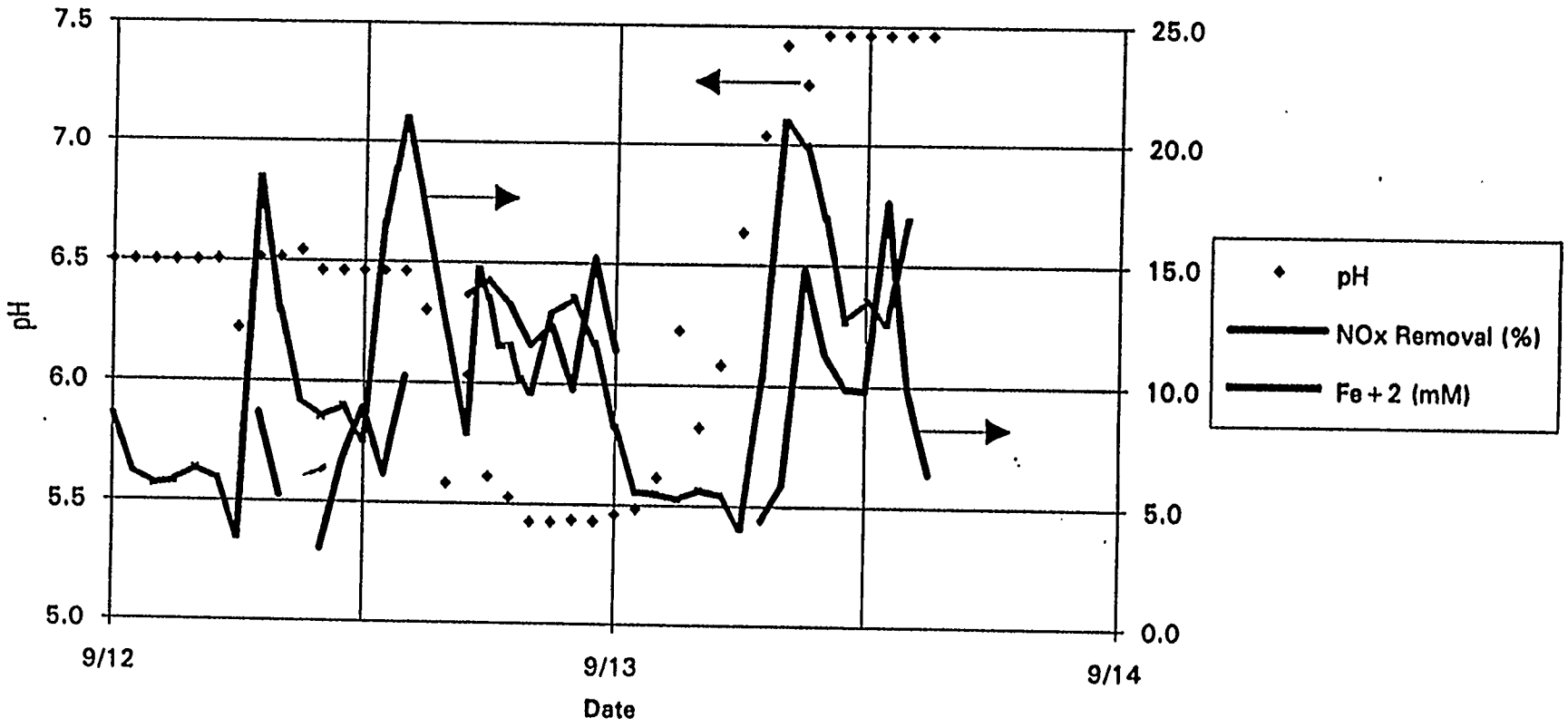

Figure 9

Figure 9

Figure 10

Miami Fort Pilot Plant
Task 3.1.2.3 Revisited
Effect of Recycle Tank pH on Ferrous Reduction

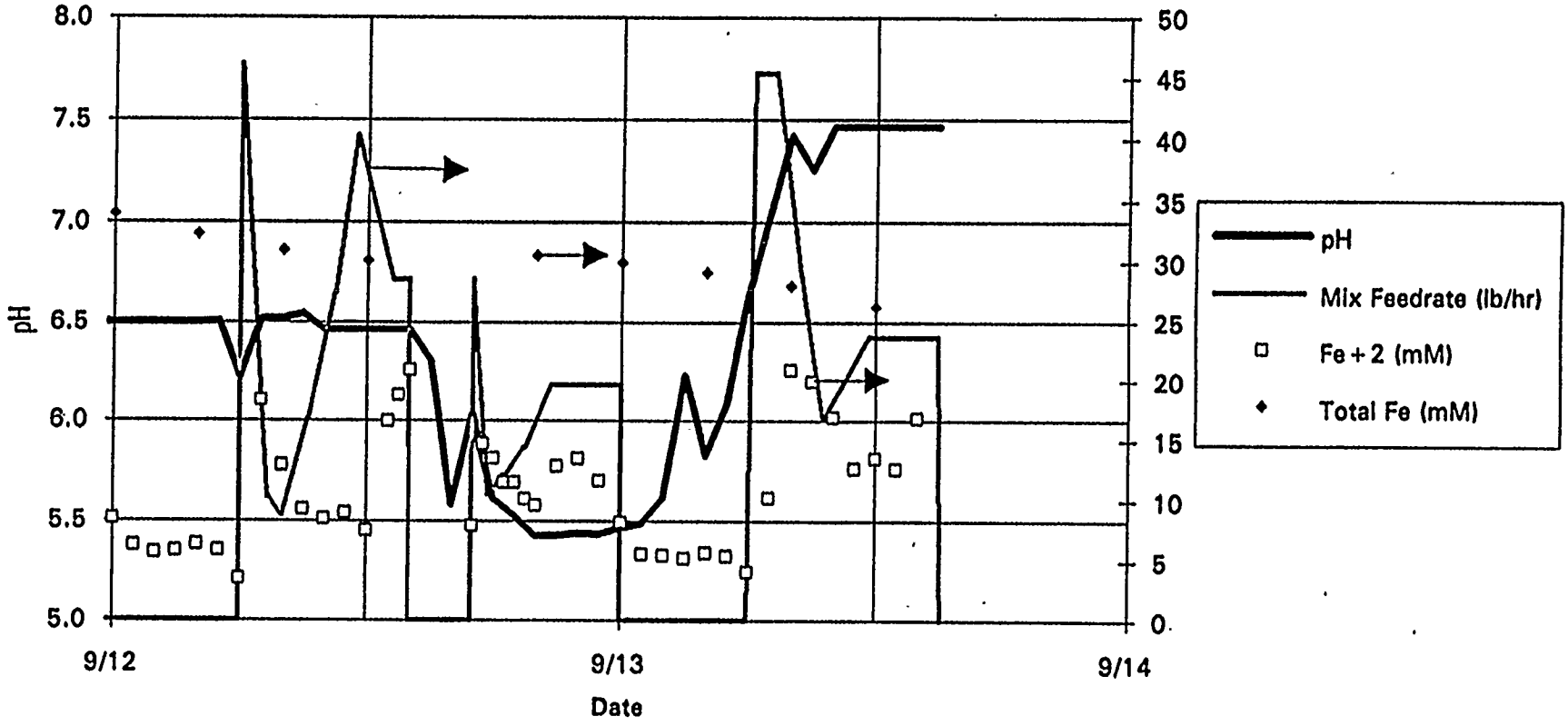

Figure 10

Figure 10

Figure 11
Miami Fort Pilot Plant
Phase 2
Solids Settling & Filtration Data

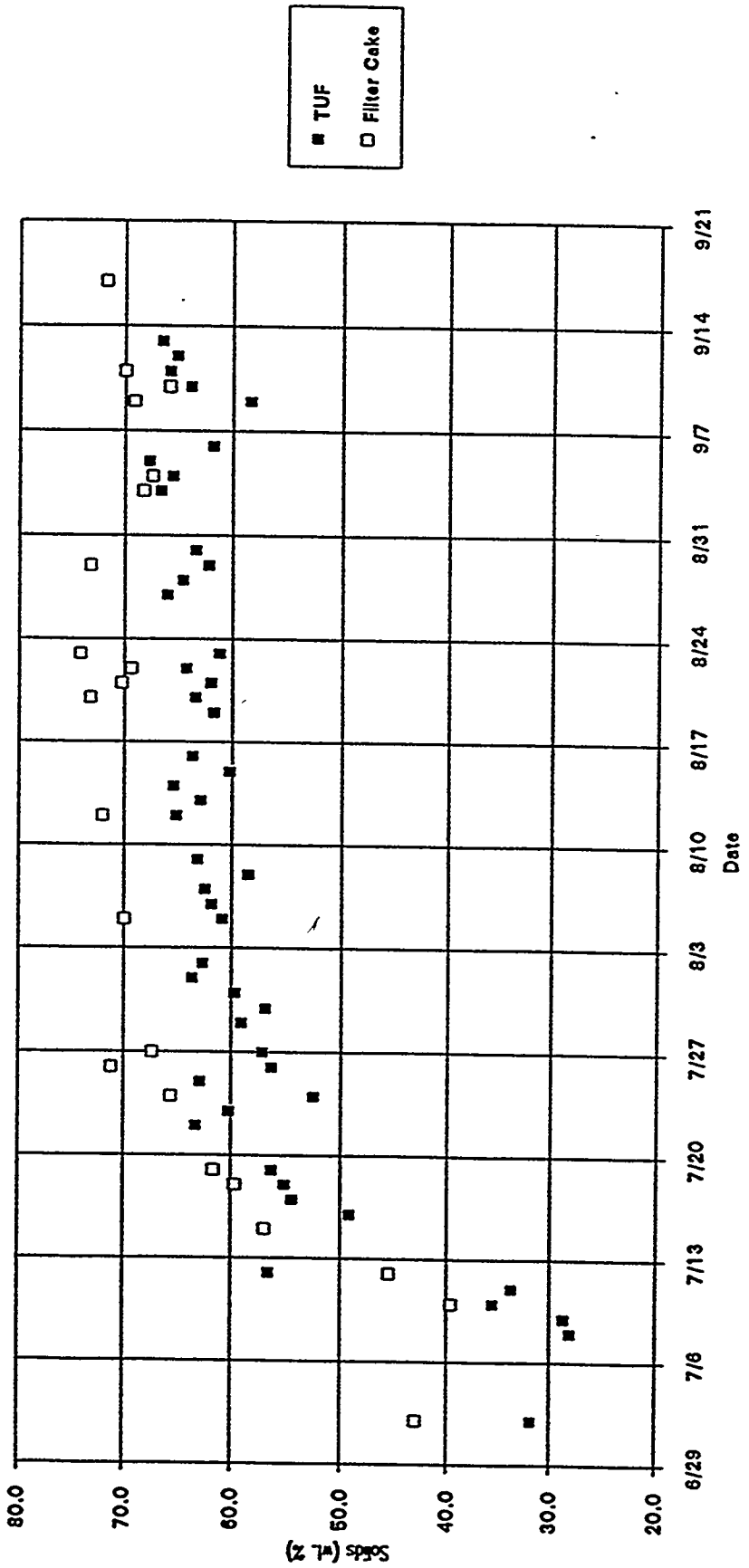

Figure 11

Figure 11

Table • \ Summary of Velocity Tests

Date	Test	NTU SO2	RT Alka.	SO2 In	SO2 Out	O2 In	NTU NOx	Fe + 2	NOx In	NOx Out	FGVEL	R2	R3	Total Liquid	L/G	Tower DP
			ppmwt.	ppmv.	ppmv.	%		mM	ppmv	ppmv	fps	gpm	gpm	gpm		In. WC
8/1/91 12:30	A	3.61	2840	2449	67	5.8	0.16	15	658	559	9.8	121	120	301	89	3.2
8/1/91 20:30	C	4.04	2978	2502	45	5.9	0.15	19	725	625	7.6	121	120	301	114	2.5
8/1/91 16:30	B	4.90	2962	2478	19	6.3	0.21	16	699	567	4.9	122	119	300	178	2.1
8/2/91 15:30	D	3.00	2971	2446	122	6.3	0.14	17	707	612	10.2	92	91	243	69	2.8
8/2/91 11:30	F	3.59	3068	2519	68	7.4	0.17	10	656	552	7.3	90	88	238	94	2.1
8/2/91 19:00	E	4.32	3114	2622	35	6.9	0.20	17	646	529	5.2	91	88	239	133	1.9

Figure • ___
Miami Fort Pilot Plant
Task 3.1.2.4 Fine Spray Tests

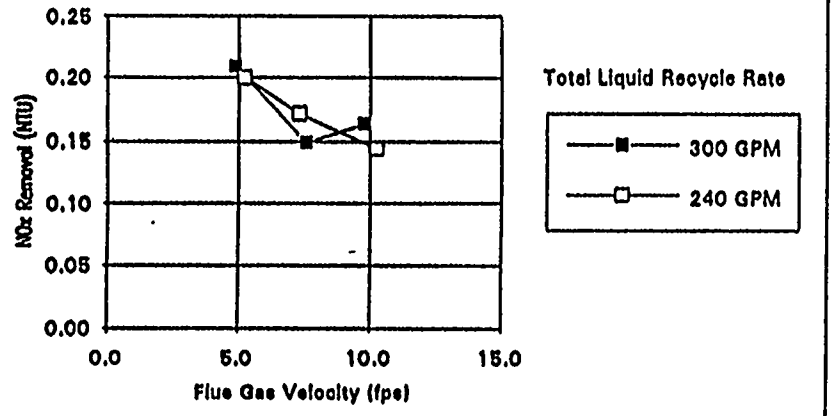

Figure • ___
Miami Fort Pilot Plant
Task 3.1.2.4 Fine Spray Tests

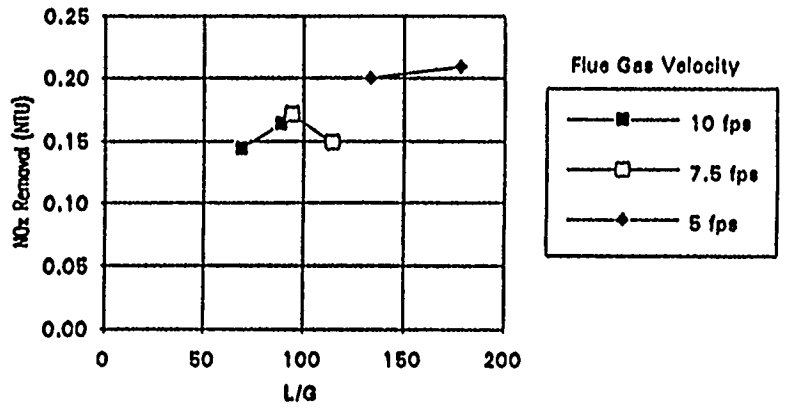

Figure • ___
Miami Fort Pilot Plant
Task 3.1.2.4 Fine Spray Tests

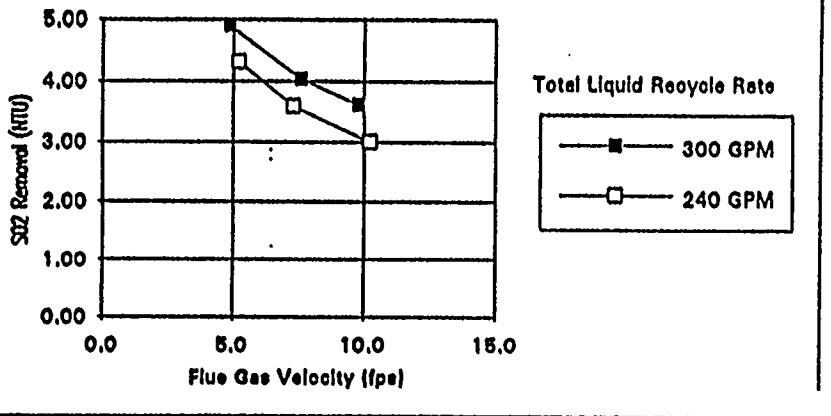

Figure • ___
Miami Fort Pilot Plant
Task 3.1.2.4 Fine Spray Tests

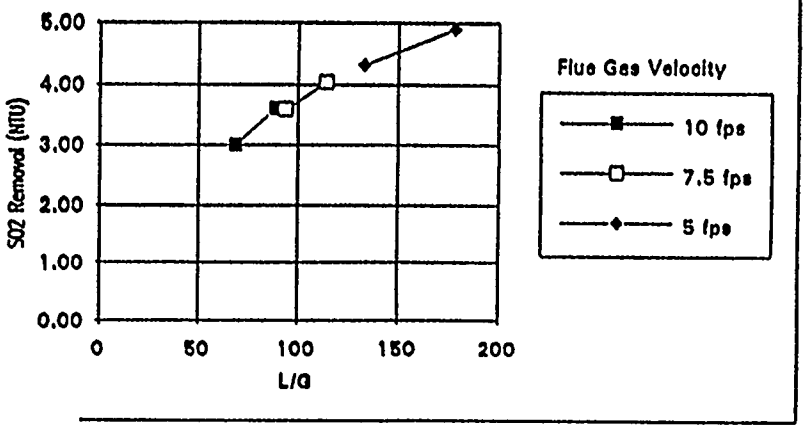

Table 1

Table 1

Table - 2 Summary of Velocity Tests with 3" Saddle Packing

Date/Time	Test	SO2 Rem.	Alka.	SO2 In	SO2 Out	O2	NOx Rem.	NOx Rem.	Fe+2	NOx In	NOx Out	FGVEL	R2	R3	Recycle Liq.	L/G	Pack. Bed DP
		NTU	ppmwt.	ppmv	ppmv	%	NTU	%	mM	ppmv	ppmv	fps	GPM	GPM	GPM		Inch WC
8/6/91 18:30	3	4.93	3028	2546	18	7.8	0.20	18	20	591	485	5	0	90	90	44	2.9
8/6/91 21:30	4	5.55	3028	2541	9	7.9	0.20	18	21	566	463	7	0	90	90	28	6.1
8/7/91 19:00	7	7.44	3437	2498	2	6.6	0.26	23	24	646	501	9	0	90	90	24	11.5
8/7/91 11:00	5	6.13	3587	2548	6	7.5	0.23	20	16	590	470	6	0	119	119	50	3.3
8/7/91 15:00	6	6.46	3517	2606	4	6.4	0.25	22	19	678	530	8	0	119	119	37	8.4
8/7/91 22:30	8	6.85	3783	2509	3	8.1	0.34	29	25	555	397	5	0	132	132	64	3.8

Figure - ___
Miami Fort Pilot Plant
Task 3.1.2.5 - 3" Packing Tests
Quench Flow Excluded

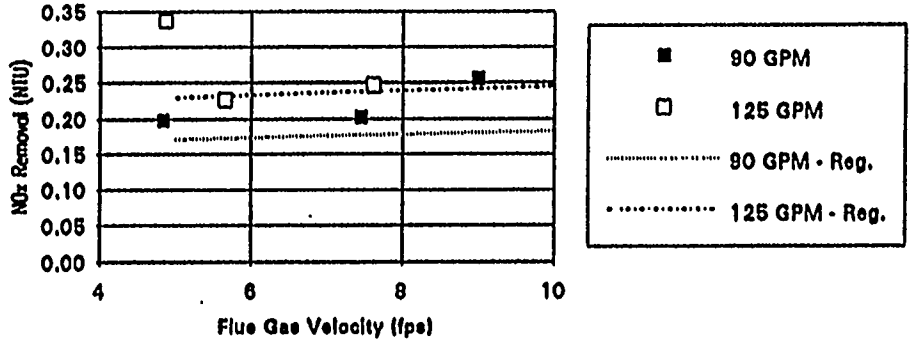

Figure - ___
Miami Fort Pilot Plant
Task 3.1.2.5 - 3" Saddle Packing Tests

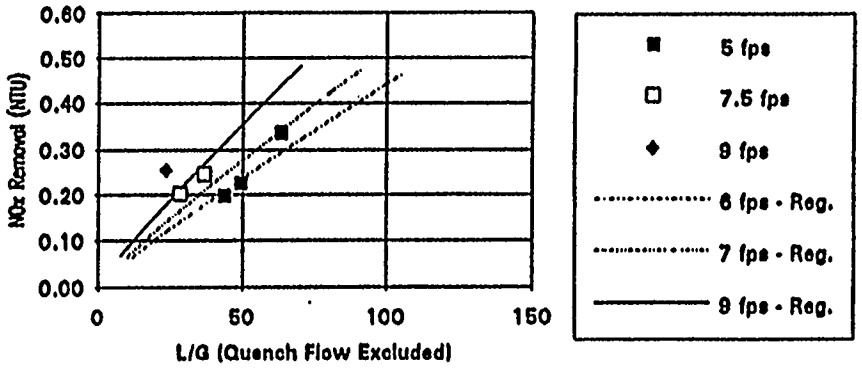

Figure - ___
Miami Fort Pilot Plant
Task 3.1.2.5 - 3" Saddle Packing Tests

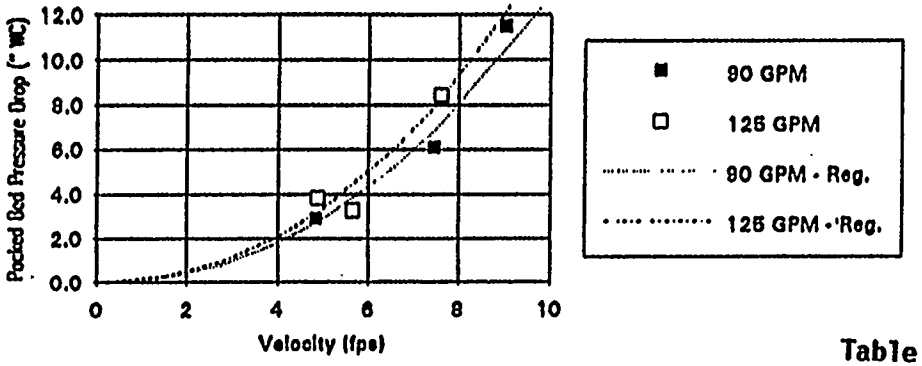

Figure - ___
Miami Fort Pilot Plant
Task 3.1.2.5 - 3" Saddle Packing Tests

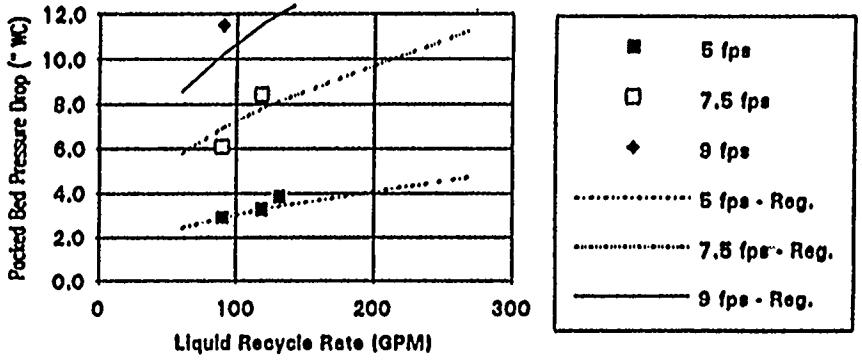

Table 2

Table - 3 Summary of Velocity Tests with 2" Saddle Packing

Date/Time	Test	SO2 Rem.	Alka.	SO2 In	SO2 Out	O2	NOx Rem.	NOx Rem.	Fe+2	NOx In	NOx Out	FGVEL	R2	R3	Recycle Liq.	L/G	MT DP
		NTU	ppmwt.	ppmv	ppmv	%	NTU	%	mM	ppmv	ppmv	fps	GPM	GPM	GPM		Inch WC
8/15/91 19:00	7	10.00	3893	2495	0	6.3	0.10	10	18	687	620	10	0	26	26	6	11.0
8/15/91 12:00	5	6.79	3759	2593	3	7.4	0.26	23	19	609	472	6	0	59	59	22	2.7
8/16/91 15:30	10	10.00	4075	2598	0	7.0	0.38	31	18	649	445	6	0	90	90	39	2.3
8/14/91 10:30	2	7.16	3993	2608	2	8.3	0.22	19	15	566	457	7	0	90	90	29	5.1
8/13/91 18:30	1	7.96	3699	2537	1	8.3	0.20	18	14	583	476	9	0	90	90	25	12.1
8/15/91 14:00	6	10.00	3853	2031	0	7.1	0.38	32	18	634	433	6	0	120	120	51	2.9
8/14/91 14:30	3	7.27	3851	2575	1	8.5	0.36	30	15	573	401	6	0	124	124	52	2.9
8/15/91 22:00	8	10.00	3893	2412	0	6.9	0.40	33	13	641	429	6	118	120	238	88	11.8
8/16/91 11:30	9	10.00	4193	2591	0	7.1	0.77	54	17	650	301	5	155	120	275	131	5.1
8/14/91 18:30	4	7.48	3991	2588	1	8.4	0.56	43	13	574	329	5	151	125	276	131	5.2

Figure - ___
Miami Fort Pilot Plant
Task 3.1.2.5 - 2" Packing Tests
Quench Flow Excluded

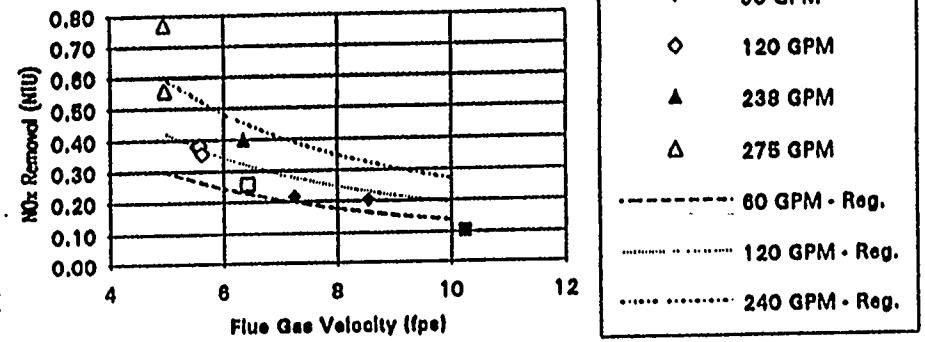

Figure - ___
Miami Fort Pilot Plant
Task 3.1.2.5 - 2" Packing Tests

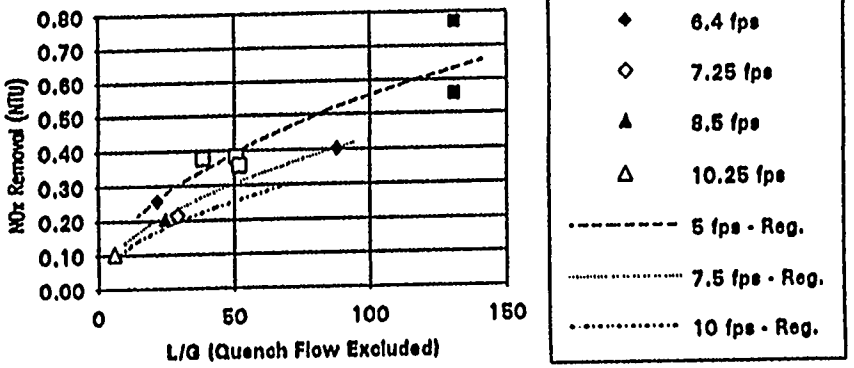

Figure - ___
Miami Fort Pilot Plant
Task 3.1.2.5 - 2" Packing Tests

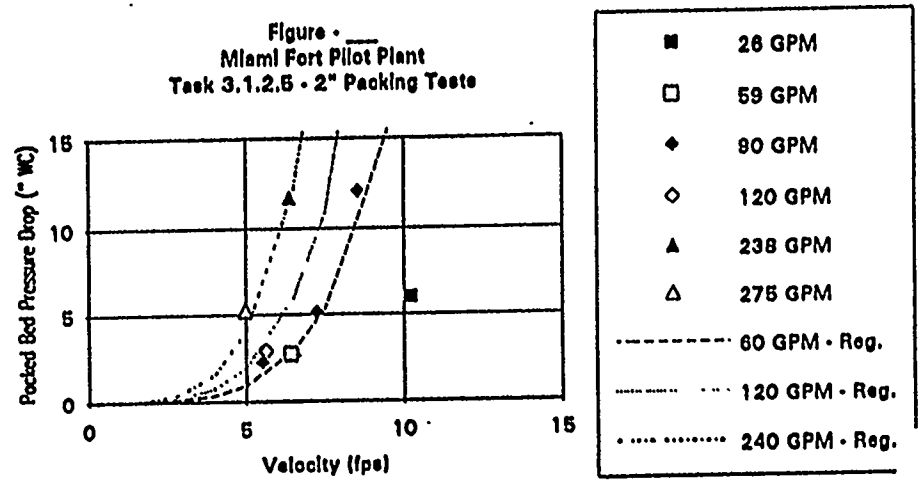

Figure - ___
Miami Fort Pilot Plant
Task 3.1.2.5 - 2" Packing Tests

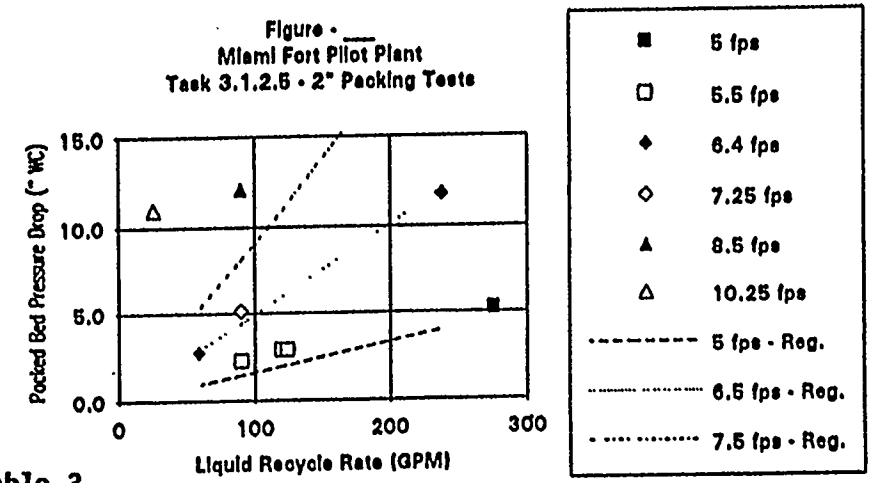

Table 3

Table - 4 Summary of Velocity Tests with Snowflake Packing

Date/Time	Test	SO2 Rem.	Alka.	SO2 In	SO2 Out	O2	NOx Rem.	NOx Rem.	Fe+2	NOx In	NOx Out	FGVEL	R2	R3	Recycle Liq.	L/G	Pack. Bed DP
		NTU	ppmwt.	ppmv	ppmv	%	NTU	%	mM	ppmv	ppmv	fps	GPM	GPM	GPM		Inch WC
8/21/91 16:30	6	10.0	3973	2387	0	7.5	0.24	21	16	568	450	6	90	0	90	37	1.0
8/21/91 11:00	5	10.0	4558	2692	0	8.0	0.24	21	21	588	464	7	90	0	90	30	1.6
8/21/91 20:00	4	10.0	4472	2604	0	8.5	0.20	18	18	567	463	9	90	0	90	25	2.5
8/20/91 19:00	2	10.0	4289	2137	0	6.4	0.30	26	19	544	495	6	0	120	120	45	1.1
8/20/91 21:30	3	10.0	4458	2454	0	7.5	0.25	22	17	594	463	7	0	120	120	40	1.6
8/20/91 16:00	1	10.0	4139	2549	0	7.1	0.21	19	18	629	510	9	0	120	120	32	4.4
8/23/91 10:30	7	10.0	4586	2525	0	7.8	0.53	41	18	615	362	6	149	118	267	114	1.9

Figure - ___
Miami Fort Pilot Plant
Task 3.1.2.6 - Snowflake Packing Tests
Quench Flow Excluded

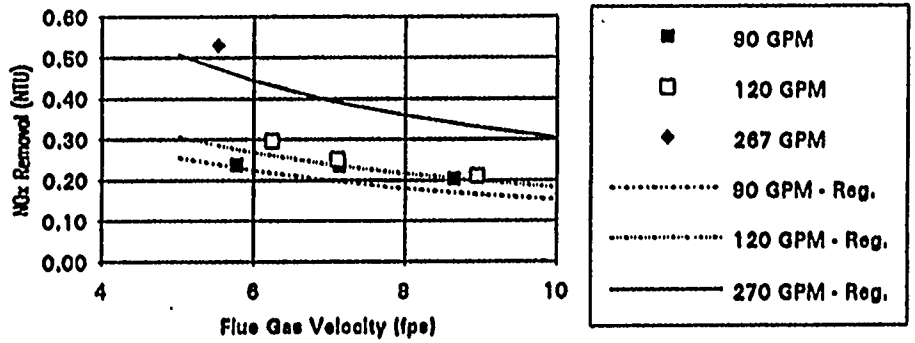

Figure - ___
Miami Fort Pilot Plant
Task 3.1.2.6 - Snowflake Packing Tests

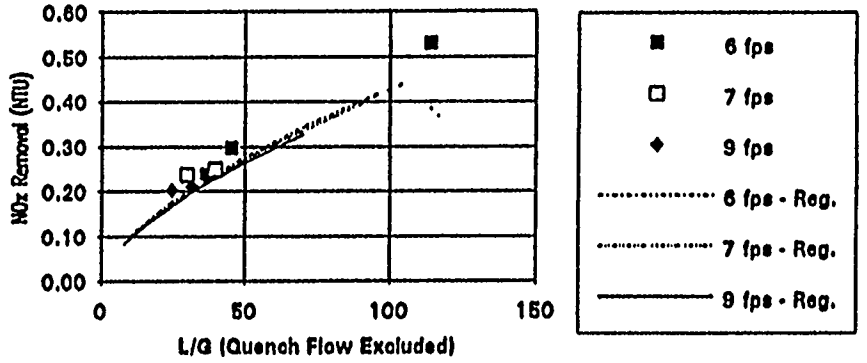

Figure - ___
Miami Fort Pilot Plant
Task 3.1.2.6 - Snowflake Packing Tests

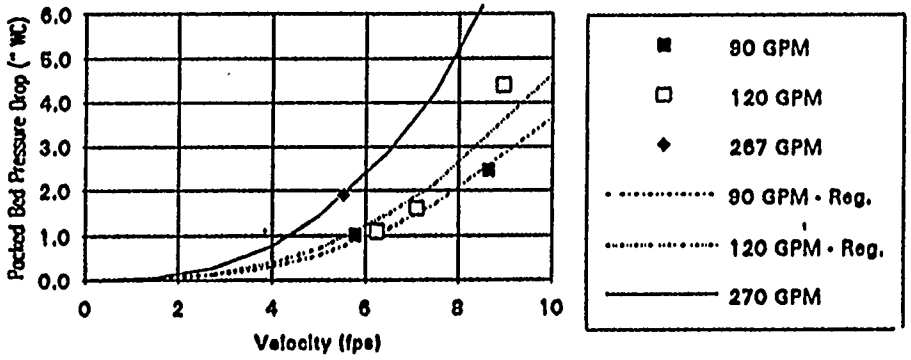

Figure - ___
Miami Fort Pilot Plant
Task 3.1.2.6 - Snowflake Packing Tests

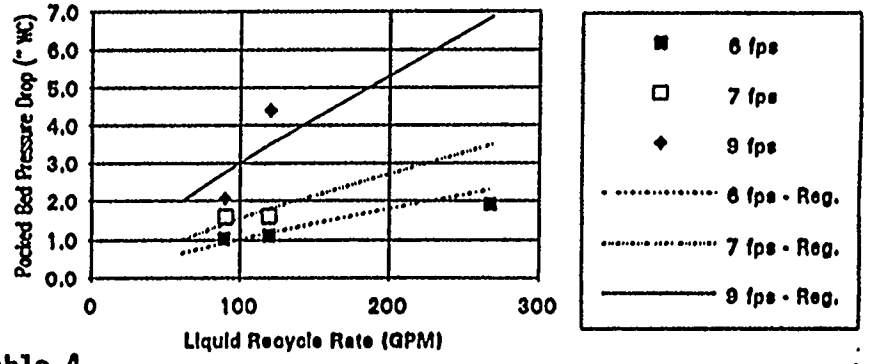

Table 4

Table - 5 Summary of Velocity Tests with PN Fill Packing

Date/Time	Test	SO2 Rem.	Alka.	SO2 In	SO2 Out	O2	NOx Rem.	NOx Rem.	Fe+2	NOx In	NOx Out	FGVEL	R2	R3	Recycle Liq.	L/G	Pack. Bed DP
		NTU	ppmwt.	ppmv	ppmv	%	NTU	%	mM	ppmv	ppmv	fps	GPM	GPM	GPM		Inch WC
8/27/91 19:00	1	10.0	4549	2555	0	6.7	0.22	19	17	631	509	9	0	110	110	29	2.5
8/30/91 10:30	8	10.0	5158	2472	0	8.1	0.10	10	14	530	478	9	0	105	105	28	2.4
8/27/91 22:30	2	10.0	4762	2502	0	7.9	0.26	23	8	629	483	7	0	110	110	36	1.2
8/29/91 0:00	4	10.0	5068	2510	0	9.3	0.19	17	16	462	382	7	0	106	106	35	1.3
8/29/91 12:00	5	10.0	4902	2604	0	7.1	0.26	23	15	608	467	7	0	103	103	34	1.1
8/28/91 21:00	3	10.0	4486	2696	0	6.5	0.25	22	17	578	449	6	0	108	108	43	1.0
8/30/91 13:00	9	10.0	5028	2540	0	7.7	0.20	18	11	569	463	9	145	105	250	67	10.3
8/29/91 23:30	7	10.0	5144	2414	0	8.7	0.29	25	15	533	397	7	146	104	250	83	3.3
8/29/91 19:00	6	10.0	4876	2610	0	6.7	0.55	42	13	659	382	6	146	106	252	107	1.7

Figure - ___
Miami Fort Pilot Plant
Task 3.1.2.7 - PN Fill Packing Tests
Quench Flow Excluded

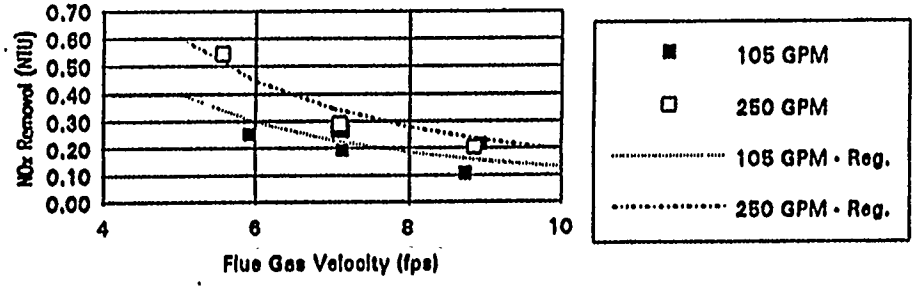

Figure - ___
Miami Fort Pilot Plant
Task 3.1.2.7 - PN Fill Packing Tests

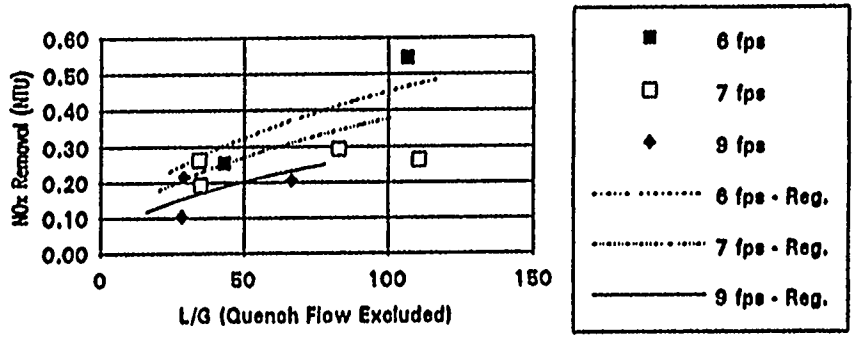

Figure - ___
Miami Fort Pilot Plant
Task 3.1.2.7 - PN Fill Packing Tests

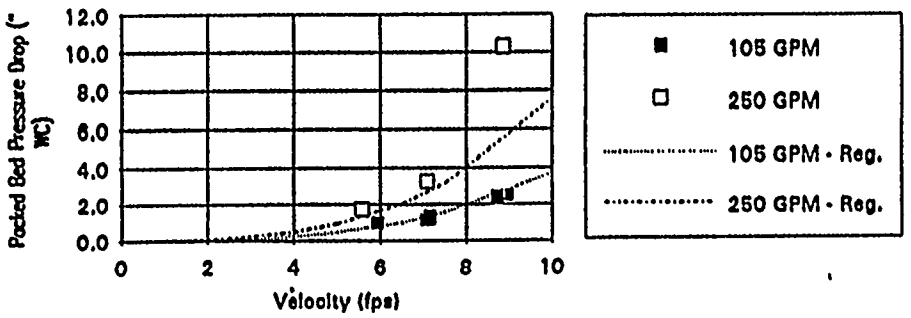

Figure - ___
Miami Fort Pilot Plant
Task 3.1.2.7 - PN Fill Packing Tests

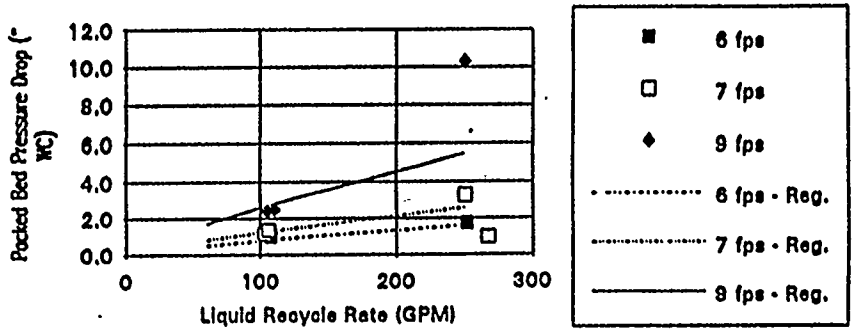

Table 5

Table - 6 Summary of Velocity Tests with PN Fill Packing; Week 2

Date/Time	Test	SO2 Rem.	Alka.	SO2 In	SO2 Out	O2	NOx Rem.	NOx Rem.	Fe+2	NOx In	NOx Out	FGVEL	R2	R3	Recycle Liq.	L/G	Pack. Bed DP
		NTU	ppmwt.	ppmv	ppmv	%	NTU	%	mM	ppmv	ppmv	fps	GPM	GPM	GPM		Inch WC
9/6/91 20:30	16	5.3	5598	2518	13	8.0	0.37	31	18	605	417	6	0	98	98	36	0.9
9/6/91 18:00	15	5.0	5598	2353	15	7.1	0.21	19	21	580	468	9	0	99	99	27	2.1
9/4/91 16:30	10	10.0	4670	2408	0	8.9	0.35	29	10	453	313	6	92	103	195	77	1.4
9/5/91 17:00	11	7.6	4836	2516	2	8.0	0.24	21	13	532	414	7	95	102	196	65	2.1
9/5/91 20:00	12	7.7	5176	2547	2	8.7	0.28	25	16	493	372	9	94	101	194	52	6.0
9/6/91 11:00	13	7.7	5827	2548	2	9.2	0.48	37	23	444	277	6	144	100	245	96	2.0
9/6/91 15:00	14	7.8	5845	2498	1	7.6	0.39	32	21	605	410	9	145	100	245	66	9.7

Figure - ___
Miami Fort Pilot Plant
Task 3.1.2.7 - PN Fill Packing Tests; Week 2
Quench Flow Excluded

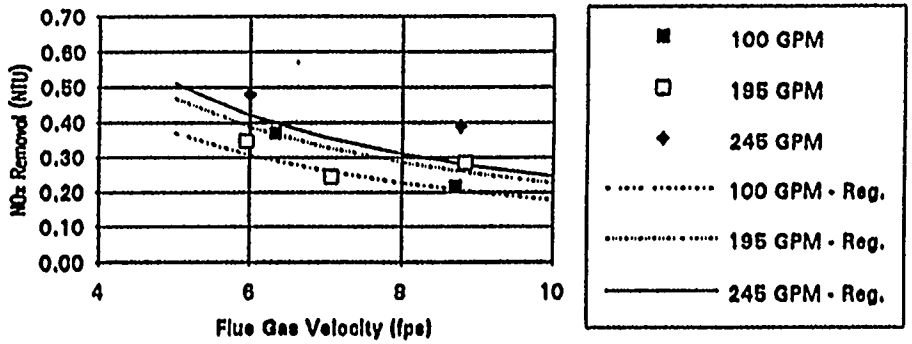

Figure - ___
Miami Fort Pilot Plant
Task 3.1.2.7 - PN Fill Packing Tests; Week 2

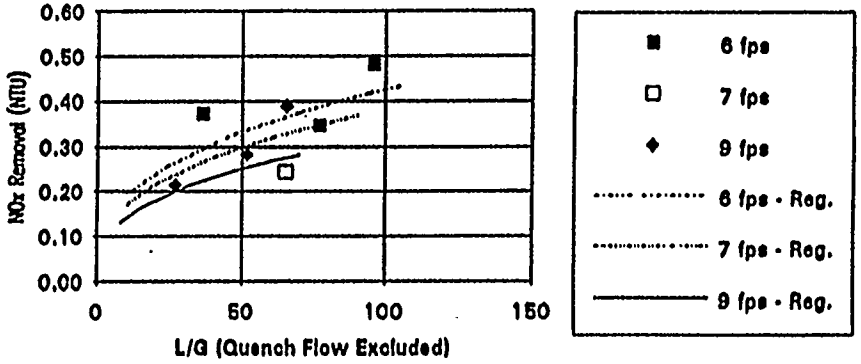

Figure - ___
Miami Fort Pilot Plant
Task 3.1.2.7 - PN Fill Packing Tests; Week 2

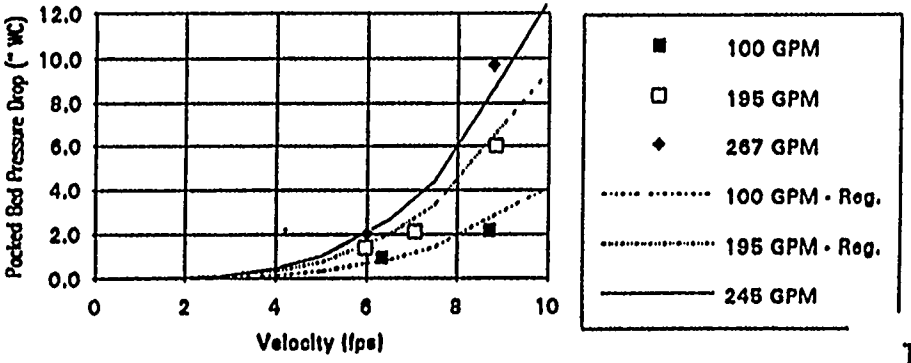

Figure - ___
Miami Fort Pilot Plant
Task 3.1.2.7 - PN Fill Packing Tests; Week 2

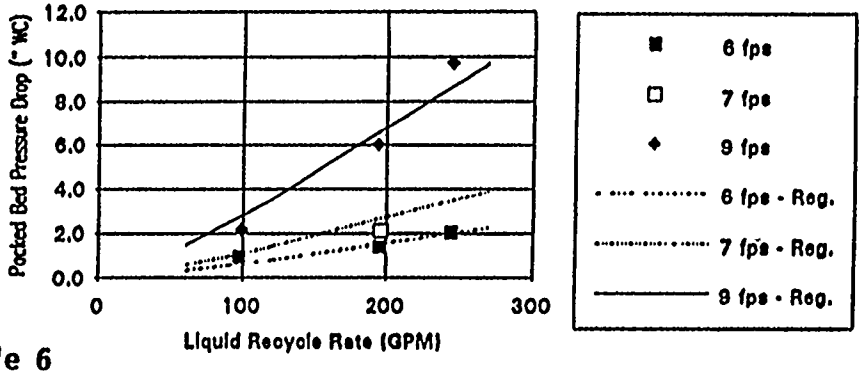

Table 6

Table - 1 Summary of Spray Nozzle Tests with Single 40% Open Tray

Date/Time	Test	SO2 Rem.	Alka.	SO2 In	SO2 Out	O2	NOx Rem.	NOx Rem.	Fe+2	NOx In	NOx Out	FGVEL	R2	R3	Recycle Liq.	L/G	Tower DP	Nozzle
		NTU	ppmwt.	ppmv	ppmv	%	NTU	%	mM	ppmv	ppmv	fps	GPM	GPM	GPM		Inch WC	Type
9/11/91 12:30	6	5.0	6733	2562	17	7.0	0.13	12	16	534	468	6	75	74	149	57	1.6	TF28
9/11/91 0:00	5	3.9	6955	2567	49	7.7	0.19	18	20	515	424	8	75	76	151	42	2.2	TF28
9/10/91 21:00	4	3.7	5811	2639	66	6.3	0.13	12	23	574	506	11	75	73	149	32	3.0	TF28
9/9/91 18:00	1	5.0	5104	2571	17	7.1	0.23	21	17	563	447	7	91	89	181	64	3.1	TF28
9/9/91 21:00	2	4.2	5040	2639	39	6.6	0.19	17	18	605	501	9	92	91	183	50	3.9	TF28
9/10/91 0:00	3	3.8	5236	2549	62	9.2	0.13	12	16	467	411	11	92	89	181	40	4.5	TF28
9/11/91 19:00	7	4.2	6177	2540	38	7.3	0.13	12	12	578	507	6	89	89	178	68	1.6	TF40
9/11/91 22:00	8	3.2	6177	2485	98	7.6	0.14	13	14	548	478	8	89	89	177	51	1.9	TF40
9/12/91 12:30	9	2.7	6393	2535	161	9.3	0.08	8	14	496	456	11	90	91	181	40	2.7	TF40

Figure - ___
Miami Fort Pilot Plant
Task 3.1.2.4 - Fine Spray Tests Revisited
Quench Flow Excluded

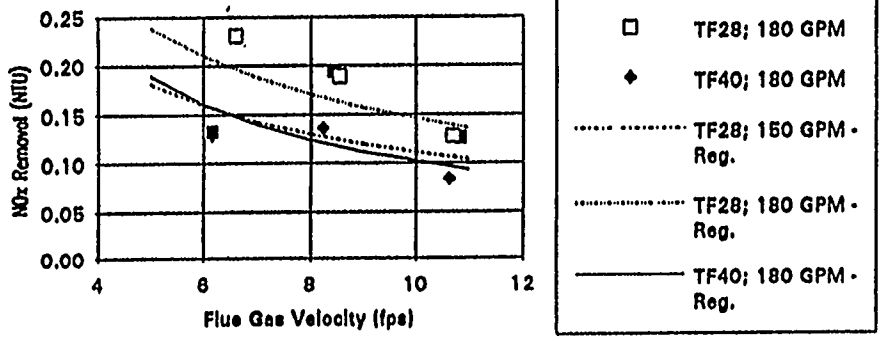

Figure - ___
Miami Fort Pilot Plant
Task 3.1.2.4 - Fine Spray Tests; Revisited

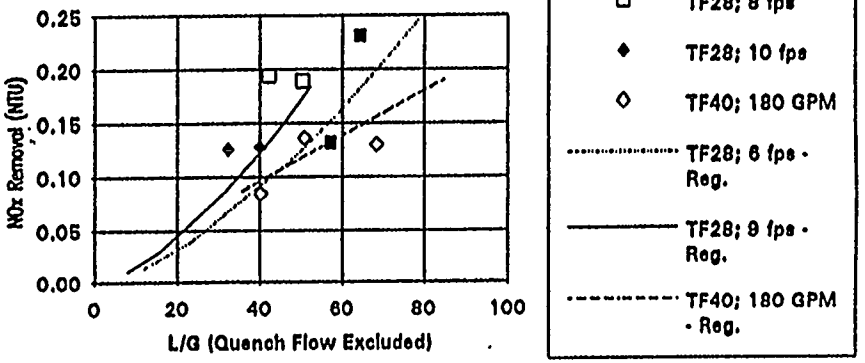

Figure - ___
Miami Fort Pilot Plant
Task 3.1.2.4 - Fine Spray Tests Revisited

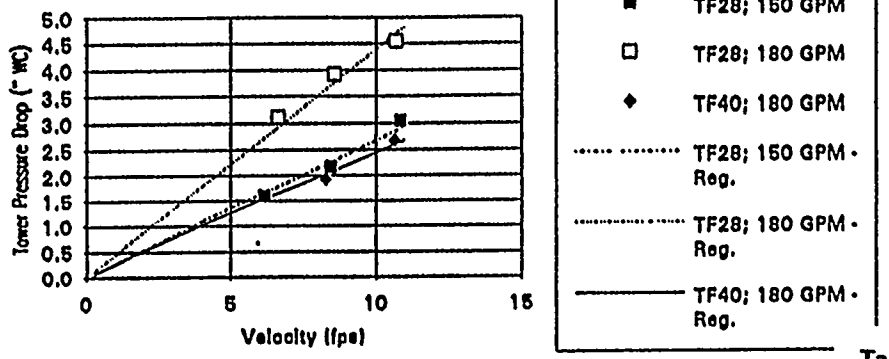

Figure - ___
Miami Fort Pilot Plant
Task 3.1.2.4 - Fine Spray Tests Revisited

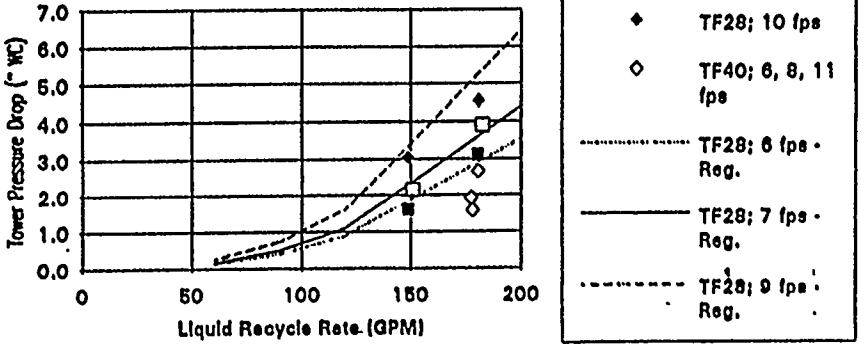

Table 7

Table - 8 Summary of Spray Nozzle Tests with Single 40% Open Tray

Date/Time	Test	SO2 Rem.	SO2 Rem.	Alka.	SO2 In	SO2 Out	O2	FGVEL	R2	R3	Recycle Liq.	L/G	Tower DP	Nozzle
		NTU	%	ppmwt.	ppmv	ppmv	%	fps	GPM	GPM	GPM		Inch WC	Type
9/11/91 12:30	6	5.0	99.4	6733	2562	17	7.0	6	75	74	149	57	1.6	TF28
9/11/91 0:00	5	3.9	98.1	6055	2567	49	7.7	8	75	76	151	42	2.2	TF28
9/10/91 21:00	4	3.7	97.5	5811	2639	66	6.3	11	75	73	149	32	3.0	TF28
9/9/91 18:00	1	5.0	99.3	5104	2571	17	7.1	7	91	89	181	64	3.1	TF28
9/9/91 21:00	2	4.2	98.6	5040	2639	39	6.6	9	92	91	183	50	3.9	TF28
9/10/91 0:00	3	3.8	97.7	5236	2549	62	9.2	11	92	89	181	40	4.5	TF28
9/11/91 19:00	7	4.2	98.6	6177	2540	38	7.3	6	89	89	178	68	1.6	TF40
9/11/91 22:00	8	3.2	96.0	6177	2485	98	7.6	8	89	89	177	51	1.9	TF40
9/12/91 12:30	9	2.7	93.5	6393	2535	161	9.3	11	90	91	181	40	2.7	TF40

Figure - ___
Miami Fort Pilot Plant
Task 3.1.2.4 - Fine Spray Tests Revisited
Quench Flow Excluded

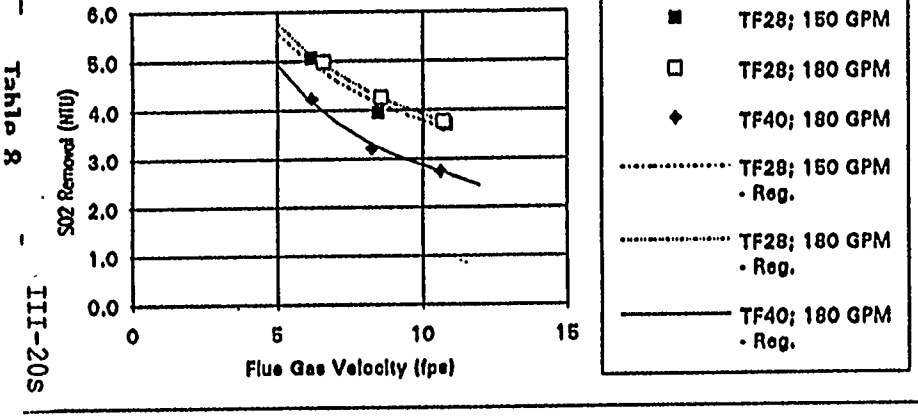

Figure - ___
Miami Fort Pilot Plant
Task 3.1.2.4 - Fine Spray Tests Revisited

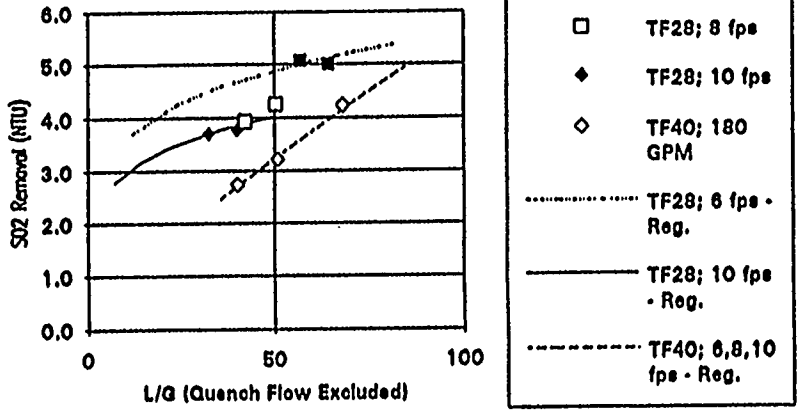

Table - ___ SO2 Removal Data Regression Analysis of Velocity
Tests with TF28 Nozzles & Single 40% Tray
(Corrected Velocity)

	LOG(GPM)	LOG(Vel)	k	
	0.19	-0.57	0.73	
Std. Err. Coeff.	0.16	0.07	0.35	Std. Err. Coeff.
R^2	0.95	0.02	Std. Y Est.	
F Statistic	32	3	d.f.	
SSreg.	0.02	0.00	SSresid.	

Table - ___ SO2 Removal Data Regression Analysis of Velocity
Tests with TF40 Nozzles & Single 40% Tray
(Corrected Velocity)

	LOG(Vel)	k	
	-0.80	1.25	
Std. Err. Coeff.	0.09	0.08	Std. Err. Coeff.
R^2	0.99	0.02	Std. Y Est.
F Statistic	79	1	d.f.
SSreg.	0.02	0.00	SSresid.

Table 8

1. Effects of Glyoxal Addition

In order for Thiosorbic/Ferrous (Fe(II)) EDTA Simultaneous SO_2/NOx Removal to proceed in a controlled fashion, it is necessary to maintain an optimal ferrous iron concentration in the scrubber liquor. The rate-limiting step in the NOx removal scheme is the removal of NO from the scrubber liquor via formation of a nitrosyl metal chelate adduct. The chemistry described herein is strictly liquid phase and does not address the absorption of the NO gas into the liquid phase, a gas-film limited process which also determines the overall reaction rate.

This liquid phase rate-limiting adduct is formed with iron chelate only when the iron is in the (+2) oxidation state, as illustrated by the following simplified reactions:

$$Fe(II)\text{-}EDTA + NO \longrightarrow Fe(II)\text{-}EDTA(NO) \qquad \text{eq.(1)}$$

$$Fe(III)\text{-}EDTA + NO \longrightarrow N.R. \qquad \text{eq.(2)}$$

Due to the strong oxidizing environment inherent in FGD systems, the bulk of the iron chelate is rather quickly converted to the inactive ferric form. Thus it is necessary to regenerate the iron chelate to the ferrous form, that is, reduce the ferric chelate to the ferrous chelate.

One of the chemical reducing agents studied at Miami Fort Pilot Plant (MFPP) for this purpose was glyoxal ($C_2H_2O_2$). Glyoxal is an attractive chemical reducing agent for ferrous chelate regeneration in NOx scrubbing for several reasons:

- Cost effectiveness
- Potentially high ferric reduction ratio (1:6) at 100% utilization:

$$C_2H_2O_2 + 2H_2O + 6Fe^{+3} \text{ ---> } 2CO_2 + 6H^+ + 6Fe^{+2} \qquad \text{eq.(3)}$$

- Ease of handling, process injection, and addition control when delivered as a 40% glyoxal in water solution

- Potentially cleaner scrubber liquor matrix upon complete utilization: no cations introduced and only CO_2 as a major reaction product.

Glyoxal addition was first initiated at MFPP during the last week of Phase I testing into a scrubber liquor that had been previously subjected to ferric chelate reduction through addition of a sodium dithionite/ascorbic acid mixture. The duration of this glyoxal addition was four days.

Glyoxal addition was reinitiated at the beginning of Phase II. However, the scrubber liquor from Phase I had been purged from the system for Phase II. A fresh thiosorbic/iron chelate scrubber liquor was prepared by operating the scrubber for two days while adding freshly prepared batches of ferrous EDTA. Desirable magnesium levels were obtained by adding magnesium hydroxide in batches to the system. Glyoxal addition was then initiated on the third day. Thus in Phase II, initial glyoxal addition occurred at sodium levels of slightly under 4000 ppm as opposed to sodium levels of +20,000 ppm upon initial Phase I addition.

GLYOXAL ADDITION EFFECTS NOTED: The following discussion will deal with the effects of glyoxal addition primarily with respect to the recycle tank chemistry, mainly its effect on ferrous iron concentration ferrous concentration, and its correlation to NOx removal and general scrubber operation.

a. Lag time between initial glyoxal addition and anticipated increase in ferrous iron concentration.

In Phase I, initial addition of glyoxal did not result in an immediate or substantial increase in ferrous concentration. This was somewhat surprising based upon the relatively fast response noticed with sodium dithionite based reducing agent. At the time of initial glyoxal addition, the ferrous concentration was approximately 7mM and it was not until over 6 hours later that the ferrous concentration had reached the 12 mM level, the lower end of the preferred 12 mM - 18 mM operating range.

In Phase II, initial addition of glyoxal proceeded the elevation to the 12mM ferrous concentration threshold by over 18 hours (see Figure 1). Once the operating range of ferrous concentration was established, it stabilized rather well at a constant glyoxal feed rate.

After the lag time period, glyoxal proved to be an effective reducing agent with generally increasing ferrous concentration resulting from increasing glyoxal feed rate. An exception to this trend was observed under low load, high inlet oxygen conditions as shown in Figure 2. This is not unusual, however, as chemical reducing agent feed rate is normally increased under these conditions to compensate for increased ferrous-EDTA oxidation.

b. Increase in Calcium Concentration:

Coincident to the lag in increased ferrous concentration was a marked increase in calcium concentration calcium concentration upon glyoxal addition to the system. During Phase I calcium concentration (determined by atomic absorption analysis) increased from 146 ppm on day #1 to 794 ppm on day #4 (See Table I). It is unusual for a thiosorbic based FGD system to have >200 ppm calcium in the scrubber liquor because of calcium concentration suppression by elevated magnesium levels. In fact, laboratory testing at Miami

Fort does not normally include calcium during NOx testing as the test endpoint is usually arrived at before titration due to the EDTA levels present. In this case, total hardness is credited solely to magnesium and calcium concentration is expressed as zero. However for quality control, samples are also analyzed at Dravo Research Center by atomic absorption (AA) spectroscopy so that historical data was available for study.

During Phase II, this trend toward higher calcium concentration took on dramatic proportions. (All calcium concentration by AA). Before glyoxal addition, a baseline calcium concentration of 59 ppm was established. By the end of the first day calcium concentration was 322 ppm. By the end of the second day of glyoxal addition calcium concentration was 1345 ppm. By day three over 3000 ppm calcium was present (See Table II).

During week #2 of Phase II testing, calcium levels had reached an unprecedented +6000 ppm, necessitating addition of magnesium hydroxide to the scrubber liquor to suppress the calcium concentration and remove the threat of scaling throughout the scrubber system.

c. Unclear Endpoint on Sulfite Analysis:

As Phase II proceeded, it became more and more difficult to achieve a clear endpoint in the sulfite lab analysis via titration with iodine solution. At first the endpoint was fuzzy and as time progressed the endpoint (blue color) would be reached only for the solution to turn clear again, require more iodine titration, reach the endpoint, turn clear again, etc. The analyst had to make a qualitative decision regarding which endpoint to choose and thus the degree of confidence in this analytical method was eroded. In addition, the normal correlation in thiosorbic chemistry of increased alkalinity with increased sulfite concentration and vice versa was compromised, diminishing the predictive capacity of the analytical data.

PROPOSED EXPLANATION FOR NOTED EFFECTS:

FORMATION OF A BISULFITE ADDITION PRODUCT

All three of the noted effects discussed above, lag time for ferrous concentration increase, increased calcium concentration, and unreliable sulfite analysis iodine endpoint, can be explained by the formation of an aldehyde-bisulfite addition product (BSAP). This hypothesis is based on the following:

In "Organic Chemistry", 2nd Edition, Morrison and Boyd note(pp. 632, 639-640) that:

[Sodium] bisulfite adds to most aldehydes ... to form bisulfite addition products:

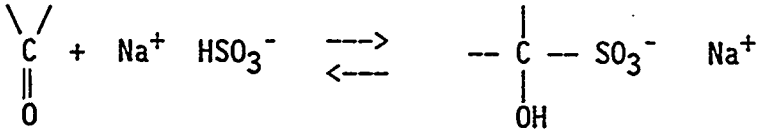

eq.(1)

, and

Like other carbonyl addition reactions, this one is reversible. Addition of acid or base destroys the bisulfite ion in equilibrium with the addition product and regenerates the carbonyl compound.

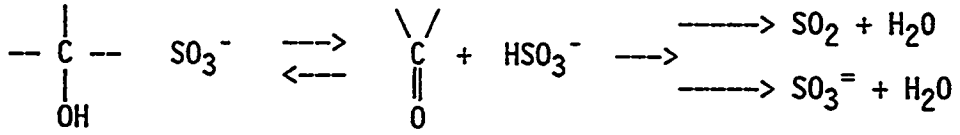

eq.(2)

There is certainly no shortage of bisulfite ions in the scrubber liquor. With hindsight, it is quite plausible to perceive initial glyoxal addition to the scrubber liquor resulting in this reaction:

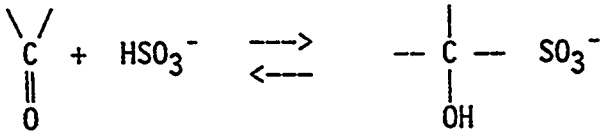

eq.(3)

The glyoxal reacts preferentially with bisulfite rather than with ferrous EDTA:

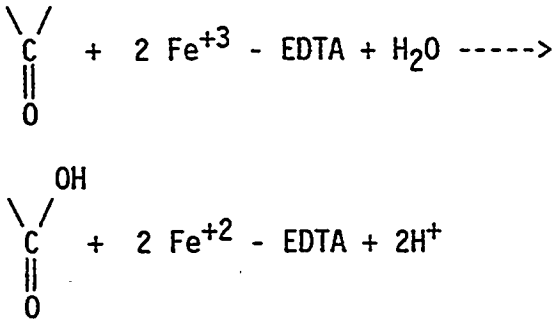

eq.(4)

That is, nucleophilic attack by bisulfite ion on the carbonyl carbon would proceed more quickly than the redox reaction, at least until reaction 4 reached equilibrium. At this point enough glyoxal would be available for the reduction of ferric chelate to ferrous chelate to proceed. This would explain the "lag" time observed upon initial glyoxal addition.

Once at equilibrium and with continued glyoxal addition it is easy to visualize a considerable amount of the bisulfite addition product (BSAP) present in the liquor. This imparts a much higher amount of anionic charge to the liquor than would normally be present. This negative charge must be counter-balanced by an increased cationic presence.

Calcium, usually suppressed by magnesium's solubility, now has impetus to stay in solution due to the increasing presence of the anionic BSAP. In order to satisfy the equilibrium requirements of reaction 4, continual addition of glyoxal would lead to a constantly increasing level of the BSAP. This would in turn lead to an increasing cationic concentration supplied primarily by calcium via lime addition. Until corrective action was taken through magnesium hydroxide addition, calcium concentrations increased with time of glyoxal addition (See Table II).

In the same manner, the equilibrium requirements of reaction 4 would apply to reactions involved in the iodine titration during sulfite analyses. Iodine oxidizes the sulfites and sulfite-like species. The endpoint of the tiration is characterized by a blue endpoint signalling an excess of iodine and the complete oxidation of the "sulfites". When the glyoxal induced BSAP is present in solution, any oxidation of bisulfite is accompanied by formation of more bisulfite. As the bisulfite component is oxidized and an iodine excess exists, the equilibrium in eq.(4) shifts to the left forming more bisulfite. The excess iodine reacts with bisulfite and the endpoint disappears (solution once again becomes clear). Upon additional iodine titration, the entire equilibrium driven scenario repeats itself and a definitive endpoint is difficult to ascertain.

ADDITIONAL EVIDENCE FOR BSAP FORMATION

Lower than Expected NOx Removals

Much of the research effort on this project was shaped by using a mathematical NOx removal model to predict NOx removals and to serve as a guide for manipulating variables. The form of this model is:

$$\text{NO Removal (NTU)} = \frac{(k_2\,[Fe^{++}]\,D_{NO})^{1/2}}{H/P_T} \quad \frac{a\ Z}{p_M\ v}$$

It can be seen that NOx removal is dependent on ferrous ion concentration ferrous concentration to the 0.5 power in this model. Testing in Phase I proved this to be very nearly the case, that is, that NOx removal in NTU's increased as the square root of the increased ferrous concentration. This was not the case when utilizing glyoxal as reducing agent. NOx removals were consistently lower for a given ferrous concentration than when sodium dithionite was used as reducing agent in Phase I. The regression analysis of Fe^{+2} vs NOx removal shown in Figure 3, shows that NOx removal in NTU's is dependent on ferrous concentration to the 0.77 power when using glyoxal as reducing agent. This result is inconsistent with the NOx removal model. It is surmised that the increased ionic strength of the scrubber slurry solution due to the elevated calcium and BSAP levels suppressed the solubility of the NO gas into the liquid phase. Possible additional impacts of increased ionic strength on the NO removal model include decreasing of the reaction rate constant, k_2, lowering the diffusivity, D_{NO}, and effecting a change in the Henry's Law Constant, H.

Another important factor in explaining lower than expected NOx removal at any certain ferrous concentration is the role of sulfites in the NOx removal mechanism. The role of sulfites is perceived as follows:

The ferrous EDTA-NO adduct formed in eq (1) reacts irreversibly with dissolved sulfite, present from absorption of SO_2, to regenerate ferrous EDTA and form primarily hydroxylamine disulfonate (HADS). HADS further reacts to form other nitrogen-and-sulfur-containing products:

$$[Fe^{+2}EDTA\text{-}NO]^{=} + 2\ SO_3^{=} + H_2O \text{ ---> } [Fe^{+3}EDTA\text{-}NO]^{-} + HON(SO_3)^{=} + OH^{-} \qquad \text{eq.(5)}$$

The rate of reaction 5 has been studied, but its mechanism is complex. The rate is proportional to sulfite concentration and to ferrous EDTA-NO concentration and inversely proportional to ferric EDTA concentration.

The rate of disappearance of ferrous EDTA-NO via reaction 5 is thought to be fast at high sulfite concentrations compared to its formation by reaction 1. In this case reaction 1 is the rate-controlling reaction. If the sulfite concentration in absorber liquid is reduced, the rate of NO removal might decrease even at constant ferrous EDTA concentration since in this case reaction 5 would also begin to control the overall rate. In addition, if enough bisulfite is tied up in the BSAP there would be a corresponding decrease in sulfite concentration predicted by the sulfite/bisulfite equilibrium reaction:

$$SO_3^{-2} + H^+ \underset{<-----}{\overset{----->}{}} HSO_3^- \qquad \text{eq.(6)}$$

This reduction in sulfite concentration could be large enough to slow down the "capture" of NO from the ferrous EDTA-NO adduct. In such a case the adduct would show up analytically as ferrous iron but would be in an "unavailable" form for NOx removal. This situation would be reflected in observing lower than expected NOx removals for any certain set of absorber conditions and ferrous concentration than the model predicts.

Effect on Sulfur-Nitrogen Compounds:

Another piece of evidence linking the formation of the BSAP to glyoxal use is the change in the relative concentrations of the sulfur-nitrogen compounds formed in the NOx removal process. Chang et al have proposed the reaction pathways for S-N compound formation shown in Figure 4. Monitoring the concentrations of four S-N compounds, HAMS, ATS, ADS, and SA during the glyoxal addition process reveals an interesting trend.

During sodium dithionite based ferric reduction in Phase I, the range and mean concentrations (in mM) of the four species during the eighth and final week of the run were as follows:

	ATS	ADS	HAMS	SA
range	(3-6)	(43-87)	(4-9)	(35-49)
mean	3.6	61	6.5	44

In contrast, during the glyoxal based ferric reduction, the range and mean concentrations (in mM) of the four species during the third week of the glyoxal run were as follows:

	ATS	ADS	HAMS	SA
range	N.D.	(22-44)	(93-165)	(30-54)
mean	N.D.	32	129	38

The dramatic twenty-fold increase in HAMS concentration (See Figure 5) is strong evidence of the reaction pathway having switched from bisulfite chemistry pre-glyoxal to non-bisulfite or hydrolysis chemistry after the addition of glyoxal. This implies that the bisulfite normally present to form ADS preferentially over HAMS has been bound up in the BSAP in the glyoxal based ferric reduction.

Effect of pH Change on Ferrous Iron Concentration:

A final piece of evidence implicating the formation of the BSAP is the change in ferrous concentration with pH in the scrubber liquor at a constant glyoxal addition rate. One of the conditions tested in week three of Phase II testing was to vary the pH from 6.5 to 7.5 to 5.5 and return to 6.5 (the normal pH of the system) at a constant ferrous concentration (15 mM) and observe how NOx removal with pH (See Figure 6).

A relatively stable level of ferrous concentration (10-15mM) was maintained with constant glyoxal addition at the pH = 7.5 level phase. The ferrous concentration began to drop to near the 5mM during the latter half of the pH = 5.5 phase. At this point research personnel had strongly suspected the presence of the BSAP and it was decided to suspend glyoxal feed before raising the pH back to the 6.5 level. If the BSAP was present, a noticeable increase in Fe^{+2} would be forthcoming, an increase attributable solely to glyoxal freed from the BSAP and not from fresh glyoxal feed. As Figure 3 amply demonstrates, the rise in ferrous iron was striking and immediate. Within an hour of incrementally beginning to raise the pH from 5.5, ferrous iron was at 24 mM,

peaking at 30 mM at the two hour mark when the pH = 6.5 level was achieved. The Fe^{+2} level stayed over 20 mM for a full seven hours after the pH increase began and remained over 12 mM for fifteen hours after glyoxal feed had been stopped. This behavior was strong evidence for the existence and the mechanism of operation of the BSAP.

During the pH = 7.5 level phase the BSAP formation equation was at equilibrium, with a constant glyoxal feed and a relatively stable.

At equilibrium, a steady state existed wherein enough newly added glyoxal was available to maintain the reaction in eq.(4). Upon lowering the pH to 5.5, the concentration of the bisulfite ion increased, forcing the reaction in eq.(3) to the right and effectively tying up the glyoxal and making it unavailable for ferric iron reduction. The Fe^{+2} began to drop even with glyoxal addition to the system. Once again it seems that glyoxal reacts preferentially with bisulfite rather than with the iron chelate.

At lower pH conditions there is a higher concentration of bisulfite present due to the sulfite/bisulfite equilibrium reaction:

$$SO_3^{-2} + H^+ \underset{<-----}{-----\!>} HSO_3^- \qquad \text{eq.(7)}$$

Due to the greater (100X) hydrogen ion concentration at pH 5.5 vs pH 7.5 the equilibrium previously established in eq (3) now shifts the reaction to the right because of increased bisulfite concentration. At low pH, the amount of glyoxal present for ferric reduction is diminished by increased formation of the BSAP.

Conversely, upon increasing the pH, the hydrogen ion concentration is decreased tenfold from pH = 5.5 to pH = 6.5 resulting in decreased bisulfite concentration. Now reaction 3 is shifted to the left to keep the equilibrium satisfied. The BSAP formation is reversed to keep the bisulfite ion in equilibrium. This causes enough glyoxal to be "freed" into the solution to raise the Fe^{+2} sharply. Gauging from the

persistence of the Fe^{+2} in solution after the suspension of glyoxal feed, the BSAP must be stable, long lived, and of a relatively high concentration. Perhaps BSAP increases in strength linearly under constant pH conditions with glyoxal concentration.

SUMMARY:

Despite the attractive features of using glyoxal as a chemical reducing agent in Thiosorbic based iron chelate simultaneous SO_2/NOx removal, the formation of an aldehyde-bisulfite addition product resulted in the following undesirable side-effects:

- A noticeable "lag time" between initial glyoxal addition and a commensurate chemical reduction of ferric-EDTA to ferrous- EDTA. In general, poorer utilization of glyoxal for regeneration of the iron chelate than would be stoichiometrically predicted.

- Increased calcium concentration in the scrubber liquor as a result of charge balance requirements to offset the buildup of the anionic BSAP.

- Effect on endpoint of sulfite analyses, diminishing the usefulness of that analyte as a monitoring and predictive tool.

- Lower than expected NOx removal for any ferrous iron concentration than would be predicted by the NOx removal model due to:

  * increased ionic strength of the solution caused by the elevated cationic calcium levels and anionic BSAP levels.

  * decreased activity of the sulfites to cleave the ferrous EDTA-NO adduct of the NO, thus rendering some ferrous iron unavailable for NOx removal.

- Decreasing glyoxal utilization with decreasing pH.

SUGGESTED FUTURE RESEARCH STUDIES:

- Formation rate of the bisulfite addition product, especially as a function of pH.

- Analytical methods development to better quantify free glyoxal, the bisulfite addition product, and bisulfite and sulfite ions.

- Glyoxal utilization studies as a function of ferrous concentration and NOx removal.

- Determination of the effects of increased ionic strength on the variables of the NOx removal model and on the activity coefficients of the major chemical species.

FIGURE 1

Miami Fort Pilot Plant
3.1.2.1 Phase 2 Start-Up
Effect of Glyoxal Feedrate and O2
on Recycle Tank Fe+2 Concentration

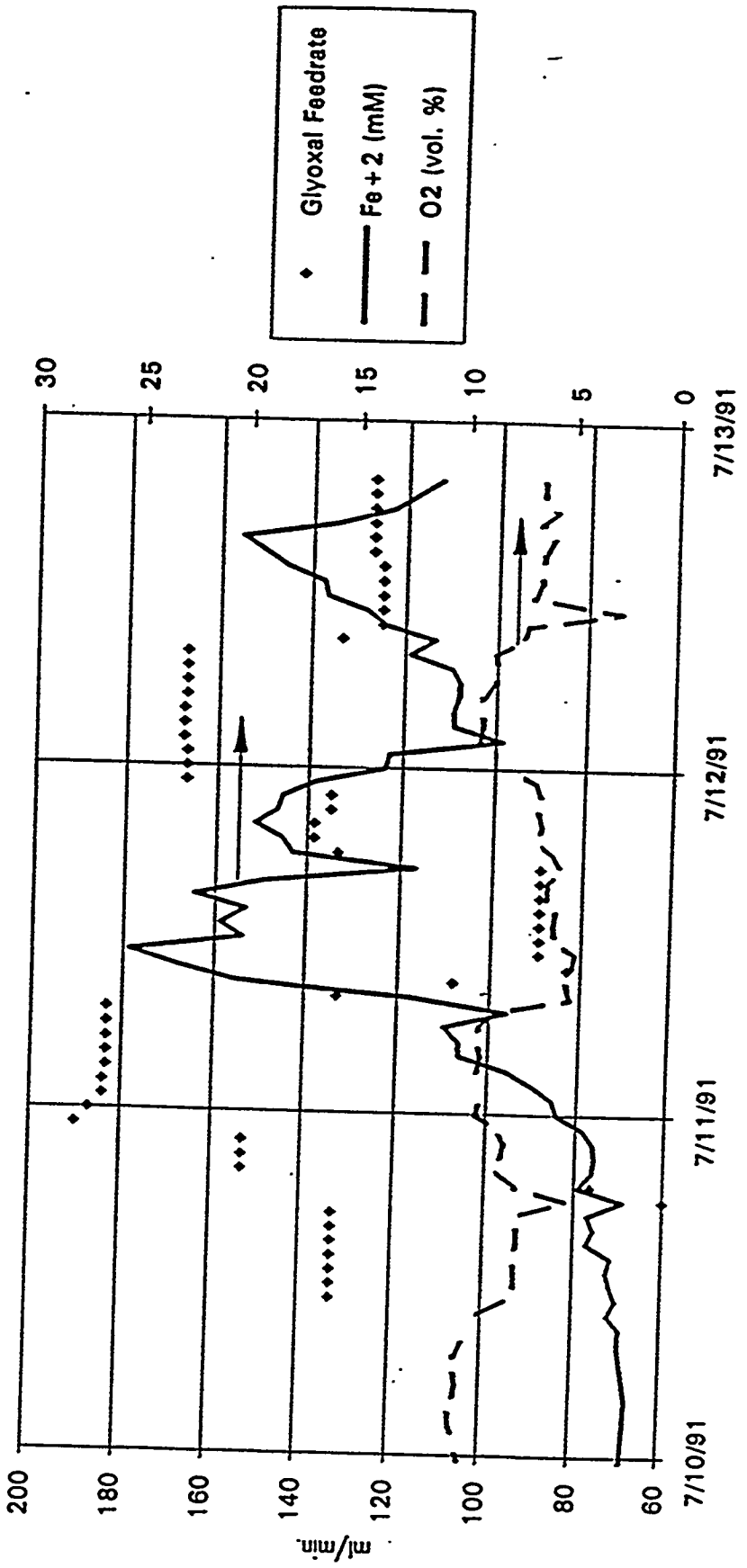

Figure 1

Figure 1

FIGURE 2

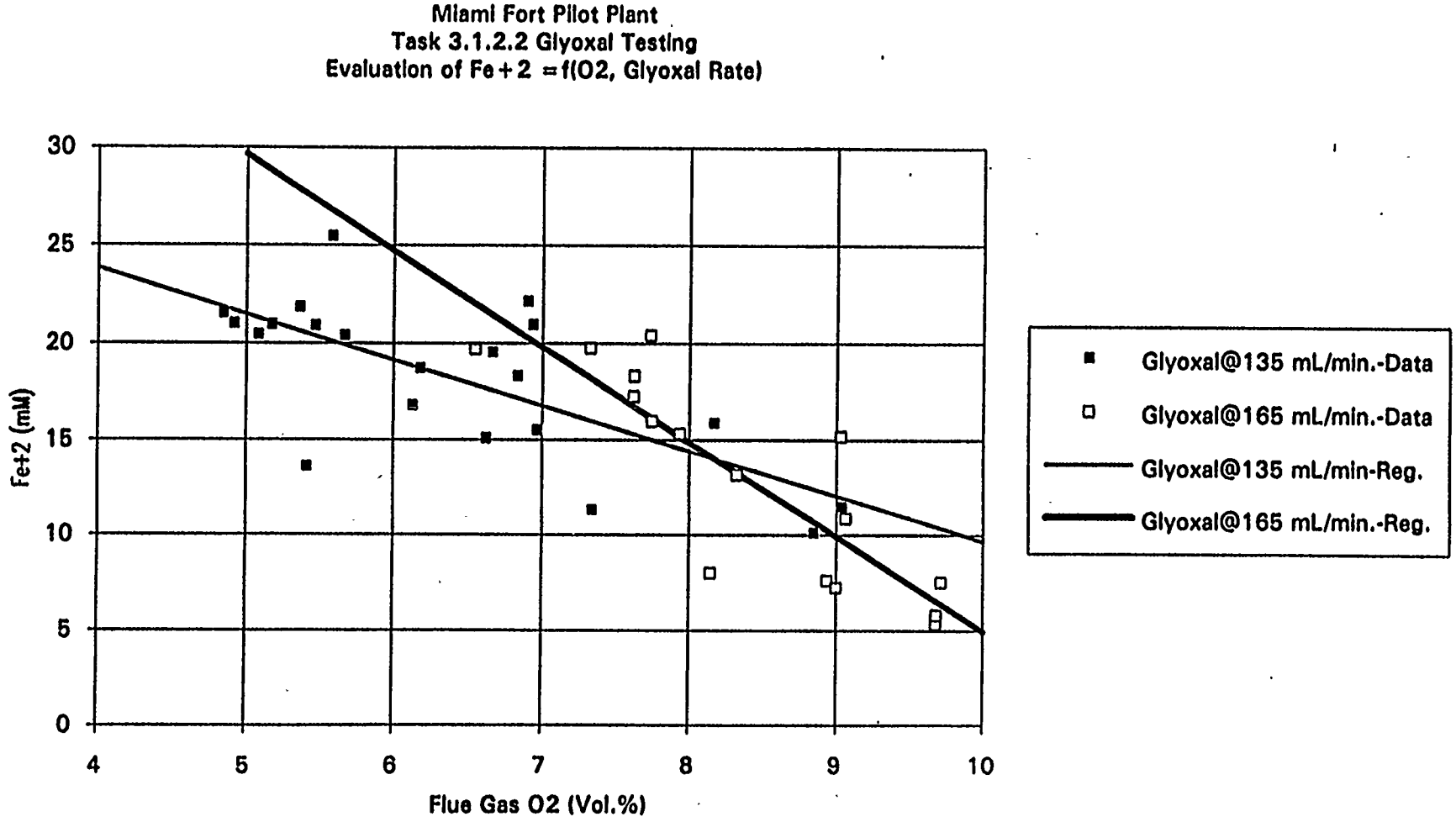

Figure 2

Figure 2

FIGURE 3

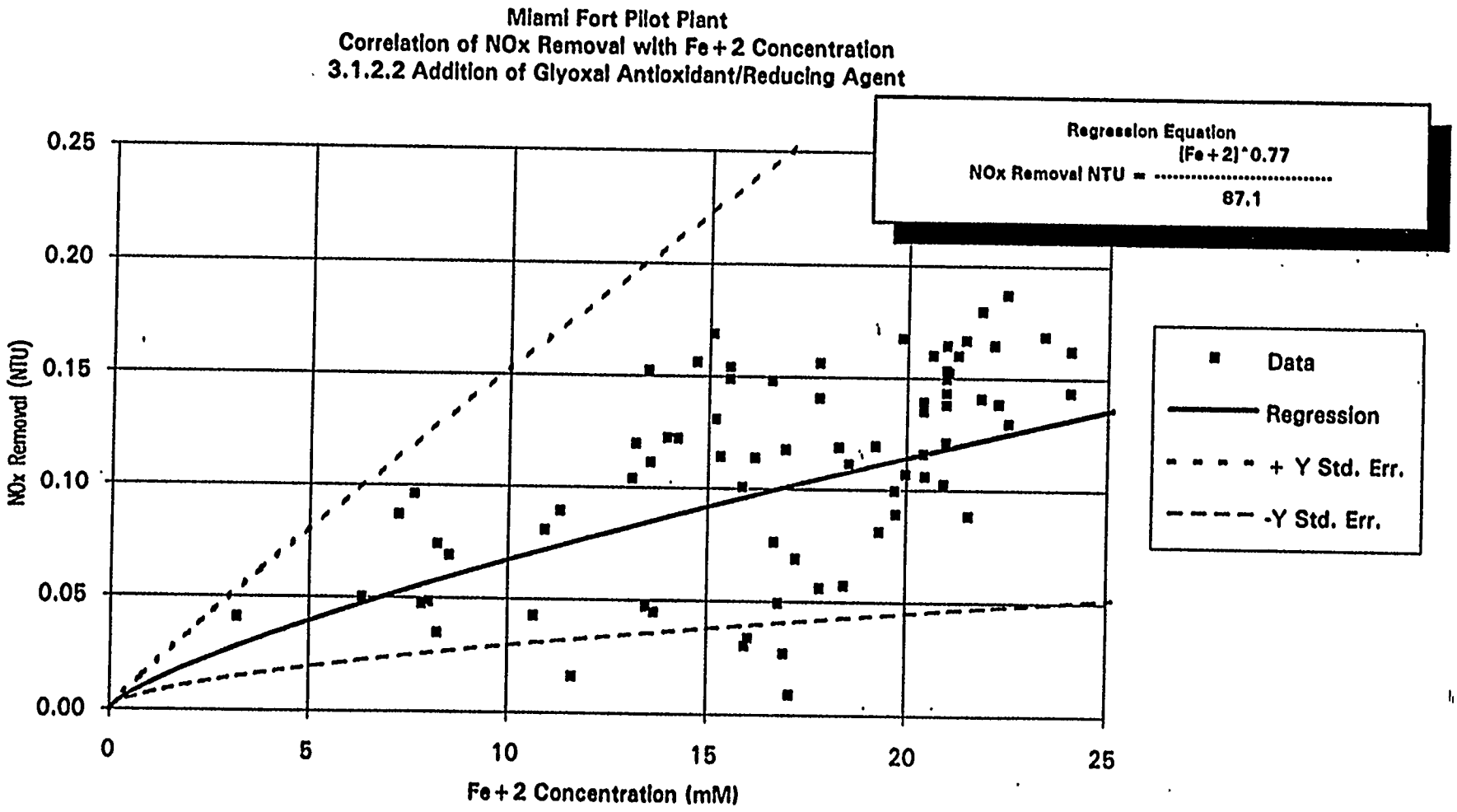

Figure 3

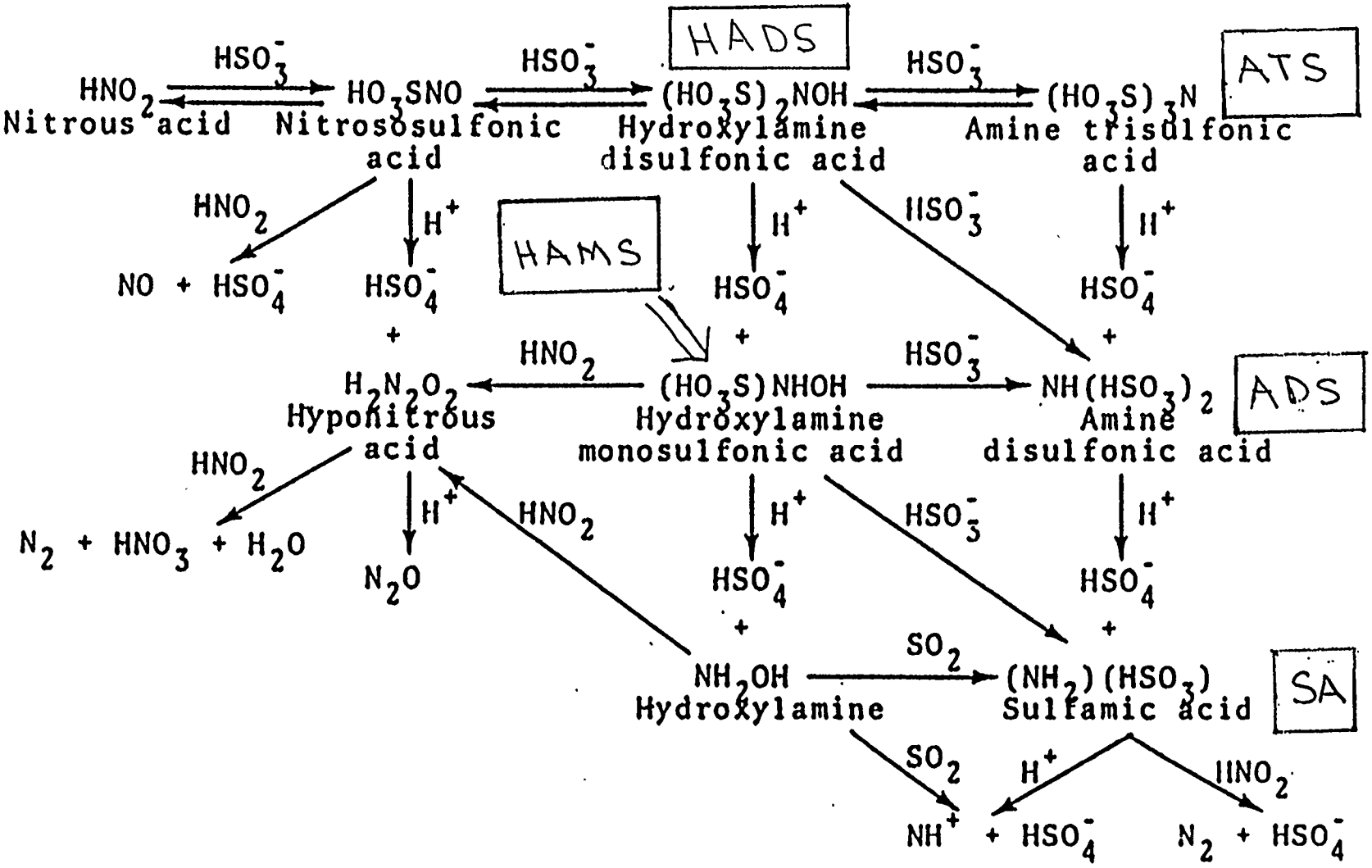

III-33d

Figure 4

FIGURE 4 **Summary of reactions that can take place as a result of interactions between nitrite and bisulfite ions.**

Figure 4

FIGURE 5

Miami Fort Pilot Plant
Task 3.1.2.2 Glyoxal Testing
Trend of S-N Compounds and Ca+2

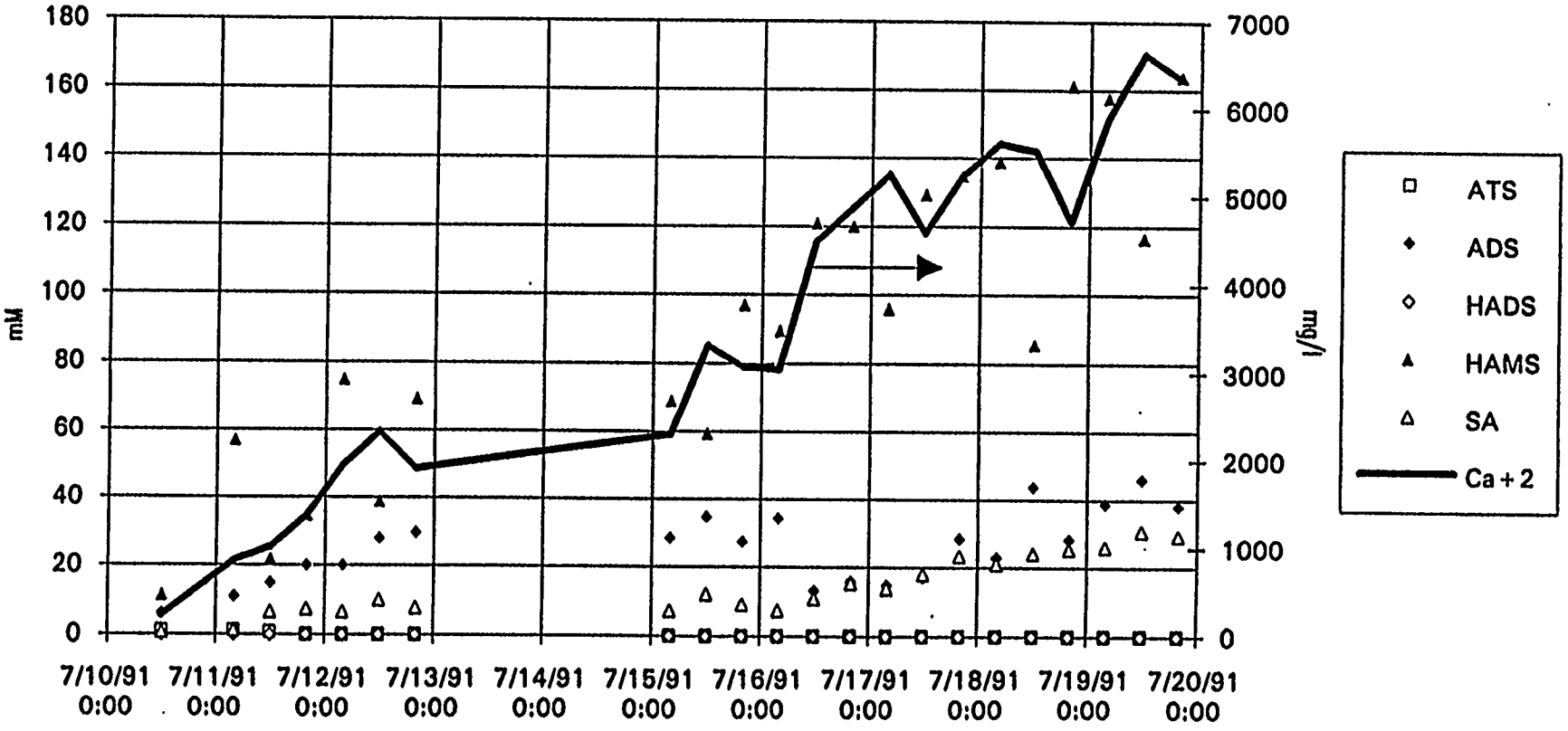

Figure 5

FIGURE 6

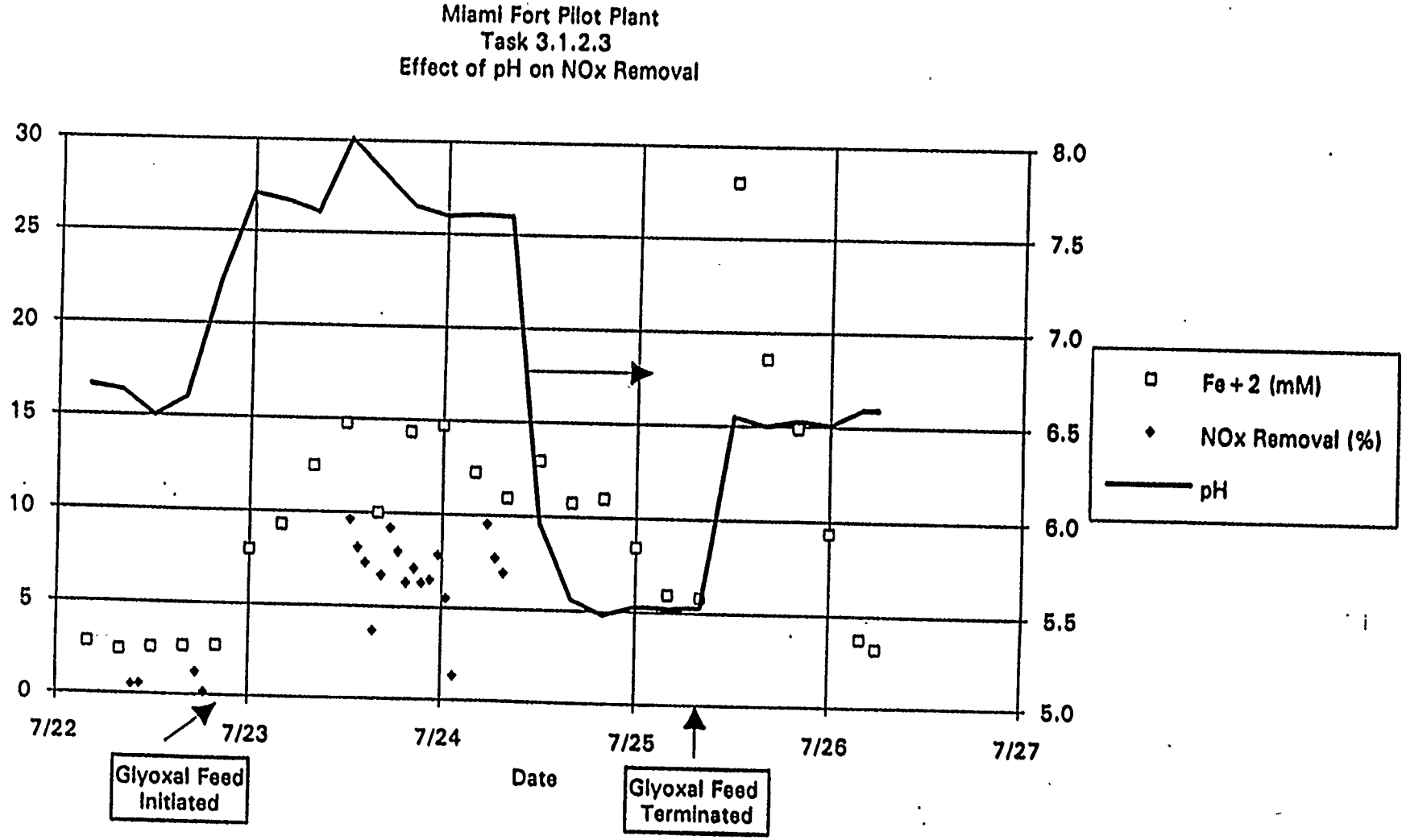

Figure 6

TABLE I

DATE	TIME	Ca. CONC.	t / HR.	NOTES
5-28-91	1200	146	0	
	2000	176	8	
5-29-91	400	232	16	
	1200	262	24	
	2000	372	32	
5-30-91	400	368	40	
	1200	663	48	
	2000	336	56	
5-31-91	400	328	64	
	1200	580	72	
	1900	794	79	END PHASE I

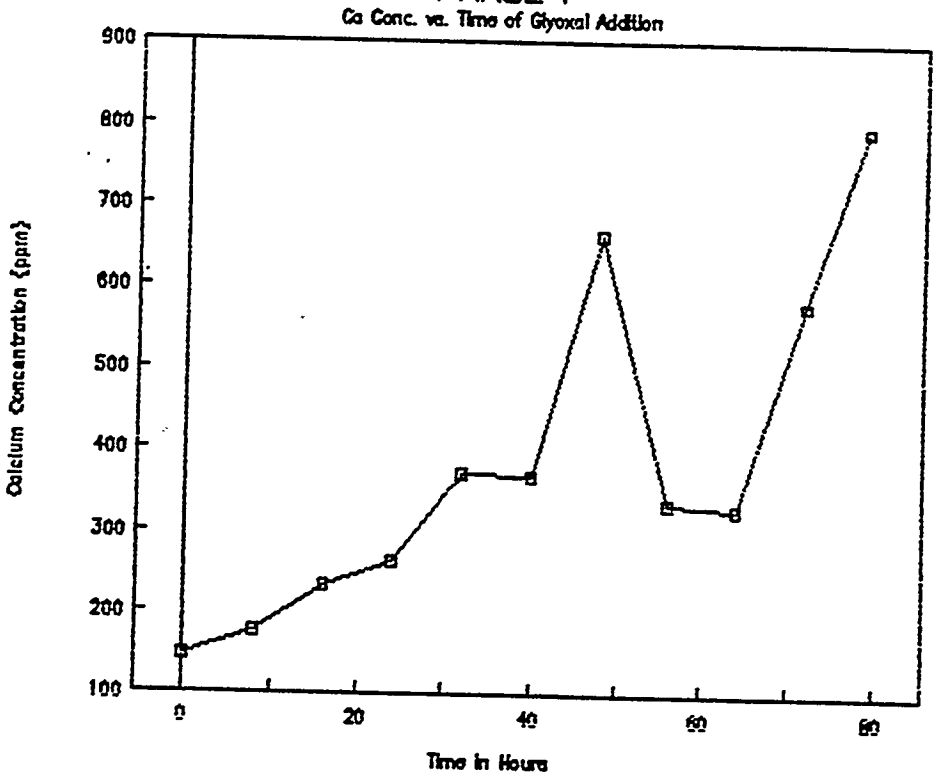

Table 1

TABLE II

DATE	TIME	Ca. CONC.	t / HR.	NOTES
7-08-91	1300	59	-	BASELINE
7-10-91	1200	211	0	
	2000	322	8	
7-11-91	0400	834	16	
	1200	985	24	
	2000	1345	32	
7-12-91	0400	1927	40	
	1200	2038	48	
	2000	1888	56	
7-15-91	0400	2302	60	
	1200	3314	68	
	2000	3073	76	
7-16-91	0400	3043	84	
	1200	4493	92	
	2000	4880	100	
7-17-91	0400	5255	108	
	1200	4590	116	
	2000	5235	124	
7-18-91	0400	5605	132	
	1200	5520	140	
	2000	4718	148	
7-19-91	0400	5898	156	
	0800	6948	160	
	1200	6634	164	
	2000	6353	172	STOP GLYOXAL FEED
7-22-91	0400	5819		START MgOH2 ADDN
	1200	2453		
	2000	4050		pH = 7.1
	2200			pH = 7.5
	2300			RESUME GLYOXAL FEE
7-23-91	0400	2580	176	
	1200	4893	184	
	2000	4333	192	
7-24-91	0400	3949	200	
	1200	2821	204	pH = 5.5
	2000	3834	212	
7-25-91	0400	4527	220	
	0800		224	STOP GLYOXAL FEED
	1000			pH = 6.5
	1200	3508	224	
	2000	3533		
7-26-91	0400	3453		
	0600	3305		

Table 2

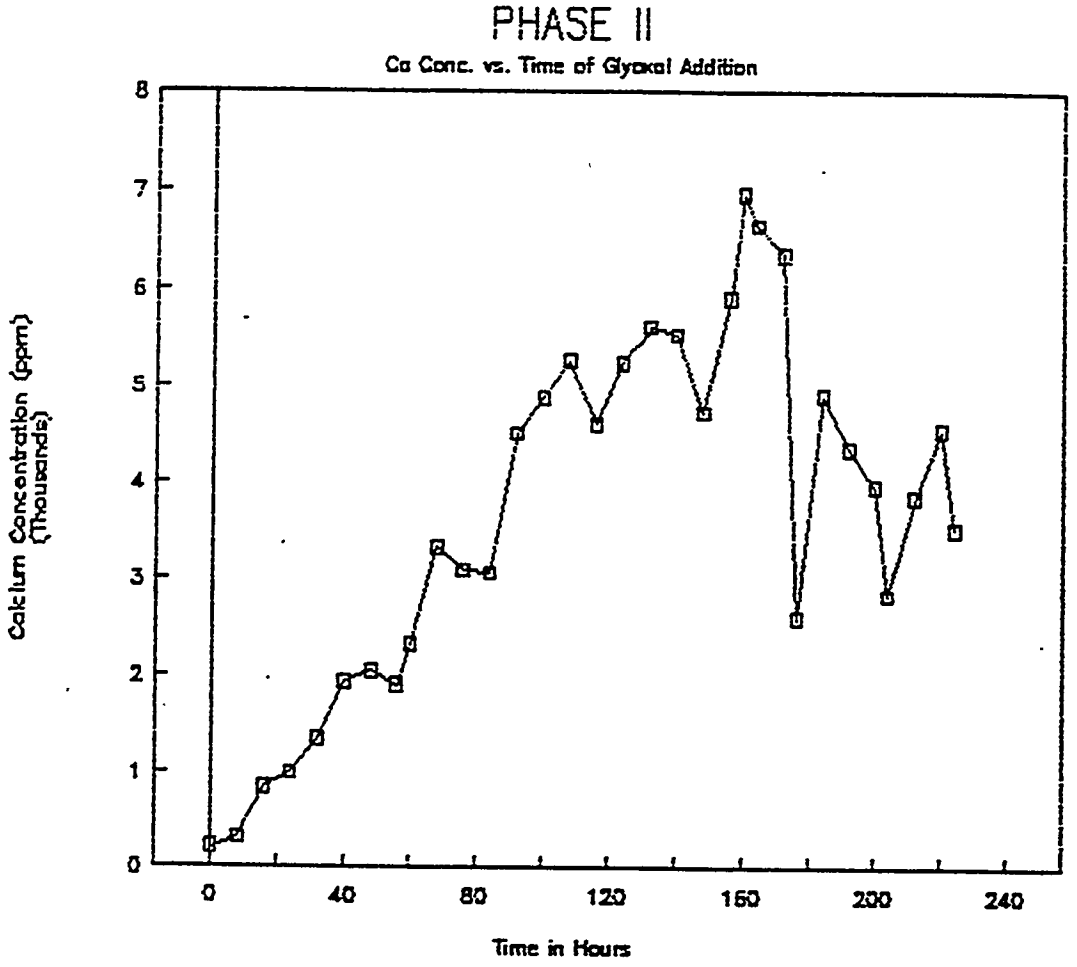
PHASE II
Ca Conc. vs. Time of Glyoxal Addition
Calcium Concentration (ppm)
(Thousands)
8
7
6
5
4
3
2
1
0
0
40
80
120
160
200
240
Time in Hours

2. NOx Removal Model Verification

A major component of this project has been the derivation, application, and verification of a NOx (or NO) removal model based upon ferrous chelate addition to the scrubbing liquor of a magnesium enhanced lime (MEL) flue gas desulfurization (FGD) process. This model is an equation that relates NOx removal to absorber operating conditions, including flue gas velocity, absorber liquid flow rate, absorber liquid ferrous EDTA concentration, gas-liquid interfacial area, and absorber height. The model serves as the basis for correlation of NOx removal data obtained in the test program. The complex process of NOx removal is simplified with this useful tool. Section H shows how the model equation was derived. The previous "Summary of Testing" sections for Phase I and Phase II describe using the model for correlation of NOx removal data.

This section summarizes the methodology utilized in model verification based upon the results of testing at the pilot (1.5 MW) scale. The parameters of interest are studied in detail. Correlations are established from the removal data and the values of constants obtained from the correlations compared with those expected based on the model. The statistical significance of the correlations was high and the constants obtained from the correlations of NOx removal data agreed well with those expected based on the model. The model was then used as a guide to set up absorber configurations for Phase III tests and to predict NOx removals that would be obtained in these tests.

Model Parameters

The derivation of the NOx removal model equation is based upon well established scientific and engineering precepts. The incorporation of several chemical engineering principles via a rigorous mathematical treatment resulted in the NOx removal model equation used in this project. Its derivation is summarized in section H. The resulting

equation includes four parameters, ferrous EDTA concentration, absorber flue gas velocity, absorber liquid rate, gas-liquid interfacial area, and absorption zone length. These parameters can be varied so that the NOx removal data generated from the scrubber NOx analyzers can be correlated back to the equation for verification purposes. In addition, the results of manipulation of one or more parameters can be studied for their effect on NOx removal and thus serve as a readily available "fitness" test for the model.

The NOx removal equation is:

$$\text{NO Removal (NTU)} = \frac{(k_2\,[Fe^{++}]\,D_{NO})^{1/2}}{H/P_T} \quad \frac{a\ Z}{p_M\ v}$$

where:

NTU = -ln (1 - % removal/100) = NO removal expressed as number of transfer units, dimensionless

k_2 = reaction rate constant for the second-order reaction between dissolved, unreacted NO and ferrous-EDTA. This constant has a value of 2.2445×10^{12} ft^3/lb-mole-sec @ 122^oF.

$[Fe^{++}]$ = ferrous-EDTA concentration in absorber liquid in mM.

D_{NO} = diffusivity of dissolved NO in absorber liquid. The value of this parameter is 4.4×10^{-8} ft^2/sec @ 122^oF.

a = gas-liquid interfacial surface area per volume of contact zone, expressed as ft^2/ft^3.

Z = length of gas-liquid contact zone in feet.

p_M = molar density of the flue gas = 2.404×10^2 lb-mol/ft^{-3} at 50^oC and 1 atm.

v = flue gas velocity in absorber in ft sec^{-1}.

p_T = total pressure. This parameter has a value of 1 atmosphere.

H = Henry's Law constant for NO in water. This constant has a value of 11383.25 ft^3/lb-mole @ 122^oF. (if flue gas is saturated with water vapor, the effective solubility of NO in water is 12813.56 ft^3/lb-mole @ 122^oF.)

Process Parameters

Use of the model is facilitated by assuming the following parameters to be constant: k_2, D_{NO}, H, p_T, and p_M. Each of these parameters is expected to be constant at fixed temperature and pressure. The absorber operating pressure is essentially atmospheric, and absorber temperature is fixed at about 122^oF, the adiabatic saturation temperature of the flue gas entering the absorber.

This narrows process parameters to manipulate to four: flue gas velocity, ferrous-EDTA concentration, interfacial surface area, and length (or height) of contact zone. Varying one or more of these factors and noting the change in NOx removal from one set of conditions to another provides a means to test the model.

For removal efficiency of 20% or less, removal efficiency expressed as a fraction (e.g., 0.2 or 20%) is nearly equal to removal efficiency expressed as NTU. In this range of removal, increases in NTU translate directly into increases in percent removal efficiency. For percent removal greater than 20%, percent removal increases less than NTU as shown in the table:

Percent removal	NTU
10	0.105
20	0.223
30	0.357
40	0.511
50	0.693
60	0.916
70	1.204
80	1.609
90	2.303

Examination of the model equation indicates that removal efficiency as NTU is expected to increase with the square root of the ferrous-EDTA concentration. This suggests a practical limit on ferrous EDTA concentration since a doubling its concentration would result in an increase in removal efficiency of only 1.4.

Removal efficiency as NTU is expected to increase in direct proportion to the gas-liquid interfacial area. This suggests a more efficient means of increasing removal efficiency since various combinations of spray nozzles and tower packing can be utilized to increase interfacial area.

Removal efficiency as NTU is expected to increase in direct proportion to absorber height, particularly as it applies to the height of packing installed. Although it is true that increasing the height of a spray tower will increase removal efficiency it is more economical and efficient to increase the height or depth of tower packing since the increase in interfacial area is so much greater.

Removal efficiency as NTU is expected to decrease in inverse proportion to absorber gas velocity. In absorber operation this requires decreasing flue gas velocity in order to increase removal efficiency. A 50 percent reduction of absorber gas velocity would thus double removal efficiency.

For pilot plant operation, the ferrous-EDTA concentration was maintained at about 15 mM. Tests were conducted using four different absorber packings at a height of six feet. Tests were also conducted without packing using fine spray nozzles. During tests in this phase, the spray nozzles and packing were used to vary interfacial area. Flue gas velocity and absorber liquid flow rate were also varied.

Forms of Correlation NOx Removal Data

Various configurations of spray nozzles, packing, and flue gas velocities and liquid rates were tested for their effects on NOx removal. The reader is referred to the "Summary of Testing" section of this report for specific configurations tested. The data resulting from these tests were subjected to regression analyses.

The following equations were used to correlate the data:

$$\text{NTU @ 15 mM Fe++} = \text{NTU} * (15/[\text{Fe++}], \text{mM})^{1/2}$$

$$\text{NTU @ 15 mM Fe++} = (v, \text{ft/sec})^{a} * (L, \text{gpm})^{b} * 10^{c}$$

$$\log \text{NTU @ 15 mM Fe++} = a * \log(v) + b * \log(L) + c$$

where v = flue gas velocity in feet per second
L = liquid recycle rate in gallons per minute

Multiple linear regression was applied using the last equation to determine the value of the constants a, b, and c for each series of tests.

Gas pressure drop data obtained during the NOx removal tests was also correlated with flue gas velocity and liquid rate using the following empirical equation:

$$\text{Packed Bed Pressure Drop (inches WC)} = v^{A} * L^{B} * 10^{C}$$

This equation was made linear by taking the logarithm of both sides; multiple linear regression was then used to determine the value of the constants A, B, and C. The pressure drop equation applies only to the range of gas and liquid rates tested. The equation <u>cannot</u> be used to estimate pressure drops at low liquid rates or for a dry packing.

The pressure drop correlation was performed because of its operational significance. Pressure drop through the packing limits the flue gas velocity that can be achieved. In addition, at very high pressure drops loading and flooding of the packing occurs resulting in liquid entrainment and limitations on effectiveness of packing on NOx removal.

Effective interfacial areas of the packing was also determined by correlation of the data. Rearrangement of the model to solve for "a", the interfacial area resulted in the following equation:

$$a_{eff} = 340.8 * NTU * v * [Fe^{++}]^{-0.5} * Z^{-1}$$

Entering the appropriate values from pilot plant results in the right side of the equation yields the effective interfacial area for any set of absorber conditions and allows comparison of effective interfacial areas of various packing and among each other and with known dry surface areas. For packing, effective interfacial area is expected to depend only on packing type and on liquid flow rate and is expected to be independent of gas velocity for the range of velocities tested.

The a_{eff} calculated with the above equation includes the effective interfacial areas of the spray above the packing, and the rain falling from the bottom of the packing. A full evaluation of the effective interfacial area contributions of PN Fill packing and spray "end effects" will be discussed later.

Summary of Correlation Data

Tables 1 - 8 of the "Summary of Testing" section of this report gives the NOx removal and pressure drop data obtained with each of the four packing tested and for the fine spray testing. These data were used in the correlations. Figure 1 shows the basis for the correlation data associated with the interfacial area and the normalization procedure for the ferrous-EDTA concentration to 15 mM. Figure 2 summarizes results of the correlations and the values of the constants a, b, c, A, B, C for NOx removal and pressure drop. Figure 3 contains a table of interfacial areas calculated for the 2" saddle packing generated from the testing data as well as the correlation coefficients and regression constants associated with it.

Model Verification Criteria & Results

Two approaches were used in selecting and applying verification criteria regarding the model correlations. One approach was to make straightforward generalizations from the model equation and to see how well the generated data "fit" the model. The other approach was to peruse the chemical engineering literature for mass-transfer generalizations and whatever published data was available that was applicable to the testing performed. The model correlations were then subjected to comparison with these accepted standards. Few definitive criteria actually exist in the realm of gas-liquid mass-transfer operations and therefore the bulk of the model verification process consists of approximations and general tendencies. Nevertheless, the correlations should fall within reasonably close agreement to these broad established boundaries to justify model verification.

Perry's Chemical Engineering Handbook, 6th Edition, McGraw-Hill, 1984, is cited in the following sections. Its gas liquid mass-transfer sections (Chapters 14 & 18) were drawn on to provide the literature verification criteria.

NOx or NO Removal:

For NOx removal recall that the overall model equation is

$$\text{NO Removal (NTU)} = \frac{(k_2\,[Fe^{++}]\,D_{NO})^{1/2}}{H/P_T} \quad \frac{a\ Z}{p_M{}^{v}}$$

and the statistical correlation form equation is

$$(1)\quad \text{NOx Removal (NTU)} = FGV^{a} * L^{b} * 10^{c}$$

A glance at the model equation shows that NOx removal should be expected to be a function of flue gas velocity to the minus one power.

The values for coefficient a in Figure 2 (-0.72 to -1.13) show relatively good agreement with minus one. The only exception is for the #3 saddles, a special case in which NOx removal actually increased with an increase in absorber gas velocity. A detailed explanation for this exception to model behavior is given in the "Summary of Testing" section of this report. Inspection of the model equation reveals that for this close agreement with the velocity coefficient to occur, the interface area (a) the model equation would need to be constant under varying velocities for any packing. The literature states, "Whereas the interfacial area generally increases with increasing liquid rate, it apparently is relatively independent of the superficial gas mass velocity below the flooding point."

In regards to the liquid flow rate L, packing interfacial area is expected to be independent of the gas rate and to increase as the 0.2-0.5 power of L. The values for coefficient b in Figure 2 (0.35 to 0.62) are in good agreement with these values with the exception of the #3 saddle packing.

Pressure Drop:

For pressure drop the correlation form equation is

(2) Packed Bed Pressure Drop (inches WC) = $FGV^A * L^B * 10^C$

Verification of the correlation form equation for pressure drop is not as direct as it was for NOx removal. A more indirect approach must be taken for which the packed tower terms "loading" and "flooding" are necessary. For most random packing, the pressure drop experienced by the gas is influenced by the gas and liquid flow rates. The phenomena of loading and flooding are usually defined by examination of the slope of the line drawn as a plot of the log of the gas velocity vs. the log of pressure drop over height. The slope of this line for dry packing is usually in the range 1.8 to 2.0. Thus pressure drop for dry packing is proportional approximately to the square of the gas velocity. At a fixed gas

velocity, the gas-pressure drop increases with increased liquid rate. For all liquid rates, a zone is reached where pressure drop is proportional to a gas-flow power distinctly higher than 2. This zone is called the loading zone. As the liquid holdup increases, the change in pressure drop is quite great with only a slight change in gas rate. The phenomenon is called flooding and is analogous to entrainment flooding in a plate column. The slope of the line rises almost exponentially at this point. Initial loading and flooding are frequently determined by the change in slope of the pressure-drop curves rather than through any visible effect. It is not practical to operate a tower in a flooded condition. Most towers operate just below, or in the lower part of, the loading region.

Pressure drop at flooding for commonly used packing is around 2 inches WC per foot of packing. For operation at about 50% of flooding the pressure drop is roughly 0.5 inches WC per foot of packing and at 70% of flooding the pressure drop will be about one inch WC per foot of packing.

For the most part, the pressure drop in the packed tower was between 2 and 6 inches WC indicating that the absorber operated in the approximate range of 35% to 70% of flooding. This would be in the loaded but not yet flooded zone. The pressure drop correlation data from Figure 2 support this range of operation with a gas coefficient A ranging from 2.67 to 4.25. Once again the exception is the #3 saddle packing which carries a coefficient of 2.15, barely higher than dry packing. This is consistent with the premise that this packing wetted least effectively of all those tested.

An evaluation of the liquid coefficient B requires its comparison with the gas coefficient A. "For gas flow through dry packing, pressure drop may be estimated by use of the orifice equation, with suitable correction for the presence of liquid. On this basis, Leva developed the following correlation for pressure drop in irrigated packed beds:

$$\text{Delta } P = C_2 * 10^{C_3 u_t} * p_g * U_t^2,$$

where p_g = gas density, C_2 and C_3 are constants, u_t = the superficial liquid velocity and U_t = the superficial gas velocity". Although the pressure drop model correlation equation and the Leva pressure drop equation are not similar, is interesting to note the relative influence of gas and liquid rates in each. The gas rate factor in the Leva equation exerts far more influence than does the liquid rate factor, especially considering that the reported values for C_3 are all on the order of 10^{-2}. A comparison of A and B in Figure 2 reveals that here too, the influence exerted by the gas rate factor A is significantly greater than that of the liquid rate factor B.

The correlation data thus obtained with respect to pressure drop measurements is consistent with established norms and shows that the absorber behaved in the classic manner of a packed tower and generated pressure drop regression data which at least indirectly supports the NOx removal model verification.

Interfacial Area:

Recall from page 4 of this section that another correlation drawn from the results of testing was a result of the calculation of the "effective" or wetted interfacial areas of the various packing tested.

Effective area should not be confused with 'wetted area'. While film flow of liquid across the packing surface is a contributor, effective area includes also contributions from rivulets, drippings, and gas bubbles. Because of this complex physical picture, effective interfacial area is difficult to measure directly.

As stated above, a mathematical approach was taken to arrive at a "calculated" effective interfacial area. Rearrangement of the model to solve for "a", the interfacial area, coupled with substitutions for the value of all constants including Z (6 feet) results in the following equation:

$$a_{eff} = 61.27 * NTU * FGV * [Fe^{++}]^{-1/2} \text{ mM}$$

Entering the appropriate values from pilot plant test results into the right side of the equation yields the "calculated" effective interfacial area for any set of scrubber conditions and allows the comparison of effective interfacial areas of various packing and how these calculated values compare to the assigned dry interfacial surface areas. A correlation can also be drawn between the calculated areas and liquid and gas rates.

Although the interfacial area is independent of the flue gas velocity below the flooding point, NOx removal is inversely proportional to flue gas velocity and therefore highly dependent upon it. In order to arrive at a calculated effective interfacial area it is necessary to take into account NOx removal and the associated gas velocity as well as the ferrous-EDTA concentration in the absorber liquid.

Figure 3 shows the calculated effective interfacial areas arrived at for various gas velocities and NTU's for the #2 saddle packing. These calculated effective areas (15.0 - 57.6 ft^2 ft^{-3}) are on the same order of magnitude as the assigned dry interfacial area of 33 ft^2 ft^{-3} for this packing. These are an acceptable range of results considering the previous discussion of contributions to the effective area and provide a general verification of the removal model.

The most convincing model verification data is generated by plotting the calculated effective areas versus the liquid recycle rates in effect at the time. A correlation can then be drawn between the calculated effective interfacial area and the liquid rate and compared to the reported literature values and approximations. Figures 4, 5, and 6 show the results of this approach for the three packing that were thoroughly tested.

The literature reveals that studies undertaken to date consistently show the effective area to be proportional to the liquid rate L to roughly the 0.5 power. The results of the correlations reveal the effective areas to be proportional to L to: the 0.515 power for the #2 saddle packing, the 0.566 power for the snowflake packing, and the 0.477 power for the PN Fill packing. These correlations show excellent agreement with the published results and serve as powerful evidence for the model verification.

SO_2 Removal Data:

Absorption of NO with ferrous EDTA is considered to be liquid-film controlled. In contrast, SO_2 absorption is considered to be gas-film controlled. The solubility of SO_2 is about 2000 times greater than that of NO. That is, the Henry's law constant for SO_2 is about 2000 times less than that for NO. The presence of 50-100 mM sulfite in absorber liquid at pH 6.5 which can react with absorbed SO_2 produces a large enhancement factor for SO_2. These two factors combine to reduce the liquid side resistance for absorption of SO_2. The gas-side resistance then becomes the controlling resistance for absorption of SO_2.

The difference in control mechanisms between absorption of NO and SO_2 has several implications. One is that the percent removal of SO_2 will be greater than the percent removal of NO since the gas side coefficient will generally be much greater than the liquid side coefficient. The expression for the removal efficiency for SO_2 can be written as:

SO_2 removal (NTU)

$$NTU = -\ln(1 - \%\ \text{removal}/100) = k_g \frac{a\ Z}{p_M\ v}$$

where k_g is the gas-phase coefficient.

Another important implication is that removals of NO and SO_2 will vary differently with flue gas velocity. For NO, removal should clearly increase as flue gas velocity is decreased since the mass transfer coefficient does not depend on gas velocity. In contrast for SO_2 removal, the gas-side mass transfer coefficient k_g depends strongly on gas velocity. This coefficient would be expected to vary with the 0.5 to 1.0 power of gas velocity. Subsequently a decrease in gas velocity would also decrease k_g and SO_2 removal would increase only slightly (since the decrease in k_g in the numerator partially compensates for the decrease in v in the denominator). Similarly, SO_2 removal would decrease only slightly as flue gas velocity is increased. In contrast, NO removal clearly would be expected to decrease with an increase in gas velocity.

The practical consequence of these removal differences is that since velocity has a less pronounced effect on SO_2 removal and ferrous-EDTA has no effect, the major effect on SO_2 removal in NOx testing will be the dramatic increase in interfacial area and height of contact zone, Z, introduced by the tower packing. This indeed turned out to be the case as SO_2 removals consistently approached 100% with all packings tested. This was not the case for the open spray tower tests. The predictable behavior of the SO_2 removal using the same removal equation basis implies that the NOx removal trends are real and that the model works.

Utilization of Model Predictions for Phase III Testing

Having applied verification criteria successfully, the next step in the process is to utilize the NOx removal model as a predictive tool and extrapolate the results of previous testing to reconfigure the absorber with the intention of achieving a predetermined NOx removal based on that configuration. The good model correlation achieved in Phase II verified the need to manipulate only four variables: interfacial area, ferrous-EDTA concentration, height of contact zone, and flue gas velocity.

As a practical and economic matter, the ferrous-EDTA will be maintained at the historical 15 mM level. The height of contact zone, Z, will be doubled from 6 feet to 12 feet (See Figure 7) which is expected to double NOx removal NTU's with the reservations expressed below. This will leave only the interfacial area and the flue gas velocity to vary.

Prediction of "a" is a major challenge in scale-up/prediction of gas absorption. When packings are used, "a" depends primarily on absorber liquid flow rate. Therefore, the effect on removal of absorbing liquid flow rate is contained in "a". For absorption using spray nozzles, "a" depends on the size and type of nozzle, the absorber liquid flow and the flue gas velocity. These make variables prediction of interfacial area very uncertain when spray nozzles are used exclusively. Spray nozzle use also imparts a degree of uncertainty when using packings. Determining the contribution of spray nozzles, or more precisely the spray zone, on the "a" and Z terms of the model is difficult. Effective interfacial area has been shown to be determined only by experimentation using simplifying assumptions. The portion of "a" due to the spray zone is uncertain. Likewise, the effect the spray zone imparts on Z is unknown. On the surface, doubling the height of packing should double Z and thus double NO removal. However, if the spray zone is decreased and if it has a significant contribution to either "a" or Z, the matter of predicting removal becomes more complicated.

The predictive strategy nevertheless assumes Z to double and thus variation of liquid and gas rates is all that is required to make NOx removal predictions once a particular packing is chosen. Regression data were utilized to compare parameters of importance between the different packings used in Phase II. Figures 8 and 9 plot NOx removal and pressure drop as functions of flue gas velocity for the three packings of interest. The liquid rates chosen for the regression analyses, 110 GPM and 250 GPM, are generally representative of low and high liquid rates. Inspection of these graphs reveals an unacceptable pressure drop for the #2 saddle packings at both liquid rates. The pressure drops associated with the PN Fill and snowflake packings are acceptable.

PN Fill was chosen as the packing for use in Phase III partly for its slightly better NOx removal performance but mainly for the fact that it is a packing already in commercial FGD use. The reader may refer to the attached Munter's brochure for further information regarding this packing.

The final determination of the crucial liquid and gas rates to utilize in Phase III reflect the notion of "retrofit" (>8 fps absorber gas velocity) and "new construction" (<8 fps absorber gas velocity) applications. As can be seen in Fig. 10, the retrofit mode is predicted to have NOx removals of 30% to 35% and the new construction mode is predicted to have NOx removals of 54% to 69%.

Derivation of NO Removal Model Equation

In a countercurrent absorber, the rate of absorption of NO into liquid containing ferrous EDTA is:

$$N_{NO} = K_g \, a \, S \, Z \, (p_{NO})_{ln\ mean} \qquad (1)$$

where: N_{NO} = rate of absorption of NO, lb-moles/hr

K_g = overall mass transfer coefficient, defined based on the gas phase, lb-moles/hr-ft^2-atm

a = gas-liquid interfacial area per volume of contact zone, ft^2/ft^3

$(p_{NO})_{ln\ mean}$ = logarithmic mean partial pressure (concentration) difference between absorber inlet and outlet,

$$atm = (p_{NOin} - p_{NOout})/ln(p_{NOin}/p_{NOout})$$

S = horizontal cross-sectional area of absorber, ft^2

Z = length of gas-liquid contact zone, ft

It is helpful to recognize that the above expression is a simple rate equation like Ohm's law, i.e., the rate is equal to a driving force (the concentration difference between inlet and outlet) divided by a resistance to flow. The equation can be written as:

$$N_{NO} = \frac{1}{1/K_g} \; a \; S \; Z \; (p_{NO})_{ln\ mean} \qquad (2)$$

where the mass transfer coefficient K_g is shown in the form of a resistance, $1/K_g$.

For NO to be absorbed, it has to pass first through both a gas film and then through a liquid film on each side of the gas-liquid interface. These two films and their resistances to mass transfer are in series, so the overall resistance $(1/K_g)$ is the sum of the individual gas and liquid film resistances:

$$(1/K_g)\ (\text{overall resistance}) = (1/k_g)\ (\text{gas film resistance}) + H/k_l\ (\text{liquid film resistance}) \qquad (3)$$

where: k_g = gas-film mass transfer coefficient, lb-moles/hr-ft^2-atm

k_l = liquid-film mass-transfer coefficient, ft/hr

H = Henry's law coefficient, atm/(lb-mole/ft^3)

As seen from the equation, a large value of H increases the liquid side resistance when compared to the gas-side resistance and decreases the overall mass transfer coefficient. Since NO is only slightly soluble in water (i.e., a large value of H), the resistance of the liquid film is large compared to the gas-side resistance. Therefore the liquid-side resistance controls the rate of NO removal and the resistance of the gas film can be neglected.

The liquid-side coefficient can depend on both hydrodynamics and on chemical reaction of the absorbed gas in the liquid. The extent to which the liquid-film coefficient is increased over its value for physical absorption only is expressed by an "enhancement factor", E:

$$k_l \text{ (liquid-film coefficient)} = E\, k_l^{\,o} \qquad (4)$$

where: E = enhancement factor for absorption with chemical reaction, dimensionless

$k_l^{\,o}$ = liquid-film mass-transfer coefficient for physical absorption only (i.e., unenhanced by chemical reaction), ft/hr

The enhancement factor depends on the order of reaction, the diffusivity of NO in absorber liquid, the second order rate constant of the reaction between dissolved NO and ferrous EDTA, and whether this reaction is rate controlling and reversible or irreversible. For the case where the reaction is fast and irreversible and where the concentration of ferrous EDTA in the bulk liquid is greatly in excess of the concentration of NO dissolved at the gas-liquid interface (almost always the case because of the low solubility of NO in water), the enhancement factor for absorption of NO by ferrous EDTA is:

$$E = (k_2\, [Fe^{++}]\, D_{NO})^{1/2}/k_l^{\,o} \qquad (5)$$

where: k_2 = reaction rate constant for second-order reaction between dissolved (but not yet reacted) NO and ferrous EDTA = 1.4×10^8 l/M-sec at 50^oC.

$[Fe^{++}]$ = ferrous EDTA concentration in absorber liquid, lb-moles/ft^3

D_{NO} = diffusivity of dissolved NO in absorber liquid = 4.1×10^{-5} cm^2/sec

The expression for the overall mass transfer coefficient then becomes:

$$(1/K_g) = H/(E\ k_l^o) \qquad (6)$$

Substitution of E into equation 6 yields the following expression for the overall mass transfer coefficient for removal of NO:

$$K_g = (k_2\ [Fe^{++}]\ D_{NO})^{1/2}/(H/p_T) \qquad (7)$$

The rate of absorption of NO by the liquid was written earlier in equation (1) as:

$$N_{NO} = K_g\ a\ S\ Z\ (p_{NO})_{ln\ mean} \qquad (1)$$

where: N_{NO} = rate of absorption of NO, lb-moles/hr

K_g = overall mass transfer coefficient, defined based on the gas phase, lb-moles/hr-ft^2-atm

a = gas-liquid interfacial area per volume of contact zone, ft^2/ft^3

$(p_{NOin}-p_{NOout})_{ln\ mean}$ = logarithmic mean of absorber inlet and outlet partial pressure (concentration)

S = horizontal cross-sectional area of absorber, ft^2

Z = length of gas-liquid contact zone, ft

The logarithmic mean NO concentration difference is equal to:

$$(p_{NO})_{ln\ mean} = (p_{NOin}-p_{NOout})/ln\ (p_{NOin}/p_{NOout}) \qquad (8)$$

The rate of NO absorption by the liquid must be equal to the rate at which NO is lost from the gas, which is:

$$N_{NO} = p_M \, v \, S \, (p_{NOin} - p_{NOout})/p_T \qquad (9)$$

where: N_{NO} = rate of absorption of NO, lb-moles/hr

p_M = molar density of flue gas, lb-moles/ft^3

v = flue gas velocity in absorber, ft/hr

$(p_{NOin} - p_{NOout})$ = difference in flue gas NO concentration between absorber inlet and outlet, atm

p_T = total pressure, atm

S = horizontal cross-sectional area of absorber, ft^2

Combining equations 1, 8, and 9 to eliminate N_{NO} and solving for $\ln(p_{NOin}/p_{NOout})$ yields:

$$\ln (p_{NOin}/p_{NOout}) = K_g \; a \, P_T \, Z \, / \, (p_M \, v) \qquad (10)$$

The term on the left-hand side is the number of transfer units, or NTU, which is related to percent removal by:

$$NTU = \ln (p_{NOin}/p_{NOout}) = -\ln(p_{NOout}/p_{NOin})$$

$$-\ln(1 - \% \text{ removal}/100) \qquad (11)$$

Combining equation 10 with the expression for K_g from equation 7 for removal of NO with ferrous EDTA yields a single equation that describes the dependence of NO removal on ferrous EDTA concentration, flue gas velocity in the absorber, the length of the absorption zone, and the effective interfacial area:

$$NTU = -\ln(1 - \%\ removal/100) = \frac{(k_2\ [Fe^{++}]\ D_{NO})^{1/2}}{H/p_T} \quad \frac{a\ Z}{p_M\ v} \qquad (12)$$

where: NTU = NO removal as number of transfer units, dimensionless

k_2 = reaction rate constant for second-order reaction between dissolved (but not yet reacted) NO and ferrous EDTA = 1.4×10^8 $(M\text{-}sec)^{-1}$ @ 50^oC.

$[Fe^{++}]$ = ferrous EDTA concentration in absorber liquid, mM * $6.2362*10^{-5}$ = lb-mole/ft^3.

D_{NO} = diffusivity of dissolved NO in absorber liquid = 4.4×10^{-8} ft^2/sec @ 122^oF.

a = gas-liquid interfacial area per volume of contact zone, ft^2/ft^3.

Z = length of gas-liquid contact zone, ft.

p_M = molar density of flue gas = 0.00235 lb-moles/ft^3 @ 50^oC.

v = flue gas velocity in absorber, ft/sec.

p_T = total pressure = 1 atm.

H = Henry's law constant for NO in water = 710.7 atm/M @ 50^oC.
11383.25 ft^3/lb-mole @ 122^oF.
(12813.56 ft^3/lb-mole if flue gas is saturated with water vapor.)

References

1. Perry's Chemical Engineering Handbook, 6th ed., p. 13-33.

PROCESS PARAMETERS

[Fe++], a, Z, v

"a" is a function of liquid rate and packing type for packings, so "a" contains the dependence of removal on liquid rate. It is expected for each packing that:

a = constant * (liquid rate, gpm)^{b} where b is a constant. "b" is expected to be <0.5

"a" depends on liquid rate and nozzle type for spray nozzles, but also on gas velocity and absorber diameter. It is expected to be difficult to predict or correlate.

FORM OF CORRELATION OF NO REMOVAL DATA

NTU @ 15 mM Fe++ = NTU * (15/[Fe++], mM)$^{1/2}$

NTU @ 15 mM Fe++ = (v, ft/sec)^{a} * (L, gpm)^{b} * 10^{c}

log NTU @ 15 mM Fe++ = a * log(v) + b * log(L) + c

Figure 1

Comparison of Regression Constants								
	NOx Removal Correlations				Pressure Drop Correlations			
Packing	a	b	c	R2	A	B	C	R2
#2 Saddle	-1.13	0.49	-0.61	0.99	4.25	1.04	-4.84	0.93
#3 Saddle	0.09	0.9	-2.59	0.88	2.15	0.44	-1.91	0.92
Snowflake	-0.74	0.62	-1.3	0.99	2.67	0.83	-3.74	0.87
PN Fill	-1.06	0.35	-0.39	0.72	3.64	1.26	-5.54	0.96
Single 40% Tray								
w/TF28XPN	-0.72	1.51	-3.52	0.65	0.99	2.72	-6.47	0.98
w/TF40XPN	-0.9	n/a	-0.09	0.79	0.95	n/a	-0.56	0.97
Double Trays								

Figure 2

Equation (1) NOx Removal (NTU) = (FPS)^a*(GPM)^b*10^c

Equation (2) Packed Bed Pressure Drop ("WC) = (FPS)^A*(GPM)^B*10^C

Notes

1) #3 Saddle and TF40XPN test series limited in scope.
2) PN Fill correlation coefficients derived from dry additive feed test points only.

Figure 2

EFFECTIVE INTERFACIAL AREA OF #2 SADDLES
FROM MEASURED NO REMOVAL DATA

			a eff., ft2/ft3	
Recycle Liq	V, ft/sec	NTU	calc'd	correl.
26	10.2	0.10	15.0	14.7
58	6.4	0.26	23.0	22.5
90	5.5	0.38	30.1	28.0
90	7.2	0.22	24.7	27.9
90	8.5	0.20	28.4	27.9
120	5.6	0.38	31.3	32.4
124	5.6	0.36	32.2	32.9
238	6.4	0.40	42.8	46.0
275	4.9	0.77	57.6	49.6
276	5.0	0.56	47.8	49.7

CORRELATION OF CALC'D AREA VS.
LIQUID AND GAS RATES

	L	k
	0.515137	0.439022
	0.036053	0.074628
R^2	0.962291	0.034635
	204.1529	8
	0.244895	0.009597

	V	L	k
	-0.159055	0.474907	0.649318
	0.184882	0.059415	0.255946
R^2	0.965897	0.035211	#N/A
	99.13063	7	#N/A
	0.245813	0.008679	#N/A

Figure 3

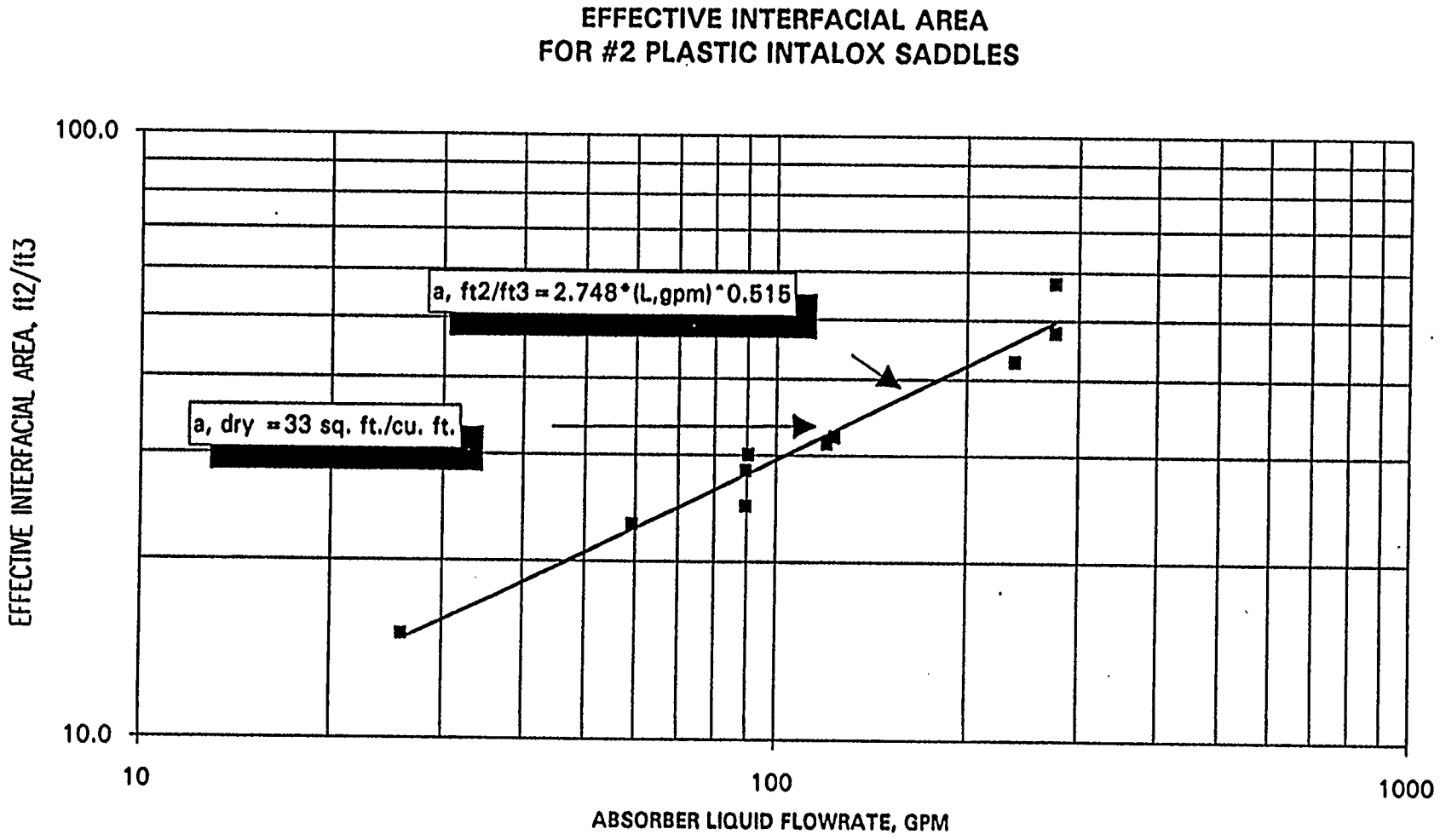
EFFECTIVE INTERFACIAL AREA
FOR #2 PLASTIC INTALOX SADDLES
100.0
10.0
EFFECTIVE INTERFACIAL AREA, ft2/ft3
a, ft2/ft3 = 2.748*(L,gpm)^0.515
a, dry = 33 sq. ft./cu. ft.
10
100
1000
ABSORBER LIQUID FLOWRATE, GPM

Figure 4

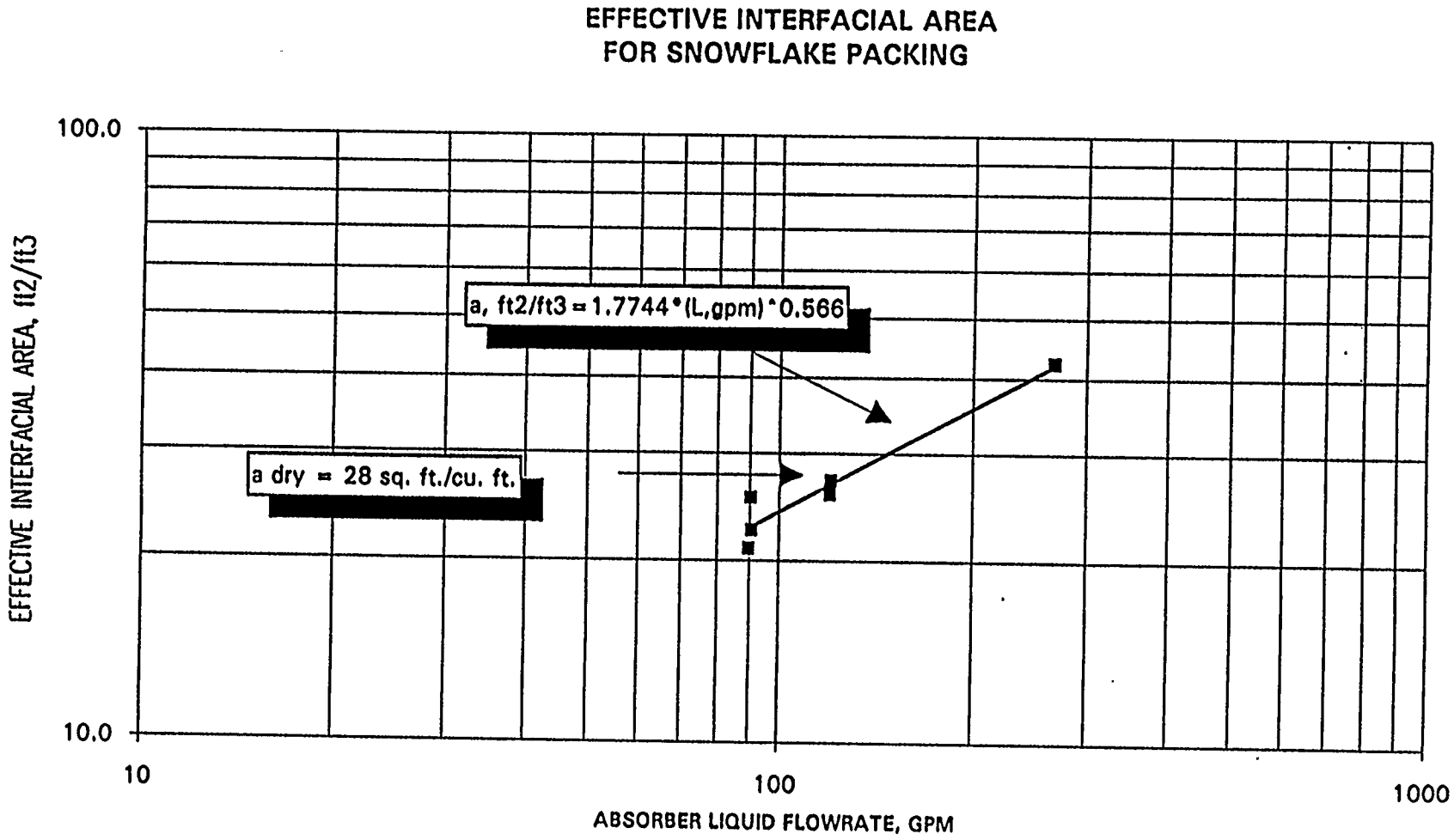
EFFECTIVE INTERFACIAL AREA
FOR SNOWFLAKE PACKING
100.0
10.0
EFFECTIVE INTERFACIAL AREA, ft2/ft3
a, ft2/ft3 = 1.7744*(L,gpm)^0.566
a dry = 28 sq. ft./cu. ft.
10
100
1000
ABSORBER LIQUID FLOWRATE, GPM

Figure 5

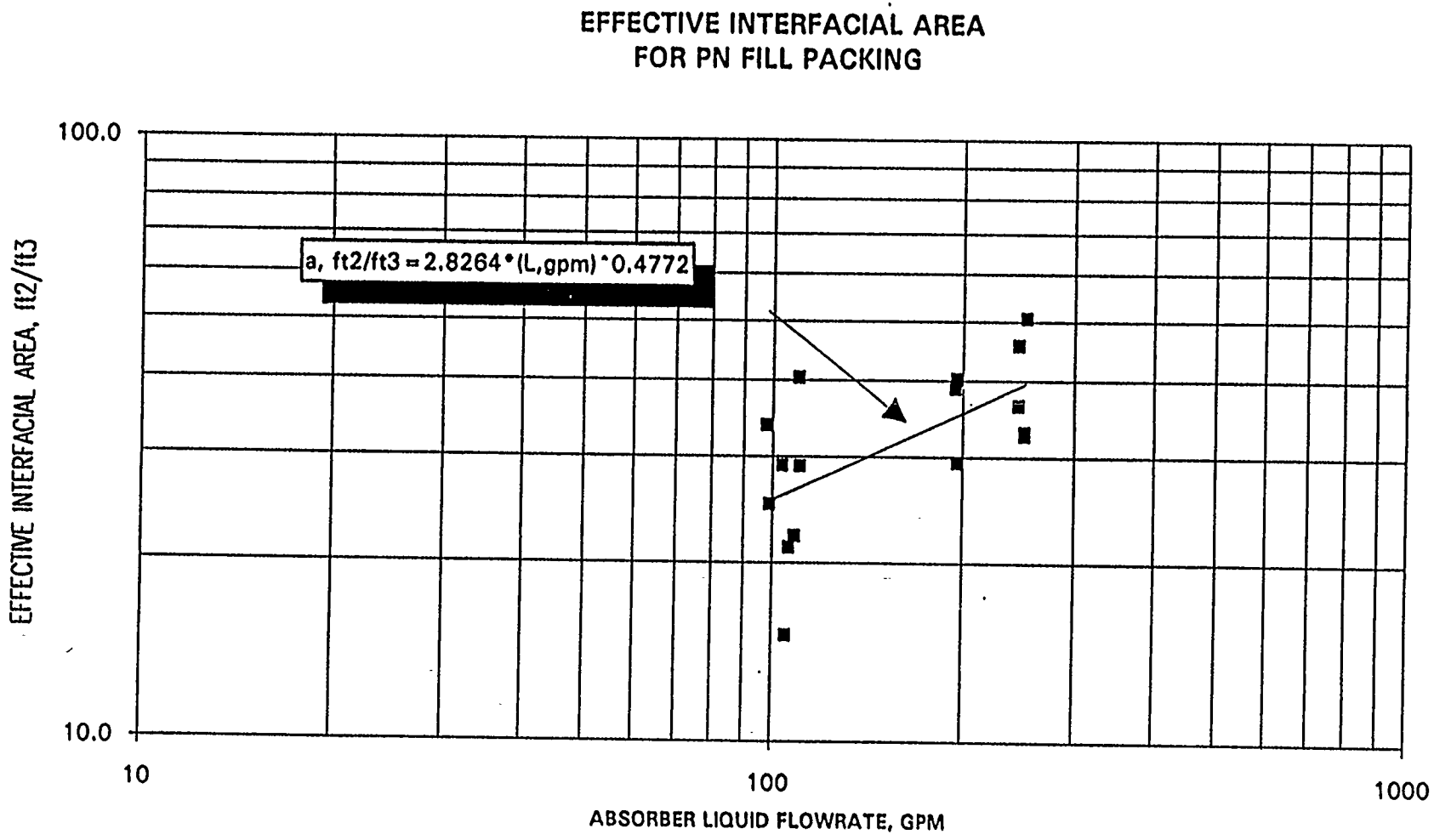
EFFECTIVE INTERFACIAL AREA
FOR PN FILL PACKING
100.0
10.0
a, ft2/ft3 = 2.8264*(L,gpm)^0.4772
EFFECTIVE INTERFACIAL AREA, ft2/ft3
10
100
1000
ABSORBER LIQUID FLOWRATE, GPM

Figure 6

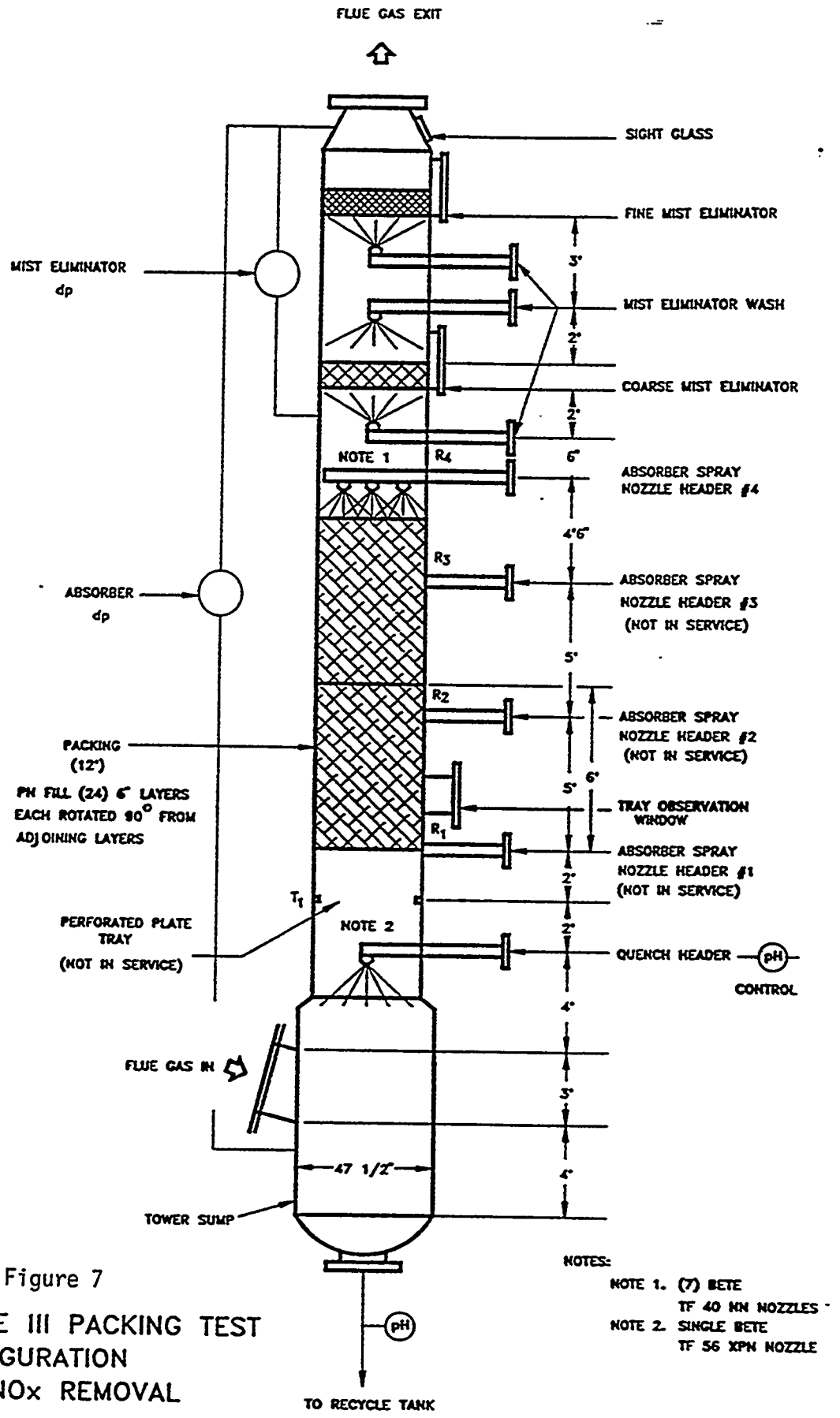

Figure 7

PHASE III PACKING TEST
CONFIGURATION
FOR NOx REMOVAL
3' DIAMETER TOWER

Figure 7

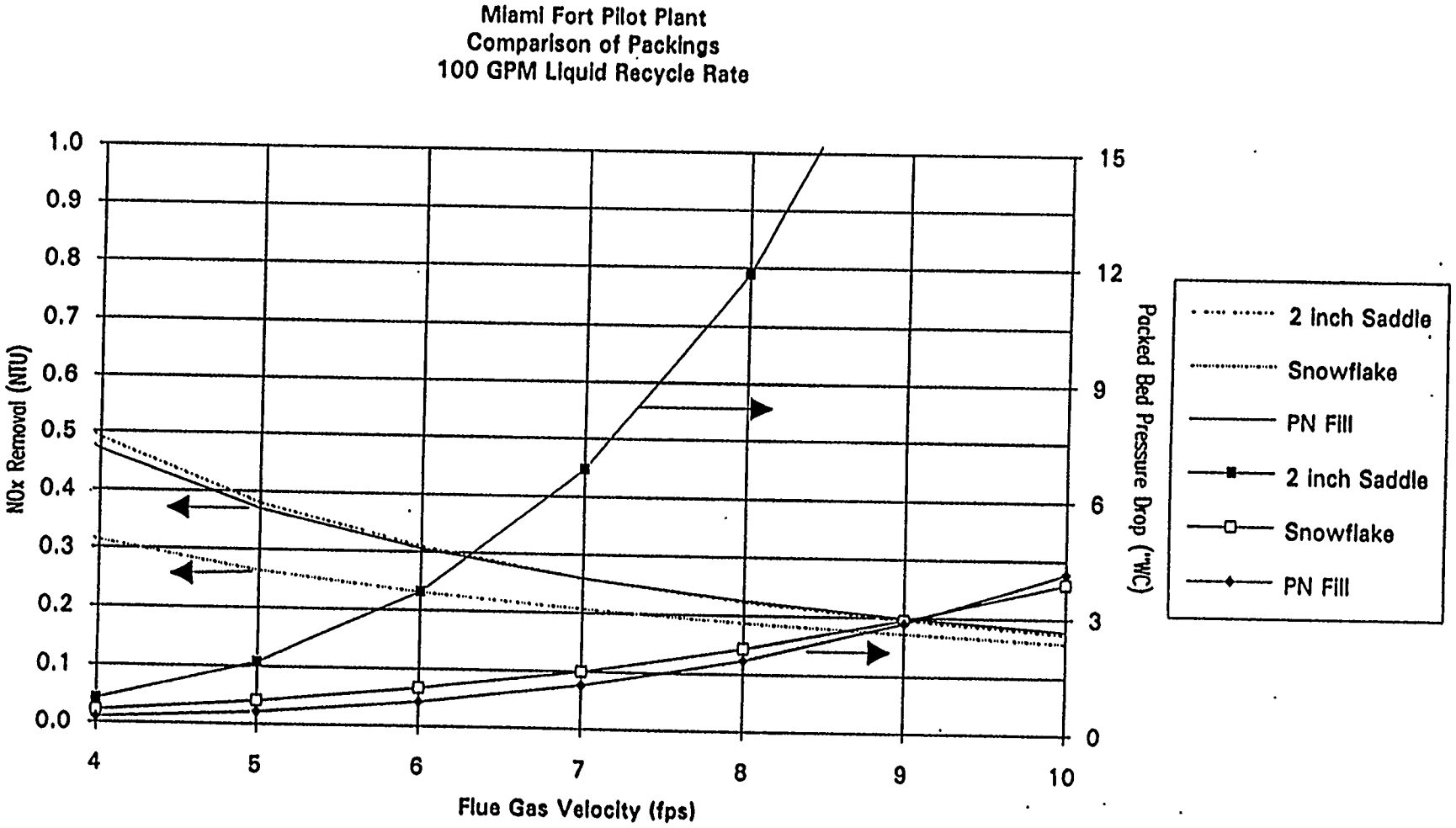
Miami Fort Pilot Plant
Comparison of Packings
100 GPM Liquid Recycle Rate
NOx Removal (NTU)
Packed Bed Pressure Drop ("WC)
Flue Gas Velocity (fps)
1.0
0.9
0.8
0.7
0.6
0.5
0.4
0.3
0.2
0.1
0.0
15
12
9
6
3
0
4
5
6
7
8
9
10
2 inch Saddle
Snowflake
PN Fill
2 inch Saddle
Snowflake
PN Fill

Figure 8

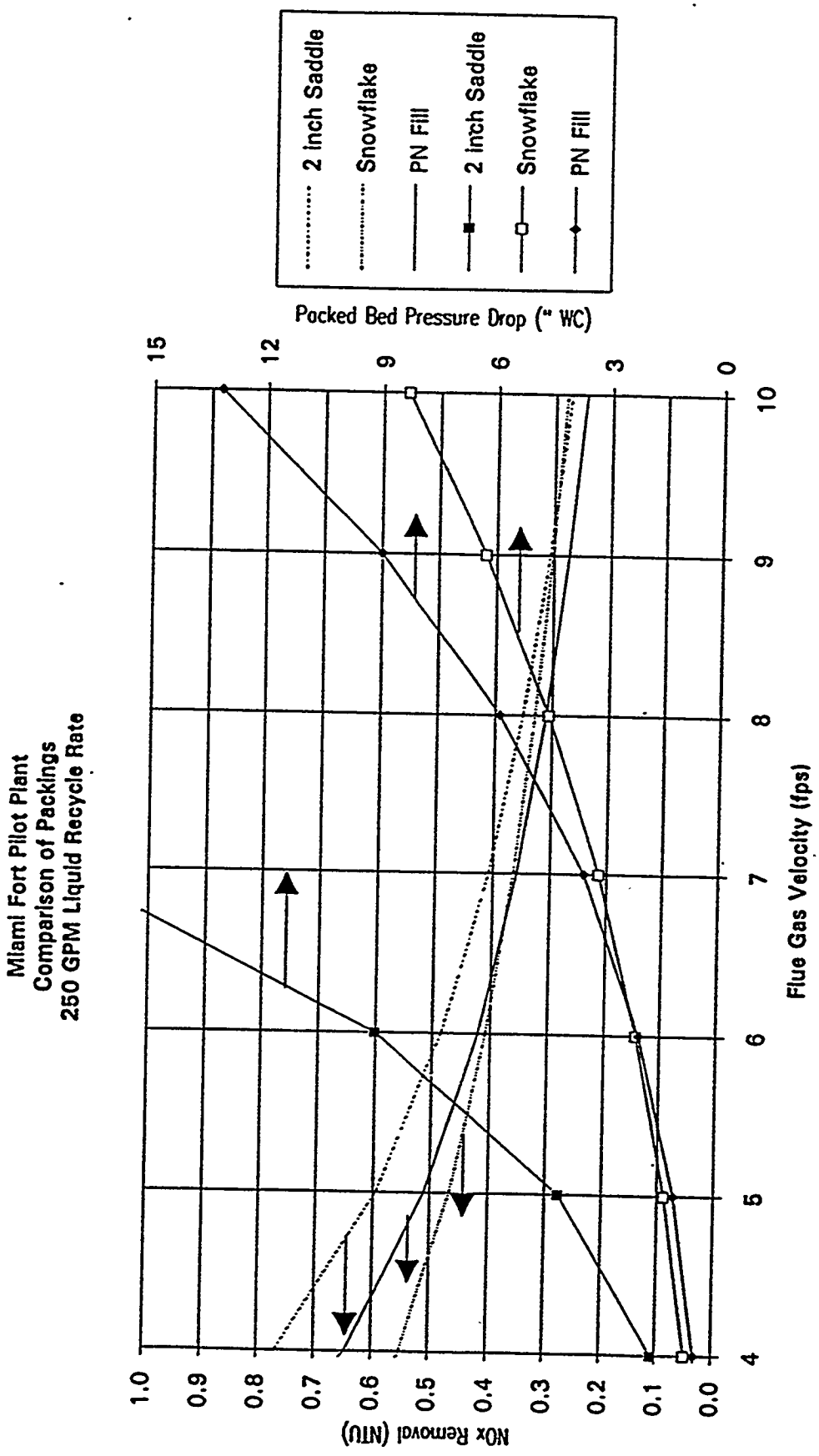

Figure 9

Figure 9

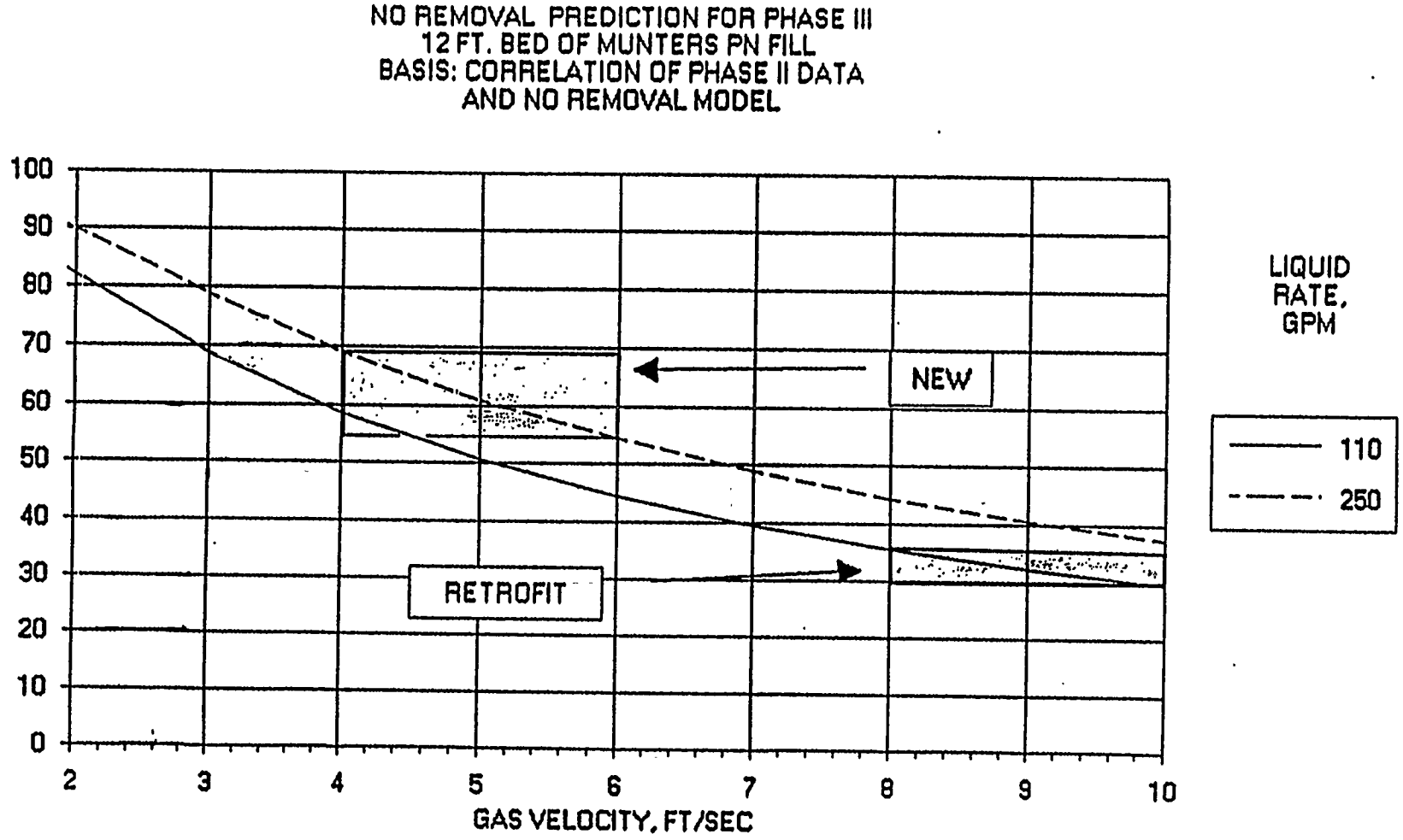

Figure 10

Figure 10

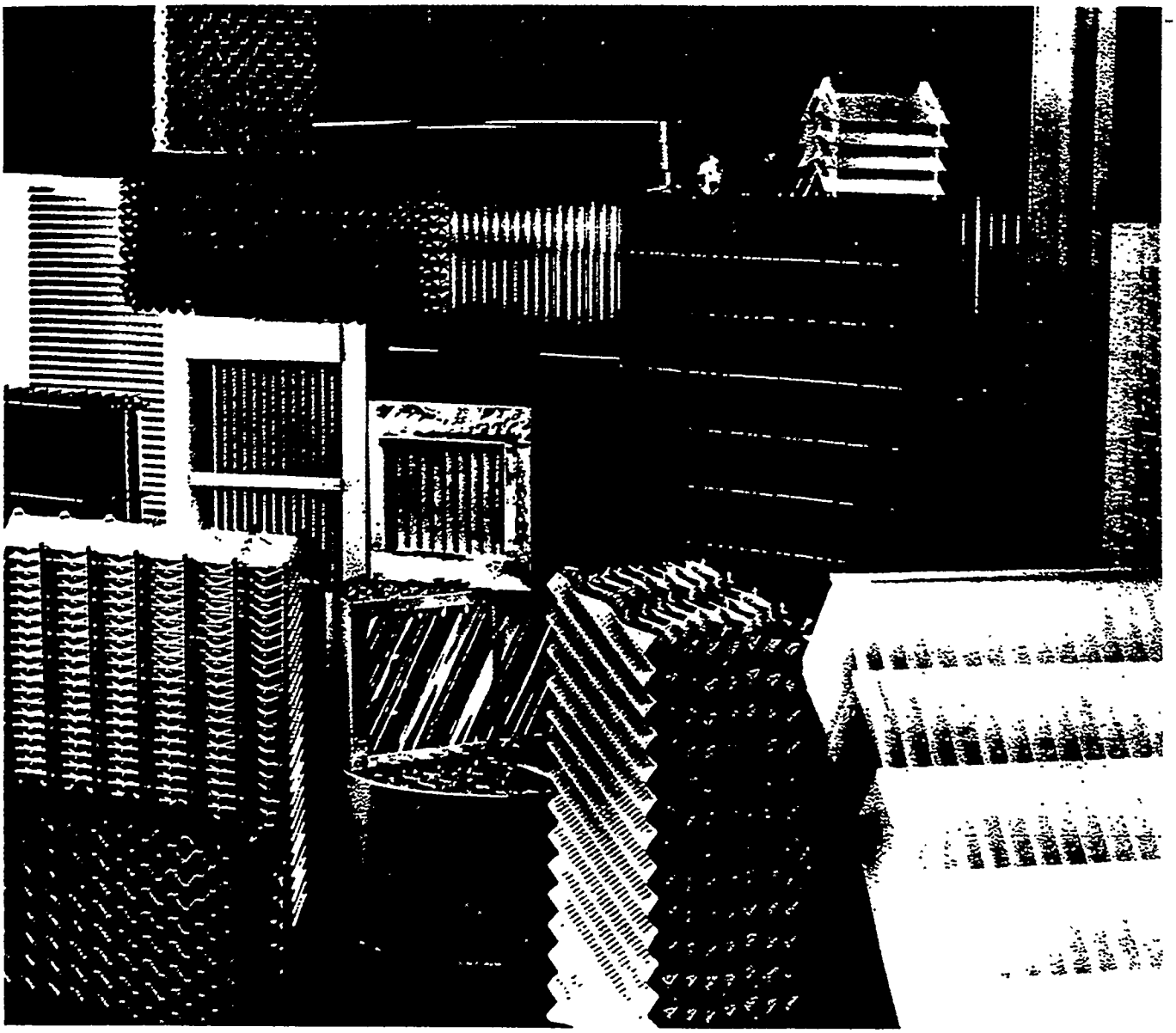

Munters

The Munters Corporation, Gas Cleaning Division
P.O. Box 6428 Fort Myers, FL 33911, U.S.A.
Customer Service Center:
Toll Free 1-800-446-6868 (USA and Canada) All others call: (813) 936-1555

3000/9-8/11

Munters

Introducing PN Fill, a New Design in Tower Packing

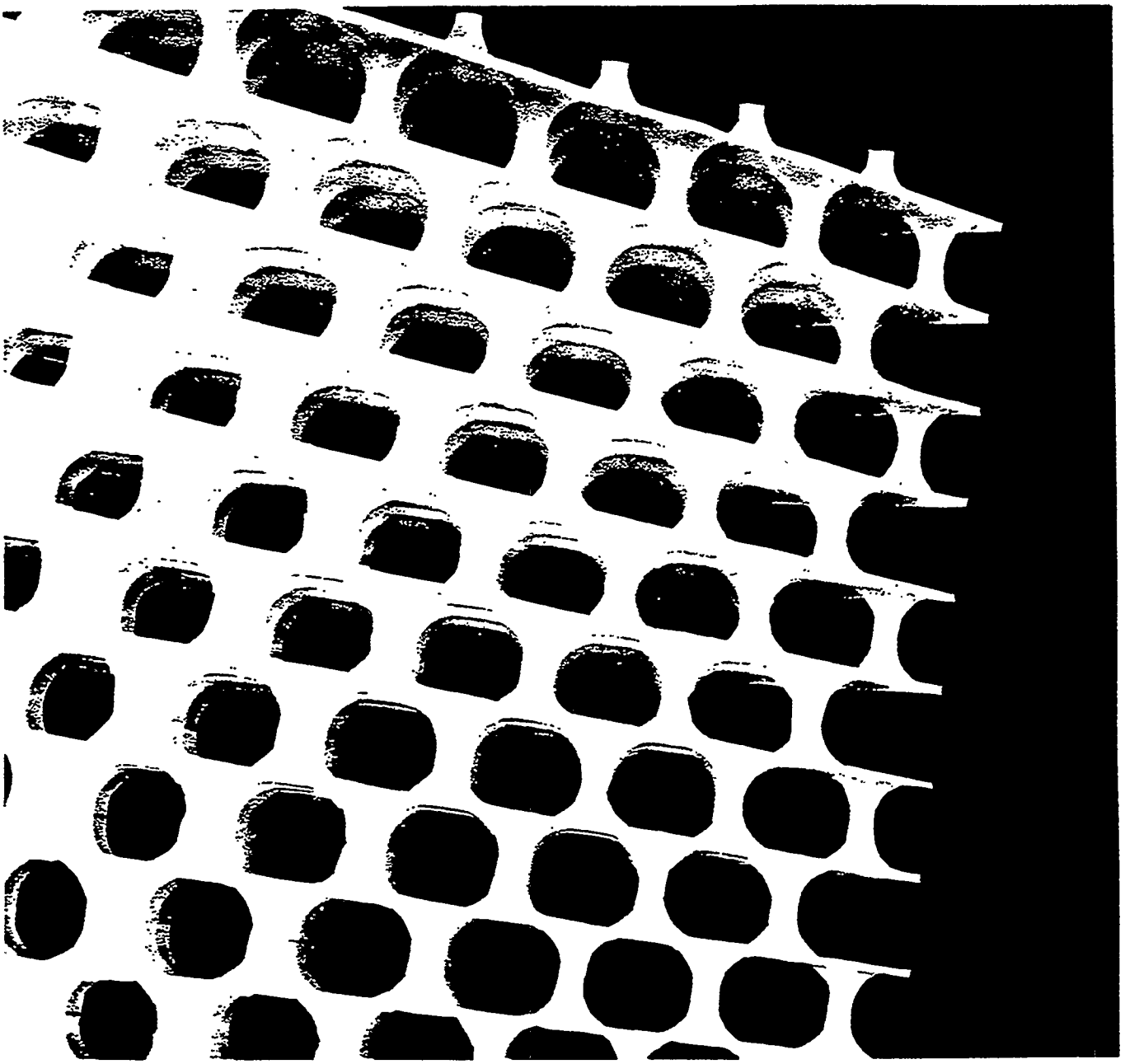

Yet Another Addition to Our Unmatched Range of Gas Cleaning Components

Shaped like no other structured packing, because no other packing is quite like it.

Don't let the egg carton shape of our PN Fill fool you. There is nothing fragile about it. On the contrary, we specially designed PN Fill for durability and high performance.

The main reason for the egg carton shape is to facilitate high-pressure washing. After careful research, we arrived at a design which is less susceptible to clogging than any other material available on the market.

Each sheet of the PN pack is individually injection molded with integral mechanical fasteners. The resulting packs can withstand extremely high pressure washing. Packs have withstood field blasting with water lances operating at pressures in excess of 4000 psi without damage to the pack or the rigid polypropylene surface of the PN fill.

PN's off-white color also makes it easy to spot areas that require washing or where solids have built-up. This feature minimizes washing cost and down time by allowing you to concentrate your efforts where they are needed, often without need to remove the packing from the tower for inspection or cleaning.

Proven low pressure drop, together with high heat and mass transfer performance characteristics, make PN Fill ideal for high-solids mass and heat transfer applications. PN is ideally suited for lime and limestone high solids FGD applications.

Like all Munter's products, PN Fill is designed with the end-user in mind. It is easy to clean and has excellent performance characteristics, but also — very importantly — it is purposely shaped in 3′ x 2′ packs designed to span existing support systems, and ease of installation. It, too, can be cut to suit the contour of your tower cross section.

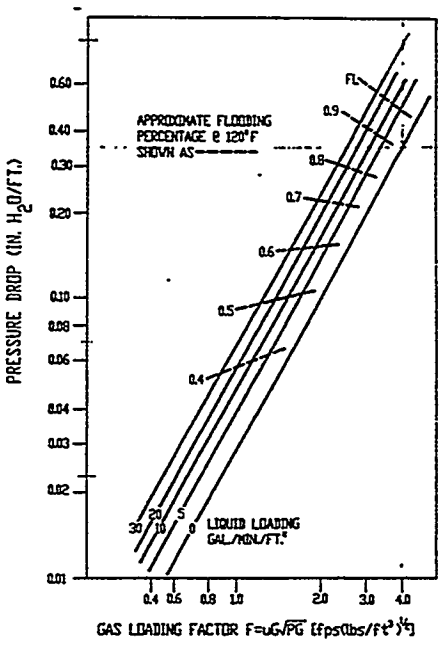

PRESSURE DROP — MUNTERS PN FILL

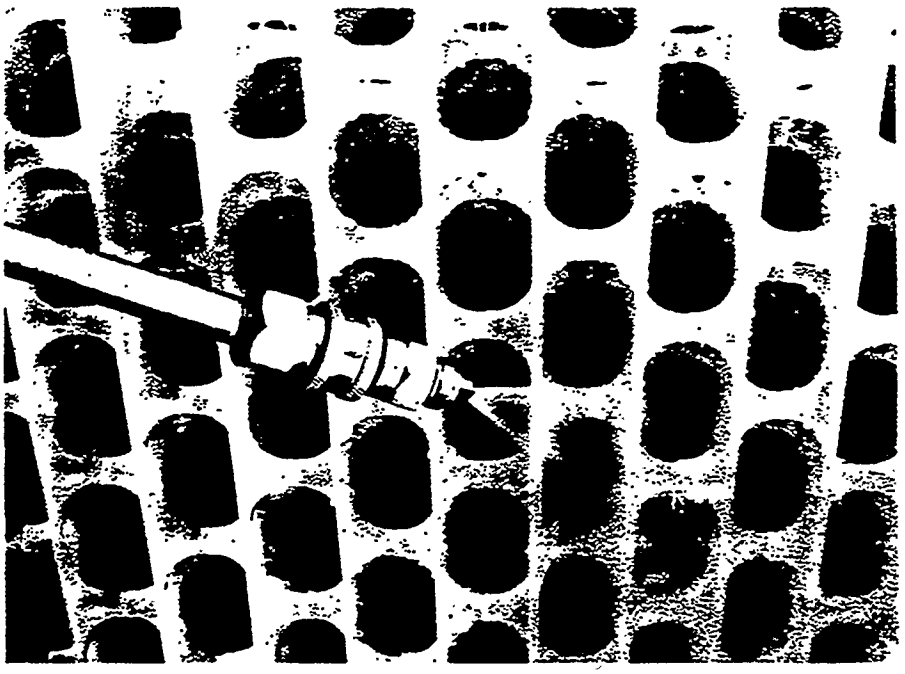

PN's rugged construction withstands high pressure cleaning.

PN Compliments our Plastic & Metallic Structured Packings.

We revolutionized packing geometry with our cross-fluted PLASdek and METAdek fills. Today other manufacturers offer cross-fluted plastic media similar to our PLASdek fill but there are still many areas where Munters is far superior. This superiority is due in part to our unique, continuous forming process, which is patented.

We manufacture our cross fluted sheets by means of a continuous rolling process. The material is formed-without being "drawn" into the forming molds.

Continuous forming gives us sizing flexability and allows us to continually form our patented DUBLfold® edge. DUBLfold® means extra strength where you need it — at the edges. Other manufacturers vacuum-form their material, sheet by sheet, limiting them to fixed lengths without a DUBLfold feature, which we alone can offer. The competition has no answer to DUBLfold®, although some try.

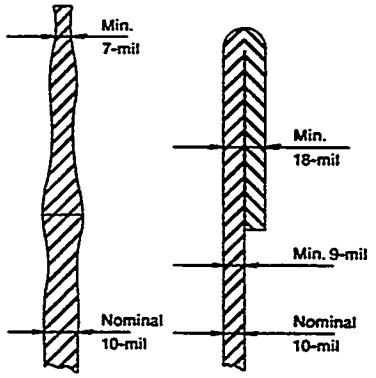

Munters DUBLfold® edges vary between 18 and 22 mil in thickness, while other processes leave edges as thin as 7 mil.

Our continuous process always leaves one end free, which minimizes thickness variations.

Our continuous rolling process means minimum sheet thickness variation throughout the pack. On 10 mil material, our tolerance is ±1 mil after forming. The competition has a substantially higher thickness variation on their vacuum formed sheets, normally more than 30 percent. On the same 10 mil sheet the thickness of the edge may be only 7 mil. Not to mention that the entire sheet will have numerous thin areas.

Vacuum-formed competitive products come in only a few standardized sizes and materials. Munters continuous formed packs can be sized to order — to any length between 4 and 10 feet and variable pack depths to minimize waste and cutting cost.

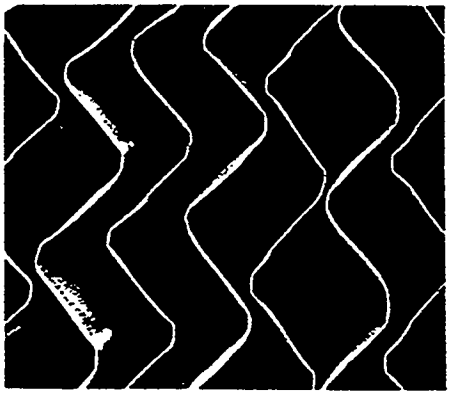

Munters also provides greater operational flexibility by offering various flute sizes and materials to meet your process needs, including polypropylene, PVC, CPVC, and high temperature glass coupled polyproplyene.

Our METAdek Fill is a cross fluted metallic packing that can be custom-tailored to a variety of heat and mass-transfer requirements.

It is continuously formed as is PLASdek, and can be provided with a DUBLfold® edge. It can also be contoured to suit your vessel cross section.

Available in various flute sizes, METAdek provides high mass and heat transfer efficiencies at very low pressure drops and recirculation rates. It can be constructed from most stainless and alloy steels.

For customers looking for a combination of low pressure drop, high efficiency, high temperature resistance and good corrosion resistance, PLASdek and METAdek can meet those needs. In fact, Munters has the right fill for your scrubbing, mass transfer and heat transfer needs.

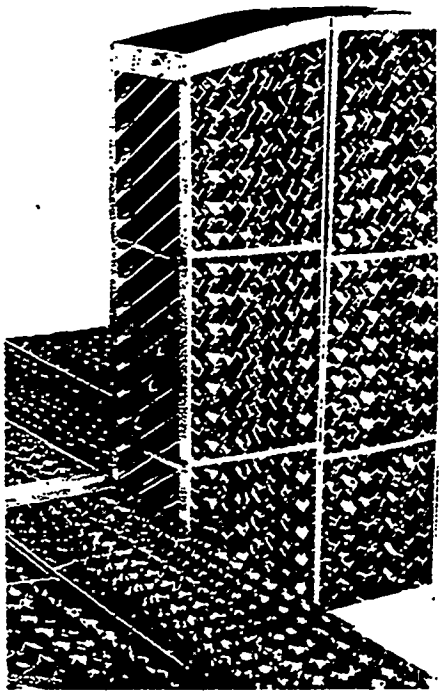

C. PHASE III SUMMARY OF TESTING

This section summarizes the results of testing performed in Phase III of the project, "Enhanced NOx Removal in Wet Scrubbers Using Metal Chelates". Each task's testing will be briefly reviewed with emphasis placed on the purpose of testing, measures of success, results of testing including any unexpected data or problems encountered, and an interpretation of the result of each task's tests. Tables and graphs are included where necessary. An effort was made to generate testing data to support the liquid-film limited, pseudo-first order absorption rate NO removal model having the following form wherein NO removal is expressed in NTU (Number of Transfer Units):

$$\text{NO Removal (NTU)} = \frac{(k_2 [Fe^{++}] D_{NO})^{1/2}}{H/P_T} \quad \frac{a Z}{p_M v}$$

where NTU = -ln(1 - % removal/100)

The terms in the above NO removal model equation are as defined earlier in Section II A of this document.

All testing was performed under test series 3.1.3, "Process Testing of Most Promising Conditions."

TESTING PERFORMED:

TASK 3.1.3.1: Model Confirmation Tests:

Purpose of Test: To confirm whether NOx removal will increase in direct proportion to an increase in packing height.

Measures of Success: Determine the effect of a change in packing height on NOx removal efficiency and on scrubber pressure drop. Perform parametric tests to confirm the effect of L/G and flue gas velocity on NOx removal efficiency. Determine if the NOx removal rates predicted from the model verification studies of Phase II can be achieved at given sets of scrubber operating conditions.

Results of Tests: The absorber tower began operation for this task outfitted with 12 feet of Munter's PN Fill packing (as opposed to 6 feet of the same packing during Phase II testing) with the configuration shown in Figure 1. Model Confirmation Testing was conducted for two weeks. After two days the seven Bete TF 40NN nozzles on recycle header #4 were replaced with seven Bete TF 28XPN nozzles. This nozzle changeover occurred throughout this testing phase as the 40NN nozzles, having a larger orifice, were used whenever 250 GPM of flow was desired and the 28XPN nozzles were utilized whenever 110 GPM of flow was required. The reducing agent/antioxidant additives sodium dithionite and ascorbic acid (250#/55# ratio) were added continuously at rates required to maintain a ferrous iron concentration of about 15 mM. On the fourth day of testing, three 36 inch rubber gaskets were installed at two foot intervals in the upper 6 foot layer of packing to serve as distribution rings to insure good liquid flow distribution and deter "wall-wetting" effects. Due to the initial design of the scrubber, distribution rings were already present in the lower six feet of packing as tray rings at the T2 through T5 tray locations, the T2 ring being situated at the bottom of the packing and followed at two foot intervals by rings at the T3 and T4 locations with the T5 ring one foot above the T4 location.

Changes made to the absorber during the second week of this task included: replacing the upper six foot section of PN Fill packing with six feet of Norton Snowflake packing to further insure good liquid distribution; placing a 40% open area sieve tray at the T1 location, two feet below the packing section, to insure even distribution of the flue gas prior to reaching the packing; and the moving of the fine mist eliminator to the coarse mist eliminator position, elimination of the coarse mist eliminator, and the placement of a sieve tray in the fine mist eliminator position in two open area configurations of 7.5% open area and 4.4% open area. This placement of a nearly closed sieve tray at the fine mist eliminator position was for the purpose of restricting flue gas flow so that very low flue gas velocities could be achieved. The modifications outlined above were made to insure even distribution of flue gas and liquor throughout the scrubber.

Figure 2a shows the results of NO removal during the two week testing period compared to the NO removal predictions made by the model. Despite the above efforts to modify the scrubber internals, the predicted doubling of the NO removal efficiency as NTU from those achieved with six feet of packing did not occur. On average the overall NTU increase in removal was by a factor of 1.5.

Examination of the correlation data resulting from the regression analyses of the NOx removal and pressure drop equations (See Table 1) for this task indicates a cause and effect relationship that was quite acceptable with respect to values expected from the NOx removal model and the chemical literature. For example, Table 1A shows that NOx removal varied as the -0.95 power of velocity, a finding very much in agreement with the model prediction of NOx removal dependence on velocity to the -1 power. Table 1A also shows that NOx removal varied as the 0.41 power of liquid rate, a result quite consistent with established values from the chemical mass transfer literature wherein removal is generally considered to vary as the ~0.5 power of liquid rate. As can be seen, these correlations are statistically significant at the 90% confidence level.

Interpretation: An objective of the model confirmation testing was to verify the model premise that doubling the packing height, Z, would double NO removal as expressed in NTU. The doubling of packing height significantly improved NO removal but not to the extent of doubling that removal. Since considerable effort was made to insure good gas and liquid flow distributions, the interfacial area,"a", must be assumed to have reached its effective value. This leaves the contribution of the "spray zone" from the factors "a" and Z to consider. In Phase III the spray zone length was six feet shorter than in the Phase II configuration. In addition, one spray header was used in Phase III testing whereas two headers were utilized in Phase II testing which provided a more intense spray zone. In Phase II the two headers were located 4.5 and 9 feet above the top of the packing; in Phase III the single header was located 3.25 feet above the top of the packing. If the spray zone imparts a significant contribution to either "a" or Z, the NOx removal may not double with a doubling of Z, the height of packing. NO removal in NTU at a flue gas velocity (FGV) of 8 feet per second (fps) was 0.1 NTU lower at 110 gpm and 0.2

NTU lower at 250 gpm than that predicted from the model based on the NO removal obtained with six feet of packing. It is clear that the surface area in the spray zone must be considered when making model predictions. Modeling of surface area provided by spray nozzles is a complex endeavor. One tool available to estimate spray zone surface area is FGD PRISM^{R}, an absorption computer model developed by EPRI.

To separate the effective interfacial area contribution of the packing and spray, parametric data from test runs conducted at 6 ft and 12 ft of PN Fill packing height were evaluated. Separate multiple linear regressions, for each packing height, were performed after normalizing for ferrous concentration of 15 mM. The results of the regression analyses for the 6 and 12 ft packing data appear in the upper left tables in Figure 2b. In the lower left table of Figure 2b trends for varying velocity (5 & 8 fps), liquid rate (110, 180, 250 gpm), and packing height (0, 6 and 12 feet) were developed using the appropriate regression constants for 6 and 12 feet of packing height. The values for NTU at zero packing height were extrapolated from the 6 and 12 foot packing height treads. This is graphically presented by the two graphs for 5 and 8 ft/sec displayed in Figure 2b. These values represent the NO removal taking place in the spray zone above and below the packing and are labled "end effects".

The NTU difference column subtracts the NTU valve for zero packing height from the 6 and 12 foot packing NTU value respectively. The result is the NO removal attributable solely to the packing. Note also that the NO removal (expressed as NTU) of the 12 foot packing condition is almost exactly double the removal of the 6 foot packing condition in all cases. This shows clearly that increasing packing height will in direct proportion increase its contribution to NO removal.

The effective surface area for the packing and spray end effects are estimated using the equation:

$$a_{eff} = 340.8 * NTU_{diff} * V * [Fe^{+2}]^{-1/2} * Z^{-1}$$

where: V = 5 or 8 ft/sec

$[Fe^{+2}]$ = 15 mM

Z = 6 or 12 ft for packing and 12 ft spray for 0 ft packing case

NTU_{diff} = NTU_{diff} for 6 and 12 ft packing cases (NTU for 0 ft packing case).

The a_{eff} for the packing cases of the two different packing heights are nearly identical as they should be. These values, estimated for Munters PN Fill packing, are useful in scaling the process to commercial size. The a_{eff} estimated for spray "end effects" are on the other hand unique to the pilot configuration and not useful for scale up.

Armed with this new understanding of effective surface area, it is possible to revise the prediction trends of Figure 2a. Effective surface area (a) and contact length (Z) can be discribed as:

$$a_{total}\ Z_{total} = (a_{spray}\ Z_{spray} + a_{packing}\ Z_{packing})$$

i.e. for the 8 ft/sec, 250 gpm, 12 ft packing case:

$$a_{total}\ Z_{total} = (8.7\ ft^2/ft^3 * 1.5\ ft + 17.7\ ft^2/ft^3 * 12\ ft)$$
$$= 225.45$$

Figure 2c shows the results of NO removal during the same two week tesing period as Figure 2a, with NO removal predictions made by the model using the above equation for $a_{total}\ Z_{total}$. Much better agreement between the prediction trends and actual results is seen.

TASK 3.1.3.2: Retrofit Operation:

Purpose of Test: To simulate the performance of a magnesium enhanced lime (MEL) FGD system that has been retrofitted to effect NOx removal. Operate the system in a continuous mode at a single operating condition to evaluate the effect of boiler load and flue gas oxygen content on antioxidant mixture consumption and NOx removal and to study the chemistry of the system to denote any significant changes occurring over a period of time.

Measures of Success: Determine trends between boiler load, flue gas oxygen content, antioxidant consumption, and NOx removal. Determine if the chemistry of the system tends to stabilize and at what point in time it occurs.

Results of Tests: NOx removal in this configuration was expected to average 35%. However, NOx removals for the first week of this task test period averaged 32% and for the second week NOx removals averaged 28%. SO_2 removal consistently averaged over 99.8% during this task. The operating conditions for this continuous run were as follows: flue gas velocity of 8 feet per second, recycle liquid rate of 110 GPM for an L/G of 33 (45 including 40 gpm quench flow), seven Bete TF 28XPN nozzles, a 40% open area sieve tray two feet below 12 feet of PN Fill packing, and three redistribution rings located 7, 9, and 11 feet from the bottom of the packing along with the tray rings at the T2 through T5 levels located 0, 2, 4, and 5 feet from the bottom of the packing. The antioxidant additives sodium dithionite/ascorbic acid were added on a continuous basis (250#/55# ratio) to maintain a 15 mM ferrous iron concentration. The duration of testing for this task was two weeks.

During the first week of retrofit mode operation these expected relationships developed: flue gas oxygen varied inversely to boiler load (historical trend), ferrous iron concentration (and subsequently NOx removal) decreased with an increase in flue gas oxygen content, and antioxidant consumption increased with an increase in flue gas oxygen. These trends for the week are depicted in Figure 3. During this first week, sulfite concentration slowly and consistently increased. Thiosulfate concentration cycled directly with antioxidate feed rate. There appeared to be no influence of either sulfite or thiosulfite on ferrous iron concentrations at these levels. (See Figure 4)

During the second week of retrofit mode operation the relative trends between flue gas oxygen, antioxidant feed rate, and ferrous iron concentration remained consistent with those of the previous week. Sulfite concentration reversed its trend of the previous week by decreasing slowly as the week progressed. Thiosulfate also reversed its behavior of the previous week, cycling inversely with antioxidant feed rate instead of cycling directly with it. (See Figure 5)

Interpretation: Results from continuous operation under relatively consistent operating conditions over the two week task test period were consistent with the trends established in the first two Phases of the project regarding boiler load, flue gas oxygen level, antioxidant consumption rate, ferrous iron concentration, and NOx removal. These are summarized in the section above.

The interesting trends are those for sulfite and thiosulfate and the reversal of these trends in the second week of the task. It is somewhat difficult to make a straightforward interpretation of the trends in sulfur chemistries in FGD systems because of the various sulfur forms present. Relationships between sulfur forms in this NOx removal regime are made more complex by the additional factors of a sulfur/sodium based reducing agent and the role of sulfites in the NO removal mechanism. A number of sulfur forms in the (-2) oxidation state exist in FGD systems, and the interactions among them are not well understood. With sodium levels in the +20,000 ppm range, there are undoubtedly elevated levels of these sulfur forms in solution in order to satisfy the required charge balance. Although some of the intermediate species and reaction pathways are well defined, it is not easy to determine under what conditions any particular chemical species or chemical equilibrium will be present to control the sulfur chemistry. Hence consistent trends in sulfur species concentrations and tendencies are not often observed. There is a certain limitation to applying simple relationships to such a complex set of interactions and this should be borne in mind when interpreting the chemical data. One possible explanation for the reversal of trends seen in the second week of this testing involves the following proposed reaction pathway:

$$S_2O_4^{-2} \text{ -----> } S + SO_4^{-2} \qquad (1)$$

$$S + SO_3^{-2} \text{ -----> } S_2O_3^{-2} \qquad (2)$$

$$S_2O_4^{-2} + SO_3^{-2} \text{ -----> } S_2O_3^{-2} + SO_4^{-2} \qquad (1+2)=(3)$$

which in sum represents the reduction of dithionite to thiosulfate accompanied by the oxidation of sulfite to sulfate. It is felt that dithionite is a strong enough reducing agent for reaction (1) to occur, especially within the localized confines of the recycle tank where the dry antioxidant mixture enters. Any excess of dithionite would have reduced all the local ferric-EDTA present and thus could be available for "self-reduction" to elemental sulfur.

Under conditions of increasing sulfite concentration reaction (3) would tend to increase thiosulfate concentration whereas under conditions of decreasing sulfite concentration the reverse would be true and thiosulfite concentration would tend to decrease.

TASK 3.1.3.3: New Construction Operation:

Purpose of Test: To simulate the performance of a magnesium enhanced lime (MEL) FGD system that has been designed for higher NOx removal. Operate the system in a continuous mode at a single operating condition to once again evaluate the relationships between boiler load, flue gas oxygen content, antioxidant mixture consumption and NOx removal; and to study the chemistry of the system to denote any significant changes occurring over a period of time.

Measures of Success: Determine trends between boiler load, flue gas oxygen content, antioxidate consumption, and NOx removal. Determine if the chemistry of the system tends to stabilize and at what point in time it occurs.

Results of Tests: NOx removal in this configuration was expected to approach 60%. During the first half of the week the L/G was held at 175 resulting in NOx removals of 43% - 54%. With the L/G maintained at +200 during the latter part of the week, NOx removals ranged from 55% to 65%. SO_2 removal during this task averaged over 99.5%. The operating conditions for this continuous run were as follows: flue gas velocity of 4 feet per second, sufficient recycle liquid rate to achieve an L/G of 155 (not including quench), seven Bete TF 40NN nozzles, a 40% open area sieve tray two feet below 12 feet of PN Fill packing at the T1 location, and seven redistribution rings located as before at 0, 2, 4, 5, 7, 9, and 11 feet from the bottom of the packing. In order to maintain flue gas velocity at a low level and promote even flue gas distribution, the coarse mist eliminator was removed and replaced by the fine mist eliminator; a sieve tray of 10% open area was then placed at the fine mist eliminator position. Measurement of flue gas velocity by pitot tube traverses revealed the flue gas velocity to be approximately one fps higher than measured and recorded by plant instrumentation. For instance, when plant instrumentation recorded the flue gas velocity as 4 fps, the actual velocity as measured by pitot tube traverse measurements was in the range of 4.5 to 4.8 fps. Since NOx removal increases with a decrease in flue gas velocity, the inability to meet predicted removals may be partly explained by this flue gas velocity measurement error. Since the estimate for flue gas velocity may be off by as much as 1 fps at the low flow condition, the trends projected from the multiple linear regression analysis, which use flue gas velocity, are also affected. The trend of higher NOx removal with increased residence time in the absorber tower does not change. However, the predicted NOx removal may be slightly higher than actually achieved. The antioxidant additives sodium dithionite/ascorbic acid were added on a continuous basis (250#/55# ratio) to maintain about 15 mM ferrous iron concentration. The duration of testing for this task was two weeks.

During the first week of new construction mode operation the cyclic trend of the boiler caused the ferrous iron concentration and the antioxidant feed rate to reflect similar trends as shown in Figure 6. During this first week, both sulfite and thiosulfate concentrations tended to trend similarly, both ending the week at higher levels than they started at.

Neither anion had a trend similar to the antioxidant feed rate. Figure 7 trends ferrous iron, sulfite, and thiosulfate concentrations for the week. Note that the ferrous iron and thiosulfate concentrations cycled inversely for the week, with ferrous iron peaks occuring at thiosulfate minimums and vice versa. NOx removal for the week trended with ferrous iron concentration.

During the second week of new construction mode operation cyclic boiler loadings of from 260 to 540 MW resulted in flue gas oxygen content of from 6% to 10%. Antioxidant feed rate trended with flue gas oxygen, that is cycled inversely with boiler load. Sulfite and thiosulfate concentrations trended upward all week but cycled inversely to each other throughout the week. Thiosulfate concentration trended similar to antioxidant feed rate. Ferrous iron concentration peaked during thiosulfate concentration minimums and vice versa throughout the week. Figures 8 and 9 depict these interesting trends. Lower antioxidant mix consumption during the latter part of the week is evident from Figure 8 coinciding with increased sulfite and thiosulfate levels. During this second week of testing, L/G was held constant at 210 and NOx removal trended as a function of ferrous iron concentration ranging from 43% to 60%.

Interpretation: Continuous operation under relatively consistent operating conditions over the two week task test period revealed the expected trends regarding boiler load, flue gas oxygen level, antioxidant consumption rate, ferrous iron concentration, and NOx removal.

Again the interesting trends are those for sulfite and thiosulfite concentrations and their relationships to antioxidant feed rate and ferrous iron concentration. The difficulty in arriving at a straightforward interpretation of the trends in sulfur chemistries in FGD systems is illustrated by the trends exhibited during this task. Recall that an explanation given for the trends in the previous task centered on the proposed reaction pathway:

$$S_2O_4^{-2} + SO_3^{-2} \text{ -----> } S_2O_3^{-2} + SO_4^{-2} \quad (3)$$

which effectively explains the similar increasing trends for the sulfite and thiosulfate concentrations observed during the first week of testing, assuming excess dithionite is available in solution. To assess the relationshiop of ferrous-EDTA and sulfur species requires a look at the primary ferric-EDTA reduction reaction

$$S_2O_4^{-2} + 2Fe^{+3} + 2H_2O \text{ -----> } 2SO_3^{-2} + 2Fe^{+2} + 4H^+ \quad (4)$$

which implies that the reduction of the iron chelate (that is an increase in ferrous iron) should be directly accompanied by an increase in sulfite and indirectly via reaction (3) by an increase in thiosulfate in the presence of excess dithionite. By combining reactions (3) and (4) the sulfite intermediate is eliminated resulting in the overall reaction:

$$3S_2O_4^{-2} + 2Fe^{+3} + 2H_2O \text{ -----> } 2SO_3^{-2} + 2SO_4^{-2} + 2Fe^{+2} + 4H^+ \quad (5)$$

which directly implies that the reduction of the iron chelate should be accompanied by an increase in thiosulfate concentration. Moreover, in excess, the self-reduction of dithionite can lead directly to thiosulfate with production of dithionate by self-oxidation:

$$3S_2O_4^{-2} \text{ -----> } 2S_2O_3^{-2} + S_2O_6^{-2} \quad (6)$$

The predicted results of reactions (5) and (6) are proposed to explain the inverse cycling of the ferrous iron and thiosulfate concentrations during this testing task. A manual feedback loop was used at the pilot plant to maintain a 15 mM level of ferrous iron in the recycle tank. Whenever the ferrous level dropped ~2 mM below that level, the feed rate of the dry antioxidant mix was manually increased and conversely decreased when ferrous levels went ~2 mM above 15 mM. As seen in Figure 6, this feedback loop was not highly precise, being based on hourly ferrous analyses and subject to flue gas oxygen swings, which often resulted in fairly drastic "peaks and valleys" of antioxidant use

and ferrous levels. At high ferrous levels antioxidant use was low. This would result in low levels of dithionite and subsequently thiosulfate. At low ferrous levels antioxidant use was high. This would result in high levels of dithionite and subsequently thiosulfate.

In the second week of this task both sulfite and thiosulfate levels trended upward all week but cycled inversely to each other. Reaction (3) explains the concurrent rise in levels, but fails to explain the inverse cycling of levels. Other reaction pathways and/or intermediates are apparently in operation. One reaction pathway proposed by Rochelle, Owens, et al. involves oxidation of sulfite via the thiosulfate mediated formation of tetrathionate, $S_4O_6^{-2}$, with subsequent formation of trithionate, $S_3O_6^{-2}$, and its hydrolysis to thiosulfate and sulfate. The authors summarize by stating the net effect of the above reactions is oxidation of sulfite to sulfate with little or no loss of thiosulfate. This oxidation proceeds only under conditions of high thiosulfate levels, which occur at low ferrous level, high antioxidant use conditions. (See Figure 8)

TASK 3.1.3.3 B: High Iron Level Testing:

Purpose of Test: To raise the total iron level in the scrubber liquor to double and triple the normal operating level of 35 mM in order to determine the feasibility of utilizing sulfite reduction of ferric-EDTA to maintain operational ferrous-EDTA levels. Determine if antioxidant mix usage can be significantly reduced or eliminated.

Measures of Success: Determine operating levels of total iron that minimize or eliminate antioxidant consumption. Determine need for use of other additives to maintain proper chemistries.

Results of Tests: No specific prediction of NOx removal was made for this task as it was uncertain what ferrous iron levels would result from sulfite reduction of the ferric iron. Over the two week course of the task, NOx removal generally was in the 20-25% range and SO_2 removal was very nearly 100% except for a brief period when it fell to 99.5%. The operating conditions for this task's run were as follows: flue gas velocity of 8 feet per second, recycle liquid rate of 110 GPM for an L/G of 35 (45 including quench), seven Bete TF 28XPN nozzles, a 40% open area sieve tray two feet below 12 feet of PN Fill packing, and redistribution rings located at 0, 2, 4, 5, 7, 9, and 11 feet from the bottom of the packing. The conventional mist eliminator configuration was restored with the coarse section followed by a fine mist section. This was essentially a repeat of the retrofit mode configuration. Addition of the antioxidant mixture was discontinued. The duration of testing for this task was two weeks.

Unususally heavy rainstorms during the first two days of the task diluted the chemistry of the system necessitating addition of ferrous sulfate and sodium EDTA to re-establish desired total iron levels. A maintenance dose of sodium thiosulfate was added on the fourth day to keep sulfite and thiosulfate at desired levels. The sulfite, thiosulfate, and ferrous iron level trends for the week are illustrated in Figure 10. Ferrous iron concentration continued to peak during thiosulfate minimums and vice versa. This was particularly evident when the system was spiked with the ferrous chelate solution. Figure 11 plots NOx removal as a function of ferrous concentration in the recycle tank. Measured data points show highly unusual scatter between ferrous concentrations of 5 mM and 15 mM. The regression equation in Figure 11 shows NOx removal to be a function of ferrous concentration to only the 0.28 power as opposed to the expected ~0.5 power.

On the first day of the second week of testing the thiosulfate level was incrementally raised to 2500 ppm and on the second day it was raised to 7500 ppm while maintaining all other conditions constant. During the next 48 hours, ferrous concentration was maintained between 10 mM and 15 mM without use of any other antioxidant/reducing agent additives to the system. Ferrous oxidation tests were conducted on each of the final two days of the task. The recycle tank was isolated from the rest of the system, 50# of sodium dithionite was

added to it, the ferrous level was allowed to reach a baseline concentration, and then a study was made of the ferrous concentration versus time. Table 2 lists the data from these two oxidation tests as well as an oxidation test conducted previously at a total iron level of 36 mM. The oxidation runs conducted with elevated total iron levels (97mM and 86 mM) resulted in ferrous iron concentrations stabilizing 13 mM higher than the low total iron level test.

The plots of the sulfite, thiosulfate, and ferrous iron levels for the week are shown in Figure 12 with the week's events highlighted. Strong correlations between the three parameters were not obvious. Figure 13 plots NOx removal as a function of ferrous iron concentration; as seen for the previous week, there is much scatter and the regression equation shows NOx removal to be a function of ferrous concentration to only the 0.18 power.

NOTE: Post test inspection of the absorber tower revealed that one of the seven nozzles had fallen off. A review of the header pressure showed this event to have occurred in the first few hours of Phase III-B operation. A check of the spray pattern subsequently emerging revealed spray coverage of only 80% of the top of the packing due to starvation of the nozzles opposite the open pipe where the nozzle was missing. This condition existed for the entire time Phase III-B (TASK 3.1.3.3 B) was conducted. NOx removal was obviously adversely affected and that fact should be kept in mind when evaluating the data.

Interpretation: The relationship between ferrous iron levels and sulfite levels would seem to be obvious from the reduction of ferric-EDTA by sulfite:

$$2SO_3^{-2} + 2Fe^{+3}\text{-EDTA} \text{ -----> } S_2O_6^{-2} + 2Fe^{+2}\text{-EDTA} \qquad (7)$$

The two should trend similarly. The test data from the two week period shows no strong correlation. It is apparent that this reduction of iron chelate will proceed to a much greater extent at higher total iron levels when sufficient sulfite is present. It is unclear why it does not proceed in a more direct proportion to sulfite concentration. Perhaps the role of sulfite in the NOx removal mechanism plays a part. No doubt the numerous intermediate sulfur

species and reaction pathways likely to be present have an effect as well. The curious inverse cycling of ferrous and thiosulfate levels during the first week cannot be accounted for by the dithionite mechanisms proposed earlier. This suggests a more direct relationship between the two species that unfortunately also remains unclear. The fact that the inverse cycling did not occur during the elevated thiosulfate levels of the second week hints at a certain equilibrium component to this relationship. Given the precarious nature of any interpretative foundations based upon FGD sulfur chemistries such equilibria as may participate cannot be easily delineated.

Although thiosulfate apparently does not directly participate in ferric-EDTA reduction, it is believed to inhibit sulfite oxidation. As less sulfite is oxidized, more becomes available to reduce the ferric chelate to the active ferrous form through reaction (7).

The disparity in NOx removals for any certain ferrous level during this task with the historical relationship is due in part to the missing spray nozzle which had a detrimental effect on gas-liquid interfacial area. The disparity (dependence on ferrous concentration to the ~0.5 (approximately) power earlier versus to the ~0.2 (approximately power now) is too large to be explained by the missing nozzle alone. Another factor contributing heavily to decreased NOx removal is the unprecedented level of dissolved solids in the scrubber liquor. Approaching 20%, this level of dissolved solids is believed high enough to inhibit the solubility of NO and possibly impart sufficient ionic strength to the solution to suppress the activities of the ferrous chelate and sulfite species. Another contribution to lower than expected NO removals may be the increase formation of the ferrous EDTA-NO adduct. This may be feasible since sulfites react slowly with this adduct at typical scrubber temperatures.

SUMMARY OF PHASE III TESTING:

Meeting of Model-Predicted NOx Removal Objectives:

The extent to which the Phase III testing program met the model prediction NOx removals are illustrated in Figure 2. The main reasons for the inability to achieve predicted NOx removals were that the NOx removal dynamics of the spray zone contribute to the removal criteria in a manner that affects both the gas-liquid interfacial area and height of packing zone in the manner discussed under Task 3.1.3.1, and that the high dissolved solids content of the scrubber liquor possibly affects NO solubility and the activities of crucial chemical species involved in the NOx removal mechanism. Operating at flue gas velocities 0.5 to 1.0 fps higher than planned (by pitot tube traverse measurements) also contributed to lower than predicted NOx removals. Generally speaking the removals did correspond well to the doubling of packing height. One of the benefits of correlating test data to model predictions is to discern those areas of the model that can be modified so that the model becomes a more useful predictive tool. Two such areas are noted above.

Another potential model parameter modification area studied extensively in Phase III was the ferrous iron concentration component, specifically the oxidation of the iron chelate as it passes through the absorber. The rationale for this study was that if the ferrous concentration decreases appreciably as it contacts the oxygen-laden flue gas on its way down the column then the NOx removal in lower portions of the packing would be lower than the model predicts and a certain ferrous/removal gradient would exist in the absorber. Extensive analyses of recycle tank (absorber feed) and downcomer (absorber return) liquor samples performed throughout this phase show that the ferrous levels dropped from 1 mM to 4 mM as the absorber liquor passed through the tower with the norm being 1 mM to 2 mM lower ferrous concentration in the downcomer. It may therefore be concluded that the bulk of the ferrous iron oxidation occurs from dissolved oxygen present in the recycle tank since antioxidant consumption is much higher than needed to compensate for the levels of ferrous iron differential occuring through the "scrubbing zone". Although this decrease in

ferrous level affects the NOx removal it is not considered significant enough to warrant a modification to this model parameter. It is suggested that such data be collected for larger scale applications to determine if significant ferrous/NOx removal gradients exist.

Sulfur Dioxide Removal Efficiency:

Throughout this phase of testing SO_2 removal efficiencies consistently exceeded 99.5%. This was expected considering the large surface area and low flue gas velocities utilized. The important conclusion to be drawn here is that SO_2 removal will approach these levels whenever a scrubber is retrofitted or designed to achieve NOx removals. This fact could become significant if and when NOx removal credits are implemented because simultaneous SO_2/NOx scrubbing will generate additional SO_2 credits.

Solids Dewatering:

The dramatic improvement over conventional magnesium enhanced lime FGD in belt filter cake solids dewatering during the NOx removal process continued in Phase III. Regardless of whether the sodium dithionite/ascorbic acid reducing agent/antioxidant was used or if high total iron/high thiosulfate chemistry prevailed, the solids content of the belt filter cake was consistently in the 70% range (See Table 3) as compared to normal thiosorbic based filter cake solids in the 35% to 45% range. In fact after two weeks of operation without the use of the antioxidant mix high solids dewatering actually improved.

This excellent dewaterability of the filter cake is one of the significant outcomes of the project. It translates into lower consumption of chemical additives because of the tight water balance. Lower disposal costs because of the reduced sludge volume generated. This excellent solids dewaterability represents a cost reduction for this NOx removal process over the life of a commercial plant.

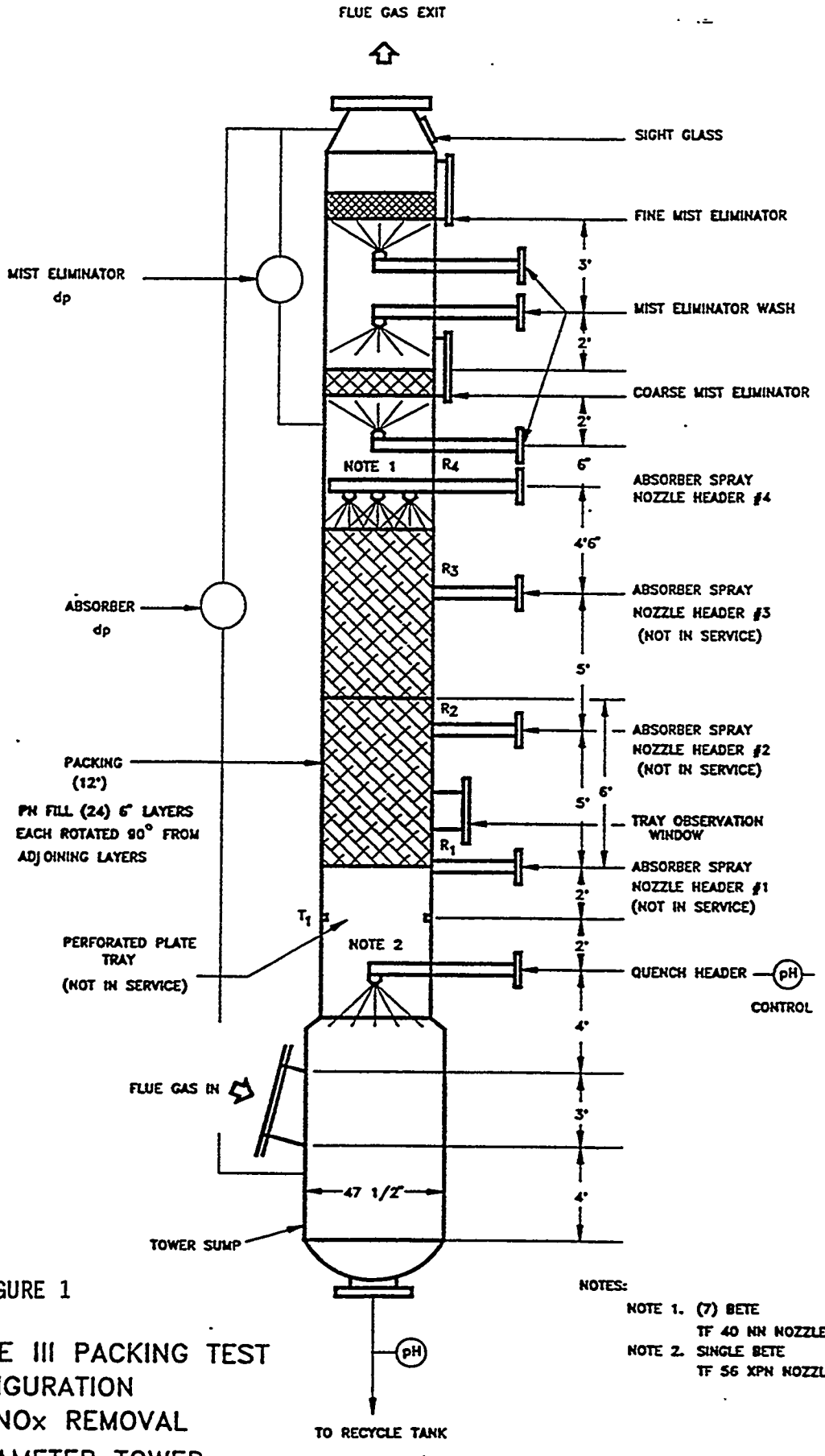

FIGURE 1

PHASE III PACKING TEST
CONFIGURATION
FOR NOx REMOVAL
3' DIAMETER TOWER

NOTES:

NOTE 1. (7) BETE
TF 40 NN NOZZLES

NOTE 2. SINGLE BETE
TF 56 XPN NOZZLE

Figure 1

FIGURE 2

NO REMOVAL PREDICTION FOR PHASE III
12 FT. BED OF MUNTERS PN FILL
BASIS: CORRELATION OF PHASE II DATA
AND NO REMOVAL MODEL
DATA NORMALIZED TO [Fe+2] = 15 mM

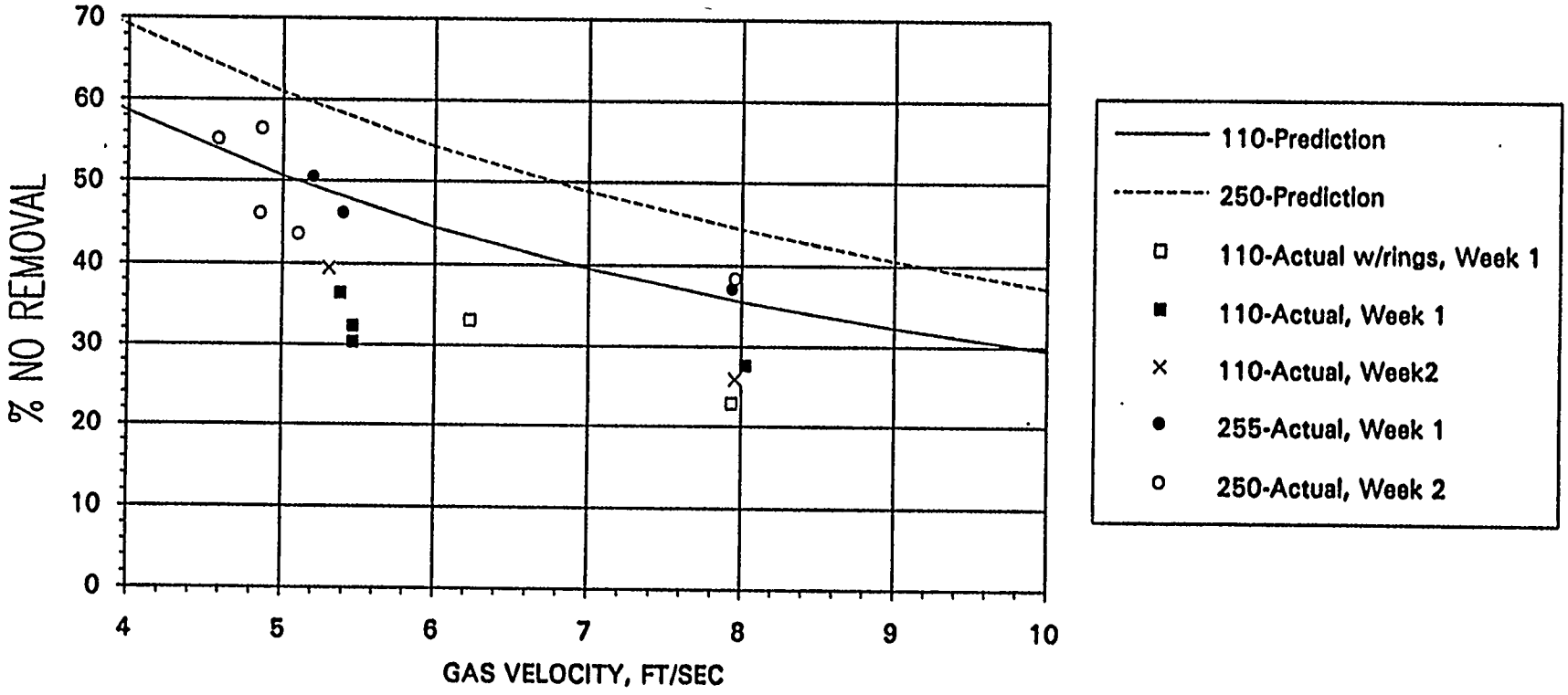

Figure 2

Figure 2

FIGURE 3

Miami Fort Pilot Plant
Task 3.1.3.2
Retrofit Operation Test

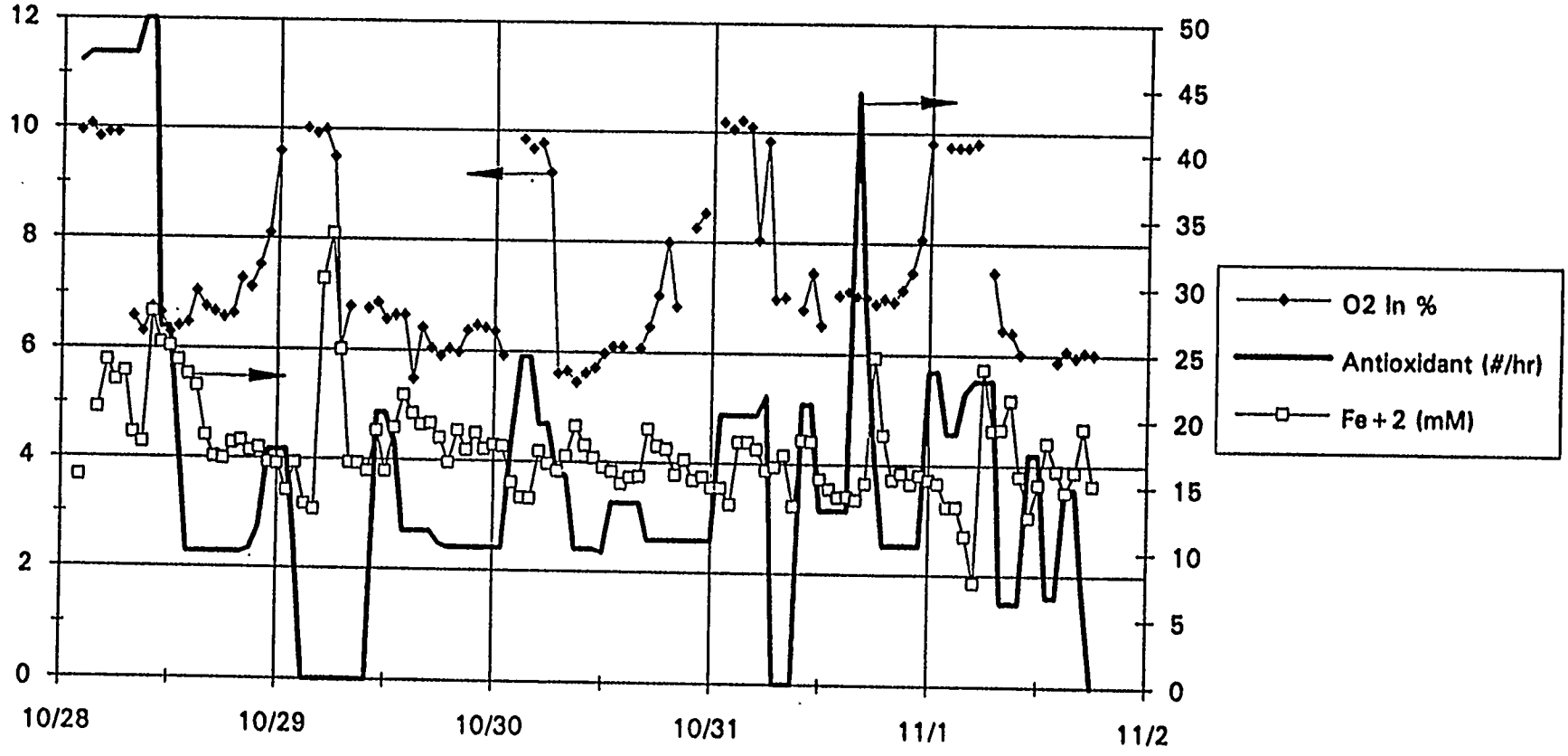

Figure 3

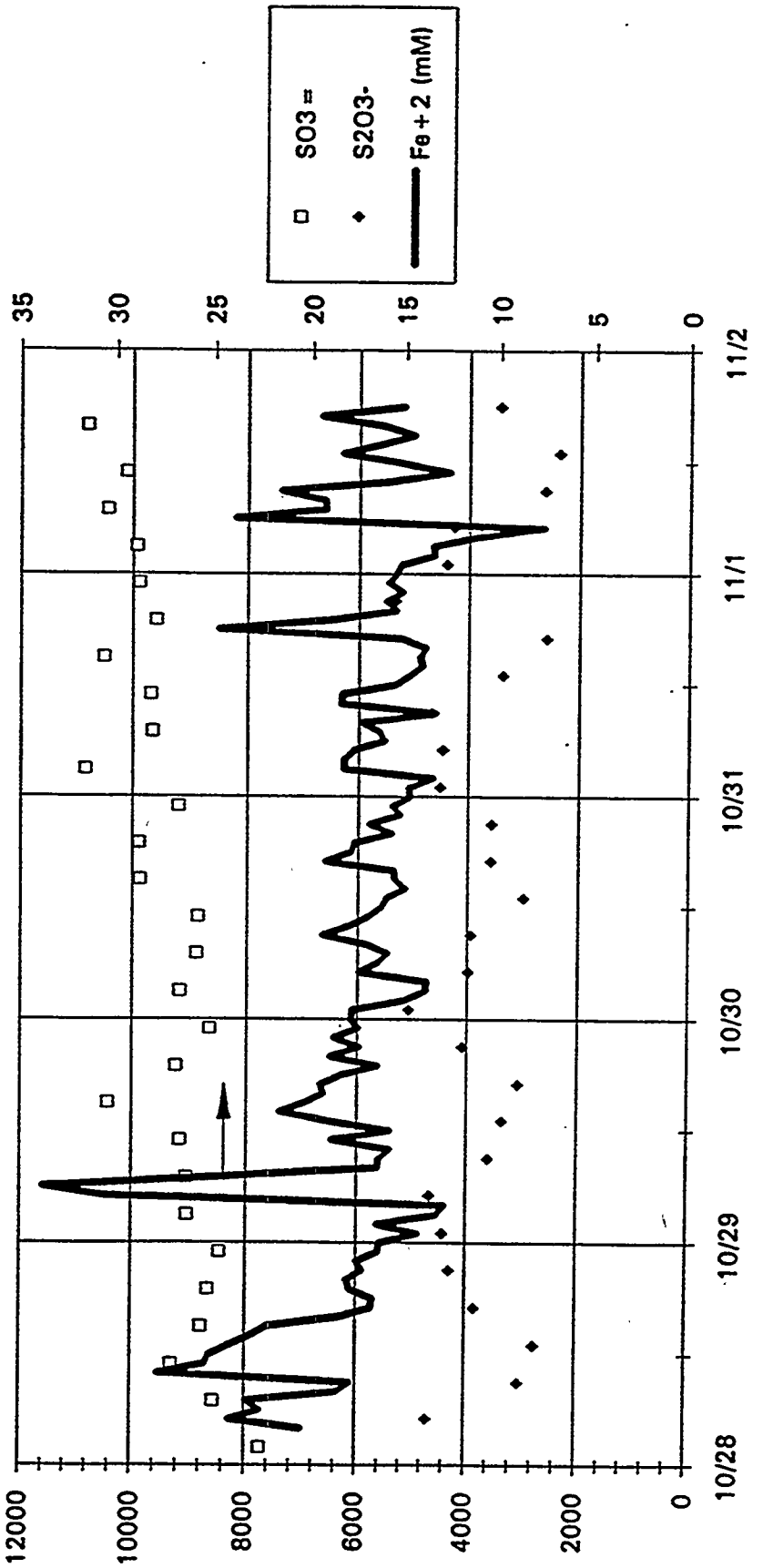

FIGURE 4
Miami Fort Pilot Plant
Task 3.1.3.2
Retrofit Operation Test

Figure 4

Figure 4

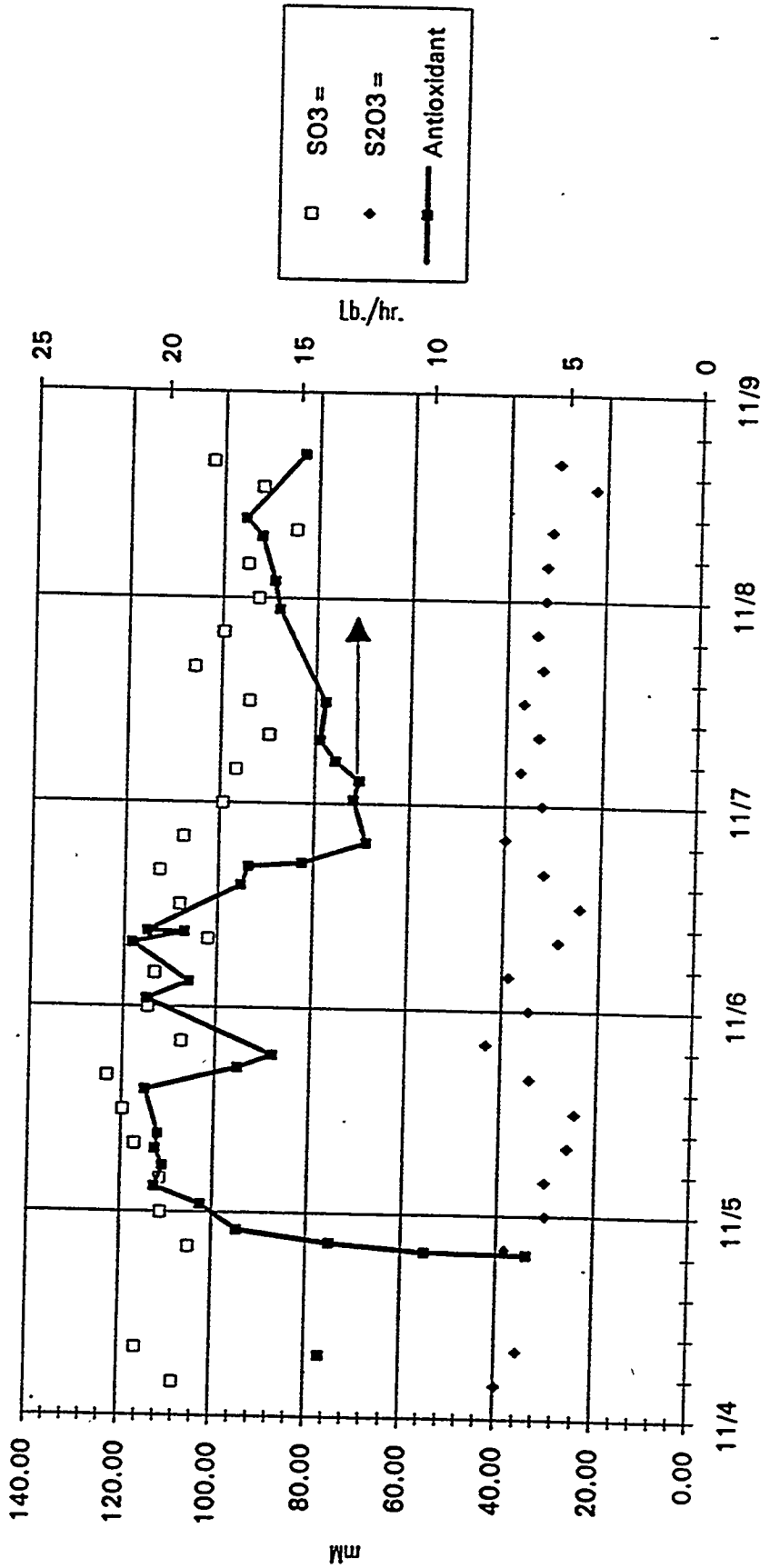

FIGURE 5
Miami Fort Pilot Plant
Task 3.1.3.2
Retrofit Operation Test; Week 2

Figure 5

Figure 5

FIGURE 6

Miami Fort Pilot Plant
Task 3.1.3.3
New Construction Operation Test; Week 1

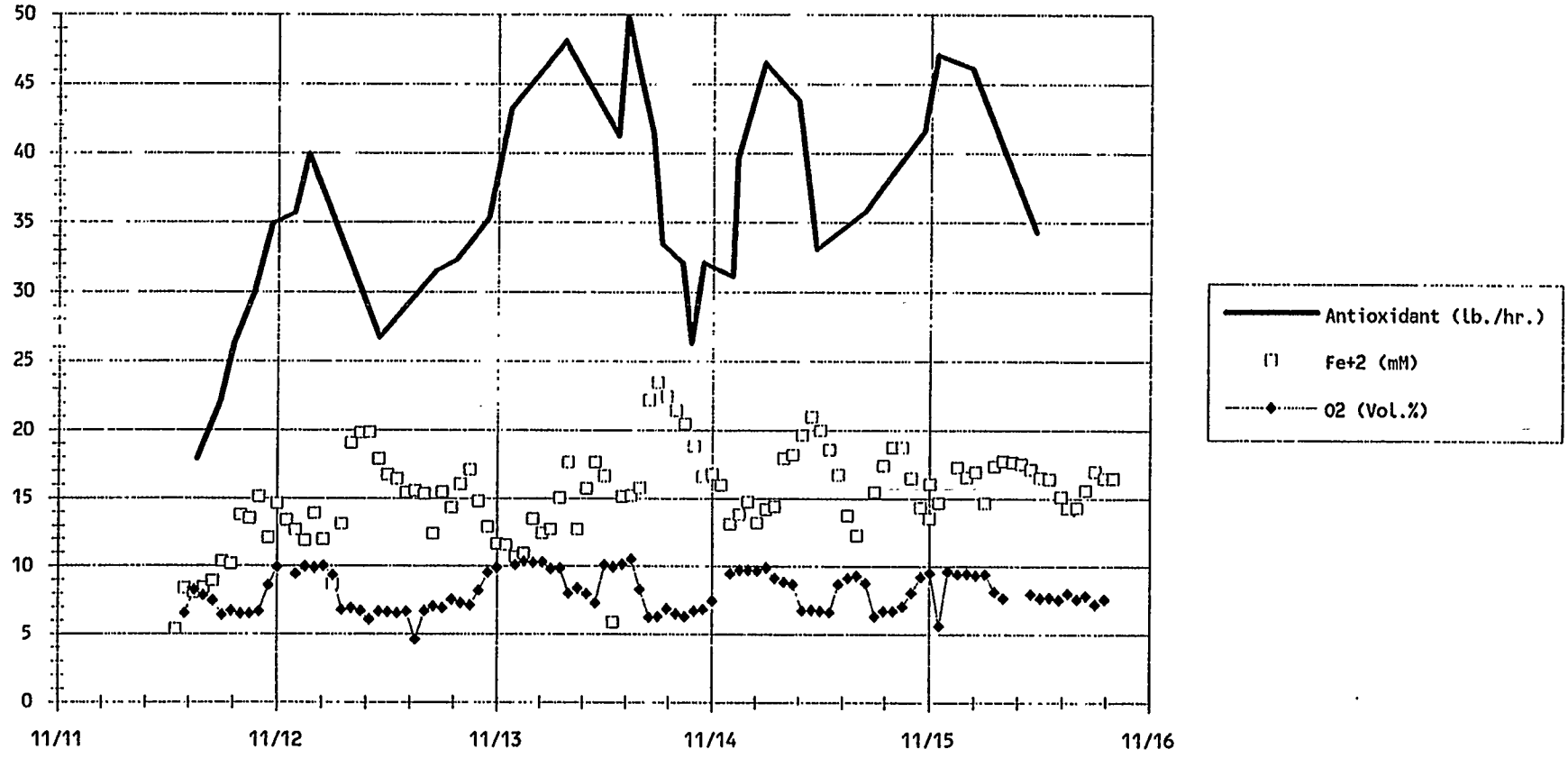

Figure 6

III-71f

Figure 6

FESXOX.XLC

FIGURE 7

Miami Fort Pilot Plant
Task 3.1.3.3
New Construction Operation Test; Week 1

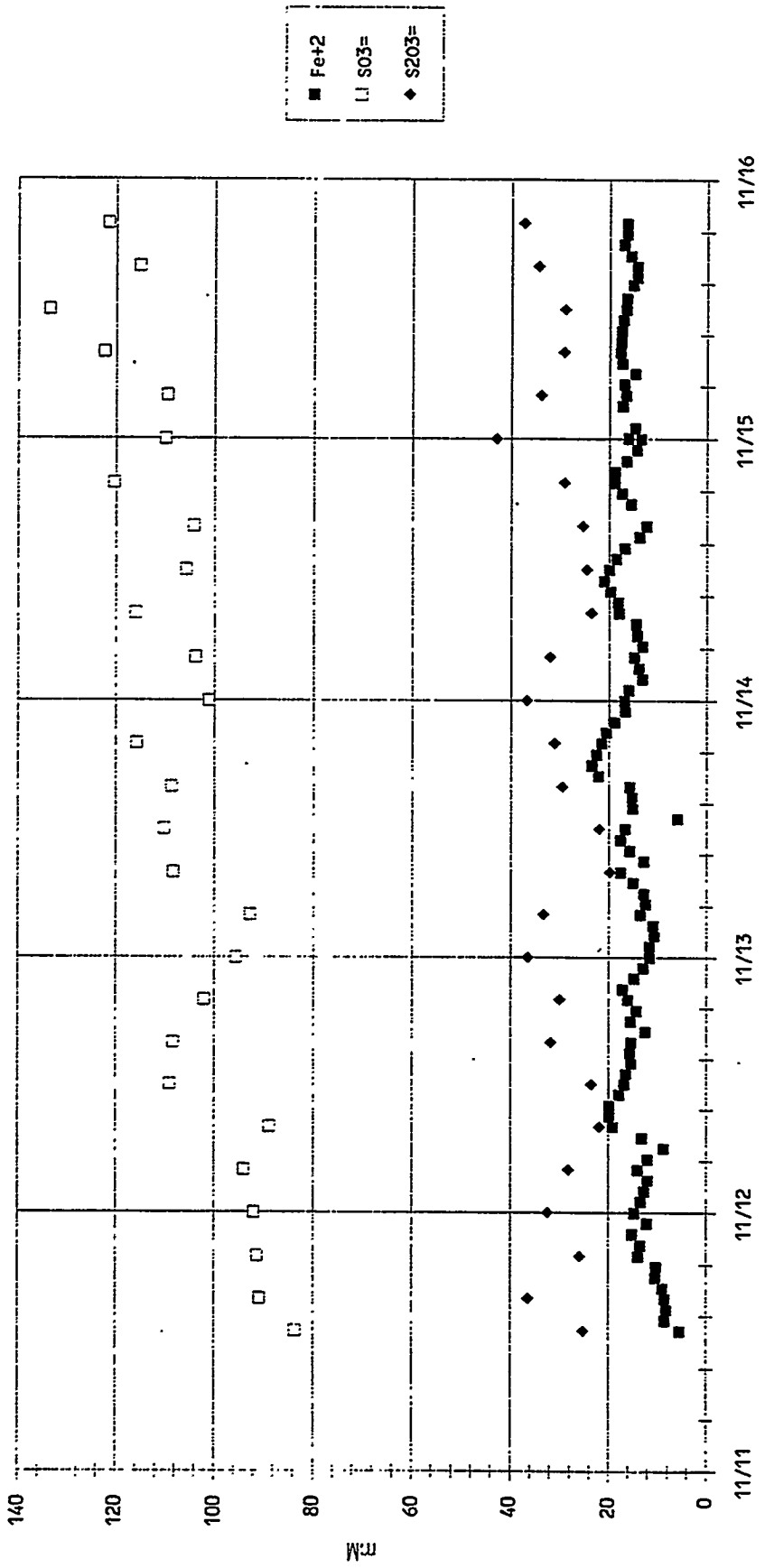

Figure 7

Figure 7

ADSXOX.XLC

FIGURE 8

Miami Fort Pilot Plant
Task 3.1.3.3
New Plant Construction Operation Test; Week 2

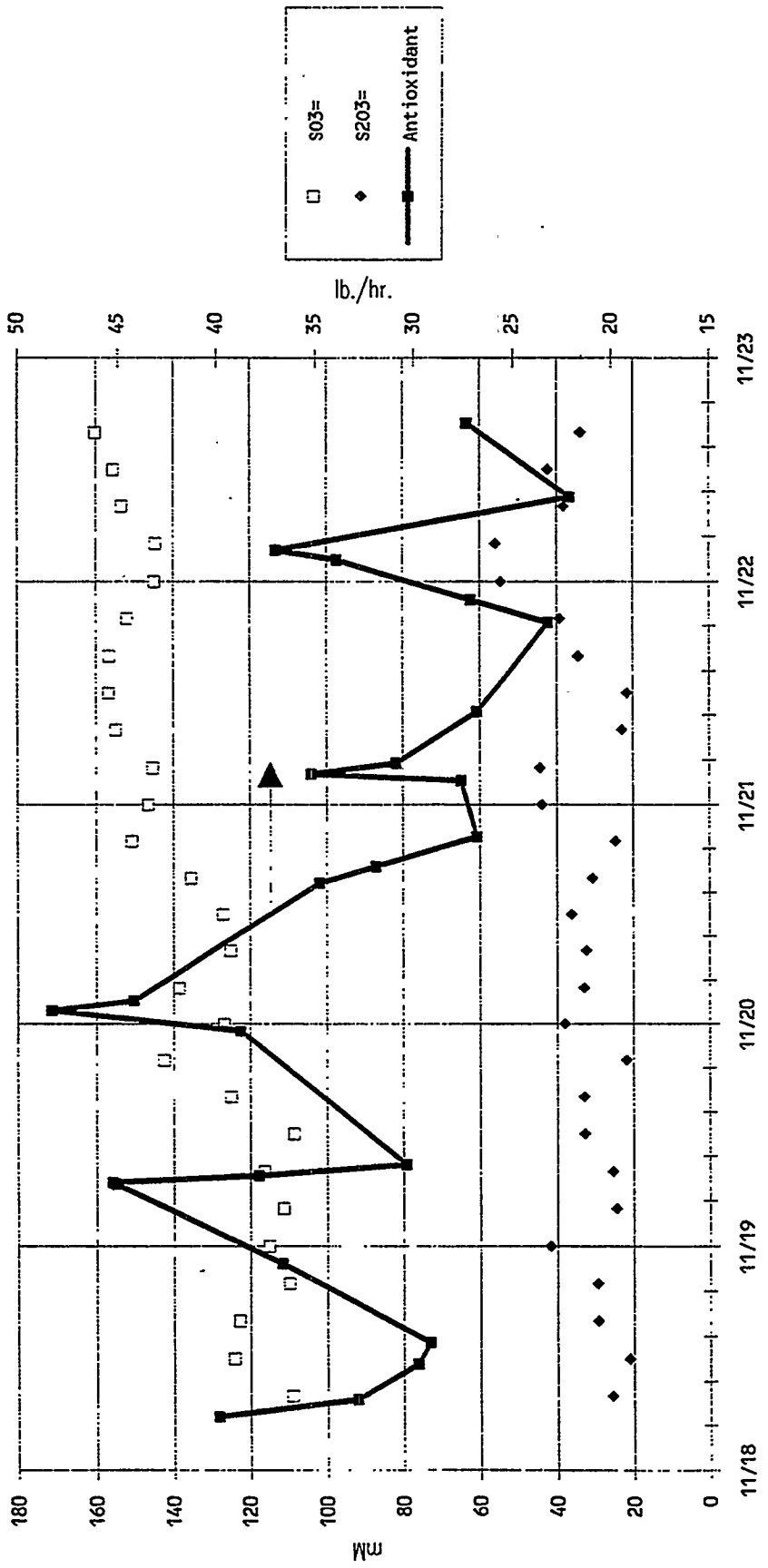

Figure 8

Figure 8

FESXOX.XLC

FIGURE 9

Miami Fort Pilot Plant
Task 3.1.3.3
New Plant Construction Operation Test; Week 2

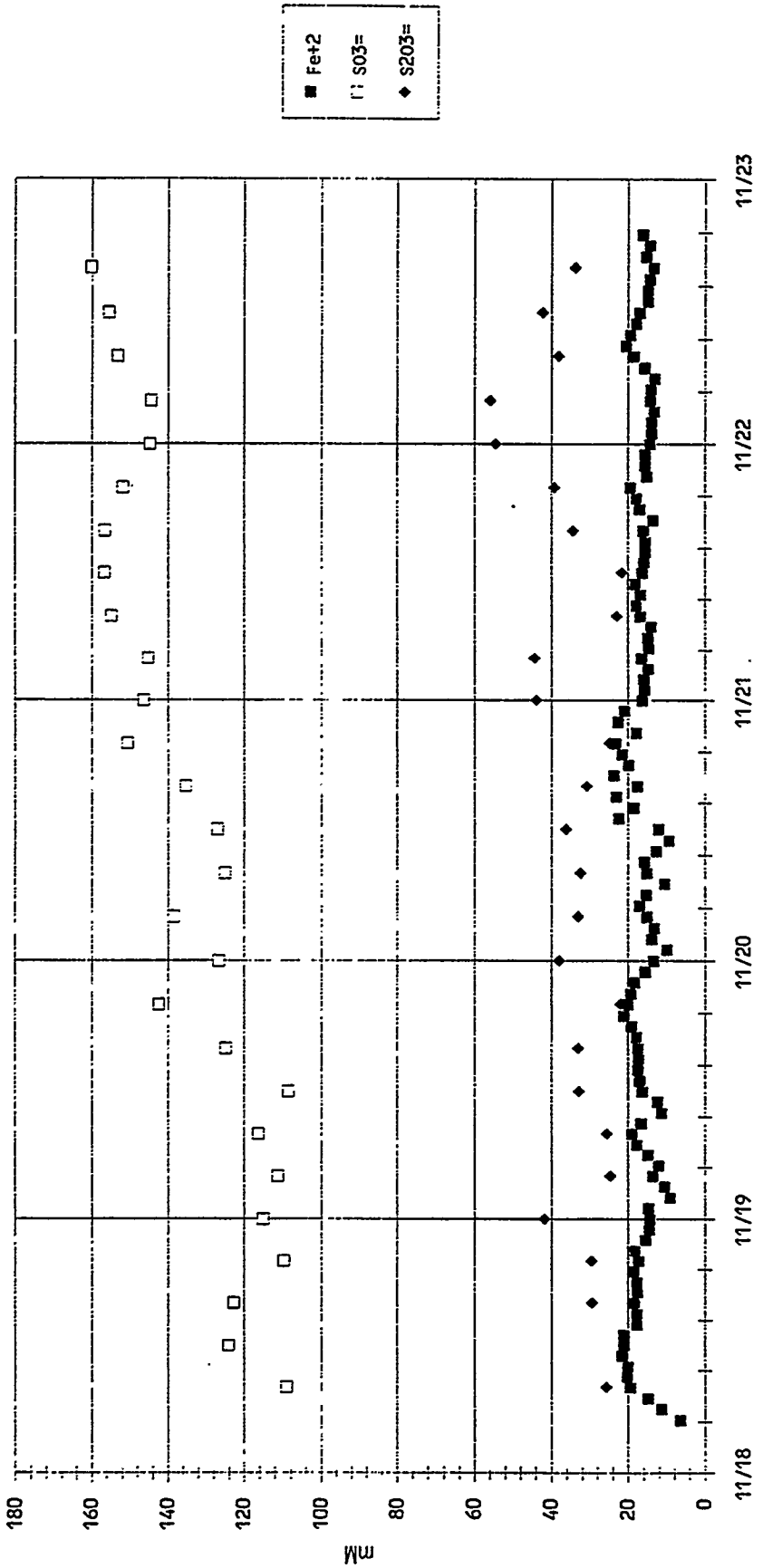

Figure 9

Figure 9

FIGURE 10

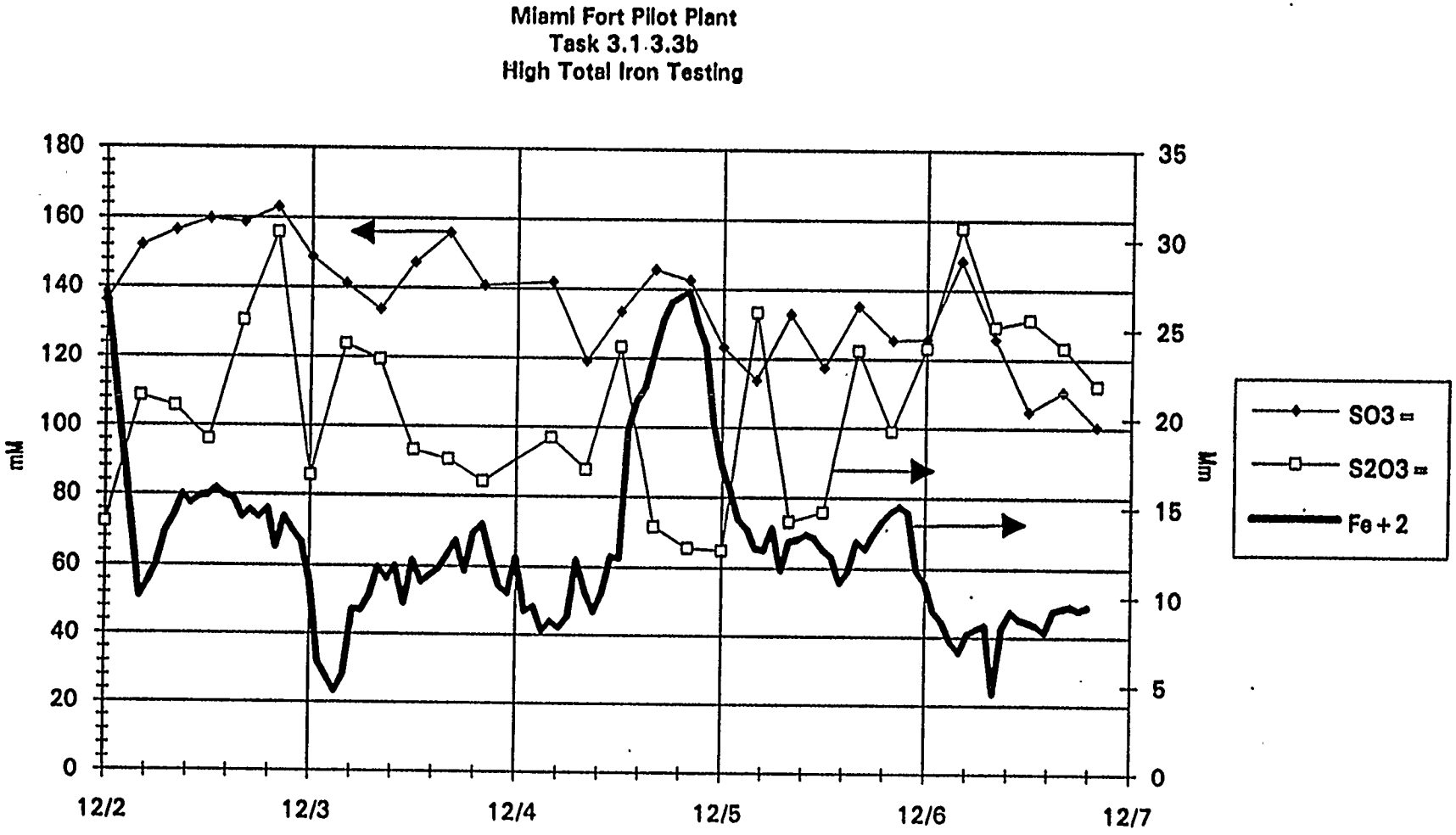

Figure 10

FIGURE 11

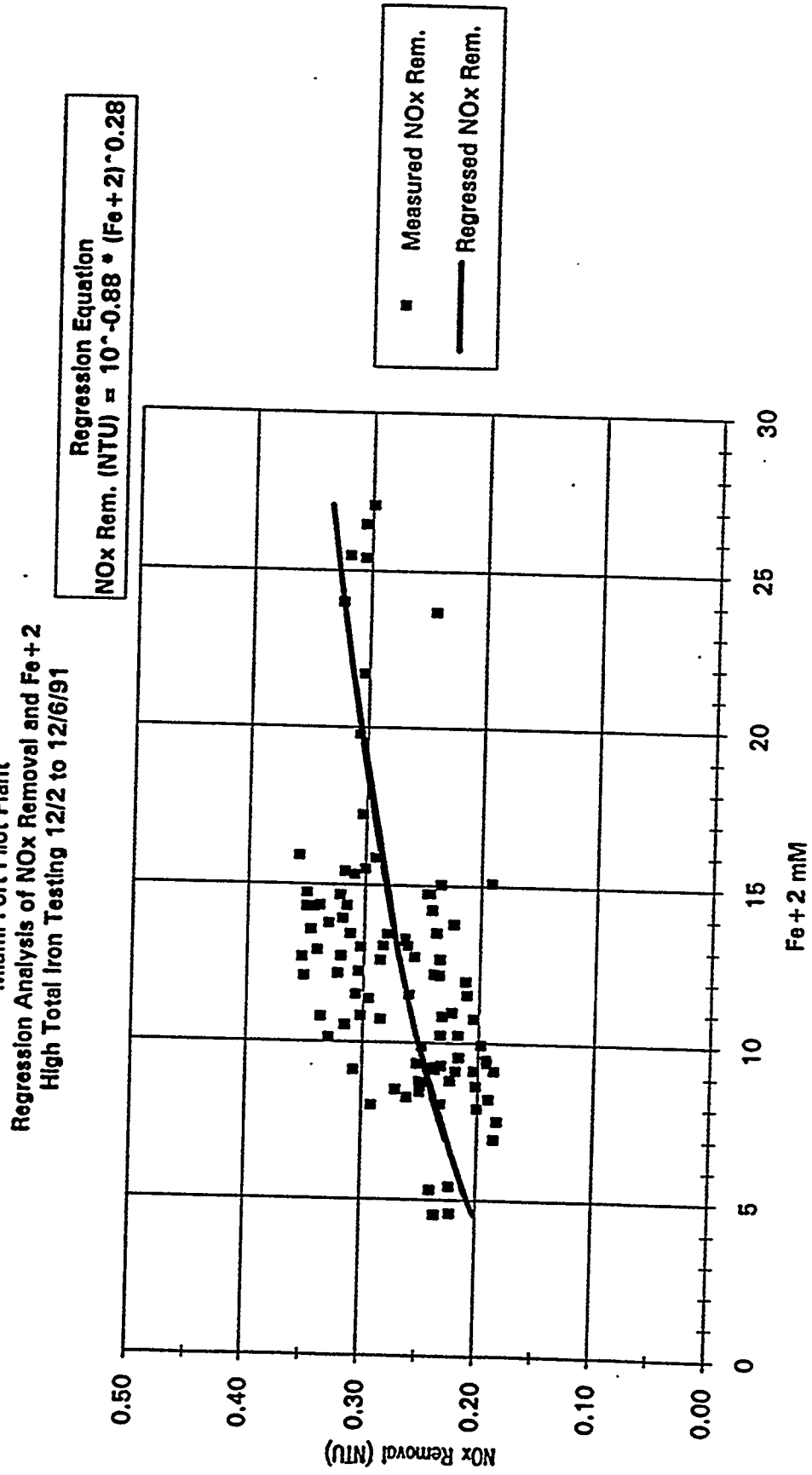

Figure 11

Figure 11

FIGURE 12

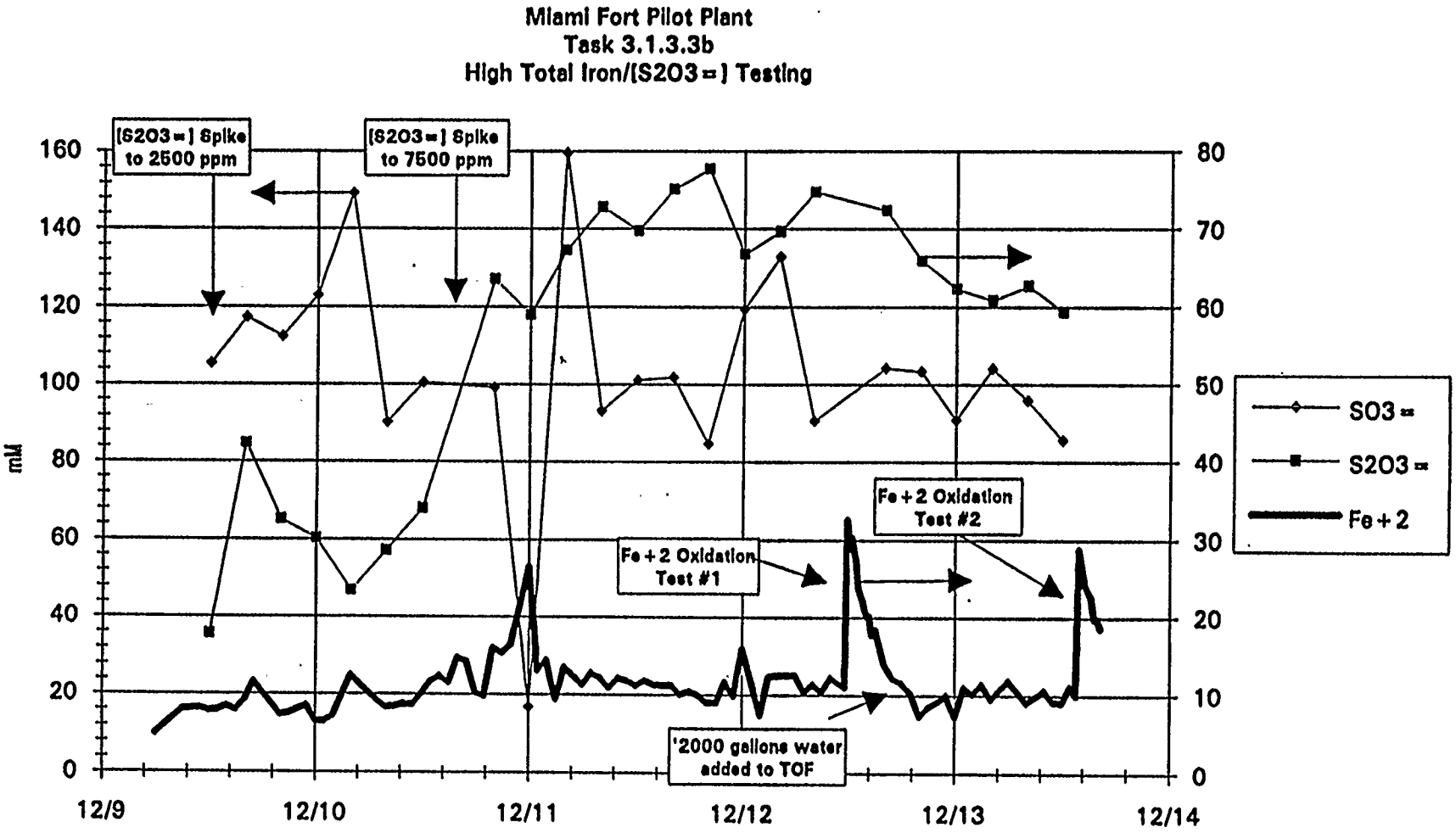

Figure 12

FIGURE 13

Miami Fort Pilot Plant
Regression Analysis of NOx Removal And Fe+2
High Total Iron Testing 12/9 to 12/13/91

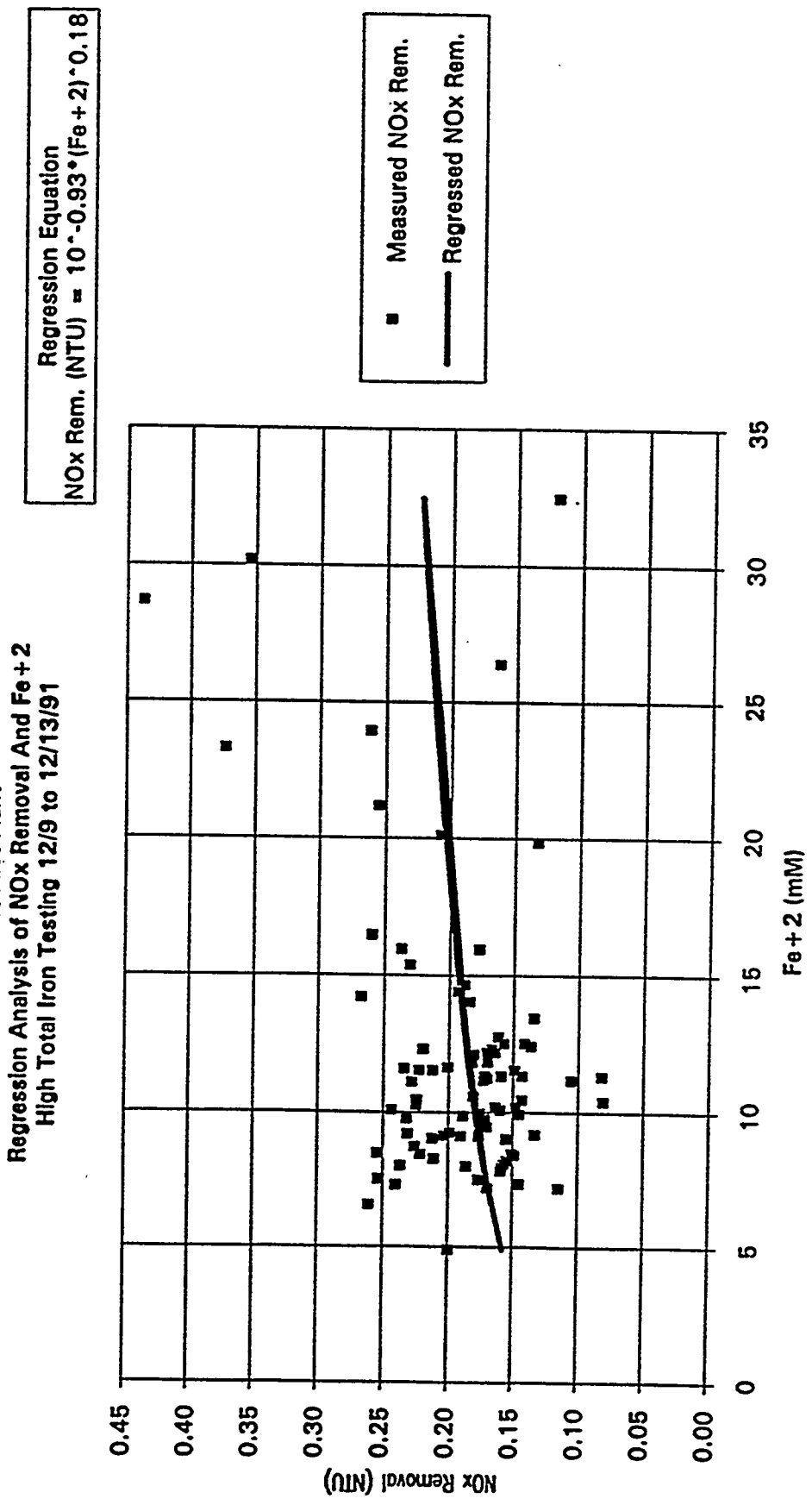

Figure 13

Figure 13

TABLE 1

Table - 1A NOx Removal Data Regression Analysis of Model Confirmation Tests w/ PN Fill / Snowflake Packing (Normalized to Fe+2 = 15 mM and Corrected Velocity)

	LOG(GPM)	LOG(Vel)	k	
	0.41	-0.95	-0.48	
Std. Err. Coe	0.15	0.22	0.45	Std. Err. Coeff.
R^2	0.90	0.06	Std. Y Est.	
F Statistic	28.12	6.00	d.f.	
SSreg.	0.19	0.02	SSresid.	

NO_x Removal (NTU) = $L^a \times V^b \times 10^c$

Table - 1B Pressure Drop Data Regression Analysis of Model Confirmation Tests w/ PN Fill / Snowflake Packing (Corrected Velocity)

	LOG(Vel)	LOG(GPM)	k	
	2.00	1.02	-3.34	
Std. Err. Coe	0.34	0.23	0.70	Std. Err. Coeff.
R^2	0.86	0.09	Std. Y Est.	
F Statistic	18.36	6.00	d.f.	
SSreg.	0.30	0.05	SSresid.	

Pressure Drop ("WC) = $V^a \times L^b \times 10^c$

where: L = liquid rate in gallons per minute

V = flue gas velocity in feet per second

c = a constant

Table 1

Ferrous Oxidation Test Summary

Fe+2 Oxidation Test #1				Oxid. Rate
Date/Time	Elapsed Time	Fe+2 (mM)	Ln( )	mM/min
12/12 11:35	0	11.1	0.000	....
12/12 11:50	15	32.5	1.078	-1.4287
12/12 12:05	30	30.2	1.004	0.1533
12/12 12:20	45	30.4	1.010	-0.0113
12/12 12:35	60	28.7	0.954	0.1107
12/12 12:50	75	27.3	0.902	0.0960
12/12 13:05	90	24.0	0.773	0.2200
12/12 13:20	105	23.0	0.730	0.0667
12/12 13:35	120	22.2	0.695	0.0540
12/12 13:50	135	21.0	0.640	0.0787
12/12 14:05	150	20.13	0.599	0.0560
12/12 14:20	165	20.24	0.604	-0.0073
12/12 14:35	180	17.72	0.471	0.1680

Fe+2 Oxidation Test #2 (Diluted System)				Oxid. Rate
Date/Time	Elapsed Time	Fe+2 (mM)	Ln( )	mM/min
12/13 13:35	0	10.0	-0.098	....
12/13 13:55	20	28.7	0.954	-0.9335
12/13 14:15	40	26.3	0.865	0.1220
12/13 14:35	60	24.2	0.782	0.1045
12/13 14:55	80	23.3	0.746	0.0430
12/13 15:15	100	22.7	0.718	0.0315
12/13 15:35	120	19.8	0.583	0.1435
12/13 15:55	140	19.9	0.585	-0.0025
12/13 16:15	160	18.7	0.523	0.0600
12/13 16:35	180	19.2	0.553	-0.0280

Fe+2 Oxidation Test #3 (Total Fe = 36 mM)				Oxid. Rate
Date/Time	Elapsed Time	Fe+2 (mM)	Ln( )	mM/min
10/17/91 1:00	0	8.5	-0.263	....
10/17 1:20	20	27.0	0.891	-0.9225
10/17 1:40	40	19.2	0.553	0.3865
10/17 2:00	60	15.1	0.308	0.2085
10/17 2:20	80	10.4	-0.060	0.2315
10/17 2:40	100	9.1	-0.194	0.0655
10/17 3:00	120	8.7	-0.237	0.0190
10/17 3:20	140	8.5	-0.267	0.0130
10/17 3:40	160	7.8	-0.347	0.0325
10/17 4:00	180	6.9	-0.478	0.0480
10/17 4:20	200	6.6	-0.516	0.0130

Miami Fort Pilot Plant
Fe+2 Oxidation Tests; Task 3.1.3.3b
Test #1 [S2O3=] = 8700 ppmwt; [Total Fe] = 97 mM
Test #2 [S2O3=] = 6900 ppmwt; [Total Fe] = 86 mM
Test #3 [S2O3=] = 5000 ppmwt; [Total Fe] = 36 mM

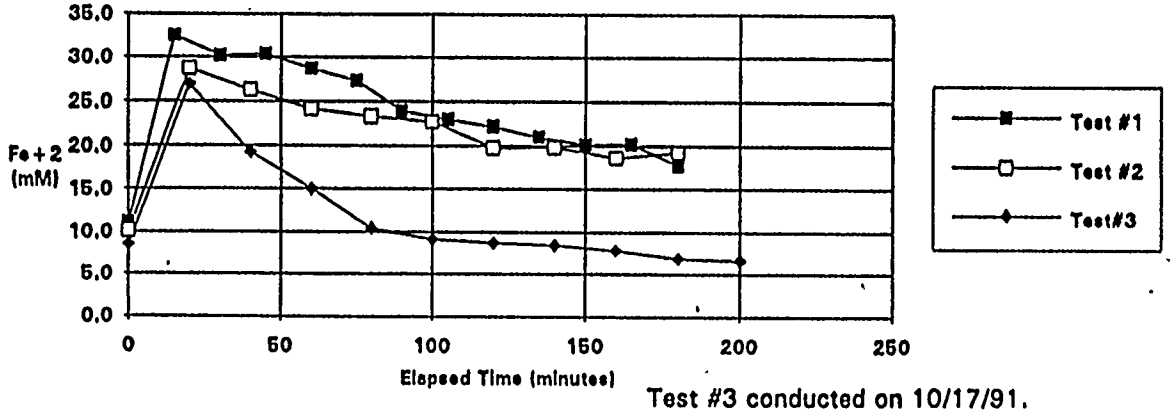

Test #3 conducted on 10/17/91.

Table 2

Table 2

TABLE 3

Solids Settling & Filtration Results Summary						
Date	Maximum Thickened Solids Conc. (~23 hrs) (wt. %)	Expected TUF Concentration w/unit area of 20 ft2/tpd (wt. %)	Actual Thickener Underflow Solids Conc. (wt. %)	Lab Filter Cake Solids (wt. %)	Actual Filter Cake Solids (wt. %)	Comments
10/14			64.2			1) All actual pilot plant data reflect the highest values recorded that day. 2) Excluded are initial readings of thickener underflow solids after restart.
10/15			62.3			
10/16	59.1	57.0	64.7	69.8		
10/17			63.2			
10/18			63.9			
10/21	56.1	52.6	62.8	65.4		
10/22	60.6	56.8	63.1	67.2		
10/23			62.0		71.0	
10/24	70.1	56.3	63.3	67.2		
10/28	56.7	53.7	59.0	64.9		
10/29	53.9	50.6	61.2	62.2		
10/30	57.8	53.2	62.9	62.9		
10/31	57.0	56.3	62.5	65.3		
11/1	59.1	59.1	60.3	66.3	69.1	
11/4	60.8	58.4		65.2		
11/5			59.2			
11/6	58.9	54.2	55.9	65.7	69.6	
11/7	63.9	59.5	64.2	69.9		
11/8			57.6			
11/11					68.8	
11/12	65.6	57.9	63.8	69.3		
11/13			63.3			
11/14	71.2	59.5	63.1	68.1		
11/15	64.0	60.0	62.0	69.4		
11/18	59.0	50.0	54.0	64.6	76.8	
11/19	65.8	60.2	62.9	69.6		
11/20			66.1			
11/21	66.8	65.4	64.4	70.9		
11/22	60.1	57.8	66.5	71.0		
11/25					69.1	
12/2			63.7			
12/3	65.7	60.5	67.2	71.1		
12/4	62.5	55.5	66.8	69.4		
12/5	65.1	61.3	66.9	71.2		
12/6	66.6	63.6	66.1	72.0		
12/9	70.2	65.9	69.7	71.6		
12/10			67.7			
12/11			67.9			
12/12			70.1			
12/13	64.0	62.9		74.3		
12/17					77.8	

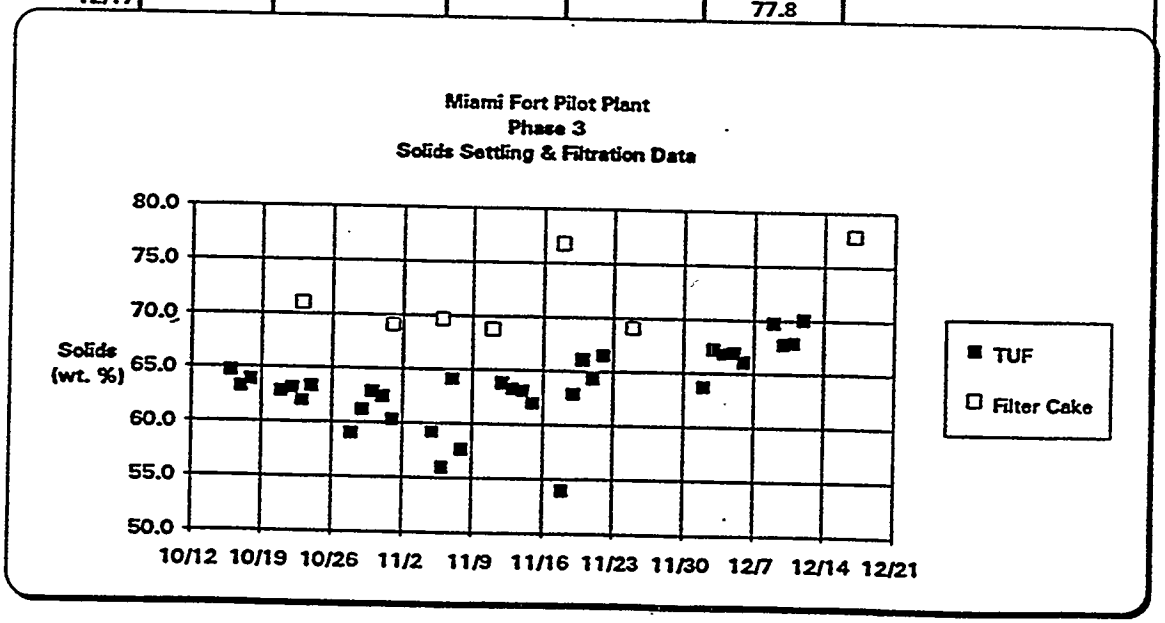

Table 3

IV. DESCRIPTION AND RESULTS OF WASTE CHARACTERIZATION STUDIES

A. BACKGROUND

An important aspect of this project has been the detailed study of the solid waste produced as a result of the simultaneous SO_2/NOx removal from coal-fired boiler flue gas at the pilot plant level. Thiosorbic lime (or magnesium enhanced lime) flue gas desulfurization (FGD) waste solids are usually dewatered by vacuum rotary filter or vacuum belt filter processes and are often referred to as FGD sludge. This material, principally calcium sulfite ($CaSO_3$) and calcium sulfate ($CaSO_4$), is usually stabilized with flyash and/or lime for landfill disposal.

This material has historically been quite amenable to stabilization techniques. A specific exclusion has been granted under RCRA [40 CFR 261.4 (b) (4)] allowing this material to be classified as a non-hazardous solid waste. Analyses conducted on the vacuum filter belt dewatered FGD solid waste from the Miami Fort Pilot Plant operating in the regular Thiosorbic mode confirmed the non-hazardous nature of this material.

The process modifications introduced to the Thiosorbic FGD process in order to effect NOx removal included the addition of several chemical reagents to the process liquor. Ferrous sulfate and tetra-sodium EDTA formed the iron chelate involved in the primary NOx removal step. Sodium dithionite, ascorbic acid, and to a lesser extent, glyoxal and sodium thiosulfate were utilized as reducing agents and/or antioxidants to maintain the iron chelate in the active ferrous form. The presence of these chemical species in the scrubber liquor along with the nitrogen compounds formed as a result of the NOx removal process have the potential to change the chemical composition and physical characteristics of the resulting sludge.

The main purpose of the waste characterization study of this NOx removal process-modified FGD sludge was to insure its suitability for land disposal in the usual manner. To this end the study centered around two criteria: the physical properties of the sludge as they apply to stabilization for disposal, and the chemical composition of the sludge as it applies to its disposal as a non-hazardous solid waste. Extensive stabilization testing and chemical analyses were conducted in conjunction with biological toxicity and microbiological tests for this determination.

B. PROGRAM OVERVIEW

1. Program Objectives

As stated above, the main purpose of the waste characterization program was to insure that the FGD sludge generated during the NOx removal project could be disposed on land in the same manner as the basic Thiosorbic process-generated sludge. The main components of this study were stabilization testing to insure physical fitness for landfilling and chemical testing to insure that the solid waste generated remained non-hazardous. The hazard determination was expanded beyond the RCRA scope of testing to include biological (aquatic) toxicity testing and a micro-biological assay. Miscellaneous physical and chemical testing such as X-Ray Florescence, particle size determination, photomicrographs, loss on ignition, total sulfur content, and others were performed primarily to monitor the consistency of the filter cake over the course of the program and to function as a quality control mechanism to alert program personnel to any major variation in sludge quality.

2. Sampling Plan

The filter cake generated at the Miami Fort Pilot Plant (MFPP) during the project was routinely sampled as it discharged from the belt filter onto a discharge conveyor belt. This discharge point provided access for the sampler to take a full-cut sample from the belt filter without stopping the filtration process. It also provided a representative sample while maintaining sampling consistency from one sampler to another throughout the duration of the project. Filter cake was typically generated in batches. The filter feed tank would reach a predetermined level (~50%-75%) and filtration would commence. When the filter feed tank was nearly empty a (~6%-10%), filtration would cease. Thus, the resulting batch of filter cake would be quite homogeneous as several days' filter feed had been mixed in the filter feed tank prior to filtration. Each batch of filter cake was a reflection of scrubber operating conditions from several previous days. Standard procedure was

for the filter feed tank to be emptied whenever a new set of operating conditions was imposed upon the scrubber. Filter cake samples hence remained representative of scrubber conditions. Sampling was conducted at roughly two-hour intervals during operation of the filter when a pair of grab samples were each collected in one gallon pails.

This duplicate pair of filter cake grab samples was assigned a sample number corresponding to the date and time of sampling in order to better determine what set of scrubber conditions prevailed at the time the solid waste was generated. On-site determinations of moisture, residual EDTA, pH, and phase (solid or liquid via paint filter test) were made. These one-gallon sample pairs were then shipped to the Dravo Research Center where they were subjected to both physical and chemical testing. One set of duplicate samples was saved and not used unless needed for sample volume makeup. The remaining set of duplicate samples provided the bulk of the material used for testing. The testing program was quite flexible and evolved in accordance with the knowledge of the sample material gained as the project progressed. Thus the sample handling and analysis process was different for each phase of the project as illustrated in Figure 1. Note that the number of individual composite samples varied in each phase. This was a reflection of the length of each phase as well as the number of major scrubber operating conditions during each phase warranting solids examination. A majority of the individual grab samples were utilized in making the individual composite samples with the primary selection criterion again being the scrubber conditions which the solids were generated. Overall composites for each phase were made for both the filter cake and the stabilized material by combining individual composite samples as well as the stabilized material resulting from each. (See Figure 1)

3. Analytical Plan

As familiarity with the solid waste was gained during the project, the analytical testing scheme was modified. As depicted in Figure 1, the bulk of testing was conducted during the first two phases of the project. Some additional testing was carried out specifically for the Phase III samples. Aquatic toxicity testing was conducted on the Phase I filtercake and Phase I stabilized material composites only. The lack of toxicity in the Phase I overall composites was considered sufficient evidence of non-toxicity to preclude the other overall phase composites from toxicity testing.

The individual composite samples of filter cake were split in the following manner: one portion was used for stabilization testing, one portion was subjected to various chemical analyses, and one portion was saved for later use in compiling the filter cake phase composites. Reference is once again made to Figure 1 for the analytical testing that was performed on samples from each phase of the project.

C. RESULTS OF STABILIZATION TESTING

Stabilization testing was conducted on material that was stabilized using the conventional method of mixing the filter cake with flyash and lime. Initially a sample of filter cake generated during the regular Thiosorbic mode was subjected to stabilization and used as a control. A large sample of the NOx removal mode-generated filter cake was then used for optimizing the relative amounts of flyash and lime to use in the stabilization tests. Flyash from Miami Fort Unit #7, the source of the flue gas, and Dravo Black River lime, the flue gas scrubbing reagent, were utilized in making the stabilized material. Evaluation of these optimization tests revealed that many mix ratios of filter cake, lime, and flyash will reach acceptable stabilization strengths given sufficient time. A minimum amount of flyash and range of lime was needed to effect stabilization. These minimum ratios were used as a starting point for the stabilization testing.

Stabilization strength testing on these samples was done using a Soil Test penetrometer. This non-destructive technique allows multiple strength determinations to be made over a period of time as the sample stabilizes. When the measured strength exceeded 4.5 tons per square foot, the stabilization period was considered ended. An unconfined compression test was conducted which is considered a measure of the stabilized material's shear strength. These two tests proved very useful in predicting the stabilized material's fitness for land disposal and constituted the core of physical testing performed on the stabilized samples.

Other physical tests were attempted with varying degrees of success. Permeability testing using the constant head technique could not be performed in a satisfactory manner due to channeling of the water around the perimeter of the sample and lexan cell wall of the test specimen. Results obtained from these flawed tests showed permeabilities to be on the order of 10^{-4} cm/sec instead of the more realistic and expected figure of ~10^{-6} cm/sec. Standard Proctor Tests were also carried out in an effort to find the mix ratio that would produce the maximum density upon compaction. The maximum densities arrived at were 92.8 #/ft^3 and 91.6 #/ft^3 for 2% lime and 4% lime mixes respectively. However, the amounts of flyash used in these mixes were above 100%, a ratio much too high to be of commercial significance.

These efforts showed neither the Standard Proctor Test or the permeability test to be useful in evaluating this material.

No attempt was made to stabilize all filter cake with the same flyash and lime mix ratios. As the program proceeded it became necessary to modify the basis of the mix ratio because of the unexpected relatively high solids content (65%-70%) of the filter cake. This necessitated basing the flyash and lime percentages on the wet weight of filter cake and percent moisture of filter cake respectively during the latter part of the program as opposed to the dry solids content of the filter cake as was done in Phase I. This adjustment in preparing mix ratios does not in any way detract from the results obtained. What is important is that all the solid waste produced was successfully stabilized with the same method of adding a specific and premixed flyash/lime mixture to the filter cake and achieving satisfactory stabilization. The varying solids content of the filter cake and the adjustments in mix ratios it necessitated allowed it to be demonstrated that an optimum mix can be determined for each range of solids content. Examples of the extensive work performed on the stabilized samples is shown in Tables 1A, 1B, and 1C, which summarize test results on the most promising stabilization mixes attempted for the three phases of the project. It is clear that optimization of the sludge stabilization process will be able to proceed smoothly for a wide range of solids handling conditions that may be encountered in the commercial application of this NOx removal process.

D. RESULTS OF TOXICITY TESTING

A major concern in commercial application of this NOx removal project was the potential that the FGD sludge produced would prove toxic and thus limit the applicability of this technology. Consequently, a significant effort to characterize the filter cake and stabilized material was undertaken to insure that the solid waste generated from the NOx removal process was non-toxic and could be landfilled.

1. Results of RCRA Testing

Although specifically excluded under the Resource Conservation and Recovery Act (RCRA) as a hazardous waste, the unique nature of this NOx removal process warranted a thorough examination from a RCRA viewpoint of the solid waste produced. Testing was conducted on all the filter cake phase composites made for the entire project and on the stabilized material from Phase I. Since FGD sludge is not a "listed" RCRA waste, samples were tested for the RCRA characteristics of ignitability, corrosively, reactivity, and Extraction Procedure (EP) or Toxic Characteristic Leaching Procedure (TCLP) toxicity (toxic metals).

The belt filter cake solids produced typically had pH values in the 6 to 8 range, similar to the 6.5 operating pH of the scrubber liquor. Therefore on a pH basis, the sludge was not considered corrosive. Testing at the Dravo Research Center showed the sludge not to be ignitable as well. Extensive testing for toxic metals was conducted on TCLP leachates of the filter cake from all three test phases. These results are detailed in Tables 2A, 2B, and 2C. Metals analyses were also performed on the TCLP leachates from Phase I stabilized material and the results of these tests are given in Table 3. The sludge is not reactive based on testing for reactive cyanides and sulfides as shown in Table 4. In no case did levels of toxic metals approach the maximum contaminant levels (MCL) established by EPA for the definition of toxicity characterization. (Maximum allowed concentrations in Tables 2B, 2C and 3.)

In addition to the above TCLP extract metals analyses, the stabilized material Phase I composite was extracted in accordance with TCLP procedures and tested in accordance with EPA Method 8270 (semivolatile organics). None of the target compounds were detected except Di-n-Butylphthalate. This compound also appeared in the blank and is a common laboratory contaminant. Determinations of herbicides and pesticides were not conducted as they would not reasonably be expected to occur in the samples. Additionally, the TCLP Base Neutral acid (BNA) were run according to EPA Contract Lab Program (CLP) methods. No compounds on the target list were found. A library search was conducted on all unidentified peaks and all compounds were identified.

The results of these tests thus show the FGD sludge generated from this process, as well as the stabilized material derived from it, to be nonhazardous under current RCRA definition.

2. Results of Bioassays

Although evaluation of the toxicity of potentially hazardous materials is not required under RCRA the ultimate disposition of solid waste generated by this process could lead to degradation of water quality if the waste material possessed a significant toxic affect on marine animals. Toxicity is a function of dose which is a product of concentration and time of exposure. Therefore nearly all substances can be considered toxic if the concentration is sufficiently high. However, in evaluating the suitability of the waste material for disposal, potential for environmental impacts at expected concentrations must be addressed.

The aquatic toxicity tests were conducted by preparing a 20% by volume stock mixture of the waste in water. This mixture was then used to prepare dilutions ranging from zero to 100% stock solution. The 100% stock solution would represent a case where the receiving water would be all leachate, a useful upper bound test condition. Test animals were placed in each dilution with the temperature maintained at 21^{o}C and the survival rate noted after exposure for a specified time period. The two test animals selected were Daphnia pulex, a freshwater invertebrate, and Pimephales promelas (fathead minnow), a freshwater vertebrate.

The tests of the Phase I filtercake composite sample is regarded as the more conservative test since it is unlikely that unstabilized filter cake solids would be landfilled in actual practice. Statistical analysis of the 24 hour Daphnia pulex survival responses yielded a median lethal concentration (LC_{50}) of 39% test media. Statistical analysis of the 96 hour fathead minnow test yielded a lethal concentration of 169% test media. This indicates survival of over 50% of the test animals at a concentration of 100% test media. Examination of the Phase I stabilized composite material yielded a LC_{50} of 34% using the Daphnia pulex. Statistical analysis of the 96 hour Pimephales promelas yielded no significant difference in survival for any test treatment including 100% of the sample. That is to say, the material had no effect.

It can be seen from the above that the stabilization of the belt filter solids rendered the material nearly innocuous and even the native unstabilized material did not have a heavy negative impact on the aquatic system in which it was tested.

3. Microbiological Testing

Some evidence of microbiological activity was noted during long term storage of many of the samples. Samples which showed the most evidence of change (odor and color changes) were selected for identification of bacteria by gas chromatography of cellular fatty acids. Computer examination of the chromatograms produced a positive identification of Bacillus as the genus but identification of the species was not possible. A second sample produced an identification of Altoromonas/Pseudomonas putridrefaciens. None of the bacteria detected are pathogenic and they are considered common. These findings are considered unremarkable.

E. RESULTS OF MISCELLANEOUS TESTING

Several tests and measurements were conducted to evaluate the concentration of analytes which are not known to be toxic or harmful but about which questions have been raised from time to time. It was not intended to provide a final answer on the possible environmental impacts of these substances but simply to note their presence and attempt to measure their concentrations.

1. Sulfur-Nitrogen Compounds

The direct measurement of sulfur-nitrogen compounds (SNC) in the filter cake was not attempted. However, exhaustive measurements were made of the concentration of these compounds in the liquor and the amount of liquor in the solids is known from the total solids measurement of the filter cake. Thus at least a minimum SNC concentration in the solid phase may be calculated. This calculation was carried out using EDTA data and compared to a direct measurement of EDTA in the filter cake with excellent agreement.

Analyses for total nitrogen were carried out on the filter cake composites and are summarized in Figure 2.

2. EDTA

The EDTA concentration of the filter cake was measured by extracting the EDTA from the sample followed by titration. Values obtained are summarized in Figure 2. The values were as expected from the moisture analysis of the cake and the EDTA concentration in the liquor.

3. XRF Analysis

Filter cake composite samples were subjected to major component analysis by wavelength dispersive X-Ray spectroscopy. Determinations were made of silicon, aluminum, iron, calcium, magnesium, and sulfur. These were calculated to the oxide basis as per convention. These results are summarized in Figure 3. A reasonably uniform product is demonstrated to have been formed in spite of numerous process changes.

4. Physical Examination

Filter cake samples were characterized by particle size and shape and particle size distribution (PSD). It was initially believed that particle size distribution and mean particle size would be closely correlated with the total solids concentration of the filter cake. A Microtrac particle size analyzer was used for this purpose. Data summarized in Table 5 show the general trends of the average PSD for the filter cake solids for the entire project as they correlate to solids content. Table 6 summarizes the PSD values for some arbitrarily selected samples representing typically high and low percent solids filter cake. This data is graphically presented in Figure 4. The selected Microtrac analyses sheets are included in the Addendum to this section. Figure 4 shows almost no agreement between PSD and percent solids, thus limiting the usefulness of this technique for determining or predicting the solids content of the filter cake.

Photomicrographs of each filtercake sample were taken and evaluated. Several of these samples were then selected for closer examination by Scanning Electron Microscope (SEM). Reproductions of these photomicrographs and SEM's appear following this section.

F. SUMMARY

Some of the process modifications made in conjunction with the simultaneous SO_2/NOx removal project conducted by Dravo Lime Company at the Miami Fort Pilot Plant were chemical in nature. The nitrogen oxides removed from the flue gas and possibly the chemical additives and their degradation products were absorbed by the scrubbing liquor. Consequently, these compounds were expected to appear in the solid waste stream and could have an unpredictable effect on the chemical and physical properties of the solid waste produced. Thus it was necessary to determine if the waste material could be disposed of as easily as conventional magnesium enhanced lime (MEL) FGD product. Disposal was considered from two points of view: the possibility that the waste would be difficult to stabilize using ordinary methodology, and the possibility that the waste could be found to be a hazardous waste, either under RCRA or under a broader consideration of whether the waste could be otherwise shown to be hazardous or toxic.

1. Stabilization Tests

Unmodified MEL FGD waste solids (sludge or belt filter cake) are normally stabilized by the addition of lime and flyash. The pozzolanic activity of such mixtures causes the product to harden into a material which can be landfilled. A major goal of this study was to determine if the material from the modified MEL process can be similarly treated. It was decided to attempt to stabilize the belt filter solids using conventional methods. A number of test mixes were made by varying the amounts of flyash and lime mixed with the scrubber solids. The strength of each mixture was monitored over time using a penetrometer and estimating the unconfined compressive strength of the mix from the penetrometer readings. When the strength by penetrometer reached 4.5 tons per square foot the unconfined compressive strength was determined in a testing machine on a companion specimen.

After evaluation of the early runs it became clear that many mix ratios of product, lime, and flyash could reach the target strength if given sufficient time. It was also determined that there is a minimum amount of flyash and range of lime needed for good results. It should be noted that no attempt was made to stabilize all material with the same mix ratios. The large variation in filter cake solids content, ranging from 39% to nearly 80%, rendered such an approach infeasible. What is noteworthy is that all waste material produced was successfully stabilized with the same method. More importantly,the data indicate that an optimum stabilization mix can be determined for each range of belt filter cake solids content that occurred during the project.

2. Toxicity Tests

Examination under RCRA requirements indicate that the waste material does not exhibit any of the characteristics of corrosively, ignitability, reactivity or EP/TCLP toxicity. The results of the TCLP extraction and the EP Toxicity for metals showed that the content of all metals in the waste were orders of magnitude lower than the regulatory limits and in most cases would even meet drinking water standards. Results of the organic analysis show all regulated compounds to be below the detection limit of the method. The results of the aquatic toxicity tests indicate that the unstabilized material is of low toxicity and that stabilization renders it nearly innocuous.

3. Miscellaneous Tests

A number of tests were run in order to determine if the composition of the sludge was uniform enough to permit generalizations to be drawn covering the entire data set. The results from all parameters tested indicated the belt filter cake to be essentially similar over the course of the entire NOx removal project.

4. Conclusions

In order to achieve commercial acceptance the MEL modified simultaneous SO_2/NOx removal technology must demonstrate that the resultant FGD waste product can be disposed of as a non-hazardous and benign solid waste. An intensive effort was undertaken during this project to determine that the waste was indeed non-hazardous and that it could be stabilized in accordance with accepted and standard stabilization techniques for landfill.

From both standpoints, the waste characterization program was an unqualified success. A battery of chemical and physical tests was conducted on both the belt filter cake and the stabilized material derived from it. In some ways, this material has been scrutinized and characterized more than the waste from conventional FGD processes which is protected by a RCRA exclusion. Stabilization studies conducted over a wide range of filter cake solids content show the waste product to be very amenable to standard stabilization techniques. The disposal of solid waste from this process should therefore pose no obstacle to its commercial acceptance.

The encompassing scope of work performed in the solid waste characterization of the FGD sludge produced from the magnesium enhanced lime simultaneous SO_2/NOx removal process not only proved the material's non-hazardous, nontoxic nature and its suitability for landfill disposal, it also provides a rich research base for operations and regulatory personnel should the technology be commercialized.

FIGURES & TABLES

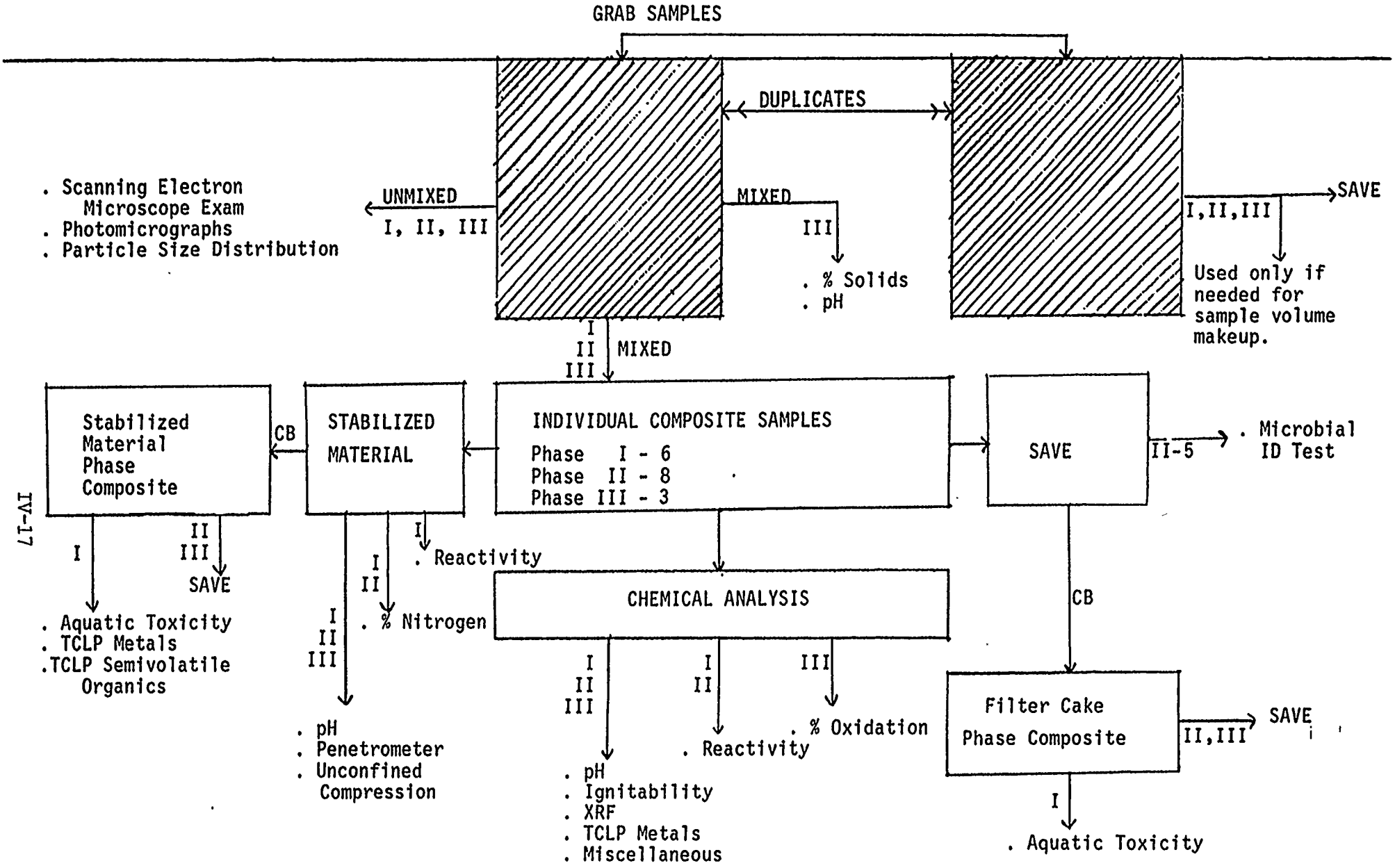

FIGURE 1: SOLID WASTE SAMPLE HANDLING/ANALYSIS FLOWSHEET

NOTE: I, II, III = Phases; SAVE = No Analyses Performed; CB = Combined

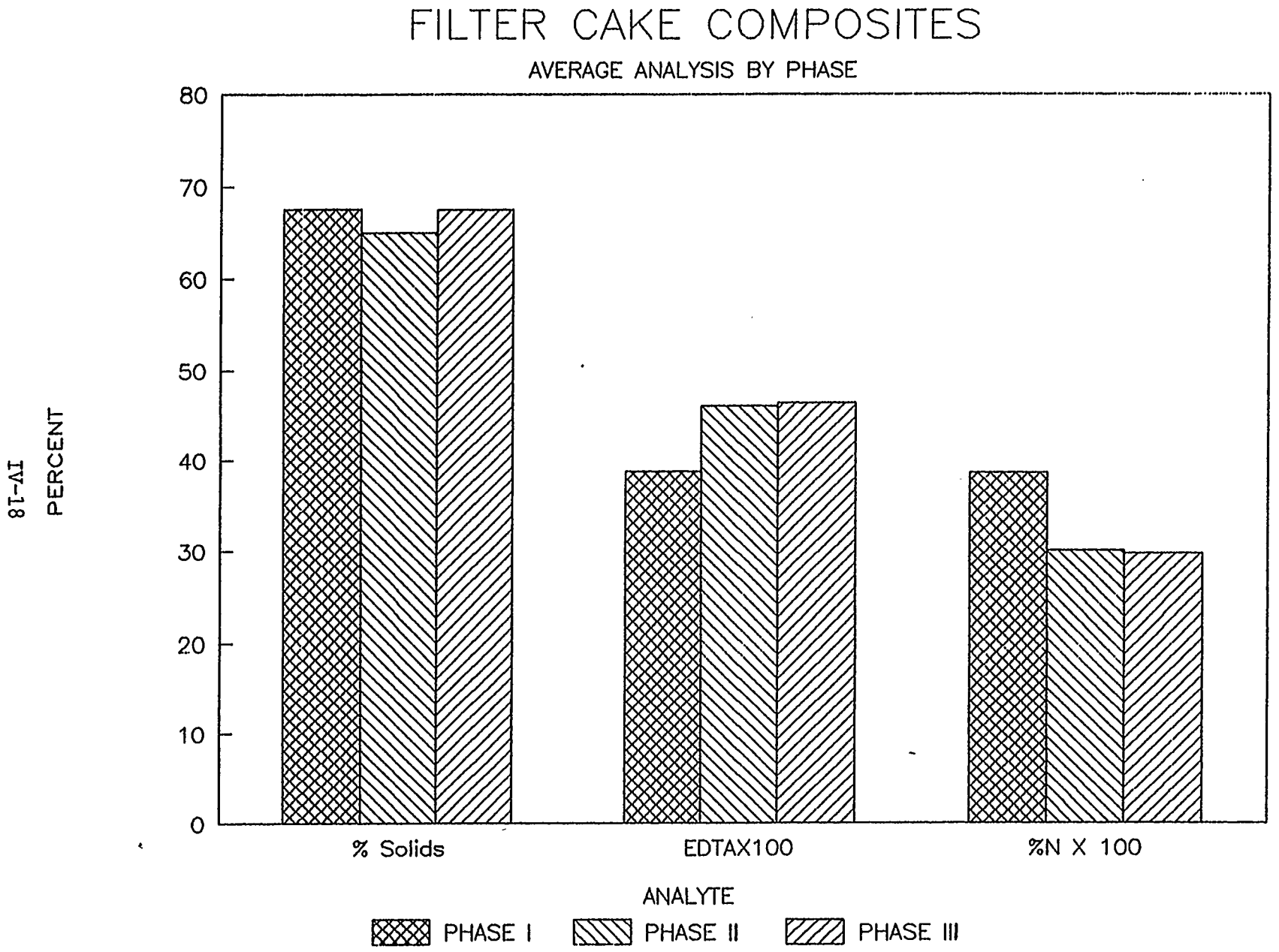
FILTER CAKE COMPOSITES
AVERAGE ANALYSIS BY PHASE
PERCENT
80
70
60
50
40
30
20
10
0
% Solids
EDTAX100
%N X 100
ANALYTE
PHASE I
PHASE II
PHASE III

FIGURE 2

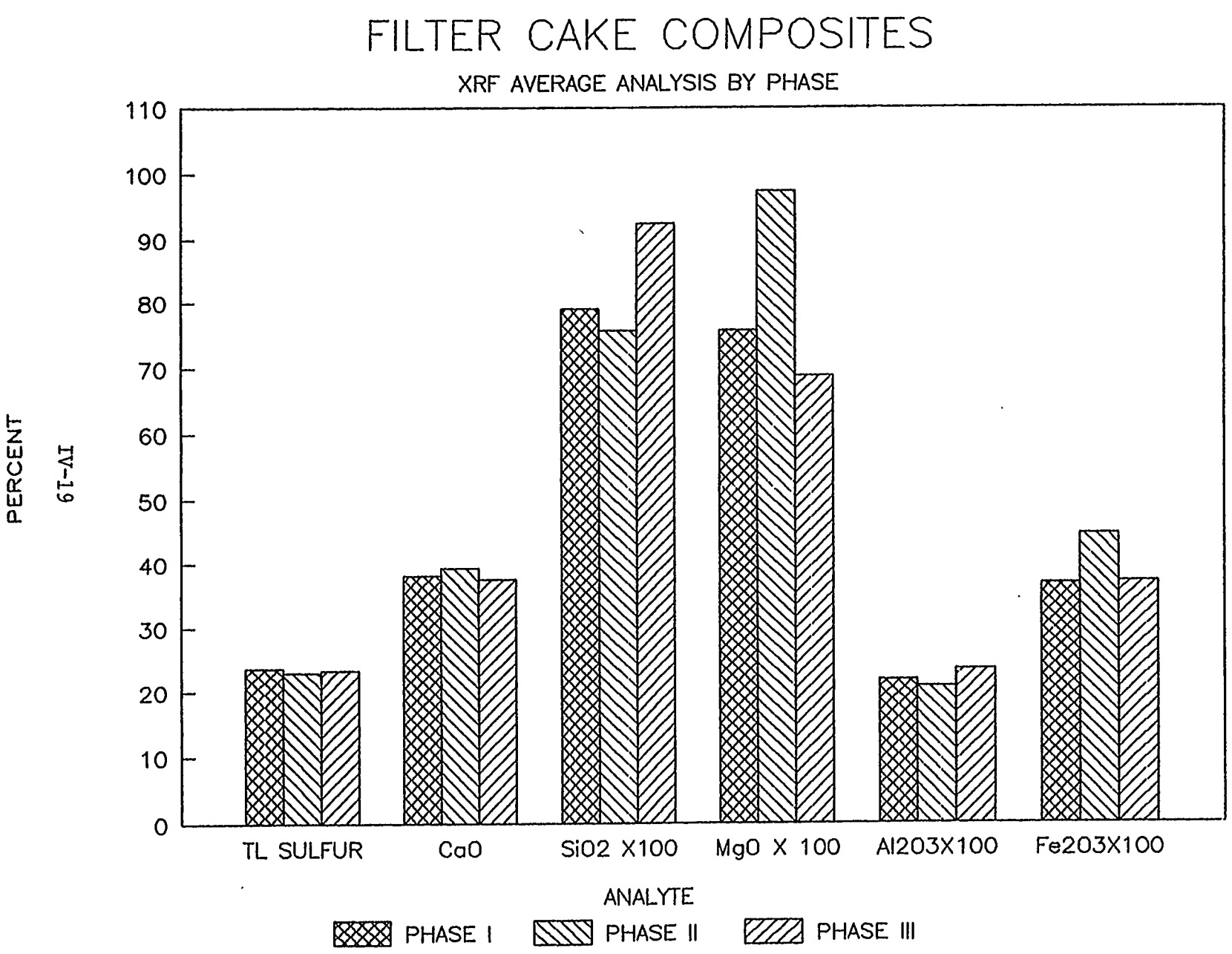
FILTER CAKE COMPOSITES
XRF AVERAGE ANALYSIS BY PHASE
PERCENT
110
100
90
80
70
60
50
40
30
20
10
0
TL SULFUR
CaO
SiO2 X100
MgO X 100
Al203X100
Fe203X100
ANALYTE
PHASE I
PHASE II
PHASE III

FIGURE 3

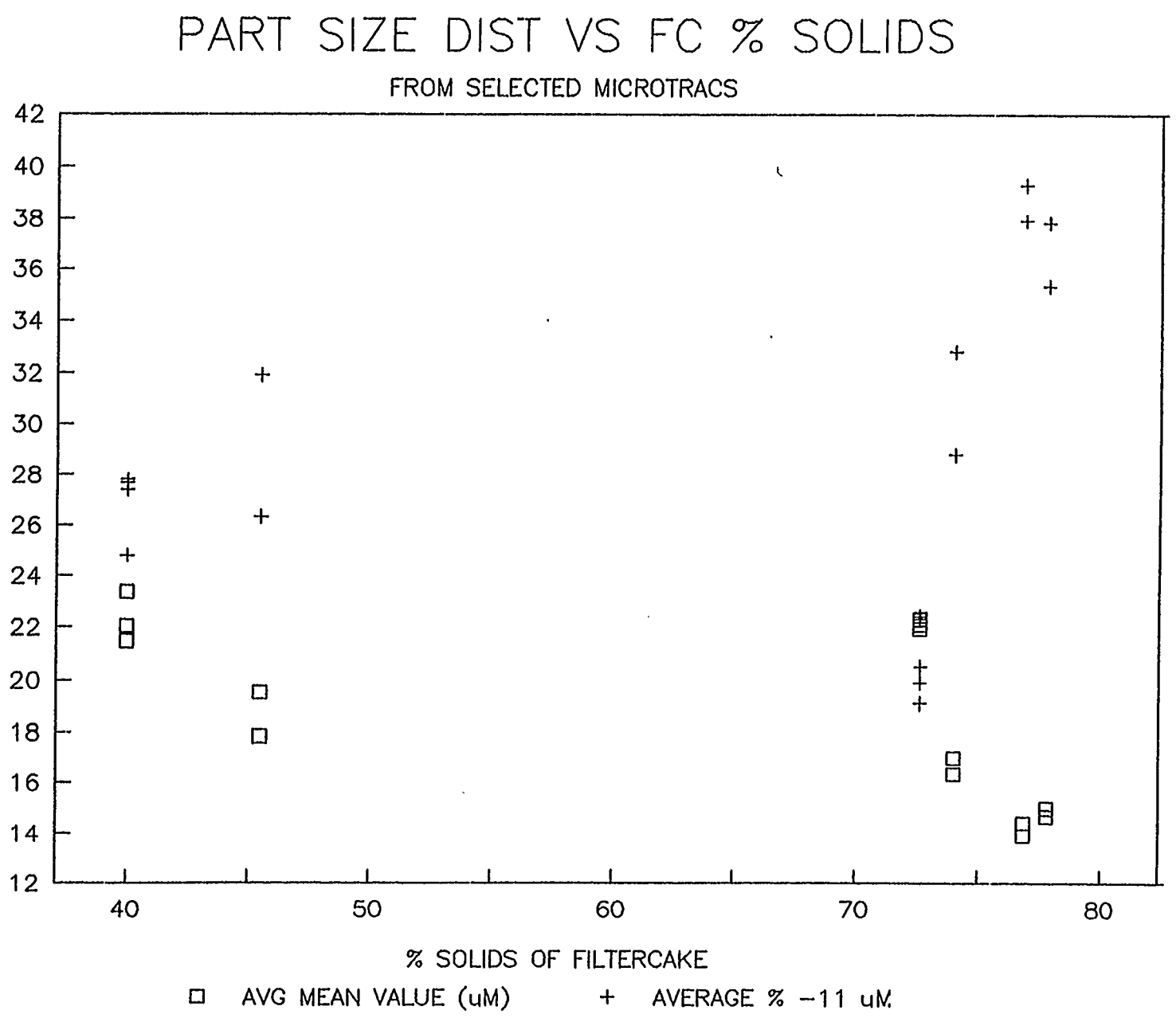
PART SIZE DIST VS FC % SOLIDS
FROM SELECTED MICROTRACS
42
40
38
36
34
32
30
28
26
24
22
20
18
16
14
12
40
50
60
70
80
% SOLIDS OF FILTERCAKE
AVG MEAN VALUE (uM)
AVERAGE % -11 uM

FIGURE 4

TABLE 1A PHASE I

SUMMARY OF STABILIZATION TESTING
FOR SAMPLES REACHING +4.5 TONS/SQ FT

SAMPLE ID	% SOLIDS FC	FLYASH %	LIME(CaO)%	% SOLIDS SM	pH SM	STABLE @ DAY #	UNCONFND COMPRESS psi
CONTROL	43.0	50.0	4		9.8	81	35
		50.0	6		11.5	14	46
		75.0	6		11.3	14	46
		100.0	4		9.0	21	63
		100.0	6		10.3	14	66
I-1	68.6	37.3	2	76.3	8.8	28	
		53.2	2	77.8	8.5	35	
		62.3	2	78.3	8.0	14	
I-2	67.0	47.8	2	75.8	8.9	35	
		64.9	2	77.8	8.2	28	
		74.6	2	78.7	8.2	14	
I-3	66.3	52.5	2	76.1	8.8	49	
		70.2	2	78.1	8.3	42	
		80.2	2	79.3	8.1	28	
I-4	67.8	59.0	2	78.0	8.3	81	
		68.4	2	79.1	8.3	14	
I-6	67.0	64.9	2	78.1	8.1	56	
		74.6	2	79.2	8.1	35	

TABLE 1B PHASE II

SUMMARY OF STABILIZATION TESTING
FOR SAMPLES REACHING +4.5 TONS/SQ FT

SAMPLE ID	% SOLIDS FC	FLYASH %	LIME(CaO)%	SOLIDS SM	pH SM	STABLE @ DAY #	UNCONFND COMPRESS psi
II-1	39.0	50	4	61.5	9.5	56	19
		75	4	66.4	9.2	56	27
II-2	53.9	75	4	74.8	9.8	28	59
		100	4	78.0	9.4	28	92
II-3	59.6	75	4	78.0	9.3	7	59
		100	4	80.3	9.0	7	73
II-4	63.5	75	4	80.0	9.5	7	44
		100	4	83.1	9.3	3	29
II-5	68.2	50	4	81.0	9.8	7	63
		75	4	83.7	9.3	3	47
II-6	69.6	30	4	78.0	9.5	14	57
		50	4	81.6	9.2	3	139
II-7	68.9	30	4	77.1	9.3	14	64
		50	4	80.2	9.1	3	114
II-8	67.0	30	4	76.0	9.3	28	36
		50	4	79.2	9.3	7	58
II-9	69.4	30	4	77.4	9.1	21	67
		50	4	80.6	9.2	3	115

TABLE 1C PHASE III

SUMMARY OF STABILIZATION TESTING
FOR SAMPLES REACHING +4.5 TONS/SQ FT

SAMPLE ID	% SOLIDS FC	FLYASH %	LIME(CaO)%	% SOLIDS SM	pH SM	STABLE @ DAY #	UNCONFND COMPRESS psi
III-1	65.3	30	7	74.8	9.6	60	59
		50	7	78.3	9.5	2	45
III-2	66.0	30	7	75.1	9.6	60	45
		50	7	77.7	9.4	2	42
III-3	71.1	30	7	77.4	9.7	7	38
		50	7	81.3	9.4	14	19

RECAP OF MIX RATIOS

SAMPL SET	% FLYASH BASED ON	% LIME BASED ON
CONTROL	WET FILTER CAKE	DRY FILTER CAKE
PHASE I	DRY FILTER CAKE	DRY FILTER CAKE
PHASE II	WET FILTER CAKE	DRY FILTER CAKE
PHASE III	WET FILTER CAKE	% MOISTURE FC

TABLE 2A

Miami Fort Waste Characterization Study
Toxicity Characteristic Leaching Procedure
Toxic Metals Analyses

PHASE I Filter Cake Composites

LAB ID #	91-2611	91-2612	91-2613	91-2614	91-2615	91-2616	Blank
Arsenic mg/l	0.030	0.018	0.10	0.009	0.008	0.010	<0.005
Barium mg/l	0.066	0.060	0.059	0.058	0.058	0.062	0.018
Cadmium mg/l	<0.040	0.047	<0.040	0.053	<0.040	0.053	<0.040
Chromium mg/l	0.048	0.059	0.076	0.060	0.072	0.086	<0.040
Lead mg/l	0.2	0.2	0.2	0.3	0.3	0.3	<0.1
Mercury mg/l	<0.003	<0.003	<0.003	<0.003	<0.003	<0.003	<0.003
Selenium mg/l	0.067	0.044	0.055	0.041	0.041	0.038	<0.005
Silver mg/l	0.067	0.044	0.055	0.051	0.020	0.026	<0.005

TABLE 2B

Miami Fort Waste Characterization Study
Toxicity Characteristic Leaching Procedure
Toxic Metals Analyses

PHASE II Filter Cake Composites

LAB ID #	91-3453	91-3454	91-3455	Blank	91-3638	91-4459
Arsenic mg/l	0.007	0.013	0.011	<0.005	0.006	0.007
Barium mg/l	0.086	0.091	0.060	0.018	0.057	0.047
Cadmium mg/l	<0.040	0.043	0.048	<0.040	<0.015	<0.015
Chromium mg/l	<0.040	0.040	0.055	<0.040	0.340	0.150
Lead mg/l	0.1	0.1	0.3	<0.1	<0.1	<0.1
Mercury mg/l	<0.003	<0.003	<0.003	<0.003	<0.003	<0.003
Selenium mg/l	0.026	0.025	0.012	<0.005	0.013	0.015
Silver mg/l	0.015	0.018	0.027	<0.005	0.017	0.017

LAB ID #	91-4623	Blank	91-4623 DUPL.	91-4624	91-4625	Blank	Maximum Allowed Concentration mg/l
Arsenic mg/l	0.009	0.005	<0.050	<0.050	<0.050	<0.050	5.0
Barium mg/l	0.049	<0.005	0.028	0.023	0.019	<0.005	100.0
Cadmium mg/l	<0.015	<0.015	<0.015	<0.015	<0.015	<0.015	1.0
Chromium mg/l	0.190	0.062	0.041	0.052	0.060	<0.015	5.0
Lead mg/l	0.100	<0.1	<0.150	<0.150	<0.150	<0.150	5.0
Mercury mg/l	<0.003	<0.003	<0.003	<0.003	0.004	<0.003	0.2
Selenium mg/l	<0.005	<0.005	0.042	0.046	0.042	<0.025	1.0
Silver mg/l	0.020	<0.005	0.017	0.015	0.016	<0.005	5.0

TABLE 2C

Miami Fort Waste Characterization Study
Toxicity Characteristic Leaching Procedure
Toxic Metals Analyses

PHASE III Filter Cake Composites

LAB ID #	92-0063	92-0064	92-0065	Blank	Maximum Allowed Concentration mg/l
Arsenic mg/l	<0.010	<0.010	<0.010	<0.005	5.0
Barium mg/l	0.032	0.034	0.033	<0.005	100.0
Cadmium mg/l	<0.005	<0.005	<0.005	<0.005	1.0
Chromium mg/l	0.048	0.042	0.035	<0.015	5.0
Lead mg/l	<0.150	<0.150	<0.150	<0.150	5.0
Mercury mg/l	<0.003	<0.003	<0.003	<0.003	0.2
Selenium mg/l	0.036	0.029	0.027	<0.005	1.0
Silver mg/l	0.022	0.027	0.027	<0.005	5.0

TABLE 3

Miami Fort Waste Characterization Study
Toxicity Characteristic Leachate Procedure
Phase I Stabilized Material

TCLP Metals

Sample ID	91-2611 SM	91-2612 SM	91-2613 SM	91-2614 SM	91-2615 SM	91-2616 SM	Blank	Maximum Allowed Concentration mg/l
Arsenic mg/l	0.28	0.23	0.24	0.24	0.18	0.16	.005	5.0
Barium mg/l	0.45	0.54	0.56	0.52	0.39	0.58	<.005	100.0
Cadmium mg/l	<0.015	<0.015	<0.015	<0.015	<0.015	<0.015	<0.015	1.0
Chromium mg/l	0.48	0.28	0.21	0.29	0.17	0.41	0.062	5.0
Lead mg/l	0.1	0.2	0.1	<0.1	0.1	0.2	<0.1	5.0
Mercury mg/l	<0.003	<0.003	<0.003	<0.003	<0.003	<0.003	<0.003	0.2
Selenium mg/l	0.075	0.058	0.12	0.075	0.089	0.11	<0.005	1.0
Silver mg/l	0.024	0.022	0.024	0.020	0.018	0.019	<0.005	5.0

SM =Material Stabilized With Lime And Fly Ash

TABLE 4

Miami Fort Waste Characterization Study
Reactivity: Cyanide/Sulfide

Sample #	Reactivity, Cyanide Spec Rate Release mg/kg sec	Total Available mg/kg	Reactivity Sulfide Spec Rate Release mg/kg sec	Total available mg/kg
91-2611	<0.0003	<0.5	<0.0003	<0.5
91-2612	<0.0003	<0.5	<0.0003	<0.5
91-2613	<0.0003	<0.5	<0.0003	<0.5
91-2613	<0.0003	<0.5	<0.0003	<0.5
91-2614	<0.0003	<0.5	<0.0003	<0.5
91-2615	<0.0003	<0.5	<0.0003	<0.5
91-2616	<0.0003	<0.5	<0.0003	<0.5
91-3453	<0.0003	<0.5	<0.0003	<0.5
91-3454	<0.0003	<0.5	<0.0003	<0.5
91-3455	<0.0003	<0.5	<0.0003	<0.5
91-3638	<0.0003	<0.5	<0.0003	<0.5
91-4459	<0.0003	<0.5	<0.0003	<0.5
91-4623	<0.0003	<0.5	<0.0003	<0.5
91-4624	<0.0003	<0.5	<0.0003	<0.5
91-4625	<0.0003	<0.5	<0.0003	<0.5
91-2611 SM	<0.0003	<0.5	<0.0003	<0.5
91-2612 SM	<0.0003	<0.5	<0.0003	<0.5
91-2613 SM	<0.0003	<0.5	<0.0003	<0.5
91-2614 SM	<0.0003	<0.5	<0.0003	<0.5
91-2615 SM	<0.0003	<0.5	<0.0003	<0.5
91-2616 SM	<0.0003	<0.5	<0.0003	<0.5

TABLE 5

REVIEW OF RESULTS OF MICROTRAC ANALYSES

FOR SCRUBBER LIQUORS

DOE NOX REMOVAL PROJECT

GENERAL TRENDS

PHASE #	% SOLIDS RANGE	AVG MEAN uM VALUE	CUT 11 uM AVG VALUE
I	< 60	19.71	24.46
	> 60	20.67	23.27
II	< 50	21.58	23.21
	50 - 65	13.30	44.99
	> 65	16.07	33.28
III	> 68	16.57	31.37

TABLE 6

REVIEW OF RESULTS OF MICROTRAC ANALYSES

DOE NOX REMOVAL PROJECT

SELECTED INDIVIDUAL SAMPLES

PHASE #	SMPL ID # RT LIQUOR	BF CAKE	DATE	% SOLIDS BF	% SOLIDS CAKE	AVG MEAN uM VALUE	CUT 11 uM AVG VALUE	MPSDA* REF #
I	095-1300		04-05-91	45.5		19.53	26.3	1
	095-2000					17.83	31.9	2
	142-1200		05-22-91	72.6		22.09	19.1	3
	142-2000					21.94	22.4	4
	143-1015		05-23-91			22.28	19.9	5
	143-1215					22.33	20.5	6
II	189-0800		07-08-91	40.0		22.05	27.8	7
	189-1300					23.39	24.8	8
		191-0930	07-10-91			21.47	27.4	9
		191-1330				21.45	27.7	10
	233-0400		08-21-91	74.0		16.33	28.8	11
	233-1200					16.96	32.8	12
III	319-1200		11-15-91	76.8		13.91	37.9	13
	319-2000					14.40	39.3	14
	347-0400		12-13-91	77.8		14.68	37.8	15
	347-1200					14.98	35.3	16

* MICROTRAC PARTICLE SIZE DISTRIBUTION ANALYSES SHEET

ADDENDUM

OPTICAL MICROSCOPE REPRODUCTIONS

ICA-1400
625X 8/13/91

FOR SEM* 625X ~~325X~~
91-130-0330 8/13/91

*Selected for SEM

OPTICAL MICROSCOPE REPRODUCTIONS

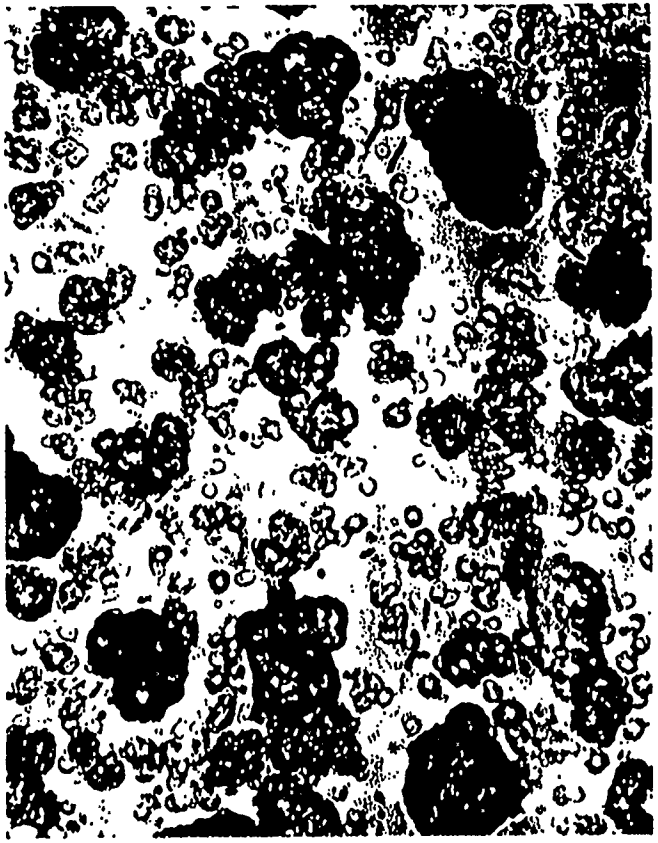

SEM*
91-155-1000
625X
8/13/91

91-143-0445
625X
8/14/91

*Selected for SEM

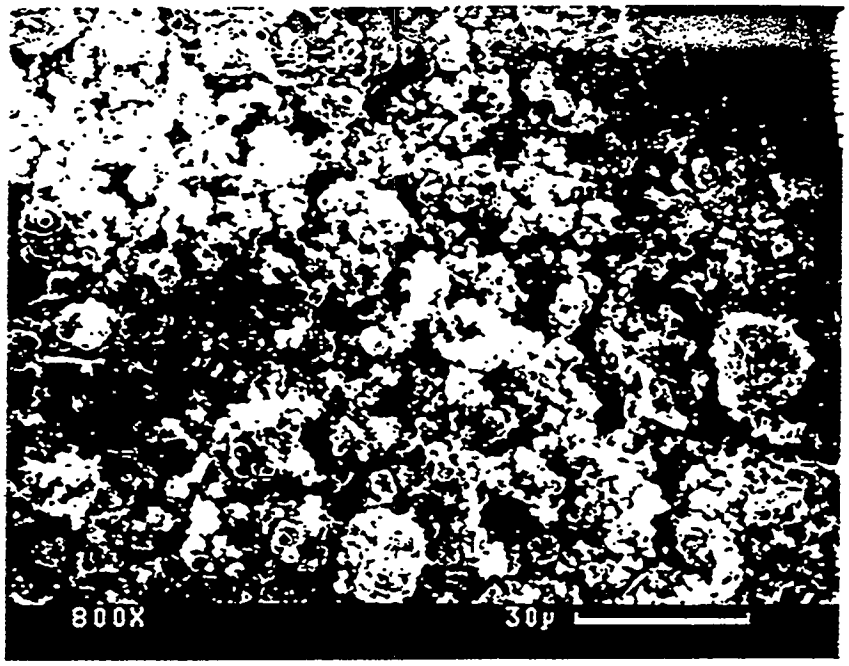

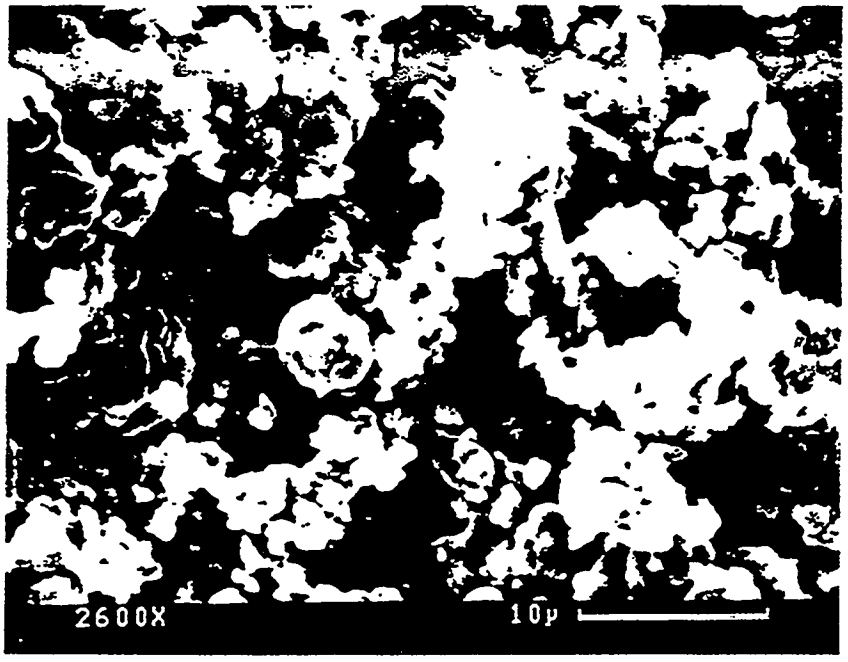

Figure 6: Sample 91-205-1830-8-12-WC.

Project #825-16347, Laboratory #MET10487

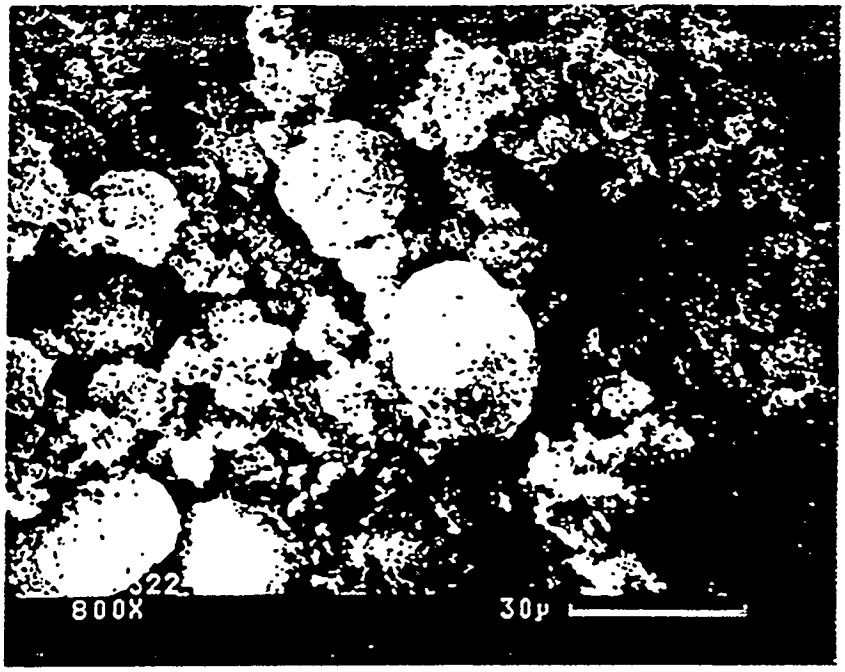

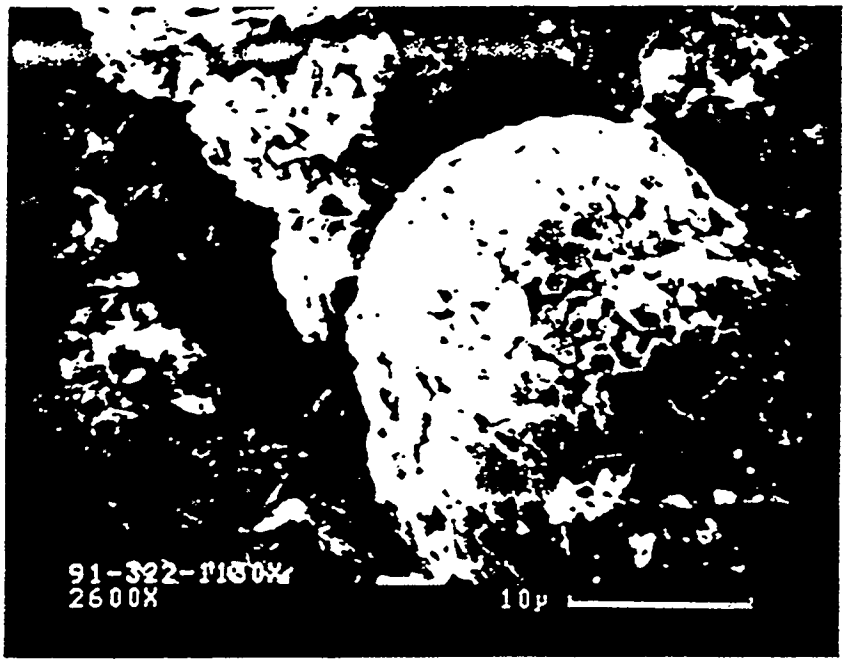

Figure 5: Sample 91-322-1130.

Project #825-26045, Laboratory #MET20062

SCANNING ELECTRON MICROSCOPE REPRODUCTIONS

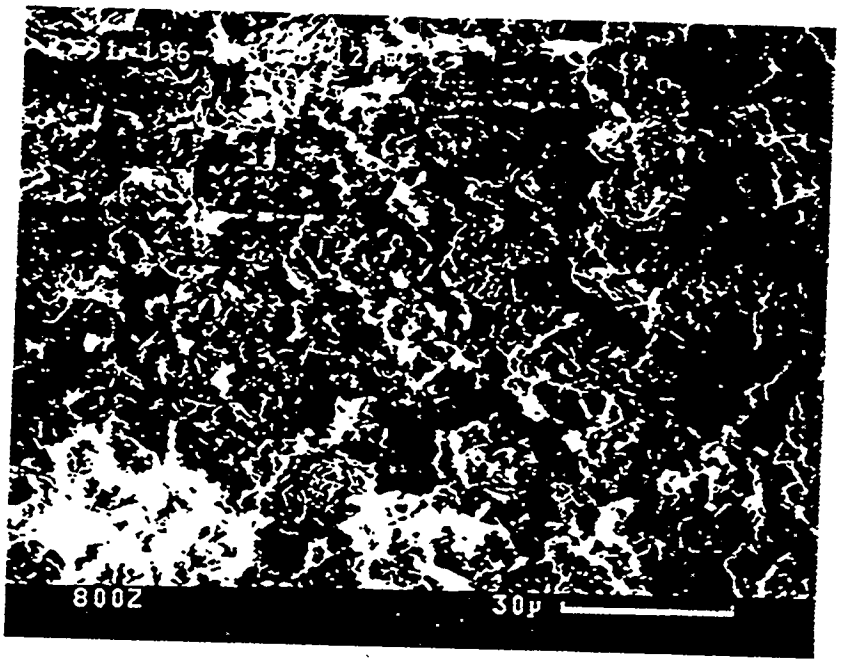

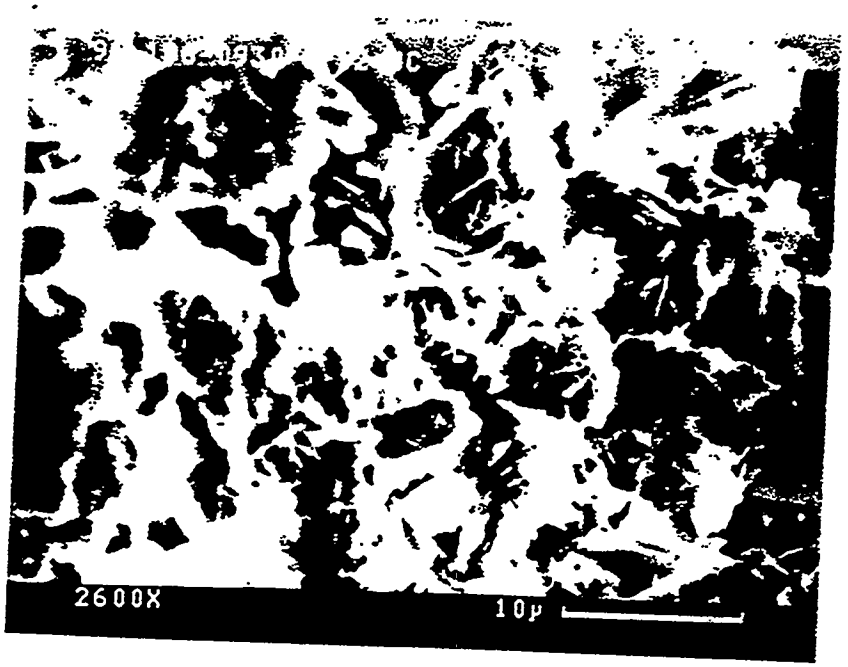

igure 4: Sample 91-196-0930-8-12-WC.

Project #825-16347, Laboratory #MET10487

SELECTED MICROTRACS

(Refer to Table 6)

DRAVO CORPORATION

5237- (91-1237)
Project No. Lab No.

Research Center

MICROTRAC PARTICLE SIZE ANALYSIS

Sample Identification: see Printout

Test No. 12104
Date 4/9/91

Division or Customer Name: OCOO/66E Miami Fort

Tested by JH

Sample Preparation: none

-REF #1-

```
5237 MIA FORT 91-095
-1300-01-01 91-1237
SAMP. TIME = 25 SEC

      DV =    0.2346
     %10 =    5.72
     %50 =   18.28
     %90 =   34.33
      MV =   19.53
      CS =    0.500

 PERCENT PASSING
CHAN.   CUM.   VOL.
=====   ====   ====
176    100.0    0.0
125    100.0    0.0
 88    100.0    0.0
 62    100.0    3.0
 44     97.0    9.4
 31     87.6   22.6
 22     65.0   24.3
 16     40.8   14.5
 11     26.3   11.3
7.8     15.0    5.6
5.5      9.5    4.5
3.9      5.0    3.1
2.8      1.9    1.5
1.9      0.4    0.4
1.4      0.0    0.0
```

```
RELATIVE VOL. GRAPH
 150  0
 106  0
  75  0
  53  *3
  38  ***9
  27  **********22
  19  ***********24
  13  *****14
 9.4  ****11
 6.6  **5
 4.7  *4
 3.3  *3
 2.4  1
 1.6  0
 1.2  0

CUMMULATIVE GRAPH
176  ***********100
125  ***********100
 88  ***********100
 62  ***********100
 44  **********96
 31  *********87
 22  *******65
 16  ****40
 11  **26
7.8  *15
5.5  9
3.9  5
2.8  1
1.9  0
1.4  0
```

NOTES:

DRAVO CORPORATION

5237-__ (91-1238)
Project No. Lab No.

Research Center

MICROTRAC PARTICLE SIZE ANALYSIS

Sample Identification: see Printout

Test No. 12105
Date 4/9/91

Division or Customer Name: 0c001666 Miami Fort

Tested by JH

Sample Preparation: none

-REF #1-

```
5237 MIA FORT 91-095
-2000-01-01 91-1238
SAMP. TIME = 25 SEC

      DV =    0.2376
     %10 =    5.04
     %50 =   16.34
     %90 =   30.95
      MV =   17.83
      CS =    0.557

 PERCENT PASSING
CHAN.   CUM.   VOL.
=====   ====   ====
176    100.0    0.0
125    100.0    0.0
 88    100.0    0.0
 62    100.0    2.5
 44     97.5    7.5
 31     90.1   18.7
 22     71.4   22.7
 16     48.7   16.9
 11     31.9   13.6
7.8     18.2    6.6
5.5     11.6    5.6
3.9      6.0    3.6
2.8      2.4    1.8
1.9      0.6    0.6
1.4      0.0    0.0
```

```
RELATIVE VOL. GRAPH
 150   0
 106   0
  75   0
  53   *2
  38   ***7
  27   *********18
  19   **********22
  13   ********16
 9.4   ******13
 6.6   **6
 4.7   **5
 3.3   *3
 2.4   1
 1.6   0
 1.2   0

CUMMULATIVE GRAPH
 176   **********100
 125   **********100
  88   **********100
  62   **********100
  44   **********97
  31   **********90
  22   ********71
  16   ****48
  11   ***31
 7.8   *18
 5.5   *11
 3.9   5
 2.8   2
 1.9   0
 1.4   0
```

NOTES:

DRAVO CORPORATION

5237 3.1
Project No.

(91/2229)
Lab No.

Research Center

MICROTRAC PARTICLE SIZE ANALYSIS

Sample Identification: See Printout

Test No. 1228

Date 5/29/91

Division or Customer Name: Miami Fort

Tested by REV

Sample Preparation: None

-REF #3-

[illegible]

05/29/91 08:54
DATE TIME

5237 MIAMI FORT
31-142-1200-1-1
SAMP. TIME = 25 SEC

DV =	0.1537
%10 =	7.92
%50 =	20.68
%90 =	38.43
MV =	22.09
CS =	0.419

PERCENT PASSING

CHAN.	CUM.	VOL.
176	100.0	0.0
125	100.0	0.0
88	100.0	0.0
62	100.0	3.0
44	97.0	16.3
31	80.7	25.9
22	54.8	22.0
16	32.9	13.7
11	19.1	9.5
7.8	9.6	3.8
5.5	5.8	2.4
3.9	3.4	2.1
2.8	1.3	1.1
1.9	0.2	0.2
1.4	0.0	0.0

RELATIVE VOL. GRAPH

150	0
106	0
75	0
53	*3
38	******16
27	**********25
19	********21
13	*****13
9.4	***9
6.6	*3
4.7	2
3.3	2
2.4	1
1.6	0
1.2	0

CUMMULATIVE GRAPH

176	**********100
125	**********100
88	**********100
62	**********100
44	**********96
31	*********80
22	*****54
16	***32
11	*19
7.8	9
5.5	5
3.9	3
2.8	1
1.9	0
1.4	0

NOTES:

DRAVO CORPORATION

5237 3.1
Project No.

(91/2230)
Lab No.

Research Center

MICROTRAC PARTICLE SIZE ANALYSIS

Sample Identification: See Printout

Test No. 12281
Date 5.29.91

Division or Customer Name: Miami Fort

Tested by REV

Sample Preparation: None

-REF #4-

```
MICROTRAC

  05/29/91   08:58
    DATE      TIME

5237 MIAMI FORT
91-142-2000-1-1
SAMP. TIME = 25 SEC

        DV =    0.1383
       %10 =    7.28
       %50 =   20.38
       %90 =   38.98
        MV =   21.94
        CS =    0.432

  PERCENT PASSING
 CHAN.   CUM.   VOL.
 =====   ====   ====
 176     100.0    0.0
 125     100.0    0.0
  88     100.0    0.0
  62     100.0    4.6
  44      95.4   14.1
  31      81.4   25.4
  22      56.0   22.2
  16      33.8   11.4
  11      22.4   11.1
 7.8      11.3    5.6
 5.5       5.7    2.3
 3.9       3.4    2.1
 2.8       1.3    1.1
 1.9       0.3    0.3
 1.4       0.0    0.0
```

```
RELATIVE VOL. GRAPH
 150  0
 106  0
  75  0
  53  *4
  38  *****14
  27  **********25
  19  *********22
  13  ****11
 9.4  ****11
 6.6  **5
 4.7  2
 3.3  2
 2.4  1
 1.6  0
 1.2  0

CUMMULATIVE GRAPH
 176  **********100
 125  **********100
  88  **********100
  62  **********100
  44  **********95
  31  *********81
  22  *****56
  16  ***33
  11  **22
 7.8  *11
 5.5  5
 3.9  3
 2.8  1
 1.9  0
 1.4  0
```

NOTES:

DRAVO CORPORATION

5237
Project No.

( )
Lab No.

Research Center

MICROTRAC PARTICLE SIZE ANALYSIS

Sample Identification: See Print out

Test No. 12607
Date 7/26/91

Division or Customer Name: Miami Fort

Tested by ST

Sample Preparation: WA - US

-REF #5-

MICROTRAC

07/26/91 14:32
DATE TIME

5237 MIA FT BLT FLT
91-143-1015
SAMP. TIME = 25 SEC

DV =	0.3135
%10 =	6.90
%50 =	20.24
%90 =	40.35
MV =	22.28
CS =	0.442

PERCENT PASSING

CHAN.	CUM.	VOL.
176	100.0	0.0
125	100.0	0.0
88	100.0	0.0
62	100.0	6.2
44	93.8	13.5
31	80.3	23.4
22	56.9	23.6
16	33.3	13.4
11	19.9	8.3
7.8	11.7	4.3
5.5	7.4	3.3
3.9	4.1	2.4
2.8	1.7	1.3
1.9	0.4	0.4
1.4	0.0	0.0

RELATIVE VOL. GRAPH

150	9
106	0
75	0
53	**6
38	*****13
27	**********23
19	**********23
13	*****13
9.4	***8
6.6	*4
4.7	*3
3.3	*2
2.4	1
1.6	0
1.2	0

CUMMULATIVE GRAPH

176	**********100
125	**********100
88	**********100
62	**********100
44	**********93
31	*********80
22	*****56
16	***33
11	*19
7.8	*11
5.5	7
3.9	4
2.8	1
1.9	0
1.4	0

NOTES: Slight +80 mesh Material

BRAVO CORPORATION

5234
Project No.

( )
Lab No.

Research Center

MICROTRAC PARTICLE SIZE ANALYSIS

Sample Identification: See Paint out

Test No. 12608
Date 7/26/91

Division or Customer Name: Miami Fort

Tested by ST

Sample Preparation: WA - US

- REF #6 -

MICROTRAC

07/26/91 14:36
DATE TIME

5237 MIA FT BLT FLT
91-143-1215
SAMP. TIME = 25 SEC

DV =	0.2708
%10 =	7.50
%50 =	20.42
%90 =	39.89
MV =	22.33
CS =	0.429

PERCENT PASSING

CHAN.	CUM.	VOL.
176	100.0	0.0
125	100.0	0.0
88	100.0	0.0
62	100.0	5.4
44	94.6	14.7
31	79.9	24.0
22	56.0	22.7
16	33.2	12.7
11	20.5	9.8
7.8	10.7	5.2
5.5	5.5	2.3
3.9	3.2	1.4
2.8	1.8	1.2
1.9	0.5	0.5
1.4	0.0	0.0

RELATIVE VOL. GRAPH

150	0
106	0
75	0
53	**5
38	*******14
27	************23
19	**********22
13	******12
9.4	*****9
6.6	**5
4.7	2
3.3	1
2.4	1
1.6	0
1.2	0

CUMMULATIVE GRAPH

176	************100
125	************100
88	************100
62	************100
44	**********94
31	********79
22	******55
16	***33
11	**20
7.8	*10
5.5	5
3.9	3
2.8	1
1.9	0
1.4	0

NOTES: Slight +80 mesh Material

DRAVO CORPORATION

5237 3.1
Project No.

(91/2418)
Lab No.

Research Center

MICROTRAC PARTICLE SIZE ANALYSIS

Sample Identification: See Printout

Test No. 12492
Date 7/16/91

Division or Customer Name: Miami Fort

Tested by REV

Sample Preparation: None

-REF #7-

MICROTRAC

07/16/91 10:09
DATE TIME

5237 MIAMI FORT
91-189-0800-1-1
SAMP. TIME = 25 SEC

DV =	0.2472
%10 =	5.00
%50 =	19.43
%90 =	41.95
MV =	22.05
CS =	0.501

PERCENT PASSING

CHAN.	CUM.	VOL.
176	100.0	0.0
125	100.0	0.3
88	99.7	0.7
62	99.0	6.9
44	92.2	13.7
31	78.5	20.5
22	58.0	18.7
16	39.3	11.5
11	27.8	10.7
7.8	17.2	5.4
5.5	11.8	5.6
3.9	6.2	4.6
2.8	1.6	1.4
1.9	0.2	0.2
1.4	0.0	0.0

RELATIVE VOL. GRAPH

150	0
106	0
75	0
53	***6
38	*******13
27	**********20
19	**********18
13	******11
9.4	******10
6.6	**5
4.7	**5
3.3	**4
2.4	1
1.6	0
1.2	0

CUMMULATIVE GRAPH

176	**********100
125	**********100
88	**********99
62	**********99
44	**********92
31	********78
22	******58
16	***39
11	**27
7.8	*17
5.5	*11
3.9	6
2.8	1
1.9	0
1.4	0

NOTES: Very little + 80 Mesh Material

DRAVO CORPORATION

5237 3.1
Project No.

(91/26 19)
Lab No.

Research Center

MICROTRAC PARTICLE SIZE ANALYSIS

Sample Identification: See Printout

Test No. 12423
Date 7/16/91

Division or Customer Name: Miami Fort

Tested by REV

Sample Preparation: None

-REF#8-

MICROTRAC

07/16/91 10:24
DATE TIME

5237 MIAMI FORT
91-189-1300-1-1
SAMP. TIME = 25 SEC

DV =	0.2896
%10 =	5.90
%50 =	20.10
%90 =	44.51
MV =	23.39
GS =	0.479

PERCENT PASSING

CHAN.	CUM.	VOL.
176	100.0	0.0
125	100.0	0.0
88	100.0	3.0
62	97.0	7.2
44	89.8	12.4
31	77.4	21.1
22	56.3	19.9
16	36.4	11.6
11	24.8	9.9
7.8	15.0	6.0
5.5	9.0	3.8
3.9	5.1	2.7
2.8	2.4	1.7
1.9	0.7	0.7
1.4	0.0	0.0

RELATIVE VOL. GRAPH

150	0
106	0
75	*2
53	***7
38	*****12
27	**********21
19	**********19
13	*****11
9.4	****9
6.6	**6
4.7	*3
3.3	*2
2.4	1
1.6	0
1.2	0

CUMMULATIVE GRAPH

176	**********100
125	**********100
88	**********100
62	**********97
44	*********89
31	********77
22	*****56
16	***36
11	**24
7.8	*14
5.5	8
3.9	5
2.8	2
1.9	0
1.4	0

NOTES: Very little + 80 mesh Material

DRAVO CORPORATION

5237
Project No.

( )
Lab No.

Research Center

MICROTRAC PARTICLE SIZE ANALYSIS

Sample Identification: See Point out

Test No. 12616
Date 7/26/91

Division or Customer Name: Miami Fort

Tested by ST

Sample Preparation: W/A - US

-REF#9-

MICROTRAC

07/26/91 15:57
DATE TIME

5237 MIA FT BLT FLT
91-191-0930
SAMP. TIME = 25 SEC

DV =	0.3598
%10 =	4.54
%50 =	19.45
%90 =	41.10
MV =	21.47
CS =	0.543

PERCENT PASSING

CHAN.	CUM.	VOL.
176	100.0	0.0
125	100.0	0.0
88	100.0	0.0
62	100.0	6.7
44	93.3	14.7
31	78.6	20.3
22	58.3	19.5
16	38.8	11.3
11	27.4	9.1
7.8	18.4	5.3
5.5	13.1	5.1
3.9	8.0	4.5
2.8	3.5	2.4
1.9	1.0	1.0
1.4	0.0	0.0

RELATIVE VOL. GRAPH

150	0
106	0
75	0
53	***6
38	********14
27	**********20
19	**********19
13	******11
9.4	****9
6.6	**5
4.7	**5
3.3	**4
2.4	*2
1.6	1
1.2	0

CUMMULATIVE GRAPH

176	**********100
125	**********100
88	**********100
62	**********100
44	**********93
31	********78
22	******58
16	***38
11	**27
7.8	*18
5.5	*13
3.9	7
2.8	3
1.9	1
1.4	0

NOTES: Slight +80 mesh Material

DRAVO CORPORATION

5237
Project No.

( )
Lab No.

Research Center

MICROTRAC PARTICLE SIZE ANALYSIS

Sample Identification: See Print out

Test No. 12617
Date 7/26/91

Division or Customer Name: Miami Fort

Tested by ST

Sample Preparation: W/A - US

-REF #10-

MICROTRAC

07/26/91 16:01
DATE TIME

5237 MIA FT BLT FLT
91-191-1330
SAMP. TIME = 25 SEC

DV =	0.3407
%10 =	4.70
%50 =	19.50
%90 =	41.07
MV =	21.45
CS =	0.551

PERCENT PASSING

CHAN.	CUM.	VOL.
176	100.0	0.0
125	100.0	0.0
88	100.0	0.0
62	100.0	6.9
44	93.1	13.6
31	79.5	21.5
22	58.0	19.2
16	38.8	11.1
11	27.7	10.0
7.8	17.7	5.4
5.5	12.3	4.5
3.9	7.7	3.6
2.8	4.1	2.6
1.9	1.6	1.3
1.4	0.3	0.3

RELATIVE VOL. GRAPH

150	0
106	0
75	0
53	***6
38	******13
27	**********21
19	*********19
13	*****11
9.4	****10
6.6	**5
4.7	**4
3.3	*3
2.4	*2
1.6	1
1.2	0

CUMMULATIVE GRAPH

176	**********100
125	**********100
88	**********100
62	**********100
44	**********93
31	********79
22	*****57
16	***38
11	**27
7.8	*17
5.5	*12
3.9	7
2.8	4
1.9	1
1.4	0

NOTES: Slight +80 mesh Material

DRAVO CORPORATION

5237-3.1 Project No.

91-3986 Lab No.

Research Center

MICROTRAC PARTICLE SIZE ANALYSIS

Sample Identification: See Printout

Test No. 13305
Date 090491

Division or Customer Name: Miami Fort

Tested by CYJ

Sample Preparation: As Received

-REF #11-

MICROTRAC

09/04/91 13:57
DATE TIME

5237-3.1 M.F.91-3981
91-233-0400-1-01
SAMP. TIME = 25 SEC

DV =	0.1250
%10 =	5.56
%50 =	15.67
%90 =	27.53
MV =	16.33
CS =	0.540

PERCENT PASSING

CHAN.	CUM.	VOL.
176	100.0	0.0
125	100.0	0.0
88	100.0	0.0
62	100.0	0.8
44	99.2	2.0
31	97.3	18.9
22	78.4	26.9
16	51.5	22.6
11	28.8	14.8
7.8	14.0	4.1
5.5	9.9	4.3
3.9	5.6	3.8
2.8	1.8	1.5
1.9	0.3	0.3
1.4	0.0	0.0

RELATIVE VOL. GRAPH

150	0
106	0
75	0
53	0
38	1
27	******18
19	**********26
13	*********22
9.4	*****14
6.6	*4
4.7	*4
3.3	*3
2.4	1
1.6	0
1.2	0

CUMMULATIVE GRAPH

176	**********100
125	**********100
88	**********100
62	**********100
44	**********99
31	**********97
22	********78
16	******51
11	**28
7.8	*14
5.5	9
3.9	5
2.8	1
1.9	0
1.4	0

NOTES:

DRAVO CORPORATION

5237-3.1 Project No.

C91-4026 Lab No.

Research Center

MICROTRAC PARTICLE SIZE ANALYSIS

Sample Identification: See Printout

Test No. 13306
Date 090491

Division or Customer Name: Miami Fort

Tested by CYJ

Sample Preparation: As Received

-REF #12-

MICROTRAC

09/04/91 14:05
DATE TIME

5237-3.1 M.F.91-4026
91-233-1200-1-01
SAMP. TIME = 25 SEC

DV =	0.1500
%10 =	5.08
%50 =	16.22
%90 =	29.23
MV =	16.96
CS =	0.564

PERCENT PASSING

CHAN.	CUM.	VOL.
176	100.0	0.0
125	100.0	0.0
88	100.0	0.0
62	100.0	1.2
44	98.8	4.9
31	93.9	20.0
22	73.9	24.8
16	49.1	16.3
11	32.8	14.4
7.8	18.4	7.1
5.5	11.2	4.7
3.9	6.5	4.2
2.8	2.3	1.8
1.9	0.5	0.5
1.4	0.0	0.0

RELATIVE VOL. GRAPH

150	0
106	0
75	0
53	1
38	*4
27	*********19
19	**********24
13	******16
9.4	*****14
6.6	**7
4.7	*4
3.3	*4
2.4	1
1.6	0
1.2	0

CUMMULATIVE GRAPH

176	**********100
125	**********100
88	**********100
62	**********100
44	**********98
31	**********93
22	********73
16	****49
11	***32
7.8	*18
5.5	*11
3.9	6
2.8	2
1.9	0
1.4	0

NOTES:

Project No: 5237
Lab no : 91-5270
Date : 11/19/91
Sampled by: Client
Test No. : 13713

.ient Name: Miami Fort
:tn: Lewis Benson

ımple Identification: 91-319-1200-1-01

-REF # 13-

Particle Size Distribution by Leeds & Northrup Microtrac

Percent Passing

Chan.	Cum.	Vol.
176.0	100.0	0.0
125.0	100.0	0.0
88.0	100.0	0.0
62.0	100.0	0.0
44.0	100.0	0.0
31.0	100.0	11.3
22.0	88.7	24.4
16.0	64.3	26.4
11.0	37.9	20.2
7.8	17.8	8.3
5.5	9.5	4.9
3.9	4.5	2.1
2.8	2.4	1.7
1.9	0.7	0.7
1.4	0.0	0.0

Relative Volume Graph

150.0	0
106.0	0
75.0	0
53.0	0
38.0	0
27.0	11
19.0	24
13.0	26
9.4	20
6.6	8
4.7	4
3.3	2
2.4	1
1.6	0
1.2	0

Cummulative Graph

176.0	100
125.0	100
88.0	100
62.0	100
44.0	100
31.0	100
22.0	88
16.0	64
11.0	37
7.8	17
5.5	9
3.9	4
2.8	2
1.9	0
1.4	0

Summary Data

%10 = 5.65
%50 = 13.28
%90 = 23.01

MV = 13.91
CS = 0.599
DV = 0.1262

Remarks: 25 sec. run

Respectfully Submitted,

Mary Lou Cupp
Laboratory Supervisor
Dravo Lime Company

Project No: 5237
Lab no : 91-5271
Date : 11/19/91
Sampled by: Client
Test No. : 13714

Client Name: Miami Fort
Attn: Lewis Benson

Sample Identification: 91-319-2000-1-01 SLR

-REF #14-

Particle Size Distribution by Leeds & Northrup Microtrac

Percent Passing

Chan.	Cum.	Vol.
176.0	100.0	0.0
125.0	100.0	0.0
88.0	100.0	0.0
62.0	100.0	0.6
44.0	99.4	0.7
31.0	98.7	14.6
22.0	84.1	23.6
16.0	60.5	21.2
11.0	39.3	16.8
7.8	22.5	8.0
5.5	14.4	6.6
3.9	7.8	4.9
2.8	2.9	2.2
1.9	0.7	0.7
1.4	0.0	0.0

Relative Volume Graph

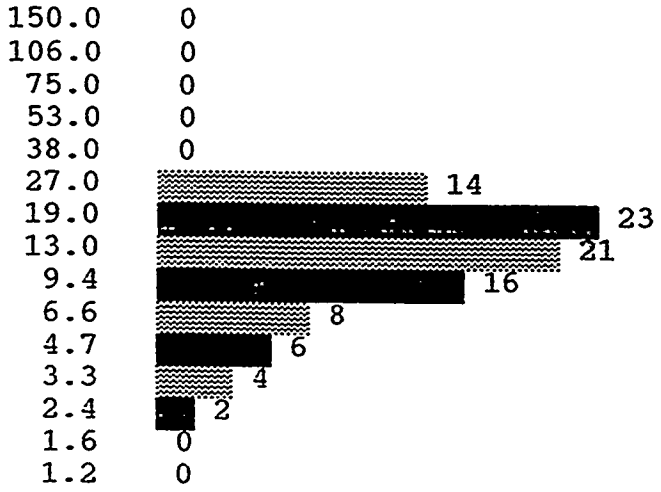

Cummulative Graph

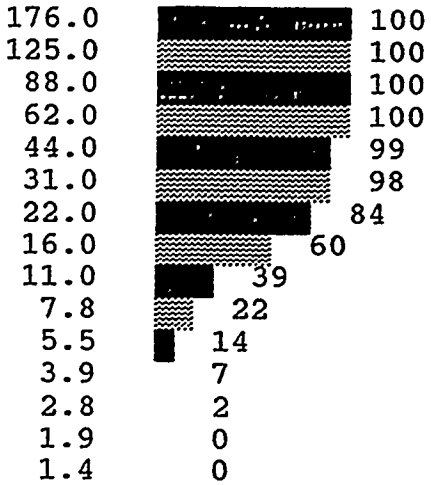

Summary Data

%10 = 4.43
%50 = 13.52
%90 = 25.61

MV = 14.40
CS = 0.643
DV = 0.1729

Remarks: 25 sec. run
traces +80

Respectfully Submitted,

Mary Lou Cupp
Laboratory Supervisor
Dravo Lime Company

Project No: 5237
Lab no : 91-5661
Date : 12/30/91
Sampled by: Client
Test No. : 13806

lient Name: Miami Fort
ttn: Lew Benson

ample Identification: 91-347-0400-1-01

-REF #15-

Particle Size Distribution by Leeds & Northrup Microtrac

Percent Passing

Chan.	Cum.	Vol.
176.0	100.0	0.0
125.0	100.0	0.0
88.0	100.0	0.0
62.0	100.0	0.0
44.0	100.0	0.0
31.0	100.0	14.7
22.0	85.3	26.7
16.0	58.6	20.8
11.0	37.8	22.4
7.8	15.4	9.0
5.5	6.4	3.3
3.9	3.1	0.7
2.8	2.4	1.5
1.9	0.9	0.8
1.4	0.1	0.1

Relative Volume Graph

150.0	0
106.0	0
75.0	0
53.0	0
38.0	0
27.0	14
19.0	26
13.0	20
9.4	22
6.6	9
4.7	3
3.3	0
2.4	1
1.6	0
1.2	0

Cummulative Graph

176.0	100
125.0	100
88.0	100
62.0	100
44.0	100
31.0	100
22.0	85
16.0	58
11.0	37
7.8	15
5.5	6
3.9	3
2.8	2
1.9	0
1.4	0

Summary Data

%10 = 6.42
%50 = 13.93
%90 = 24.89

MV = 14.68
CS = 0.565
DV = 0.1492

Remarks: 25 sec. Run Time
Trace +80

Respectfully Submitted,

Mary Lou Cupp
Laboratory Supervisor
Dravo Lime Company

Project No: 5237
Lab no : 91-5673
Date : 12/30/91
Sampled by: Client
Test No. : 13807

ient Name: Miami Fort
t.n: Lew Benson

mple Identification: 91-347-1200-1-01

-REF #16-

Particle Size Distribution by Leeds & Northrup Microtrac

Percent Passing

Chan.	Cum.	Vol.
176.0	100.0	0.0
125.0	100.0	0.0
88.0	100.0	0.0
62.0	100.0	0.0
44.0	100.0	0.0
31.0	100.0	17.9
22.0	82.1	30.2
16.0	52.0	16.6
11.0	35.3	14.0
7.8	21.3	7.2
5.5	14.1	5.1
3.9	9.1	3.9
2.8	5.1	3.0
1.9	2.1	1.6
1.4	0.5	0.5

Relative Volume Graph

150.0	0
106.0	0
75.0	0
53.0	0
38.0	0
27.0	17
19.0	30
13.0	16
9.4	14
6.6	7
4.7	5
3.3	3
2.4	3
1.6	1
1.2	0

Cummulative Graph

176.0	100
125.0	100
88.0	100
62.0	100
44.0	100
31.0	100
22.0	82
16.0	51
11.0	35
7.8	21
5.5	14
3.9	9
2.8	5
1.9	2
1.4	0

Summary Data

%10 = 4.20
%50 = 15.41
%90 = 25.97

MV = 14.98
CS = 0.663
DV = 0.1608

Remarks: 25 sec. Run Time
Trace +80

Respectfully Submitted,

Mary Lou Cupp
Laboratory Supervisor
Dravo Lime Company

V. ECONOMIC ANALYSIS - PROCESS COST ESTIMATES

An economic evaluation of the iron chelate NOx removal technology has been conducted based on operating experience gained at the pilot plant level with consideration of full scale operation. The basis of this evaluation is from the EPRI Capital and Operating Cost Premise (GS-7193), Section II Magnesium Enhanced Lime Process. The EPRI economic evaluation is based on a nominal 300 MWe plant operating at full load at 1/1990.

Exceptions to the EPRI Basis Include:

1. Chelate and reducing agents costs are of February, 1992 dollars.

2. Absorber tower packing is a Munters budgetary estimate (February, 1992).

3. Magnesium enhanced lime absorber tower for new plant construction is scaled to reflect actual commercial experience and optimum NOx removal.

4. Commercial electrochemical cell capital cost is unknown. Cell operating costs for electricity and alkali are based on an assumed ferric EDTA reduction rate and with a cell voltage of 2 volts and 90% current efficiency.

5. NOx removal reagents storage and transfer facilities were estimated from similarly sized systems in GS-7193.

6. The solids dewatering and handling areas were sized to take advantage of the superior dewaterability experienced during pilot plant operation. The resulting capital and operating cost reductions are reflected in the evaluation.

The capital and operating costs have been estimated for retrofit and new plant construction versions of the iron chelate based NOx removal technology, integrated with a Thiosorbic^{R} FGD system. Three versions of this technology, each version a different method of regenerating Fe(III)EDTA with two subset versions of introducing iron and EDTA into the system, were evaluated and presented. The three major versions evaluated are:

1) High total FeEDTA concentration (100 mM) in the system with no active means of Fe^{+3} reduction either chemically or electrochemically.

2) Low total FeEDTA concentration (35 mM) in the system using chemical reduction of Fe^{+3}.

3) Low total FeEDTA concentration (35 mM) in the system using electrochemical reduction of Fe^{+3}.

Two subset versions to each of these Fe^{+3} reduction methods consider the source of iron and EDTA introduced to the system. The first source, dry bulk Na_4EDTA and $FeSO_4$ was tested in the pilot plant. Using these reagents as the source for iron and EDTA requires separate storage and transfer facilities as well as a mixed reaction tank to bring the reagents together to react and form Fe(III)EDTA. A second source is a 4 wt.% iron Fe(III)EDTA solution that is commercially available at a somewhat higher cost than the dry bulk Na_4EDTA and $FeSO_4$ combination. This approach however eliminates the need for two sets of storage and transfer facilities and a mixed reaction tank. Using the second alternative source results in a 0.1 to 0.4 mill/kW-hr increase in operating cost but a $5.00/kW decrease in capital cost, regardless of mode (retrofit or new plant construction) employed. When it was necessary to estimate a new capital cost for resized absorber towers or thickeners, the exponential cost scale factor 0.7 was used.

Retrofit Absorber Tower Design

The retrofit Thiosorbic^{R} absorber design had the following operating parameters: 1) 8 feet per second flue gas velocity; 2) L/G of 40 gpm/1000 ACFM; 3) Munters PN Fill packing 12 feet tall by 32 feet in diameter; 4) Absorber tower height of 60 feet. At these conditions, SO_2 removal is 99% and NOx removal is assumed to be 50%. NOx removal in the pilot plant at these conditions ranged from 30 to 45%. NOx removal was assumed to be 50% in the economic evaluation with the assumption that better gas liquid contacting and less wall effects would occur on a commercial scale.

New Plant Absorber Tower Design

The new plant Thiosorbic^{R} absorber, designed for optimum NOx removal, has the following operating parameters: 1) 5 feet per second flue gas velocity; 2) L/G of 200 gpm/1000 ACFM; 3) Munters PN Fill Packing 12 feet tall by 41.85 feet in diameter; 4) Absorber tower height of 78 feet. At these conditions, SO_2 removal is 99.9% and NOx removal is assumed to be 70%. At these conditions, NOx removal in the pilot plant ranged from 43 to 60%. NOx removal was assumed to be 70% in the economic evaluation for the same reasons mentioned above.

Process Parameters

The Fe^{+3} reduction rate was determined from the antioxidant/reducing agent feedrate utilized during pilot plant operation and directly scaled up to 300 MWe (0.3278 lb-moles Fe(III)EDTA reduced/MWe). Chelate and associated chemical feedrate were estimated from the total FeEDTA concentration (35 to 100 mM) specified and the liquid loss rate in the filter cake. The system pressure drop, for determining fan size and energy consumption, was set at 9.3 and 14.7 inches WC for retrofit and new plant construction respectively. These pressure drop values are similar to those experienced at the pilot plant.

Results of Evaluation

Table 1 summarizes the cost of chemical and electrochemical Fe(III)EDTA reduction. Sodium dithionite ($Na_2S_2O_4$) and ascorbic acid costs are shown as if each were the sole reducing agent. These agents were actually used in the pilot plant as a 250 to 55 lb/lb mixture of sodium dithionite and ascorbic acid respectively. The cost of this mixture is used in the detailed capital and operating cost evaluation. Glyoxal, which appears as a significantly less expensive alternative to sodium dithionite and ascorbic acid, was not evaluated further because of undesirable side reactions that occurred with its use during pilot plant operation.

The electrochemical cell estimated operating costs consist only of electricity and anode neutralization costs. Anode neutralization costs are compared using caustic and lime solutions where use of lime is 1/3 the cost of caustic. The electrochemical cell using lime slurry neutralization of the anode represents the least expensive active means of reducing Fe(III)EDTA. This method however was not tested at the pilot plant and is not available commercially at this writing. Other unknowns associated with the electrochemical cell include capital and maintenance costs that are only guessed in the detailed cost evaluation.

A final alternate method of Fe(III)EDTA reduction utilizes $SO_3^=$, which characteristically exists in high concentration in the Thiosorbic^R FGD process, as the reducing agent. Fe(III)EDTA reduction using $SO_3^=$ was found to be a slow reaction providing insufficient amounts of the Fe^{+2} ion when total FeEDTA levels throughout the system were maintained at a low level (35 mM). However, if total FeEDTA concentration was maintained at 100 mM, Fe(III)EDTA reduction by $SO_3^=$ appeared to provide sufficient levels of Fe^{+2} (10 to 15 mM) for NOx removal. Although this method of Fe(III)EDTA reduction was tested only briefly at the pilot plant (1 week), results were promising enough to include in the detailed capital and operating cost evaluation. More operating time in pilot operation would be necessary to confirm the results.

Table 2 summarizes the detailed capital and operating costs evaluation for both retrofit into an existing Thiosorbic^R FGD system and new plant construction. The tabulated costs (operating costs only for retrofit and both operating and capital costs for new plant construction) include FGD costs. Exceptions are SCR and Low NOx burner cases that represent only NOx removal costs.

The Table 2 summary indicates electrochemical Fe(III)EDTA reduction (Cases C and D) to be the least expensive in terms of operating costs for both retrofit and new plant construction. However the high (100 mM) Fe(III)EDTA concentration cases (A and B) represent the least capital expenditure with only slightly higher (0.5 to 0.9 mills/kW-hr) operating costs compared with the electrochemical cell cases. Chemical reduction of Fe(III)EDTA (Cases E and F), using the mixture of sodium dithionite and ascorbic acid, represents the most expensive option both in terms of capital and operating costs of the three iron chelate NOx removal options. Compared to SCR, the chemical reduction option capital costs would be significantly less expensive for both retrofit or new plant construction (whether including FGD costs or not) but experiences operating costs 3 times greater. These costs make chemical reduction of Fe(III)EDTA the least economically viable means of reducing NOx emissions.

In all the Thiosorbic^R/NOx removal cases alternative sources of Fe and EDTA are compared. The source used in the pilot plant was mixing powdered $FeSO_4$ and Na_4EDTA into a mixing tank of process liquor. This mixed solution was metered into the recycle tank as required to maintain desired total FeEDTA concentration. In the commercial scale evaluation, a 39 wt.% solution of Na_4EDTA replaced the powdered Na_4EDTA because it is less expensive. The alternative source of FeEDTA is a 4 wt.% Fe solution of FeEDTA that eliminates the need for one set of storage and transfer facilities and mixing tank. This results in a $5/kW decrease in capital expenditure regardless of reduction method or whether a retrofit or new plant application. However since the 4 wt.% iron FeEDTA solution is about 1/3 more expensive than the combined expense of $FeSO_4$ and Na_4EDTA, the operating costs are 0.1 to 0.4 mills/kW-hr higher depending on the application.

Tables 3 and 4 show itemized capital and levelized operating costs for retrofit and new plant construction versions respectively. The capital costs listed on the retrofit Table 3 reflect only NOx removal modifications.

Most variation in the capital costs regardless of mode occurs in the NOx reagent/reduction systems, fees and contingency, and royalty, preproduction, and inventory categories. The absorber tower capital cost remains constant for all cases as the design of the modifications for the retrofit cases, and the design of the absorber tower optimized for NOx removal, is the same throughout. The NOx reagent/reduction system cost varies due to the amount of reagent storage and transfer equipment required and the cost of electrochemical cell procurement. The fees and contingency category is factored from the various systems and thus vary as subsystem costs vary. The royalty, preproduction, and inventory category is partly factored from the capital costs of the various systems and 30 day inventory requirements for reagents. Variation in operating costs in both Tables 3 and 4 are a function the Fe(III)EDTA reduction method and the source of Fe and EDTA.

Up to this point in the economic evaluation, the approach has been to evaluate the iron chelate technology as the sole means of NOx removal. An alternate and perhaps more technically attainable approach is to combine Low NOx Burners with iron chelate NOx technology. The two technologies combined will reduce NOx emissions far lower than each can separately. Capital and operating costs are only slightly higher in retrofit cases and actually less expensive than new plant construction cases where iron chelate technology was solely used. The capital cost in the new plant construction cases are less because the absorber tower design is back to the conventional size of a standard Thiosorbic^{R} tower (32 feet in diameter and flue gas velocity 8.5 fps). Operating costs are less because the specified L/G is 50 rather than 200 which means fewer operating pumps and less pressure drop across the absorber tower. NOx removal with this absorber design will drop to 50% or less but if combined with Low NOx burners, NOx emissions will be reduced by 75% (i.e. LNB reduction: 50% of 600 ppmv = 300 ppmv; iron chelate NOx removal: 50% of 300 ppmv = 150 ppmv; therefore overall NOx reduction = (600 - 150)/600 *100 = 75%).

Table 5 lists total capital and operating costs of selected Thiosorbic^R/Iron chelate cases combined with Low NOx burner technology for both retrofit and new plant construction. Also included are retrofit and new plant construction cases where Thiosorbic^R FGD is combined with Selective Catalytic Reduction (SCR). Once again when chemical reduction of Fe(III)EDTA is used, (Thiosorbic^R/Iron chelate Case E and Low NOx burner) the operating costs, for both retrofit and new plant construction, are prohibitively high, though the capital costs are lower than Thiosorbic^R combined with SCR.

Of the remaining three cases, the Thiosorbic^R/SCR case has capital costs 2 to 3 times higher than any other retrofit case and 1.7 to 1.85 times higher than any new plant construction case. The Thiosorbic^R/SCR case, regardless of whether retrofit or new plant construction, also has operating costs roughly 3 to 4 mills/kW-hr higher. The two cases where Thiosorbic^R/Iron chelate and Low NOx burner technologies are combined represent the lowest capital and operating cost cases in their respective categories and differ only in the method of Fe(III)EDTA reduction. Case A relies on $SO_3^=$ to reduce Fe(III)EDTA while total FeEDTA is maintained at 100 mM concentration. Case C uses electrochemical reduction of Fe(III)EDTA with concentration of total FeEDTA maintained at 35 mM. As mentioned previously, while Case C shows electrochemical reduction to be a most promising means, in terms of operating cost, for reducing Fe(III)EDTA, it is not available commercially. Case A is the most likely near term application of the iron chelate NOx removal technology, but requires more study as the Miami Fort pilot plant was operated only briefly in this mode.

COST OF CHEMICAL REDUCING AGENTS/ANTIOXIDANTS

COUMPOUND	FORMULA	COST PER POUND	FORMULA WEIGHT	REDUCTION STOICHIOMETRY (NOTE 1)	RELATIVE COST, ¢ PER LB-MOLE FERRIC EDTA REDUCED (NOTE 2)	REDUCTION COST IN MILLS/kW-HR (NOTE 2)
SODIUM DITHIONATE (ANHYDROUS)	Na2S2O4	0.62	174	2	53.94	17.7
ASCORBIC ACID		6.50	176	10	98.80	31.7
GLYOXAL (NOTE 3) AT 100% UTILIZATION	C2O2H2	1.43	58	6	13.78	4.5
GLYOXAL AT 66.7% UTILIZATION	C2O2H2	1.43	58	4	20.66	6.8

ELECTROCHEMICAL REDUCTION REAGENT AND ELECTRICITY COST

ELECTRICITY COST, MILLS/kW-HR	CAUSTIC/LIME COST, ¢/LB	COST OF ELECTRICITY, ¢ PER LB-MOLE FERRIC EDTA REDUCED	COST OF CAUSTIC/LIME, ¢ PER LB-MOLE FERRIC EDTA REDUCED	TOTAL REDUCTION COST IN MILLS/kW-HR (NOTE 2)
25	0.125	0.68	2.5 <= = Caustic	1.04
25	0.028	0.68	0.392 <= = Lime	0.35

NOTE 1: STOICHIOMETRY IS NUMBER OF MOLES OF IRON REDUCED PER MOLE OF COMPOUND

NOTE 2: COST IS BASED ON REDUCTION RATE OF 98.34 LB-MOLES FERRIC EDTA REDUCED PER HOUR AT 300 MW CAPACITY.
FOR THE ELECTROCHEMICAL CELL, IT IS ALSO BASED ON CELL VOLTAGE OF 2 VOLTS AT 90% CURRENT EFFICIENCY.

NOTE 3: GLYOXAL IS SOLD AS A 40 WT.% SOLUTION AT $0.57/LB SOLUTION (CHEMICAL MARKETING REPORTER, JUNE 1991)

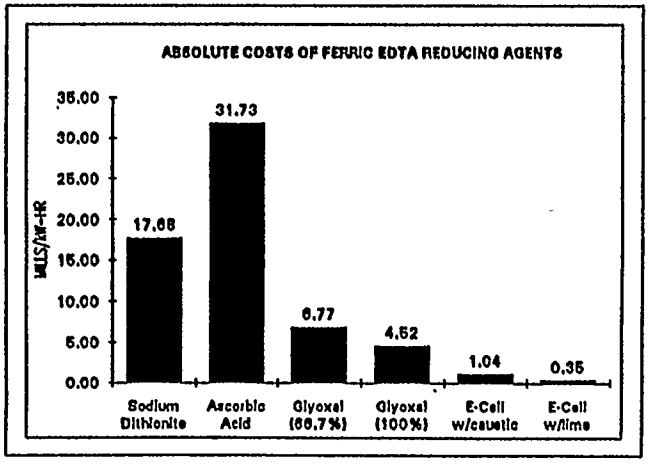

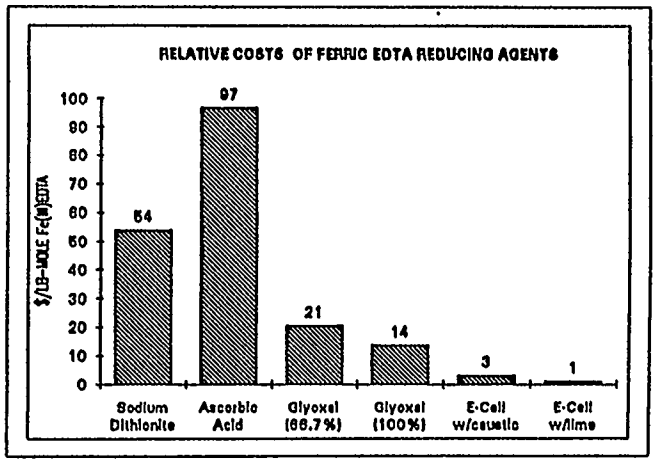

Table 1

Table 1

Table - 2

Summary of Estimated Capital and Operating Costs for Thiosorbic/Iron Chelate NOx Removal System
Dravo Lime Estimated Costs Based on EPRI GS-7193(1991) With Noted Adjustments

Costs	Units	Existing Thiosorbic System	Thio/NOx Retrofit A	Thio/NOx Retrofit B	Thio/NOx Retrofit C	Thio/NOx Retrofit D	Thio/NOx Retrofit E	Thio/NOx Retrofit F	Retrofit SCR	Retrofit Low NOx Burner
Operating Costs; First Year	mills/kW-Hr	3.0	5.9	6.3	5.5	5.5	25.5	25.5	6.8	0.46
Operating Costs; Levelized	mills/kW-Hr	4.1	7.8	8.4	7.1	7.1	34.4	34.5	6.8	0.46
Capital Costs	$/kW	- - - - -	22.0	17.0	39.0	34.0	45.0	40.0	157.7	15.4

Costs	Units	New Thiosorbic System	Thio/NOx New Plant A	Thio/NOx New Plant B	Thio/NOx New Plant C	Thio/NOx New Plant D	Thio/NOx New Plant E	Thio/NOx New Plant F	New SCR	New Low NOx Burner
Operating Costs; First Year	mills/kW-Hr	6.6	10.1	10.5	9.6	9.7	29.6	29.7	6.8	0.30
Operating Costs; Levelized	mills/kW-Hr	7.8	12.0	12.6	11.2	11.3	38.6	38.6	6.8	0.30
Capital Costs	$/kW	114.0	154.0	150.0	170.0	165.0	176.0	172.0	157.7	10.1

Notes:

Case A: High Fe(III)EDTA Concentration, No Additives, No Electrochemical Cell, Na4EDTA & FeSO4
Case B: High Fe(III)EDTA Concentration, No Additives, No Electrochemical Cell, 4% Fe-Fe(III)EDTA
Case C: Low Fe(III)EDTA Concentration, No Additives, w/Electrochemical Cell, Na4EDTA & FeSO4
Case D: Low Fe(III)EDTA Concentration, No Additives, w/Electrochemical Cell, 4% Fe-Fe(III)EDTA
Case E: Low Fe(III)EDTA Concentration, w/ Additives, No Electrochemical Cell, Na4EDTA & FeSO4
Case F: Low Fe(III)EDTA Concentration, w/Additives, No Electrochemical Cell, 4% Fe-Fe(III)EDTA
SCR and Low NOx Burner Costs were estimated using IAPCS Version 4.0 Cost Model (LNB NOx Reduction 50%; SCR Hot NOx Removal 80%)
Base Thiosorbic System SO2 Removal is 90%

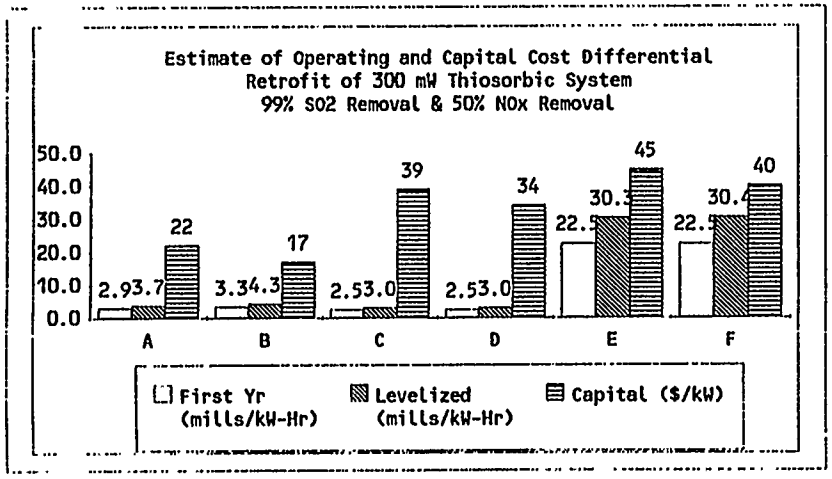

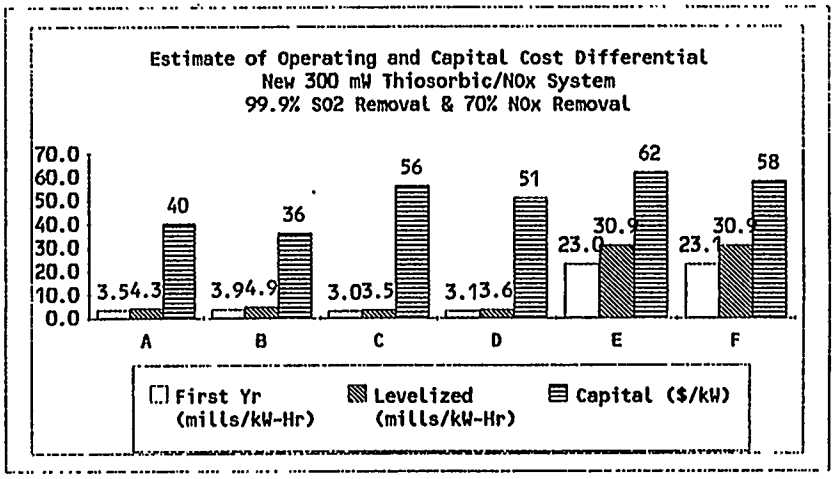

Table 2

DETAIL RETROFIT COSTS

CAPITAL COSTS ($/kW)

	A	B	C	D	E	F
ABSORBER TOWER SYSTEM	6.6	6.6	6.6	6.6	6.6	6.6
NOx REAGENT/RED. SYSTEMS	5.4	2.2	16.3	13.1	14.5	11.3
MISC. EQUIPMENT	1.3	1.3	1.3	1.3	1.3	1.3
FEES & CONTIGENCY	5.7	4.4	10.3	9	9.6	8.2
ROYALTY, PREPROD., & INVENTORY	2.9	2.7	4.1	3.6	13.2	12.8
TOTAL	21.9	17.2	38.6	33.6	45.2	40.2

LEVELIZED OPERATING COSTS (mills/kW-hr)

	MG-LIME	A	B	C	D	E	F
CAPITAL	3.66	0.7	0.55	1.24	1.08	1.44	1.29
FIXED OPERATING	1.42	1.82	1.79	1.92	1.89	1.91	1.87
REAGENT LIME	1.34	1.47	1.47	1.47	1.47	1.47	1.47
STABILIZATION LIME	0.16	0	0	0	0	0	0
NEUTRALIZATION LIME	0	0	0	0.35	0.35	0	0
ELECTRICITY	0.55	0.63	0.63	0.63	0.63	0.64	0.64
WASTE DISPOSAL	0.55	0.43	0.43	0.43	0.43	0.43	0.43
WATER	0.07	0.07	0.07	0.07	0.07	0.07	0.07
VERSENE 100	0	2.68	0	0.94	0	0.94	0
4% Fe; Fe(III)EDTA	0	0	3.47	0	1.21	0	1.21
FERROUS SULFATE	0	0.004	0	0.001	0	0.001	0
SODIUM DITHIONITE	0	0	0	0	0	20.12	20.12
ASCORBIC ACID	0	0	0	0	0	7.4	7.4
TOTAL	7.75	7.80	8.41	7.05	7.13	34.42	34.50

Table 3 V-10

Notes

Case A: High Fe(III)EDTA Concentration, No Additives, No Electrochemical Cell, Na4EDTA & FeSO4
Case B: High Fe(III)EDTA Concentration, No Additives, No Electrochemical Cell, 4% Fe-Fe(III)EDTA
Case C: Low Fe(III)EDTA Concentration, No Additives, w/Electrochemical Cell, Na4EDTA & FeSO4
Case D: Low Fe(III)EDTA Concentration, No Additives, w/Electrochemical Cell, 4% Fe-Fe(III)EDTA
Case E: Low Fe(III)EDTA Concentration, w/ Additives, No Electrochemical Cell, Na4EDTA & FeSO4
Case F: Low Fe(III)EDTA Concentration, w/Additives, No Electrochemical Cell, 4% Fe-Fe(III)EDTA
ELECTROCHEMICAL POWER CONSUMPTION ESTIMATE: 2.66 kW
CAPITAL COSTS REFLECT ONLY NOx REMOVAL SYSTEMS

DETAIL NEW PLANT COSTS

CAPITAL COSTS ($/kW)

	MG-LIME	A	B	C	D	E	F
ABSORBER TOWER SYSTEM	21.6	43.4	43.4	43.4	43.4	43.4	43.4
NOx REAGENT/RED. SYSTEMS	0	5.4	2.2	16.3	13.1	14.5	11.3
SO2 REAGENT SYSTEMS	19.1	20.4	20.4	20.4	20.4	20.4	20.4
SOLIDS DEWATERING SYSTEMS	8.6	6.3	6.3	6.3	6.3	6.3	6.3
OTHER SYSTEMS & MISC. EQUIPMENT	23.3	23.5	23.5	23.5	23.5	23.4	23.4
FEES & CONTIGENCY	31.1	42.3	40.9	47	45.6	46.3	44.9
ROYALTY, PREPROD., & INVENTORY	10.8	12.9	13	12.9	12.9	22.2	22.1
TOTAL	115	154.2	149.7	169.8	165.2	176.5	171.8

LEVELIZED OPERATING COSTS (mills/kW-hr)

	MG-LIME	A	B	C	D	E	F
CAPITAL	3.66	4.93	4.79	5.43	5.28	5.64	5.49
FIXED OPERATING	1.42	1.78	1.75	1.88	1.85	1.86	1.83
REAGENT LIME	1.34	1.47	1.47	1.47	1.47	1.47	1.47
STABILIZATION LIME	0.16	0	0	0	0	0	0
NEUTRALIZATION LIME	0	0	0	0.35	0.35	0	0
ELECTRICITY	0.55	0.63	0.63	0.63	0.63	0.64	0.64
WASTE DISPOSAL	0.55	0.43	0.43	0.43	0.43	0.43	0.43
WATER	0.07	0.05	0.05	0.05	0.05	0.05	0.05
VERSENE 100	0	2.68	0	0.94	0	0.94	0
4% Fe; Fe(III)EDTA	0	0	3.47	0	1.21	0	1.21
FERROUS SULFATE	0	0.004	0	0.001	0	0.001	0
SODIUM DITHIONITE	0	0	0	0	0	20.12	20.12
ASCORBIC ACID	0	0	0	0	0	7.4	7.4
TOTAL	7.75	11.97	12.59	11.18	11.27	38.55	38.64

Notes
- Case A: High Fe(III)EDTA Concentration, No Additives, No Electrochemical Cell, Na4EDTA & FeSO4
- Case B: High Fe(III)EDTA Concentration, No Additives, No Electrochemical Cell, 4% Fe-Fe(III)EDTA
- Case C: Low Fe(III)EDTA Concentration, No Additives, w/Electrochemical Cell, Na4EDTA & FeSO4
- Case D: Low Fe(III)EDTA Concentration, No Additives, w/Electrochemical Cell, 4% Fe-Fe(III)EDTA
- Case E: Low Fe(III)EDTA Concentration, w/ Additives, No Electrochemical Cell, Na4EDTA & FeSO4
- Case F: Low Fe(III)EDTA Concentration, w/Additives, No Electrochemical Cell, 4% Fe-Fe(III)EDTA
- ELECTROCHEMICAL CELL POWER CONSUMPTION ESTIMATE: 2.66 kW

Table - 5

Estimated Capital and Operating Costs for Combined Low NOx Burner/Thiosorbic/Iron Chelate NOx Removal System
Dravo Lime Estimated Costs Based on EPRI GS-7193(1990) With Noted Adjustments

Costs	Units		Retrofit Thiosorbic SCR	Retrofit Thio/NOx Case A & LNB	Retrofit Thio/NOx Case C & LNB	Retrofit Thio/NOx Case E & LNB
Operating Costs; First Year	mills/kW-Hr		9.8	6.4	6.0	26.0
Operating Costs; Levelized Year	mills/kW-Hr		10.9	8.3	7.6	34.9
Capital Costs	$/kW		157.7	37.3	54.1	60.6

Costs	Units		New Thiosorbic & SCR	New Thio/NOx Case A & LNB	New Thio/NOx Case C & LNB	New Thio/NOx Case E & LNB
Operating Costs; First Year	mills/kW-Hr		13.4	9.7	9.3	29.3
Operating Costs; Levelized Year	mills/kW-Hr		14.6	11.6	10.8	38.2
Capital Costs	$/kW		271.7	147.2	162.8	169.5

Notes:
- Case A: High Fe(III)EDTA Concentration, No Additives, No Electrochemical Cell, Na4EDTA & FeSO4
- Case C: Low Fe(III)EDTA Concentration, No Additives, w/Electrochemical Cell, Na4EDTA & FeSO4
- Case E: Low Fe(III)EDTA Concentration, w/ Additives, No Electrochemical Cell, Na4EDTA & FeSO4
- SCR and Low NOx Burner Costs were estimated using IAPCS Version 4.0 Cost Model (LNB NOx Reduction 50%; SCR Hot NOx Removal 80%)
- Capital costs reflect only NOx removal modifications in retrofit cases.
- Assumes LO-NOx Burner NOx Reduction of 50% (total NOx reduction w/LNB & FeEDTA 75%)
- New Plant absorber tower diameter same as retrofit absorber tower @ 32 feet.

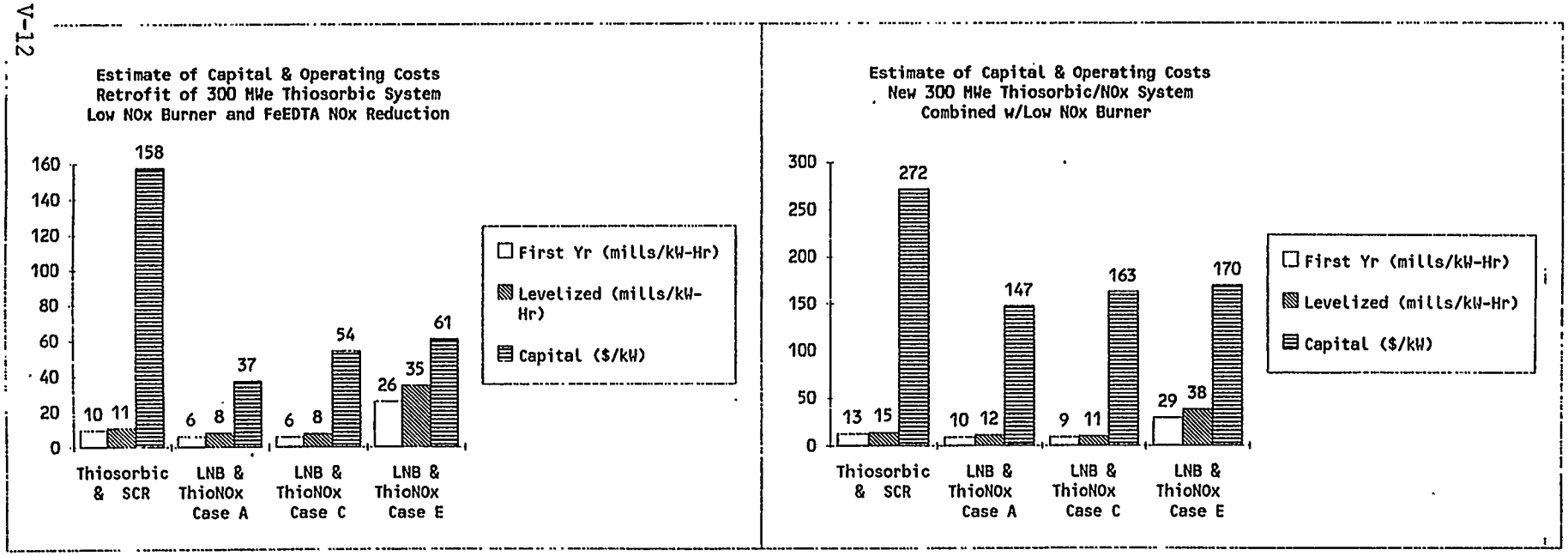

Table 5